Bioethanol production from *Parthenium hysterophorus* involving cellulase from *Bacillus amyloliquefaciens* SS35: Process development, optimization and intensification

Ph. D. Thesis

by

Shuchi Singh

Center for Energy
Indian Institute of Technology Guwahati
Guwahati – 781 039, Assam, India
December 2014

Bioethanol production from *Parthenium hysterophorus* involving cellulase from *Bacillus amyloliquefaciens* SS35: Process development, optimization and intensification

A
Thesis
Submitted in
Partial Fulfillment of the
Requirements for the Degree of

DOCTOR OF PHILOSOPHY

By

Shuchi Singh

Center for Energy
Indian Institute of Technology Guwahati
Guwahati – 781 039, Assam, India

December 2014

Dedicated to

My Parents

&

Mentors

INDIAN INSTITUTE OF TECHNOLOGY GUWAHATI

CENTER FOR ENERGY

STATEMENT

I do hereby declare that the content embodied in this thesis entitled "**Bioethanol production from *Parthenium hysterophorus* involving cellulase from *Bacillus amyloliquefaciens* SS35: Process development, optimization and intensification"** is the result of investigations carried out by me at Center for Energy, Indian Institute of Technology Guwahati, Guwahati, India under the guidance of Prof. Arun Goyal and Prof. Vijayanand S. Moholkar.

In keeping with the general practice of reporting scientific observations, due acknowledgements have been made wherever the work described is based on the findings of other investigators.

December, 2014 *Shuchi Singh*

(Roll No.: 09615103)

INDIAN INSTITUTE OF TECHNOLOGY GUWAHATI

CENTER FOR ENERGY

CERTIFICATE

This is to certify that the work described in this thesis entitled **"Bioethanol production from *Parthenium hysterophorus* involving cellulase from *Bacillus amyloliquefaciens* SS35: Process development, optimization and intensification"** by Mrs. **Shuchi Singh (Roll No.: 09615103)** for the award of degree of Doctor of Philosophy is an authentic record of the results obtained from the research work carried out under our supervision in the Center for Energy, Indian Institute of Technology Guwahati, India and this work has not been submitted elsewhere for a degree.

Dr. Arun Goyal
(FAMI, FBRS, FABAP, FNABS, FNAAS, FIFIB)
Professor
Department of Biosciences and Bioengineering
Indian Institute of Technology Guwahati
Guwahati – 781 039
Assam, India

Dr. Vijayanand S. Moholkar
Professor
Department of Chemical Engineering
Indian Institute of Technology Guwahati
Guwahati – 781 039
Assam, India

Acknowledgements

I take utmost pleasure to express my gratitude to all who made this thesis possible. I would like to take the opportunity to express my sincere gratitude to my supervisors ***Prof. Arun Goyal*** *and* ***Prof. Vijayanand S. Moholkar****. This thesis would not have been possible without their valuable suggestions, encouragement and constant support throughout my course. I earnestly thank them for imbibing scientific temperament and appreciable work ethics in me, which helped me to achieve this goal.*

I would like to express my sincere gratitude to all my doctoral committee members ***Prof. V. K. Dubey, Dr. (Mrs.) G. K. Saini*** *and* ***Prof. T. Punniyamurthy*** *for their valuable suggestions during my seminars and progress reviews that has led to the successful completion of my thesis.*

I take the pleasure to thank the head of Center for Energy, IIT Guwahati, ***Prof. Pranab Goswami*** *for providing me with the necessary facilities. My thanks and appreciation is also due for former heads of the Centre* ***Prof. Aloke Kumar Ghoshal*** *and* ***Prof. Pinakeswar Mahanta*** *for providing the necessary facilities and always being supportive to me.*

I wish to acknowledge the supports received from earlier and present staffs of Center for Energy, ***Dr. Lepakshi Borbora****,* ***Dr. Pankaj Kalita, Mr. Dhiren Huzuri, Mrs. Archana Rajbonshi Mrs. Gitanjali Hazarika****,* ***Mrs. Bornali Malakar*** *and* ***Mr. Debarshi Baruah*** *for their cooperation.*

I am thankful to my friends at IIT Guwahati ***Nayanmoni****,* ***Dipti****,* ***Sudhanshu*** *and* ***Jeetesh*** *for making my stay comfortable and cheerful in campus. I am also thankful to* ***Adreeja Di****,* ***Deepti****,* ***Pooja****,* ***Prachi****,* ***Alpana****,* ***Asrifa****,* ***Reena*** *and* ***Kanchan*** *for always being there for me whenever I needed their support. I am immensely thankful to my seniors* ***Dr. Deepmoni Deka****,* ***Dr. Shadab Ahmed****,* ***Dr. Rishikesh Shukla****,* ***Dr. Shraddha Shukla****,* ***Dr. Swati Khanna****,* ***Dr. Amrita Ranjan****,* ***Dr. Hanif Ahmed Choudhury*** *and research group members,* ***Deeplina****,* ***Damini****,* ***Anil****,* ***Arabinda****,* ***Saprativ****,* ***Jagan****,* ***Sankar****,* ***Jaykumar****,* ***Soumyadeep****,* ***Arun****,* ***Aruna****,* ***Rwivoo****,* ***Maneesh****,* ***STP Bharadwaja****,* ***Pritam****,* ***Arup****,* ***Shyamali****,* ***Ashutosh****,* ***Ritesh****,* ***Kedar****,* ***Vicky****,* ***Sachin*** *and* ***Mayank****.*

I am thankful to ***Center for Energy****,* ***Department of Biosciences and Bioengineering****,* ***Department of Chemical Engineering*** *and* ***Central Instrument Facility (CIF)*** *for providing me facilities to carry out my research work. I am also thankful to the* ***Indian Institute of Technology Guwahati*** *for providing me with the state of the art infrastructure for advance level of research.*

*I would like to thankfully acknowledge **Mr. Suryakant Moholkar** Uncle for his blessings, encouragement and providing me a homely environment in IIT Guwahati campus.*

*No words would suffice to express my gratitude to my husband **Dharmendra Kumar Singh** whose constant love, support and understanding throughout these years inspired me the dedication to work.*

*My Ph.D. endeavor would not have been successful without the love, trust, support and blessings of my **grandparents**, **parents** and **parents-in-law**. I owe my achievements to my family. I thank my Uncles and Aunts for their constant support and blessings. I thank my sister **Dr. Ruchi Singh** and my brother-in-law **Dr. Pradeep Verma** for their immense care, encouragement and moral support in achieving this level and always standing by me in all phases of my life. I thank my brother **Vivek** especially, for encouraging me and his immense care for three initial years of my course at IIT Guwahati. I would like to also thank my sister **Sakshi** for loving me selflessly and my cousins **Aparna**, **Nikita**, **Sonali**, **Manali**, **Priyanka**, **Nitin**, **Aakash**, **Saurabh** and **Ritesh** for their love and best wishes in all stages of my life.*

December, 2014 *Shuchi Singh*

Contents

List of Tables

Chapter 6

List of Figures

Chapter 3

Abbreviations

AFEX	Ammonia fiber expansion
AMIMCl	1-allyl-3- methylimidazolium chloride
ANOVA	Analysis of variance
B. amyloliquefaciens	*Bacillus amyloliquefaciens*
BDTACl	Benzyl dimethyl (tetradecyl) ammonium chloride
BH	Bushnell Haas
BLAST	Basic local alignment search tool
BM	Biomass
BMIMCl	1-n-butyl-3-methylimidazolium chloride
Bp	Base pair
CBP	Consolidated bioprocessing
CCD	Central composite design
CMC	Carboxymethylcellulose
CMCase	Carboxymethylcellulase
CrI	Crystallinity index
DEAE	Diethylaminoethyl
DF	Degree of freedom
DOE	Design of experiments
EH	Enzymatic hydrolysis
FESEM	Field emission scanning electron microscope
FID	Flame ionization detector
FSC	Forward scatter
FTIR	Fourier transform infrared spectroscopy

GA	Genetic algorithm
GAIN	Global Agricultural Information Network
GC	Gas chromatography
GHGs	Greenhouse gases
*gyr*A	Gyrase A
HEC	Hydroxyethylcellulose
HPLC	High performance liquid chromatography
kDa	Kilo dalton
MA	Mechanical agitation
MBPCl	3-methyl-N-bytylpyridinium chloride
MMT	Million metric ton
MS	Mean of Squares
MTBE	Methyl *t*-butyl ether
MTCC	Microbial type culture collection
Mtoe	Million tons of oil equivalent
NMMO	N-methylmorpholine-N-oxide monohydrate
ODE	Ordinary differential equation
OVAT	One-variable-at-a-time
P. hyseterophorus	*Parthenium hysterophorus*
*p*NP	*p*-nitrophenol
*p*NPG	4-nitrophenyl *β*-D-glucopyranoside
PTT	Pretreatment
RI	Refractive index
*rpo*D	RNA polymerase sigma factor
rRNA	Ribosomal RNA

RSM	Response surface methodology
SDS-PAGE	Sodium dodecyl sulfate polyacrylamide gel electrophoresis
SEM	Scanning electron microscope
SHF	Separate hydrolysis and fermentation
SS	Sum of squares
SSC	Side scatter
SSCF	Simultaneous saccharification and co-fermentation
SSF	Simultaneous saccharification and fermentation
TAPPI	Technical association of pulp and paper industry
TFS	Total fermentable sugar
TRS	Total reducing sugar
US	Ultrasound
XRD	X-ray diffraction

Chapter 1

General introduction and motivation for the thesis

1.1 Prologue

The earliest reported production of biofuels was in 19th century with ethanol being produced from corn and use of peanut oil as fuel in Rudolf Diesel's first engine. However, with fast growth and development of petroleum industry after World War II, the production of biofuels did not see much research and development. However, with fast depletion of fossil fuel and also growing concerns of climate change risk and global warming due to GHGs (greenhouse gases) emissions (mainly from vehicular exhaust), last one decade has seen very rapid and marked growth in biofuels production. This growth has also been supported by ambitious government policies, especially in developing countries. The main drivers for government policies on biofuels are concerns of energy security and climate change risk, in addition to provide sustenance support to agricultural sector and rural economy. The most common measure of biofuels use adopted by many countries is the blending mandate, which essentially is the proportion of biofuel mixed with conventional transportation fuel. Such mandates are often supported by incentives in taxes and

duties. The two most common blending biofuels are bioethanol and biodiesel. Biodiesel, which essentially is alkyl ester of fatty acid, is used for blending with diesel, while ethanol is used for blending with gasoline and also as oxygenate to replace conventional MTBE (methyl *t*-butyl ether). The blending targets/mandates for these biofuels in numerous developing/developed economies are given in Table 1.1.

According to International Energy Agency report (2011) the global biofuels production has risen thus, more than 5-fold from 16 billion liters in 2000 to more than 100 billion liters in 2010. The next three years have seen more than 15% growth in global biofuel production, with the total production standing at 116.6 billion liters in 2013. Out of these, the major fractions were: bioethanol - 87.2 billion liters and biodiesel - 26.3 billion liters. Global ethanol production has been dominated by United States and Brazil, which account for more than 87% of the total global production. The contribution of US to total ethanol production was 50 billion liters, while Brazil contributed 25.5 billion liters. Most of the ethanol produced in USA was derived from corn, while major feedstock for the same in Brazil was sugarcane. The major contributors to ethanol production are China and Canada with 2 billion liters and 1.8 billion liters production in 2013. As far as biodiesel is concerned, European Union is the major producer with 10.5 billion liters, followed by USA with 5.1 billion liters. The next three largest biodiesel producers in world are: Germany = 3.1 billion liters, Brazil = 2.9 billion liters and Argentina = 2.3 billion liters.

Table 1.1 Biofuel blending targets and mandates in various countries (Adopted from International Energy Agency report 2011).

Country	Current mandate/target (%, v/v)		Future mandate/target (%, v/v)	
	Ethanol	Biodiesel	Ethanol	Biodiesel
Argentina	5	7	N. A.	N. A.
Australia	4	2	6 (2011)	5 (2012)
Bolivia	10	2.5	N. A.	20 (2015)
Brazil	20-25	5	N. A.	N. A.
Canada	5	2-3	N. A.	2 (2012)
Chile	5	5	N. A.	N. A.
China	10		N. A.	N. A.
Colombia	10	10	N. A.	20
Costa Rica	7	20	N. A.	N. A.
Dominican Republic	N. A.	N. A.	15 (2015)	2 (2015)
European Union	5.75% biofuels		10% renewable energy in transport	
India	5	N. A.	20 (2017)	20 (2017)
Indonesia	3	2.5	5 (2015), 15 (2025)	5 (2015), 20 (2025)
Jamaica	10	N. A.	Renewable energy in transport: 11% (2012), 12.5% (2015), 20% (2030)	
Japan	500 Ml/y (oil equivalent)		800 Ml/y (2018)	
Kenya	10 (in Kisumu)		N. A.	
Korea	N. A.	2	2.5 (2011)	3 (2012)
Malaysia	N. A.	5	N. A.	
Mexico	2	N. A.	2 (2012)	N. A.
Mozambique	N. A.		10 (2015)	5 (2015)
Norway	3.5% biofuels		5% proposed for 2011	
Nigeria	10	N. A.	N. A.	N. A.
Paraguay	24	1	N. A.	N. A.
Peru	7.8	2	N. A.	5 (2011)
Philippines	5	2	10 (2012)	5 (2011)
South Africa	N. A.		2 (2013)	
Taiwan	3	2	N. A.	N. A.
Thailand	N. A.	3	3 Ml/d ethanol (2011), 9 Ml/d ethanol (2017)	5 (2011)
Uruguay	2	N. A.	5 (2015)	5 (2012)
United States	48 billion litres of which 0.02 billion litres cellulosic-ethanol		136 billion litres, of which 60 billion litres cellulosic-ethanol (2022)	
Venezuela	10	N. A.	N. A.	
Vietnam	N. A.		50 Ml biodiesel, 500 Ml ethanol (2020)	
Zambia	N. A.	N. A.	5 (2011)	10 (2011)

N. A., Not available

Conventional biofuels such as sugar or starch based ethanol or biodiesel produced via trans-esterification of vegetable oils such as soybean, palm and sunflower do not have attractive economics due to high cost of substrate. In developing countries like India facing severe food/fodder shortage, the food versus fuel crisis renders use of substrate used in USA and Latin American countries unviable. Research and development in advanced biofuels is necessary for large scale implementation of biofuels in these countries. These biofuels are derived from non-conventional substrates which are far cheaper and abundantly available. These substrates are essentially lignocellulosic biomass comprising of waste biomass, agricultural and forest residues.

According to the Global Agricultural Information Network (GAIN) report (2014), despite significant development of non-conventional energy sources in India in past few years, the conventional sources of coal and oil still fulfill about 2/3rd of the total energy consumption. The share of renewables such as wind, geothermal, solar, hydroelectricity and waste accounts for more than 25%, while, natural gas accounts for 7% share. The nuclear power has a minor share of just 1%. The total energy production in India as reported in Key World Energy Statistics (2014) was 544.55 million tons of oil equivalent (Mtoe), while the net import stood at 243.22 Mtoe. Thus, the total primary energy supply was 788 Mtoe. However, this supply is far too small to cater the needs of 1.236 billion population. The per capita primary energy consumption in India was meager 0.64 Mtoe. The complete statistics of the energy indicators for India are given in Table 1.2.

Table 1.2 The complete statistics of the energy indicators for India (adopted from Key World Energy Statistics 2014).

Energy indicators	Data
Population (million)	1236.69
GDP (billion 2005 USD)	1389.05
GDP PPP (billion 2005 USD)	5567.13
Energy production (Mtoe)	544.55
Net imports (Mtoe)	243.22
TPES (Mtoe)	788.13
Elect. Cons. (TWH)	939.78
CO_2 emissions (Mt of CO_2)	1954.02
TPES/pop. (toe/capita)	0.64
TPES/GDP (toe/000 2005 USD)	0.57
TPES/GDP (PPP) (toe/000 2005 USD)	0.14
Elect. Cons./pop. (kWh/capita)	760
CO_2/TPES (t CO_2/toe)	2.48
CO_2/TPES (t CO_2/capita)	1.58
CO_2/GDP (kg CO_2/2005 USD)	1.41
CO_2/GDP (PPP) (kg CO_2/2005 USD)	0.35

GDP, Gross domestic product; PPP, purchase power parity

Out of all sectors with energy demands, the transport sector stands first. According to GAIN report (2014), the population of total registered motor vehicles in India was 142 million at the end of financial year 2010-11. The approximate distribution of these vehicles was $3/4^{th}$ -two wheelers (motor bikes and scooters), $1/8^{th}$ personal cars and taxies and $1/8^{th}$ - buses and trucks. The vehicle ownership is expected grow significantly over next few years due to rising urbanization, continued economic growth, rising consumer spending and fast development of road infrastructure. It is expected that total vehicle registration in India would cross 190 million at the end of 2014. Unfortunately, the native production of crude oil and natural gas in India has not risen proportionately. The crude oil production in 2007-08 in India was 34.12 MMT, which has shown just 10% increase to 37.79 MMT in 2013-14 as mentioned in Indian Petroleum and Natural Gas Statistics (2014).

Similarly, the natural gas production has also shown highly insignificant growth from 32.42 MMT in 2007-08 to 35.41 MMT in 2013-14. On the other hand, the crude oil import has shown a staggering rise from 121.67 MMT in 2007-08 to 189.24 MMT in 2013-14. Due to high rise in international crude oil prices, the value of crude oil import has risen more than 3-fold from Rs. 2.726 trillion in 2007-08 to Rs. 8.648 trillion in 2013-14. The load on road traffic in India is growing at 9% annually. At present the road infrastructure handles 60% of goods transport and ≥ 85% of total passenger traffic. A significant part of northern and northeastern part of India is covered with hilly terrains, where building of railway infrastructure is extremely difficult. The major means of both passengers and goods transport in these states/regions is by road. Estimated petrol consumption in India in 2013 was 16 million tons, while diesel consumption was 69 million tons. The trends in fuel consumption in India are given in Table 1.3.

The oil import bill is a huge burden and potential threat to economy as well as energy security of India. In order to reduce dependence on oil import, at the same time efficiently catering to the energy needs of India, the government of India has been promoting production and blending of ethanol derived from sugar molasses with gasoline and biodiesel derived from non-edible and waste oils for blending with diesel. The program of ethanol blended petrol launched by Ministry of Petroleum and Natural Gas launched in 2003 could not achieve much success. However, sugarcane production fell drastically during 2003-2004 and 2004-2005. In November 2006, petroleum companies in India entered an agreement for procurement of over 1.4 billion liters of ethanol over a period of 3 years at an MSP of Rs. 21.5 per liter.

However, only 1/3rd ethanol of this agreement could actually be supplied to petroleum industries. The major reasons which contributed to this debacle were fluctuating availability of sugar molasses and sugarcane juice for ethanol production. Low availability of the sugar molasses coupled with rising price of molasses affected cost of ethanol production but also significant loss to sugar industry as the MSP of Rs. 26.5 per liter was much lesser than actual production cost. The current statistics of ethanol in India are given in Table 1.3.

Table 1.3 Ethanol used as fuel and other industrial chemicals (million liters) in India (adopted from GAIN report 2014).

Calendar year	2006	2007	2008	2009	2010	2011	2012	2013	2014	2015*
Beginning stocks	483	734	1374	1642	1240	1021	627	624	689	380
Production	1898	2398	2150	1073	1522	1681	2154	2057	2036	2099
Imports	30	15	70	320	92	39	34	34	50	100
Exports	37	23	12	14	53	119	177	234	175	50
Consumption	1640	1750	1940	1780	1780	1995	2015	1792	2220	2280
Fuel consumption	200	200	280	100	50	365	305	182	550	700
Ending stocks	734	1374	1642	1240	1021	627	624	689	380	249
Production capacity										
No. of refineries	115	115	115	115	115	115	115	115	115	115
Nameplate capacity	1500	1500	1500	1500	1500	1500	2000	2000	2000	2000
Capacity use (%)	127	160	143	72	101	112	108	103	102	105
Feedstock use (1,000 MT)										
Molasses	7910	9992	8958	4469	6342	7004	8975	8573	8481	8746
Market penetration										
Fuel ethanol	200	200	280	100	50	365	305	182	550	700
Gasoline	12761	14189	15368	17606	19563	20716	21842	23749	25957	28371
Blend rate (%)	1.6	1.4	1.8	0.6	0.3	1.8	1.4	0.8	2.1	2.5

Source: FAS/New Delhi Estimates based on information from trade sources
**: Forecast*

As per the GAIN report (2014) on biofuels in India, as of 2013, there are more than 330 ethanol distilleries in India, with total combined annual production capacity of over 4 billion liters of rectified spirit (alcohol) and 1.5 billion liters of fuel ethanol. The distilling capacity of about 143 distilleries is over 2 billion liters of conventional ethanol. This capacity is sufficient to meet around 7% blending target. However, the actual blending target achieved is much lower. As per GAIN report (2014), the sugar mills (which are main ethanol producers from molasses) offered 671 million liters of ethanol, when the oil marketing companies have committed to procure only 305 million liters. With carry forward of balance ethanol, in addition to increased production of another 50 million liters by December 2014, the total cumulative procurement of ethanol by oil marketing companies is estimated at 555 million liters, with which 2.5% blending target could be achieved.

Main substrate for production of ethanol in India is sugar molasses, which is a byproduct of sugar industry. Thus, availability of sugar molasses is a major factor in sustained ethanol production. The sugarcane itself is a cyclical crop in India and the optimum sugar supply levels do not always correspond with demand. Therefore, the production of sugar by the sugar mills and hence that of ethanol as well, is not uniform. The obvious consequences of this are large variations in availability of sugar molasses and high molasses prices, which ultimately affect production cost of ethanol. In many instances, the production cost of ethanol significantly exceeds the pre-negotiated fixed price and the ethanol supply to oil marketing companies is disrupted. In view of this, in the calendar year 2014, the oil marketing companies have revised the formula for fixing the benchmark price for ethanol procurement.

The proposed formula will be based on the average of refinery transfer price and cost of petrol to the oil marketing companies for the previous financial year. At present, the ceiling price of Rs. 44 per liter for ethanol is still attractive for some suppliers or sugar mills, but the average retail price of gasoline is still on higher side. With the new formula, the benchmark price will rise, which will be an incentive for stakeholders, *viz*. sugar mills and oil marketing companies. A better option will be to give flexibility to sugar mills to market cane juice for any purpose (crystallize sugar or produce alcohol) that fetches higher revenue. Another obvious option is to have government support to ethanol producers through subsidized loans, concession in taxes, levies and duties, easy export permits and no-objection certificates. Cultivation of special alternate crops with high carbohydrate content such as sweet sorghum, sugar beet, sweet potatoes, pearl millet etc. to provide sustained supply of fermentation substrate for bioethanol production is also a solution that could be assessed with partnership from private institutions/organizations.

A potential solution to boost the ethanol production on sustainable basis is to disengage it from sugar industry. This essentially points to the second generation bioethanol production from lignocellulosic biomass abundantly available in the form of agricultural and forest residues. As per the Biomass Atlas statistics (IISc Bangalore), an estimated surplus of 250 MMTPA of lignocellulosic biomass is produced in India (after fulfilling all conventional uses like cattle feed, domestic fuel etc.). This biomass could form potential feedstock for bioethanol production. This new and alternate feedstock for bioethanol has dual merit of far cheaper price than molasses (or grains, in some cases) and abundant availability throughout the year in

all Indian states. Due to this feature, the cost of production of ethanol with lignocellulosic substrate is expected to be much lower than the molasses based ethanol.

Before the new technology for ethanol production from lignocellulosic biomass is implemented commercially, significant research and development is required to meet the set of challenges and opportunities associated with it. It is in this spirit that the current thesis work is planned and implemented. The present thesis has attempted to develop, optimize and intensify a laboratory scale process for bioethanol production from waste biomass of *Parthenium hysterophorus*. All aspects of the process, starting from acid pretreatment, alkaline delignification, enzymatic hydrolysis and fermentation of both pentose (acid) and hexose (enzyme) hydrolyzate have been addressed in stepwise manner. Thus, this thesis can also be looked at as a laboratory scale technology package for bioethanol production from *Parthenium hysterophorus*. *P. hysterophorus* is a noxious weed found abundantly in India. This weed has not only destroyed arable land causing loss of billions of rupees, but has also posed potential health hazard to humans and animals. The process developed in this thesis thus also provides solution to a potential environmental problem.

1.2 Aim and scope of present thesis

Investigations in this thesis are focused on cellulase production from natural isolate *Bacillus amyloliquefaciens* SS35, pretreatment of *P. hysterophorus* biomass, enzymatic hydrolysis of pretreated *P. hysterophorus* utilizing cellulase from *B. amyloliquefaciens* SS35 and eventually bioethanol production by SHF and SSF

processes. In addition, intensification of various processes involved in above mentioned steps have also been done by applying ultrasound. The work in the thesis has been presented by the following chapters:

Chapter 2 is a comprehensive review of literature focused on bioethanol production from lignocellulosic biomass. This chapter involves the review of the studies considering following major aspects of cellulosic ethanol production:

(a) *Enzymatic hydrolysis of cellulosic biomass*: The main components of the enzymatic hydrolysis of lignocellulosic biomass are the cellulase and pretreated biomass (rich in cellulose). Also the economy of ethanol production depends more on the potential of these two components. Therefore, in foremost part of the chapter the focus was on the review of the reports on natural sources and efficient production of cellulase, followed by purification, characterization and major applications of the enzyme.

(b) *Pretreatment of lignocellulosic biomass*: The subsequent focus of the chapter was on the review of the reports on various types of lignocellulosic feedstock and the methods of pretreatment/delignification of the biomass.

(c) *Fermentation for ethanol production*: The chapter was preceded with the review of the literature on the various attributes on the different modes of ethanol fermentation.

(d) *Intensification of the bioprocesses by ultrasound*: Since the present thesis focused equally on the intensification of the processes involved in bioethanol production, a major part of this chapter included the review of the investigations in the area of ultrasound-assisted enzymatic hydrolysis and fermentation. The

chapter also included the review of the reports on mechanistic investigations of the effect of sonication on various bioprocesses using various mathematical models.

Chapter 3 deals with the isolation, screening, identification and characterization of cellulolytic bacteria from rhinoceros dung. The isolate, exhibiting maximum CMCase activity, was identified as *Bacillus amyloliquefaciens* SS35 by morphological, biochemical and phylogenetic analyses.

Chapter 4 describes the statistical optimization of CMCase production from *B. amyloliquefaciens* SS35. The statistical experimental designs were applied in two steps *viz*. medium optimization and optimization of fermentation parameters. Plackett-Burman design followed by Central Composite Design (CCD) was used for medium optimization, while for optimization of fermentation parameters one-variable-at-a-time method followed by central composite design was used.

Chapter 5 deals with the purification and characterization of CMCase from *B. amyloliquefaciens* SS35. Purification was done by ammonium sulphate fractionation method and anion exchange chromatography using DEAE-Sepharose. Molecular weight of the enzyme was determined by SDS-PAGE and zymogram analysis. Effects of physical parameters and additives on enzyme activity and stability were also investigated.

Chapter 6 describes the comparative assessment of pretreatment strategies and optimization of ultrasound-assisted alkaline delignification for *P. hysterophorus* biomass. Various physical, chemical and physicochemical methods have been employed for the pretreatment with aim of exposure of cellulose moieties in biomass

for enzymatic action during hydrolysis. In addition, the mechanistic insight into ultrasound assisted delignification of *P. hysterophorus* biomass has also been attempted in this chapter.

Chapter 7 deals with the investigations on separate enzymatic hydrolysis of *P. hysterophorus* biomass and subsequent fermentation of hydrolysate. The optimization of hydrolysis process was carried out by response surface methodology (RSM). The efficiency (in terms of yield and kinetics) of conventional hydrolysis and fermentation processes was improved by employing intermittent ultrasonic irradiation. The influence of ultrasound on rate of hydrolysis was investigated by fitting the data to Michaelis-Menten kinetic model. The effect of sonication on fermentation parameters was investigated by fitting the experimental data to a mathematical model.

Chapter 8 deals with the simultaneous saccharification and fermentation (SSF) of pretreated and delignified *P. hysterophorus* biomass. The effect of ultrasonic irradiation on SSF process was also investigated by fitting the experimental data to the saccharification/ fermentation model.

Chapter 9 represents the summary of results and overall conclusion of the thesis. Some suggestions have been made for taking the thesis work ahead.

References

Biomass Resource Atlas of India, Indian Institute of Science Bangalore, India.

Global Agricultural Information Network (GAIN) report (2014), number: IN4055.

Indian Petroleum and Natural Gas Statistics (2014) Government of India, Ministry of Petroleum and Natural Gas Economics and Statistics Division, New Delhi.

Key World Energy Statistics (2014) International Energy Agency, Paris, France.

Technology Road Map: Biofuels for Transport (2011) IEA Renewable Energy Division, International Energy Agency, Paris, France.

Chapter 2

Literature survey on lignocellulosic wastes to ethanol: process development, optimization and intensification

2.1 Introduction

World is currently facing the major problem of fossil fuel depletion, at the same time energy consumption has risen at faster rates. One viable solution to this problem is the development and implementation of technologies based on alternative sources of energy. Many countries have implemented or are implementing policies for addition of ethanol to gasoline as described previously in chapter 1. This has made ethanol a most employed liquid biofuel either as a fuel or as a gasoline enhancer (Sanchez and Cardona 2008). In this chapter an attempt has been made to present an overview of the research activities in the area of bioethanol production from lignocellulosic biomass. The review focused on the development and optimization and intensification of various processes involved in synthesis of bioethanol. The successive steps which has been reviewed extensively in this chapter, are: (1) isolation and identification of cellulase producing bacteria (2) purification and properties of cellulase enzymes (3) optimization of cellulase production by statistical methods (4) screening of lignocellulosic biomass as feedstock for ethanol

production (5) pretreatment of lignocellulosic biomass prior to enzymatic hydrolysis (6) enzymatic hydrolysis of pretreated lignocellulosic biomass (7) fermentation of enzymatic hydrolysate for ethanol production (8) ultrasound and its application in intensification of the bioprocesses.

2.2 Cellulose hydrolysing enzymes (cellulases)

Cellulose is a most abundant polymer on earth and exists exclusively as a major structural component of plant cell wall entangled with hemicellulose and lignin. The cellulose content in plant biomasses and plant fibres is in a range of approximately 35-70% of dry weight (Wiselogel *et al.* 1996, Lynd *et al.* 1999, Mather and Wardman 2011). However, some natural substances contain almost 90% cellulose on dry weight basis, for example cotton fibres (Lewin and Pearce, 1998). Hemicellulose and lignin content in plant biomass is about 20-50% and 10-30%, respectively (Wiselogel *et al.* 1996, Jorgensen *et al.* 2007). Cellulose polymer consists of a linear chain of glucose units linked by β-1,4-glycosidic linkages. Approximately, 10,000-15,000 glucose units form one cellulose molecule and 30 cellulose molecules assemble into elementary fibrils, which are linked together by extensive intra- or inter chain hydrogen bonding interactions to form larger unit called microfibrils. About 250 microfibrils assemble to form cellulose fiber (Krassig 1992). The variation in the form of crystalline and amorphous cellulose depends on the extent of hydrogen bonding, degree of polymerization of microfibrils and source of cellulose (Bayer *et al.* 2006). Thus, the abundance of cellulose content in plant biomass revealed that it has great potential for fuel ethanol production by means of

hydrolysis and fermentation. Since, the composition of the biomass and crystallinity of cellulose varies across plant taxa, various lignocellulosic biomasses can be processed by appropriate physical, chemical or biological methods for removal of hemicellulose and lignin fractions leaving behind the cellulose. Cellulose can be hydrolyzed to fermentable sugar i.e. glucose by acid or enzymatic treatment. The group of enzymes used for cellulose hydrolysis are, endoglucanase (1,4-*β*-D-glucan-4-glucanohydrolase; carboxymethylcellulase, generally known as cellulase) (EC 3.2.1.4), exocellobiohydrolase (1,4-*β*-D-glucan glucohydrolase; avicelase) (EC 3.2.1.91) and *β*-glucosidase (*β*-D-glucoside glucohydrolase, cellobiase) (EC 3.2.1.21), which act synergistically on cellulose polymer to form cellobiose and eventually glucose (Bayer *et al.* 1998). A comparison of acid and enzymatic hydrolysis has been summarized in Table 2.1.

Table 2.1 Comparison of acid and enzymatic hydrolysis of lignocellulosic biomass.

Characteristic	Acid hydrolysis	Enzymatic hydrolysis	Reference
Detoxification of hydrolysate prior to fermentation	Yes	No	Talebnia and Taherzadeh 2006
Time of treatment	Less	More	Taherzadeh and Karimi 2007
Neutralization of hydrolysate prior to fermentation	Yes	No	Chandel *et al.* 2007
Yield of hydrolysis	Low	High	Taherzadeh and Karimi 2007
Cost of catalyst	Low	High	Taherzadeh and Karimi 2007
Treatment conditions	Harsh	Mild	Taherzadeh and Karimi 2007
Utility cost	High	Low	Kuhad *et al.* 2011
Requirement of corrosion resistant vessel	Yes	No	Chen 2014

Use of acid for hydrolysing cellulose has several disadvantages, thus in this study the enzymatic hydrolysis mode was selected and in view of the focus of the

study was towards cellulase production from a natural isolate and application in hydrolysis of lignocellulosic biomass. Since the efficiency and properties of enzyme also play an important role in enzymatic hydrolysis, the source of isolation of cellulase producing bacteria was selected as dung of one horned Indian rhinoceros of Kaziranga National Park, Assam, India. The rhinoceros dung was selected as the source of cellulolytic bacteria assuming the rhinoceros's potent mechanism towards the digestion of its main food elephant grass at Kaziranga National Park.

2.2.1 Cellulase from microbial sources

Cellulase has been produced by a number of microorganisms, mainly from fungi and bacteria which have diverse characteristics based on their source of isolation. The cellulase producers most studied in past are aerobic thermophilic fungi, *Aspergillus terreus* (Vyas *et al.* 2005, Gao *et al.* 2008, Narra *et al.* 2012, Sharma *et al.* 2014), aerobic mesophilic fungi, *Trichoderma reesie* (Singhania *et al.* 2007, Deshpande *et al.* 2008, Ahamed and Vermette 2009, Jourdier *et al.* 2012, Onofre *et al.* 2014), *T. viride* (Vintila *et al.* 2010, Jiang *et al.* 2011, Irfan *et al.* 2012, Zhao *et al.* 2013, Nathan *et al.* 2014) and very few anaerobic mesophilic fungi, *Neocallimastix patriciarum* (Wang *et al.* 2011, Wang *et al.* 2014). In case of bacteria, anaerobic thermophiles, *Acetivibrio cellulolyticus* (Xu *et al.* 2003, Jindou *et al.* 2006, Hamberg *et al.* 2014), *Bacteroides* sp. (Xu *et al.* 2004) and *Clostridium thermocellum* (Dumitrache *et al.* 2013, Akinosho *et al.* 2014) and aerobic mesophiles, *Bacillus* sp. (Lee *et al.* 2008, Kim *et al.* 2009, Rastogi *et al.* 2010, Trivedi *et al.* 2011, Lin *et al.* 2012, Deka *et al.* 2013a, Dias *et al.* 2014) have been explored extensively. Few

actinomycetes have also emerged as potent cellulase producers, for example *Streptomyces* sp. (Jaradat *et al.* 2008, Hsu *et al.* 2011, Azzeddine *et al.* 2013, Yassien *et al.* 2014).

The isolation of cellulase producing bacteria from diverse habitat has been a highly active research area, because bacteria have a faster growth rate than fungi, leading to greater enzyme productivity (Lynd *et al.* 2002). Also, the recalcitrance of fungi and few anaerobic bacteria such as Clostridia towards genetic manipulation (Maki *et al.* 2009) has promoted the preference of aerobic bacteria for example Bacilli over these organisms. In this study the cellulolytic bacterium was isolated from rhinoceros dung assuming its potential towards efficient cellulose hydrolysis, enzyme activity at relatively low pH of gut (≤ 6.0) and mesophilic nature. A mesophilic bacterium producing cellulase with acidic pH optima may be useful in the advanced strategies of ethanol fermentation *viz*., simultaneous saccharification and fermentation (SSF) and consolidated bioprocessing (CBP). In these modes of fermentation either enzyme is being used with the ethanol fermenting organism or enzyme producing microorganism after genetic modification can be involved in ethanol production. Therefore, the physical conditions of enzyme action and the growth/survival of organism used for ethanol fermentation should be possible under similar conditions. Since, most of the ethanol fermenting organisms either yeast or bacteria are mesophilic and acidophilic in nature, the focus of present study was towards these aspects.

2.2.2 Cellulase producing bacteria in nature: isolation, screening and identification strategies

Isolation of cellulose hydrolysing bacteria from natural sources has been practiced by selective enrichment method using soluble cellulose (carboxymethylcellulose) as sole substrate. Plate screening method is a popular technique for selecting cellulolytic bacteria in which a minimal medium agar plate supplemented with carboxymethylcellulose is being used. The staining of culture plate is being done either by Congo red (Teather and Wood, 1982) or Gram's iodine solution (Kasana *et al.* 2008). The cellulase production efficiency of the isolates was compared on the basis of colony to clear zone ratio. This technique was not considered efficient later on because of poor correlation between enzyme activity and size of clear zone (Maki *et al.* 2009) and was limited to only preliminary or qualitative screening of cellulolytic bacteria. Determination of cellulase activity by growing the isolates in liquid medium was therefore a preferred method for screening the cellulolytic bacteria. Another advanced method of quantitative screening with higher sensitivity is use of florescent-labeled short polysaccharides (Ivanen *et al.* 2009), however, the major limitation of using florescent substrate in agar plates is the tendency of hydrolysis products to diffuse widely (Maki *et al.* 2009).

Among several cellulolytic bacteria *Bacillus* spp. are most preferred because of their diverse range of cellulases stable at extreme environments (Singh *et al.* 2001, Ariffin *et al.* 2006, Immanuel 2006, Lee *et al.* 2008, Kim *et al.* 2009, Rastogi *et al.* 2010, Trivedi *et al.* 2011, Vijayaraghavan and Vincent 2012, Akhtar *et al.* 2013, Sethi *et al.* 2013, Dias *et al.* 2014, Patagundi *et al.* 2014). The identification of

natural isolates can be done by various biochemical methods but the accuracy of these methods is limited only up to 'Genus' level. Another approach for complete identification of microorganism is its phylogenetic analysis. Currently, the phylogenetic analysis based on 16S rRNA gene sequences is most popular method for bacterial classification, but it often limited for members of closely related taxa (Fox *et al.* 1992) for example *Bacillus* spp. 16S rRNA gene sequences of these organisms are almost 99.2-99.6% similar (Ash *et al.* 1991, Nakamura *et al.* 1999) making their identification difficult. Alternatively, results from several studies (Mollet *et al.* 1997, Kim *et al.* 1999, Yamamoto *et al.* 1999, Chun and Bae 2000) report that protein coding genes exhibit much higher genetic variation, which can be used for classification and identification of closely related taxa.

2.2.3 Optimization of cellulase production

The enzyme production by a microbial strain depends on the medium components and fermentation parameters. The major medium components are carbon and nitrogen which influence the cellulase production significantly, on the other hand, fermentation parameters such as incubation temperature, medium pH, shaking speed and inoculum size also paly important role in enzyme production. The optimization of these parameters has been done by one-variable-at a-time (OVAT) approach by several researchers (Singh *et al.* 2001, Ariffin *et al.* 2008, Lee *et al.* 2008, Lee *et al.* 2010, Shabeb *et al.* 2010, Sethi *et al.* 2013, Sadhu *et al.* 2014). In this method the effect of one parameter is being investigated on enzyme production keeping other parameters constant. However, OVAT approach has limitation of not

identifying the interactive effects of the parameters and thus the erroneous optimum values (Vishwanatha *et al.* 2010). This problem can be resolved by using statistical methods of optimization. Response surface methodology (RSM) is a most popular technique used for optimizations, which is based on the fitting of a polynomial equation to experimental data and describing the behavior of the data set with statistical predictions (Box and Wilson 1951). Prior to response surface optimization the initial screening of parameters is necessary to screen the variables influencing significantly the process, which can be done by using two level fractional factorial design developed by Plackett and Burman (1946), based on the first order polynomial model. Finally to identify optimum values the experimental designs for quadratic response surfaces have been used, such as three level factorial central composite design (Deka *et al.* 2011, Vasudeo and Lew 2011, Deka *et al.* 2013b, Singh *et al.* 2014a, Singh *et al.* 2014b).

Several studies in literature reported the optimization of medium components mainly carbon and nitrogen sources. Singh *et al.* (2001) screened various carbon and nitrogen sources for *Bacillus* sp. VG1 and observed that carboxymethylcellulose (CMC) (10 g/L) and tryptone (5 g/L) enhanced the carboxymethylcellulase (CMCase) activity maximally by 72% and 91%, respectively. Another study by Ariffin *et al.* (2008) reported that the maximum cellulase activity from *Bacillus pumilus* EB3 was achieved at the optimum concentrations of CMC (10 g/L), yeast extract (2.5 g/L) and ammonium sulphate (2.5 g/L). A marine isolate *Bacillus subtilis* subsp. *subtilis* A-53 exhibited maximum cellulase activity at the concentrations of 20 g/L of rice bran and 2.5 g/L of yeast extract (Lee *et al.* 2010). Optimum

concentrations of CMC, yeast extract and peptone for *Bacillus subtilis* AS3 were obtained as 18, 4.79 and 8 g/L, respectively (Deka *et al.* 2011). In a study by Sethi *et al.* (2013) it was found that the optimum concentration of glucose and ammonium sulphate were 50 and 5 g/L for a *Bacillus subtilis* strain isolated from soil. Singh and co-workers (2014b) in their study with *Bacillus* VITRKHB replaced the carbon source CMC with xylose and observed maximum cellulase production for the concentrations of 50 and 69 g/L for xylose and beef extract, respectively.

Optimization of fermentation parameters of a process is an equally important step as optimization of medium components. Fermentation parameters or culture conditions include incubation temperature, medium pH and shaking speed or agitation. Cellulase production from *Bacillus* spp. covers a wide range of optimal temperature and medium pH which is reflected from the results of few leading reports in literature. Immanuel *et al.* (2006) in their study with *Bacillus* sp. isolated from coir retting effluents found that the strain produced maximum cellulase at 40^{o}C and pH 7.0. In another study, the optimum values of temperature and pH for cellulase production by *B. amyloliquefaciens* UMAS1002 were 40^{o}C and 7.0 (Khan and Hussaini 2006). *B. amyloliquefaciens* DL3 exhibited maximum activity at 37^{o}C and pH 6.8 (Lee *et al.* 2008). On the other hand, *B. amyloliquefaciens* UNPDV-22 isolated from hot spring showed enhanced cellulase activity at 42.24^{o}C and pH 5.25 (Vasudeo and Lew 2011). Deka *et al.* (2013a) observed the optimal conditions for cellulase production by *B. subtilis* AS3 to be 39^{o}C and pH 7.2. However, another *B. subtilis* strain isolated from soil showed 40^{o}C and medium pH 10.0 as optimal for cellulase production (Sethi *et al.* 2013).

Shaking speed or agitation is other important culture parameter which is related to the maintenance of homogeneity in fermentation broth, dispersion of dissolved oxygen into smaller bubbles thereby increasing the interfacial area and oxygen mass transfer rate resulting to the enhancement of both substrate utilization and microbial activity (Singh *et al.* 2000). However, greater agitation speed may attribute to increased shear stress on the cells leading to reduced enzyme production (Purkarthofer *et al.* 1993). *Bacillus amyloliquefaciens* UMAS 1002 showed a 2 fold enhancement in cellulase activity under shaking at a rate of 100 rpm (Khan and Hussaini 2006). Trivedi *et al.* (2011) reported agitation speed of 120 rpm as optimum for cellulase production by *Bacillus flexus* isolated from green sea weed *Ulva lactuca*. Optimum shaking speed for *B. subtilis* AS3 was found to be 121 rpm in shake flask level cellulase production (Deka *et al.* 2013b). In the present study shaking speed optimization for cellulase production from *B. amyloliquefaciens* SS35 also resulted in similar observation with a value of 120 rpm (Singh *et al.* 2014a).

2.2.4 Purification, characterization and application of cellulase

2.2.4.1 Methods of purification

Cellulase has been purified by employing various steps such as fractionation by ammonium sulphate, solvent extraction by acetone or ethanol, ultrafiltration and chromatography. In case of purification of extracellular cellulase, the cell-free supernatant has been concentrated by using salting out (Lee *et al.* 2008, Kim *et al.* 2009, Sadhu *et al.* 2013, Deka *et al.* 2013a), solvent extraction (Mawadza *et al.* 2000) or ultrafiltration (Knutsen and Davis 2004) method and this concentrated

protein mixture is further processed for purification of desired enzyme either by ion-exchange or gel filtration or by both employed stepwise. For purification of cellulase generally DEAE-cellulose (Bajaj *et al.* 2009, Vijayaraghavan and Vincent 2012), DEAE-sepharose (Trivedi *et al.* 2011, Sadhu *et al.* 2013, Deka *et al.* 2013a, Singh *et al.* 2014c) have been used as matrix. However, for cellulase purification by hydrophobic interaction chromatography, HiTrap™ Q column has been preferred (Lee *et al.* 2008, Kim *et al.* 2009). Gel filtration using sephadex (Vijayaraghavan and Vincent 2012), sephacryl (Sadhu *et al.* 2013), DEAE-sephadex (Singh *et al.* 2001, Trivedi *et al.* 2011) have also been used. Singh *et al.* (2001) reported purification of cellulase from *Bacillus* sp. VG1 by ammonium sulphate fractionation (40-80% saturation) followed by two-step gel filtration chromatography using DEAE Sephadex A-50 and Sephadex G-75. Lee *et al.* (2008) and Kim *et al.* (2009) carried out a three step purification employing ammonium sulphate precipitation, HiTrap Q and two cycles of ion exchange chromatography with Mono Q HR column. Deka *et al.* (2013a) in their study used ammonium sulphate precipitation (0-80% saturation) of cell-free supernatant of *B. subtilis* AS3, followed by ion-exchange chromatography using DEAE-sepharose.

2.2.4.2 Characterization of cellulase

2.2.4.2.1 Effect of temperature and pH on cellulase activity and stability

Literature available on cellulase from naturally isolated *Bacillus* spp. indicated that cellulase activity and stability varied in a wide range of temperature (40-75^{o}C) and pH (4.0-10.0), this is considered to be a common characteristic of cellulase from

Bacillus spp. Bajaj *et al.* (2009) reported that cellulase produced by *Bacillus* sp. M-9 showed maximal CMCase activity at 60^{o}C and pH 5.0. However, enzyme was stable at 50-70^{o}C for 1 h and retained more than 60% residual CMCase activity at pH 4.0-6.0 for 1 h. Cellulase from *Bacillus* sp. DUSELR13 exhibited maximum activity at 75^{o}C and pH 5.0 and it was a thermostable enzyme with 78% residual activity at 70^{o}C for 1 day (Rastogi *et al.* 2010). On the other hand, cellulase from *B. flexus* NT, isolated from a sea weed showed maximal activity at 45^{o}C and pH 10.0 and stability studies revealed that the enzyme was stable at 15-20^{o}C and pH 9.0-11.0 with more than 60% residual activity for 30 min (Trivedi *et al.* 2011). Another report by Lin *et al.* (2012) has revealed that cellulase from *B. thuringiensis* had an optimum activity at 40^{o}C and pH 4.0 and at 40-60^{o}C enzyme retained 50% of its initial activity for 1 h. CMCase from *B. subtilis* AS3 showed maximal activity at 45^{o}C and pH 9.2, however, enzyme was stable in a range of temperature 30-50^{o}C and pH 12.0 for 1 h with more than 60% residual activity (Deka *et al.* 2013a). Cellulase from another strain of *B. subtilis* SU40 isolated from soil exhibited maximum activity at pH 8.0 and 45^{o}C (Asha and Sakthivel 2014).

2.2.4.2.2 Effect of metal ions on cellulase activity

The effect of most commonly used metal ions Co^{2+}, Ca^{2+}, K^{+}, Na^{+} and Mn^{2+} Zn^{2+}, Fe^{3+} and Hg^{2+}, have been investigated on cellulases of different origins. Generally, Co^{2+}, Ca^{2+}, K^{+}, Na^{+} and Mn^{2+} ions enhance the cellulase activity and Zn^{2+}, Fe^{3+} and Hg^{2+} inhibit the activity. However, these trends may vary for the cellulase from different source. For example, CMCase from *Bacillus* sp. VG1 (Singh *et al.*

2001) and *B. flexus* NT (Trivedi *et al.* 2011) showed the above mentioned trends of effect of metal ions and cellulase from *B. subtilis* GN156 on the other hand showed the inhibition effect on enzyme activity by Co^{2+} and Mn^{2+} ions (Apiraksakorn *et al.* 2008). In another report by Asha and Sakthivel (2014) cellulase produced by *B. subtilis* SU40 exhibited enhancement in activity in presence of Ca^{2+} and Na^{+} and the cellulase activity was inhibited by Mn^{2+}, Zn^{2+} and Hg^{2+} ions.

2.2.4.2.3 Substrate specificity of cellulase

Many cellulases of bacterial origin are known to have multi-substrate specificity, for example cellulase from *B. amyloliquefaciens* DL-3 exhibited activity against avicel, CMC, cellobiose, *β*-glucan and xylan (Lee *et al.* 2008). However, the enzyme was not able to hydrolyze 4-nitrophenyl *β*-D-glucopyranoside (*p*NPG) which is a substrate for detecting *β*-glucosidase activity. In another study by Kim *et al.* (2009) cellulase produced by *B. subtilis* subsp. *subtilis* A-53 showed detectable activity against CMC, cellobiose, filter paper and xylan. Cellulase from *B. subtilis* AS3 showed significant activity towards CMC, lichenan and barley *β*-D-glucan (Deka *et al.* 2013a). Cellulase from *B. subtilis* SU40 interestingly, showed the presence of all the three cellulase activities *viz.* exoglucanase, endoglucanase and *β*-glucosidase, indicated by hydrolysis of avicel, CMC and *p*NPG, respectively (Asha and Saktivel 2014). It also hydrolyzed glucan and xylan significantly.

2.2.4.3 Applications of cellulases

Cellulases are regarded as third most important enzymes for applications in various industries *viz*. pulp and paper, textile, food and beverages, animal feed, detergent and currently in bioethanol industry (Nigam and Pandey 2009, Kuhad *et al.* 2011). However, few applications in waste management (Kuhad *et al.* 2010a), extraction of olive oil and carotenoids (Cinar 2005) have also been reported.

2.2.4.3.1 Paper and pulp industry

Mechanical pulping process in presence of cellulases (bio-mechanical pulping) has been preferred over mechanical pulping alone, which lead to decreased viscosity of processed material (Bhat 2000). Interestingly, several mills used cellulases for removing fine fibrils in dissolved substances for improved drainage (Kuhad *et al.* 2011).

2.2.4.3.2 Food processing and beverages

Cellulases have been used for extraction and clarification of fruit and vegetable juices as a part of macerating enzyme complex which involves cellulases, xylanases and pectinases (Youn *et al.* 2004, de Carvalho *et al.* 2008). This enzyme complex has been used to increase cloud stability and texture of purees prepared from fruits and to decrease its viscosity (Baker and Wicker 1996). Cellulases also play an important role in producing alcoholic beverages *viz*. beer and wine. Cellulase enzymes are added either during mashing or primary fermentation which results in increased dissolution of glucan, reduced viscosity of wort and thus improved filterability

(Bamforth 2009). The enzymes are also employed to obtain improved skin degradation, color extraction, clarification and improved quality and stability of the wine (Caldini *et al.* 1994).

2.2.4.3.3 Animal feed

Cellulases are useful in improving nutritive quality of forage diet of ruminants as well as cereal based diet of poultry and pigs and thus health and performance of animals (Cowan 1996, Fontes *et al.* 2004). Since the forage diet of ruminants is cellulose rich, the cellulases have been used as supplement to improve feed conversion rate when the animal suffers inadequate digestion, for example in the post-weaning period. Cellulases have been used for de-hulling and elimination of anti-nutritional factors present in cereals and grains such as starch rich grain with non-starch polysaccharide, cellulose. Reduced viscosity and thus improved emulsification of high fibre based feeds in poultry and pig has been achieved by using cellulases (Karmakar and Ray 2011, Kuhad *et al.* 2011).

2.2.4.3.4 Textile and detergent

Cellulases in textile industry have been used in the process of bio-polishing, which involves de-piling, ageing, scouring and bleaching of the fabric (Sreenath *et al.* 1996). Cellulases are also being used for bio-stoning of denim as an alternative to conventional pumice stone treatment (abrasion). In this process, cellulases dissolve the small fiber ends on the fabric surface, thereby loosening the dye with less damage of the fibers (Galante *et al.* 1998). Cellulase preparations are added to laundry

detergents to modify the structure of fibrils which in turn results to color brightness, hand feel and dirt removal from cotton garments (Karmakar and Ray 2011).

2.2.4.3.5 Lignocellulosic ethanol

Currently, the use of cellulases in bioethanol production process is the most popular application being investigated. Bioethanol production from lignocellulosic substances involves three major steps, *viz*. pretreatment of raw biomass to yield cellulose, enzymatic hydrolysis of cellulose to simple sugars and fermentation of sugars to ethanol. Lignocellulosic biomass in the form of agricultural or forest residues such as rice straw (Binod *et al.* 2010), wheat straw (Talebnia *et al.* 2010), corn cob (Itelima *et al.* 2013), sugarcane bagasse (Canilha *et al.* 2013), hard wood (Lim *et al.* 2013), saw dust (Shea tree sawdust) (Ayeni *et al.* 2013) and grasses/weeds, for example reed canary grass (Dien *et al.* 2006), switch grass (Bals *et al.* 2010), Kans grass (Kataria and Ghosh 2011), water hyacinth (Satyanagalakshmi *et al.* 2011), red sage (*Lantana camara*) (Kuhad *et al.* 2010b) and *Prosopis juliflora* (Gupta *et al.* 2009) are being utilized as potent feedstock for ethanol production. Since enzymatic hydrolysis of cellulosic substrate is an important step of bioethanol production, the efficiency of the process should be enhanced in terms of sugar yield and saccharification rate. The performance of cellulases can also be improved to reduce the cost of enzyme which will make cellulosic ethanol commercially viable. The efforts are being carried out by enzyme engineering methods (Kazlauskas and Bornschcucr 2009), high expression (Handelsman 2005), immobilization, coenzyme regeneration, multienzyme system, enzyme coupling with fermentation, asymmetric

biosynthesis and nonaqueous biocatalysis, etc. (Li *et al*. 2012).

2.3 Feedstock for bioethanol

Currently the commercial production of ethanol depends on sugar and starch based materials, such as sugarcane and corn. However, the second generation ethanol production utilizing various lignocellulosic substances such as agricultural or forest residues, grasses, weeds, industrial and municipal solid wastes is being investigated extensively (Table 2.2).

Lignocellulosic complex is the most abundant biopolymer on Earth and it comprises about 50% of world biomass. Various attempts are being made worldwide for large-scale production of ethanol from lignocellulosic biomass; however, the higher degree of complexity of biomass is the limiting factor for processing it as feedstock. The complexity of biomass varies throughout the plant genera and thus processing of different lignocellulosic biomasses are complicated, energy-consuming and not completely developed (Sanchez and Cardona 2008). Among various substrates, biomass with minimum cost and negligible food and fodder value such as weeds are of great interest. In this study, a noxious weed, *Parthenium hysterophorus* was used as feedstock for ethanol production and biomass processing and pretreatment was investigated thoroughly.

Table 2.2 Composition and key pretreatment processes for various lignocellulosic materials.

Feedstock	Content (%, w/w)			Pretreatment	Reference
	Cellulose	Hemicellulose	Lignin		
Agricultural residues					
Rice straw	32-47	19-27	5-24	Popping pretreatment (water impregnated steam explosion), ultrasound-assisted acid/alkaline treatment	Sarkar and Aikat 2012, Wi *et al.* 2013 Suresh *et al.* 2014
Wheat straw	35-45	20-30	8-15	Dilute acid, lime, alkaline peroxide, steam explosion	Kootstra *et al.* (2009),Saha *et al.* (2005), Saha and Cotta 2006, Ballesteros *et al.* (2006)
Rice hull	35.62	11.96	15.38	Alkaline peroxide, dilute acid	Saha *et al.* 2005, Saha and Cotta 2008
Sugarcane bagasse	40.5	24.5	26.4	Milling, lime pretreatment, liquid hot water	da Silva *et al.* 2010, Rabelo *et al.* 2013, Laser *et al.* 2002
Sugarcane tops	29.9	18.9	-	dilute acid pretreatment	Sindhu *et al.* 2011
Corn stover	37.5	22.4	17.6	Liquid hot water, aqueous ammonia, acid, alkali pretreatment	Kaar and Holtzapple 2000, Kim *et al.* 2003, Mosier *et al.* 2005, Um *et al.* 2003
Corn straw	38.7	21.7	19.3	Alkaline pretreatment	Chen *et al.* 2008
Forest residues					
Saw dust (shea tree)	45.9	20.3	29.9	alkaline wet air oxidation and alkaline peroxide-assisted wet air oxidation	Ayeni *et al.* 2013
Hard wood (*Quercus mongolica*+ *Robinia pseudoacacia* L.+ *Castanea crenata*)	40.9	20.0	24.9	Acid pretreatment using maleic, oxalic and sulfuric acids	Lim *et al.* 2013

Table 2.2 (…….*Continued*)

Feedstock	Content (%, w/w)			Pretreatment	Reference
	Cellulose	Hemicellulose	Lignin		
Grasses					
Wild grass (*Achnatherum hymenoides*)	51.23	30.06	18.7	Steam explosion and alkaline treatment	Das *et al.* 2013
Switch grass	33.6	19.3	21.4	Microwave-assisted alkaline treatment, ammonia fiber expansion	Hu and Wen 2008, Bals *et al.* 2010
Elephant grass (*Pennisetum purpureum*)	22.6	20.9	19.4	Alkaline delignification with NaOH, dilute acid hydrolysis, aqueous ammonia, steam explosion, alkaline peroxide pretreatment	Eliana *et al.* 2014
Kans grass (Saccharum spontaneum)	45.10	22.75	24.56	Dilute acid treatment	Chandel etal. 2011
Weeds					
Red sage (*Lantana camara*)	44.1	17.0	32.25	Dilute acid and alkaline delignification	Kuhad *et al.* 2010b
Carrot grass (*Parthenium hysterophorus*)	26.3	18.6	26.31	Biological pretreatment for delignification	Rana *et al.* 2013
Water hyacinth (*Eichhornia crassipes*)	18.4	49.2	3.55	Dilute acid treatment	Kumar *et al.* 2009
Prosopis juliflora	47.5	18.7	29.1	Acid, alkaline and chlorite treatment	Gupta *et al.* 2011
Industrial wastes					
Paper sludge	33.4	14.2	15.4	No pretreatment	Yamashita *et al.* 2008
Old corrugated cardboard	75.0	-	-	No pretreatment	Kadar *et al.* 2004
Dextran industrial waste water	58.89*	-	-	No pretreatment	He *et al.* 2014
Municipal wastes					
News paper	85	-	12	Alkaline treatment	Saxena *et al.* 1992

** total carbohydrate content*

2.3.1 *Parthenium hysterophorus* (carrot grass)

P. hysterophorus is a native of north-east Mexico and is endemic in America. Recently, this has been included in the world's seven most devastating and hazardous weeds. A single plant of *P. hysterophorus* can produce 10,000 to 15,000 seeds and these seeds can germinate to yield innumerable plants (Patel 2011). This is currently widespread in India and an estimated two million hectares of land have been covered with this weed (Singh *et al.* 2008, Dwivedi 2009).

The potential of *P. hysterophorus* as a feedstock for (mainly alcoholic) biofuels production has not been explored in depth yet. The published literature has mainly used the agricultural and forest residues as the substrates. To the best of my knowledge, very few studies have been published in recent past concerning use of *Parthenium hysterophorus* as a feedstock for ethanol production. Ghosh *et al.* (2013) have studied the kinetics and thermodynamics of dilute acid hydrolysis of *P. hysterophorus*. However, they have not studied the enzymatic hydrolysis of pretreated biomass. With this, Ghosh *et al.* (2013) have been able to determine only the pentose sugar released due to the hydrolysis of hemicellulose fraction of biomass. Secondly, they have also not attempted any other pre-treatment technique and compared the sugar yields. Thus, the complete potential of *P. hysterophorus* as biofuels substrate remained unexplored in the study of Ghosh *et al.* (2013). Pandiyan *et al.* (2013) have compared the efficiency of different pretreatment methods on enzymatic digestibility of *P. hysterophorus*. They have used acid, alkali and biological pretreatment (at fixed concentration and temperature) of *P. hysterophorus*. For the biological pretreatment lignolytic enzyme produced from *Marasmiellus*

palmivorus has been used. In a second parallel publication (Rana *et al.* 2014), the same group has used *Trametes hirsuta* for biological treatment. This is followed by enzymatic hydrolysis of pretreated biomass by the commercial enzyme mixture Accellerase®. The major limitation of the study of Pandiyan *et al.* (2014) was that they have not made an attempt to optimize the pretreatment in terms of operating parameters like concentration of acid/alkali and temperature and time of pretreatment. They have determined the sugar release only after enzymatic hydrolysis, which comprises of hexoses. They have not measured the pentose sugar release after pretreatment. The potential of any biomass as feedstock for alcoholic biofuels production is estimated from the total fermentable sugar release during pretreatment, which is inclusive of pentose sugars released during pre-treatment and hexose sugars released during enzymatic hydrolysis. The study of Pandiyan *et al.* (2014), thus, also did not bring out the complete potential of *P. hysterophorus* as feedstock for biofuels.

2.4 Pretreatment of lignocellulosic biomass

The pretreatment is carried out prior to enzymatic hydrolysis of lignocellulosic biomass to make cellulosic component of biomass accessible to enzyme action. The lignocellulosic biomass comprises of three components, *viz*. cellulose, hemicellulose and lignin. The pretreatment of biomass is aimed at separation of these components and their subsequent hydrolysis to monomeric sugars that can be fermented or chemically converted to biofuels. Cellulose is a polymeric, linear molecule made up exclusively of *β*-D-glucose units linked by 1,4-*β*-glucosidic bonds. This is the main

structural component of the cellulose material with high degree of crystallinity. Hemicelluloses are made from mainly five carbon sugars and are more abundant in the hard wood than soft wood. The composition of the hydrolyzate resulting from hydrolysis of biomass thus varies in terms of pentose and hexose sugar content. Hemicelluloses are different from celluloses in that they have side groups and short chains and they are branched in many cases. The sugar units in hemicellulose are held together by glycosidic linkages and are more accessible to chemical and physical attack. Lignin has amorphous structure and is a strengthening constituent. The components of biomass are interlinked by hydrogen bonds and glycosidic linkages and hence, separation of these components requires chemical treatment.The enzymatic hydrolysis of lignocellulose may be limited by several factors, such as crystallinity of cellulose (Chang and Holtzapple 2000), degree of polymerization (DP), moisture content, available surface area and lignin content (Koullas *et al*. 1992). However, Chang and Holtzapple (2000) mentioned that crystallinity affects the initial rate of enzymatic hydrolysis, but not the ultimate sugar yields. Zhang and Lynd (2004) mention that a slower hydrolysis rate of crystalline cellulose as compared to amorphous cellulose would increase the percentage crystallinity of the hydrolysed biomass. Thompson and Chen (1992) concluded that the relative pore size of the substrate and enzyme is the main limiting factor in the enzymatic hydrolysis of lignocellulosic biomass. Removal of hemicellulose and lignin increases the mean pore size and surface area of the substrate and thus increase in accessibility of cellulose to enzyme. There are various pretreatment processes in practice for the removal of hemicellulose and lignin (delignification) from lignocellulosic biomass.

The major categories of these methods may be classified on the basis of the agents/factors involved in the process, such as physical, chemical, physicochemical and biological pretreatments. These methods have been described in detail subsequent sections.

2.4.1 Physical pretreatment

Lignocellulosic biomass can be macerated and processed by various physical methods, such as mechanical comminution, pyrolysis, steam explosion, liquid hot water treatment and energy radiations. Mechanical comminution involves successive size reduction of raw biomass leading to increase in surface area and decreased cellulose crystallinity. This can be achieved by chipping, grinding and milling which result in the material size of 10-30 mm after chipping and 0.2-2 mm after milling or grinding (Sun and Cheng 2002, Hideno *et al.* 2009). Alvo and Belkacemi (1997) used comminuting, hammer and knife mills for processing timothy and alfalfa grass. Millet *et al.* (1976) in their study concluded that vibratory ball milling has been more effective in reducing the cellulose crystallinity of spruce and aspen chips and improving the digestibility of the biomass than ordinary ball milling. However, the power input of mechanical comminution of biomass depends on the required final particle size and biomass characteristics (Cadoche and Loopez, 1989) high energy and capital costs (Ghosh and Ghose, 2003).

The other useful physical treatment method is pyrolysis, where the biomass is heated above the temperature 300^{o}C, which results in formation of volatile products and char. The residue obtained after pyrolysis treatment can be easily hydrolysed by

dilute acids to yield reducing sugar (Sanchez and Cardona 2008).

Uncatalysed steam explosion is another popular physical treatment method which is usually being used in succession with mechanical comminution. In this method powdered biomass is being treated at very high temperature and pressure followed by sudden release of pressure, which led the biomass to undergo an explosive decompression (Zheng *et al.* 2009, Ibrahim *et al.* 2011). Das *et al.* (2013) have shown that steam explosion of wild grass at 121^{o}C, 15 psi for 1 h yielded significant amount of fermentable sugars and eventually ethanol after fermentation.

Liquid hot water treatment results in enhancement of cellulose digestibility and hydrolysis of hemicellulose i. e. release of pentose sugar, with the advantage of absence of fermentation inhibitors in the hydrolysate. In this method the treatment is being carried out at elevated pressure to maintain water in the liquid state (Rogalinski *et al.* 2008, Yu *et al.* 2010).

Use of high energy radiations, such as γ-ray (Yang *et al.* 2008), UV, ultrasound (Nitayavardhana *et al.* 2008), electron beam (Bak *et al.* 2009) and microwave heating (Hu and Wen 2008, Ma *et al.* 2009), for biomass pretreatment has also been investigated widely in recent past. However, these methods are not commercially viable because of being slow, energy intensive and strongly substrate specific (Zheng *et al.* 2009).

2.4.2 Chemical pretreatment

The chemicals used for lignocellulosic biomass pretreatment may be acids, alkali, oxidising agents, surfactants and ionic liquids. Dilute acid treatment hydrolyse

mainly amorphous part of lignocellulose i.e. hemicellulose and dissolves lignin to some extent. Thus, the sugar (mainly pentoses) present in dilute acid hydrolysate can be utilized for ethanol production by pentose fermentation. However, the residue which is rich in cellulose and lignin can be subsequently treated with alkali for removal of lignin (Kuhad *et al.* 2010b). Alkaline treatment on the other hand decreases the crystallinity of cellulose and thus increases enzyme digestibility (Ayeni *et al.* 2013, Pandiyan *et al.* 2014).

Oxidizing agent such as H_2O_2 alone or in combination with alkali or ammonia has significant effect on biomass pretreatment. The role of hydrogen peroxide is essentially to promote removal of lignin and break lignin-carbohydrates bonds. This action increases digestibility of cellulose by making it more accessible to enzyme action (Kim *et al.* 2000, Kim *et al.* 2001, Saha and Cotta 2006, Ayeni *et al.* 2013).

Few studies have showed that the surfactants can be potentially used for pretreatment of lignocellulosic biomass (Kurakake *et al.* 1994, Kim and Chun 2004, Kim *et al.* 2007). The action of surfactant is to reduce surface tension of water, which may lead to reduction in surface tension and higher wettability of the surface of biomass. Reduced surface tension may assist penetration of water molecules in small micro-sized pores of biomass matrix (Singh *et al.* 2014d).

Biomass pretreatment using ionic liquids to dissolve cellulose has recently received extensive research attention (Zheng *et al.* 2009, Rocha *et al.* 2014). The mainly used ionic liquids include include N-methylmorpholine-N-oxide monohydrate (NMMO) (Kuo and Lee 2009), 1-n-butyl-3-methylimidazolium chloride (BMIMCl) (Dadi *et al.* 2007), 1-allyl-3- methylimidazolium chloride (AMIMCl) (Zhang *et al.*

2005), 3-methyl-N-bytylpyridinium chloride (MBPCl) and benzyl dimethyl (tetradecyl) ammonium chloride (BDTACl) (Heinz *et al.* 2005).

2.4.3 Physicochemical pretreatment

This category of pretreatment may be the combination of the physical and chemical processes described in Section 2.4.1 and 2.4.2, respectively, or may occur individually for example ammonia fiber expansion (AFEX) method and ultrasound-assisted chemical treatments. The combined processes which have been used very popularly are chemical catalysed steam explosion (CO_2, SO_2, acid or alkaline treatment coupled with steam explosion) (Zheng *et al.* 1995, de Bari *et al.* 2007, Satyanagalakshmi *et al.* 2011, Ranjan and Moholkar 2013, Sindhu *et al.* 2014).

AFEX has emerged as an efficient method for pretreatment of variety of lignocellulosic wastes (Holtzapple *et al.* 1992, Balan *et al.* 2009, Bals *et al.* 2010). It is similar to the steam explosion with only difference of using ammonia at pH <12. AFEX pretreatment simultaneously decrystallizes cellulose with the removal of lignin and some hemicellulose (Zheng *et al.* 2009).

Ultrasound-assisted chemical treatments in practice, involved mainly acidic or alkaline treatments coupled with sonication (Guo *et al.* 2012). Ultrasound-assisted acidic pretreatment has been employed for various substrates (Sun and Tomkinson 2002, Ramon *et al.* 2014, Suresh *et al.* 2014) which resulted in enhanced sugar yield because of increased efficiency of hemicellulose hydrolysis. In a report (Suresh *et al.* 2014) on ultrasound-assisted acid treatment of rice straw, it was concluded that the enhanced hydrolysis yield was mainly due to the effect of ultrasound than the

cavitation. Ultrasound-assisted delignification processes using alkali as chemical agent have been explored widely in past using various lignocellulosic substrates (Sun *et al.* 2002, Sun and Tomkinson 2002, Yuan *et al.* 2010, Baxi and Pandit 2012, Li *et al.* 2012, Velmurugan and Muthukumar 2012, Subhedar and Gogate 2014). In this thesis, the same process has been employed for delignification of *Parthenium hysterophorus* biomass and the mechanistic investigation of the process has been attempted. Thus, the extended review and description of the structure of lignin and mechanism of delignification by ultrasound-assisted alkaline pretreatment (adopted from Bussemaker and Zhang 2013) has been given subsequently.

Lignin structure and reactivity: Lignin polymer is formed through enzymatic dehydrogenation of phenyl propanes followed by radical coupling. Lignin is derived from three monomer units, *viz*. trans-coniferyl, trans-sinapyl and trans-*p*-coumeryl alcohols. These units are linked randomly mostly via ether linkages at α and β positions to construct the lignin macromolecule. The reactive sites in lignin are mainly the ether linkages and functional groups, since the carbon-carbon linkages are generally resistant to chemical attack. The areas of lignin susceptible to chemical attack are the hydrolysable ether linkages (α-aryl, α-alkyl and β-aryl), phenolic and aliphatic hydroxyl groups, ester groups, methoxyl groups, the unsaturated groups and uncondensed units. Lignin is amorphous and tends to form hydrogen bonds influencing the accessibility of the groups, which in turn affects the levels of reactivity.

Lignin-carbohydrate linkages: There are three possible types of lignin-carbohydrate linkages, *viz*. ester, ether and glycosidic - which pose difficulty in separation of lignin and carbohydrate. Ester linkages can be readily hydrolyzed in alkali media unlike ether linkages, which are relatively stable under mild alkaline conditions.

Lignin Degradation: There are three main chemical mechanisms by which the lignin degrades in acidic, alkaline and oxidative environments.

Acidic environment: In this case, the benzyl oxygen can be protonated initiating acid degradations of α- and β-ether lignin units. The protonation is followed by α-ether elimination of the phenol or alcohol giving benzylic carbonium ion intermediate. This can undergo further degradation enabling depolymerization of lignin compound.

Alkaline environment: In alkaline and alkaline-oxidative environments, lignin degrades through the cleavage of the α- and β-aryl ether linkages to yield fragmentation units.

Oxidative environment: In this case, degradation is driven by cleavage of carbon-carbon linkages and the formation of acidic groups from ring degradations such as carboxylic acids. Side chains within the lignin may be displaced or cleaved in oxidative reactions through electrophillic substitution at an unsubstituted ring position and α-β-cleavages of the carbon chains.

Possible mechanisms for the extraction of lignin from lignocellulose with ultrasound: These mechanisms may include depolymerization, separation, degradation and condensation of lignin. Ultrasound can cause depolymerization and separation of lignin and these phenomena contribute to increased lignin extraction yields with ultrasound. Ultrasound, however, can also degrade lignin components.

Separation of lignin with ultrasound occurs via cleavage of the lignin-hemicellulose linkages. Cleavage of these linkages is evidenced by higher purity of lignin and hemicellulose fraction extractions with ultrasound. Depolymerization of lignin occurs through homolytic cleavages of the phenyl ether β-O-4 and α-O-4 bonds. Homolytic cleavage of these bonds has been confirmed with electron spin resonance. The extent of β-O-4 cleavages was more than α-O-4 cleavages.

Hydroxyl radicals produced from transient collapse of cavitation bubble can also induce degradation of lignin. However, this attack usually takes place on aromatic ring. This leads to hydroxylated, demethoxylated and side chain eliminated products. A small extent of hydroxyl radical attack also occurs on the side chains leading to formation of dimmers and oxidation of aromatic aldehydes to carboxylic acids. Increase in number of non-conjugated carbonyls also corroborates the hydroxyl radical induced degradation.

In addition to cleavage of inter-unitary bonds within lignin matrix and between lignin-hemi cellulose entities, evidence for condensation of lignin in presence of ultrasound has also been observed. Lignin condensation occurs during lignin extraction in the treatment of lignocellulosic biomass. In case of sonication, the lignin species can accumulate at the bubble surface - depending on solvent properties and structure of lignin molecule (which has phenolic moieties). This accumulation can enable proton transfer or promote radical scavenging in the interfacial region of the bubble (or in the thin liquid film in contact with bubble surface). This liquid film can get heated to moderately high temperatures (400-600 K) during transient collapse of the bubble. Hua *et al.* (1995) have hypothesized that the thin film of liquid near

bubble surface can reach supercritical conditions with marked rise in solubility. This further enhances the phenomenon of proton transfer and radical scavenging leading to recondensation and repolymerization reactions.

2.4.4 Biological pretreatment

Biological pretreatments have been carried out by employing wood degrading microorganisms to modify the chemical composition and/ or structure of the lignocellulosic biomass so that the modified biomass is more amenable to enzyme digestion. Brown and soft rot fungi mainly act on cellulose with minor effects on lignin; white rot fungi on the other hand degrade lignin actively (Zheng *et al.* 2009). Biological pretreatment of *Parthenium* sp. has been reported by Rana *et al.* (2013) and Pandiyan *et al.* (2014) using the fungi *Trametes hirsuta* and *Marasmiellus palmivorus* PK-27, respectively.

2.5 Enzymatic hydrolysis of pretreated lignocellulosic biomass

Cellulose rich pretreated lignocellulosic biomass is used as substrate for producing fermentable sugars by enzymatic hydrolysis. It has been observed by various researchers that the rate and yield of enzymatic hydrolysis of various lignocellulosic biomasses depend on concentration of enzymes and biomass (Kunamneni and Singh 2005, Fang *et al.* 2010, Rodhe *et al.* 2011, Thongkheaw and Pitiyont 2011, Suwannarangsee *et al.* 2012, Jamaludin *et al.* 2013, Marcos *et al.* 2013). Therefore, the optimization enzymatic hydrolysis is an important step to be considered in bioethanol production process. According to a report by Rodhe *et al.*

(2011), optimization of enzymatic hydrolysis of alkali pretreated sorghum straw increased the efficiency of the process by 70%. In another study by Fang *et al.* (2010), the optimization of enzymatic hydrolysis of steam-exploded corn stover resulted in enhanced yield of sugar with comparatively lesser enzyme dosage. In present study, the optimization of enzymatic hydrolysis of acid pretreated and delignified *P. hysterophorus* biomass has been done by Response surface methodology. Cellulase and *β*-glucosidase and *P. hysterophorus* biomass concentrations were the parameters to be optimized.

2.6 Fermentation of enzymatic hydrolysate to ethanol

In the process of bioethanol production, mainly the hydrolysate obtained from enzymatic hydrolysis of lignocellulosic biomass has been used as substrate for fermentation. However, in some cases hydrolysate obtained after dilute acid pretreatment can also be utilized for ethanol production by employing pentose fermenting microorganisms (Kuhad *et al.* 2010b). The selection of the type of fermentation process depends on characteristics of biomass, enzyme and microorganisms involved. On the basis of these factors the modes of fermentation and type of microorganisms has been described subsequently. Table 2.3 represents the summary of various reports in literature for ethanol production from lignocellulosic biomass employing various microorganisms and strategies.

Table 2.3 Ethanol production by enzymatic hydrolysis and fermentation using various lignocellulosic materials.

Lignocellulosic biomass	Microorganism	Enzyme	Mode of fermentation	Ethanol yield (g/g sugar)	Ethanol yield (g/g raw biomass)	Reference
Paper sludge	*Kluyveromyces marxianus* Y01070	Commercial cellulase + *β*-glucosidase	SSF	N. A.	0.33	Kadar *et al.* 2004
Paper sludge	*Saccharomyces cerevisiae*	Commercial cellulase + *β*-glucosidase	SSF	N. A.	0.33	Kadar *et al.* 2004
Wheat starch pre-fermentation effluent	Recombinant *Saccharomyces cerevisiae* strain REF	Commercial amyloglucosidase	SHF	0.47	N. D.	Zaldivar *et al.* 2005
Wheat starch post-fermentation effluent	Recombinant *Saccharomyces cerevisiae* strain REF	Commercial amyloglucosidase	SHF	0.46	N. D.	Zaldivar *et al.* 2005
Rice straw	*Saccharomyces cerevisiae* D4A	Commercial cellulase	SSF	N. A.	0.12	Ko *et al.* 2009
Red sage (*Lantana camara*)	*Saccharomyces cerevisiae*	Commercial cellulase + *β*-glucosidase	SHF	0.48	0.148	Kuhad *et al.* 2010b
Wheat straw	*Saccharomyces cerevisiae* TMB3400	Commercial cellulase + xylanse + *β*-glucosidase	SSCF	0.35	N. D.	Olofsson *et al.* 2010
Kans grass (*Saccharum spontaneum*)	*Pichia stipitis*	Cellulase produced by *Aspergillus oryzae* MTCC 1846	SHF	0.38	N. D.	Chandel *et al.* 2011
Kans grass (*Saccharum sponteneum*)	*Saccharomyces cerevisiae* MTCC170	Cellulase produced by *Trichoderma .reesei* NCIM 1052	SHF	0.46	N. D.	Kataria and Ghosh 2011
Water hyacinth (*Eichhornia crassipes*)	*Saccharomyces cerevisiae*	Commercial cellulase	SHF	0.04*	N. D.	Satyanagalaks-hmi *et al.* 2011

*N. A., Not applicable; N. D., not determined; *as calculated from data reported in paper, SHF, Separate hydrolysis and fermentation; SSF, Simultaneous saccharification and fermentation; SSCF, Simultaneous saccharification and co-fermentation, CBP, Consolidated bioprocessing*

Table 2.3 (…….*Continued*)

Lignocellulosic biomass	Microorganism	Enzyme	Mode of fermentation	Ethanol yield (g/g sugar)	Ethanol yield (g/g raw biomass)	Reference
Prosopis juliflora	*Saccharomyces cerevisiae* HAU	Commercial cellulase + *β*-glucosidase	SHF	0.45	N. D.	Gupta *et al.* 2012
Corn cob slurry and molasses	Recombinant strains of *Saccharomyces cerevisiae*	Enzyme not required	SSCF	0.46*	N. D.	Koppram *et al.* 2013
Rice straw	*Saccharomyces cerevisiae* AYH306	Commercial cellulase + *β*-glucosidase	SSF	N. A.	0.13	Sun and Tao 2013
Phosphoric acid swollen cellulose	Recombinant *Saccharomyces cerevisiae*	Enzyme not added	CBP	0.19*	N. D.	Yamada *et al.* 2013
Commercial cellulose	*Clostridium phytofermentans* and *Candida molischiana* or *S. cerevisiae* cdt-1	Endoglucanase	CBP	N. A.	0.22	Zuroff *et al.* 2013
Wheat straw	*Saccharomyces cerevisiae* ATCC 96581	Cellulase + *β*-glucosidase + xylanase	SHF	N. D.	0.36	Nanda *et al.* 2014
Pinewood (*Pinus banksiana*)	*Saccharomyces cerevisiae* ATCC 96581	Cellulase + *β*-glucosidase + xylanase	SHF	N. D.	0.35	Nanda *et al.* 2014
Timothy grass (*Phleum pretense*)	*Saccharomyces cerevisiae* ATCC 96581	Cellulase + *β*-glucosidase + xylanase	SHF	N. D.	0.39	Nanda *et al.* 2014
Sugarcane bagasse	Recombinant *Trichoderma reesei*	Enzyme not added	CBP	N. A.	0.10	Huang *et al.* 2014

*N. A., Not applicable; N. D., not determined; *as calculated from data reported in paper; SHF, Separate hydrolysis and fermentation; SSF, Simultaneous saccharification and fermentation; SSCF, Simultaneous saccharification and co-fermentation, CBP, Consolidated bioprocessing*

The characteristics of cellulases and fermenting microorganisms are the deciding factors for the mode of fermentation. Based on these aspects the fermentation processes may be classified as separate hydrolysis and fermentation (SHF), simultaneous saccharification and fermentation (SSF), simultaneous saccharification and co-fermentation (SSCF) and consolidated bioprocessing (CBP). In SHF, the enzymatic hydrolysis and fermentation processes being carried out separately, since, the optimum conditions for cellulase activities and growth of fermenting microorganism may not be similar. The main attraction of SHF process is that both hydrolysis and fermentation can be carried out under optimum conditions (Sanchez and Cardona 2008). Kuhad *et al.* (2010b) carried out ethanol production by SHF of *Lantana camara*, which resulted in maximum ethanol yield of 148 g/1000 g of pretreated *L. camara* biomass. The bioethanol production by SHF can be made more manageable by coupling the separate processes as SSF. The SSF is more advantageous over SHF since it eliminates the glucose inhibition to cellulases by reducing the sugar levels in the fermentation broth which also results in reduced the risk of contamination. Also it is more energy efficient process, in view of the utilization of a single vessel for two processes and thus lesser energy consumption for maintenance of physical conditions (Sanchez and Cardona 2008). Stenberg *et al.* (2000) used the resulting slurry of the steam pretreatment of SO_2-impregnated spruce for SSF and observed that the ethanol productivity was doubled as compared to SHF. The major limitation of SSF process is the compromise with the optimum conditions of two separate processes *viz*., enzymatic hydrolysis and fermentation. Most of the cellulases are optimally active at 40-50^{o}C and pH of 4.0-5.0 whereas the optimal

culture conditions of fermenting microorganisms are 30^{o}C and pH of 4.0-5.0. On the other hand, fermentation of pentose sugars is optimally performed at 30-70^{o}C and pH of 5.0-7.0 (Olsson and Hahn-Hagerdal 1996).

Another mode of ethanol fermentation is the inclusion of the pentose fermentation in the SSF, process called simultaneous saccharification and co-fermentation (SSCF). However, the major prerequisite of this mode is the compatibility of both microorganisms in terms of optimal temperature and pH. Olsson and Hahn-Hagerdal (1996) carried out SSCF of aspen by co-culturing *Pichia stipitis* and *Brettanomyces clausennii* at 38^{o}C. The use of recombinant microorganism for utilization of both pentose and hexose sugars has been preferred more currently. Ethanol production by SSCF process was carried out by Olofsson *et al.* (2010), where acid and enzymatic hydrolyzate of wheat straw were fermented by employing a recombinant *Saccharomyces cerevisiae* TMB3400 strain. Koppram *et al.* (2013) have used recombinant strains of *Saccharomyces cerevisiae* for ethanol production from corn cob slurry and molasses by SSCF process.

The other mode of ethanol production from lignocellulosic biomass is consolidated bioprocessing (CBP), also known as direct microbial conversion (DMC). CBP involves single microbial community to carry out four successive bioconversions, *viz*., production of cellulases and hemicellulases, hydrolysis of delignified biomass to sugars and fermentation of sugars to ethanol (Cardona and Sanchez 2007). Therefore, the capital and operation costs of cellulase production can be reduced by opting for this strategy (Lynd 1996). However, the optimal conditions for enzyme production, hydrolysis of biomass and fermentation are required to be

entirely compatible. Since, a single microorganism capable of performing all these processes has not been found in nature, only microbial consortium or genetically modified microorganisms can be employed in CBP (Wyman 1994, McMillan 1997, Claassen *et al.* 1999, Lynd *et al.* 2002). Zuroff *et al.* (2013) have used co-cultures of *Clostridium phytofermentans* with *Candida molischiana* or *S. cerevisiae* cdt-1 for ethanol production from cellulose. Recombinant strains of Clostridia (Maki *et al.* 2013), *S. cerevisiae* (Sun *et al.* 2012, Yamada *et al.* 2013) and *Trichoderma* sp. (Huang *et al.* 2014) has been used in recent studies.

2.7 Intensification of bioprocesses by ultrasound

It is evident from the literature that the performance of three major steps (pretreatment of biomass, enzymatic hydrolysis of pretreated biomass and fermentation of hydrolysate) of ethanol production from lignocellulosic wastes can be improved by application of ultrasound. Enhancement of pretreatment processes by ultrasound has been reviewed earlier in Section 2.4.3. In this section the effect of ultrasound on biochemical (enzyme mediated) and microbial (fermentation) processes has been discussed. Table 2.4 summarizes few significant investigations on the influence of ultrasound on biological processes.

Table 2.4 Summary of ultrasound-enhanced enzymatic hydrolysis and fermentation processes.

Substrate/ Feedstock	Bioprocess	Enzyme/ Microorganism	Ultrasonic conditions	Observations	Reference
Waste paper	Fermentation (SSF)	*Klebsiella oxytoca* P2	150 W, 15 min of exposure/240 min cycle	Ethanol production increased by 20%	Wood *et al.* 1997
Carboxymethylcellulose	EH	Commercial cellulase + *β*-glucosidase	20 kHz, 0.72-1.35 W/mL, 50°C, 20-60 min	Rate increases from 6.94×10^{-7} to 9.86×10^{-7} mol/(L s)	Imai *et al.* 2004
Glucose	EH	Glucose oxidase	23 kHz, Ultratip sonication	change in secondary structure of enzyme increased enzyme activity	Guiseppi-Elie *et al.* 2009
Lactose	Fermentation (SHF)	*Kluyveromyces marxianus*	11.8 Wcm^{-2}, 20% duty cycle	Ethanol concentration increased by 3.5 fold	Sulaiman *et al.* 2011
Glycerol	EH	1,3-propanediol dehydrogenase	35 W, 35 kHz, 75% duty cycle	K_m and V_{max} decreased and K_i increased	Khanna *et al.* 2013
Starch	EH	Commercial *α*-amylase	40 kHz, power output 132 W	Activation energy decreased by 80%, 3-fold higher enzyme activity	Souza *et al.* 2013
Sugarcane bagasse	EH	Cellulolytic enzyme complex	132 W, 40 kHz	Sugar yield increased to two-fold	Lunelli *et al.* 2014
Carboxymethylcellulose	EH	Cellulase	Intensity 17.33 W/cm^2, 30 min	Enzyme activity increased by 25%	Subhedar and Gogate 2014
Oil palm fronds	Fermentation (SHF)	*Saccharomyces cerevisiae*	200 W, 37 kHz, 5 h	Ethanol yield was increased by 43%	Ofori-Boateng and Lee 2014
Waste news paper	EH	Commercial cellulase	60 W, 70% duty cycle, 6.5 h	~2.4-fold enhancement in released sugar concentration	Subhedar *et al.* 2015

SSF, simultaneous saccharification and fermentation; SHF, separate hydrolysis and fermentation; EH, enzymatic hydrolysis.

2.7.1 Ultrasound

Ultrasound is a longitudinal wave with the frequency range from 10 kHz to 20 MHz, which passes through a compressible medium, such as air and water, in the form comprising of alternate compression and rarefaction phases. Passage of ultrasound wave introduces periodic variation in the pressure as well as density of the medium. As the sound wave propagates, the fluid elements in the medium undergo an oscillatory motion around a mean position (Shah *et al*. 1999). The main characteristics of the sound wave are frequency, velocity and pressure amplitude. For propagation of ultrasound wave through liquid, bubbles present in the medium scatter the ultrasound waves causing severe attenuation. Presence of gas bubbles in the liquid also alters the compressibility of the medium, as a result of which the speed of sound in the medium reduces. The properties of the sound wave in gaseous medium are strongly influenced by the static pressure in the medium. For sound wave propagation in liquids, the static pressure in the medium does not affect much, as the liquid properties are relatively insensitive to static pressures (at least for moderate levels of pressure). Thus, the properties of sound wave propagating in a liquid medium do not alter with static pressure of the medium for moderate rise in pressure levels. The description given in this section has been adopted from Moholkar *et al*. (2014).

2.7.1.1 Cavitation bubble dynamics

Conventionally, cavitation is known to be a fluid transportation problem which causes damages to the transport machineries such as pumps. However, in the past

couple of decades, significant research has taken place all over the world which has proven that production of controlled cavitation is a highly efficient tool for introduction of energy into the system that would eventually result in intensification of physical and chemical output from the process. The principal cause behind cavitation (which is nucleation, growth, oscillations and transient collapse of small gas bubbles) is pressure variation, or in general, energy dissipation in the system. On the basis of this criterion, cavitation can be categorized as: Acoustic cavitation - which is generated due to pressure variation generated due to passage of an acoustic wave and Hydrodynamic cavitation - which results due to pressure variation in the liquid flow due to change in the flow geometry. Theoretically, cavitation refers to creation of voids in the liquid medium by overcoming the Laplace pressure ($2\sigma/R$). This would mean that extremely high acoustic pressure amplitudes exceeding ~100 MPa would be required for generation of cavitation. However, in practical situation, actual cavitation occurs at low pressure amplitudes that are attributed to phenomenon of nucleation. Nucleation in the liquid medium occurs due to presence of solid particles or tiny free-floating bubbles present in the liquid that act as nuclei. Another source of nuclei is the gas pockets trapped in the crevices of the solid boundaries in the liquid medium. These gas pockets can grow in response to reduction in ambient pressure with passage of acoustic wave.

2.7.1.2 Radial motion of cavitation bubbles

The periodic pressure variation caused by propagation of ultrasound wave gives rise to volume oscillations of cavitation bubbles. The amplitude of the volume

oscillations of the cavitation bubbles is a function of amplitude of the acoustic wave. For relatively small acoustic pressure amplitudes, the volume oscillations of the bubble are small - driven mainly by the pressure forces and essentially in phase with the acoustic wave. For larger pressure amplitudes (typically greater than static pressure in the medium), the volumetric oscillations of the cavitation bubble become non-linear - comprising of an initial explosive growth followed by a transient collapse and few after-bounces. In this case, the volume oscillations (or radial motion) of the bubble are governed by pressure as well as inertial forces (Flynn 1975). The model for radial motion of cavitation bubbles has been a subject of investigation for more than 100 years. The first-ever mathematical analysis of an empty cavity collapsing under constant static pressure was given by Rayleigh (1917). This analysis was improved in later years by several researchers to include the effects of surface tension and viscosity of liquid. Presence of non-condensable gas and solvent vapor inside the bubble was also accounted for in the popular Rayleigh-Plesset-Noltingk-Neppiras-Poritsky (Plesset 1949, Poritsky 1952, Noltingk 1950) equation for radial motion of bubble. This equation, however, did not account for liquid compressibility, which becomes a dominant factor as the bubble wall velocity (dR/dt) becomes closer or even exceeds the sonic velocity in the medium. Later research in this area addressed this facet of bubble dynamics. The first model for cavitation bubble dynamics accounting for liquid compressibility effect was proposed by Gilmore (1954) using Kirkwood-Bethe hypothesis (Kirkwood and Bethe 1942) and Tait equation of state for liquid medium. Major developments occurred in this area during the subsequent years by Keller and Kolodner (1956), Keller and Miksis

(1980) and Prosperetti and Lezzi (1986) have resulted in more rigorous forms of models for radial motion of cavitation bubbles.

2.7.1.3 Modeling of the sonochemical and sonophysical effects

The passage of ultrasound wave through the medium gives rise to sinusoidal pressure variation in the medium. The cavitation bubbles grow from the nuclei in the medium during the rarefaction half cycle of ultrasound, when the pressure in the medium falls sufficiently below the ambient or static pressure. If the pressure amplitude of the ultrasound wave is sufficiently high, the bubble under-goes an explosive growth to several times its original size in the rarefaction half cycle of ultrasound. This expansion is accompanied by large evaporation of water at the bubble interface. The vapor molecules diffuse towards the core of the bubble after evaporation into the bubble. The vapor transport in the bubble is a crucial aspect of the cavitation bubble dynamics. This matter has been treated by numerous authors with different approaches (Flynn 1964, Colussi *et al.* 1998, Colussi and Hoffmann 1999, Kamath *et al.* 1993, Prasad *et al.* 1994, Gong and Hart 1998, Sochard *et al.* 1997, Moss *et al.* 1999, Yasui 1997a, Yasui 1997b). A review of literature treating vapor transport across bubble interface during radial motion and the entrapment of vapor in the bubble during transient collapse is given by Krishnan *et al*. (2006).

The general treatment of the vapor transport and entrapment in the cavitation bubble was given by Storey and Szeri (2000) showed that in the compression phase of radial bubble motion, counter diffusion of the vapor molecules occurs with condensation at the bubble wall. The rate of transport of vapor molecules is

proportional to the difference between partial pressure of liquid in the bubble and the saturation (or vapor) pressure at the bubble interface. However, not all of the vapor molecules that approach the bubble interface stick to it, giving rise to non-equilibrium phase change. The fraction of vapor molecules that stick to the bubble interface is the accommodation coefficient. The lower the value of this parameter, the greater the resistance to condensation and the higher the amount of vapor entrapped. The principal result of the study of Storey and Szeri (2000) was that water vapor transport in the bubble is a two-step process, i.e. diffusion to the bubble wall and condensation at the wall. Thus, it is influenced by two time scales, *viz*. time scale of diffusion (t_{diff}) and time scale of condensation (t_{cond}) (Eames 1997) and their magnitudes relative to the time scale of bubble dynamics, t_{osc}. In the initial phase of bubble collapse $t_{osc} >> t_{diff}$, t_{cond}, due to which the phase change at the bubble interface is in equilibrium and the concentration of vapor molecules at the bubble interface is essentially same as that in the bubble core. As the bubble wall acceleration increases during collapse, the time scales of bubbles dynamics and vapor diffusion becomes equal. At this stage, the rate of reduction of vapor molecules in the central region of the bubble is less than that at the bubble wall. With further acceleration of the bubble wall, $t_{osc} << t_{diff}$ condition is reached and the vapor molecules have insufficient time to diffuse to the bubble wall, which results in a fixed and uneven distribution of vapor molecules in the bubble. At this condition, the bubble composition is "freezed" and the vapor present inside the bubble is essentially "trapped" in the bubble.

Another mechanism which traps vapor molecules inside the bubble is the non-equilibrium phase change at the bubble wall. In the final moments of bubble collapse, when $t_{osc} << t_{cond}$, the condensation or phase change at the bubble wall is non-equilibrium in that not all vapor molecules that approach the bubble wall can escape the bubble by undergoing phase change and get trapped in the bubble. The exact mechanism by which water vapor gets trapped in the bubble is determined by relative magnitudes of t_{osc}, t_{cond} and t_{diff}. When the bubble dynamics time scale is smaller than either diffusion or condensation time scale, it leads to entrapment of the vapor. Storey and Szeri (2000) showed that the condition $t_{osc} << t_{diff}$ is reached well before the condition of $t_{osc} << t_{cond}$. Thus, the contribution to vapor entrapment from diffusion mechanism is more than the condensation mechanism or in other words, vapor transport in the bubble is a diffusion limited process. The entrapped vapor and gas molecules in the bubble are subjected to extreme conditions generated during transient collapse, due to which they undergo thermal dissociation to several chemical species - some of which are radical species. The bubble may get fragmented at the point of minimum radius or maximum compression. At this moment, the chemical species formed in the bubble get released into the medium where they induce the sonochemical effect such as induction of a stubborn reaction or acceleration of the kinetics of a reaction etc.

In view of the results of Storey and Szeri (2000, 2001), Toegel *et al.* (2000) developed a simple diffusion limited model using boundary layer approximation, which has become immensely popular among the sonochemical community. This model, based on ordinary differential equations, has distinct merits of being simple

yet physically realistic. This model has been validated against the full partial differential equation (PDE) model of Storey and Szeri (2000, 2001). This model does not take into account the rectified diffusion of non-condensable gas across the bubble during radial motion, as the time scale of this diffusion, approximated by ratio R_o^2/D, is of the order of milliseconds (100 ms for typical values of $R_o \sim 10$ μm and $D = 10^{-9}$ m^2/s), while the bubble motion time scale is of the order of microseconds (50 μs for 20 kHz). As a result of large difference in the two time scales, practically no diffusion of gas occurs across bubble interface for the radial motion of few hundreds of acoustic cycles and hence, the approximation of neglecting gas diffusion is good (Hilgenfeldt *et al.* 1996). Another important assumption made while estimation of the sonochemical effect is that of prevalence of chemical equilibrium in the bubble all through radial motion. This assumption is again based on the relative time scales of reactions occurring inside the bubble and the timescale of bubble dynamics. As the temperature and the pressure in the bubble at the point of maximum compression is extreme (~ 5000 K and ~ 50 MPa) and also that the concentration of different chemical species is very high due to extremely small volume. The rates of various reactions occurring between these species are also very high. As a result, chemical equilibrium prevails in bubbles all along during the radial motion (Brenner *et al*. 2002, Krishnan *et al*. 2006).

2.7.1.4 Physical effects of cavitation bubble

Ultrasound and cavitation render several physical effects on a reaction system. The main manifestation of all of these results is generation of intense micro-

convection and micro-mixing in the reaction system. A brief description of all physical effects of ultrasound and cavitation is given below (Young 1989, Leighton 1994, Mason and Lorimer 2002, Shah *et al.* 1999):

2.7.1.4.1 Micro-streaming

This is essentially small amplitude oscillatory motion of fluid elements around a mean position, which is induced by propagation of ultrasound wave. For a typical ultrasound wave with pressure amplitude of 120 kPa in water (ρ = 1000 kg/m^3, C = 1500 m/s), the micro-streaming velocity = 0.08 m/s.

2.7.1.4.2 Acoustic streaming

During propagation of ultrasound wave, the momentum of the wave is absorbed by the medium due to finite viscosity. This results in setting up of low velocity unidirectional currents of the fluid known as acoustic streaming (Kolb and Nyborg 1956, Nyborg 1958). The phenomenon of acoustic streaming also occurs in the vicinity of solid boundaries in the medium, where the oscillatory motion of fluid elements is obstructed and results in setting up of unidirectional current parallel to the boundary.

2.7.1.4.3 Microturbulence

The oscillatory motion of fluid induced by an oscillatory bubble in its vicinity is called microturbulence. This phenomenon is explained as follows: in the expansion phase of radial motion of the cavitation bubble, the liquid is displaced away from

bubble interface. During the collapse phase the liquid is pulled towards the bubble as it fills the vacuum created in the liquid with size reduction of bubble. The mean velocity of microturbulence depends on the amplitude of bubble oscillation. However, it was noted that phenomenon of microturbulence is restricted only in the region in close vicinity of the bubble. The microturbulence velocity diminishes very rapidly away from the bubble.

Acoustic (or shock) waves: During the compression phase of radial motion, as the bubble contracts void space is created in the liquid and the fluid element spherically converge (or essentially "gush") in this void space and work is done on the bubble. For a cavitation bubble containing non-condensable gas such as air, the adiabatic compression results in rapid rise of pressure inside the bubble. At the point of minimum radius (or maximum compression), the bubble wall comes to a sudden halt. At this instance, the fluid elements converging towards the bubble are reflected back from the interface. This reflection creates a high pressure shock wave that propagates through the medium. The pressure exerted by the non-condensable gas inside the bubble causes rebounce of the bubble.

2.7.1.4.4 Microjets

During radial motion driven by ultrasound wave, the cavitation bubble maintains spherical geometry as long as the motion of liquid in its vicinity is symmetric and uniform and thus there are no pressure gradients. If the bubble is located close to a phase boundary, either solid-liquid, gas-liquid or liquid-liquid, the motion of liquid in its vicinity is hindered, resulting in development of pressure

gradient around it. This non-uniformity of pressure results in the loss of spherical geometry of the bubble. Numerous authors (Plesset and Chapman 1971, Lauterborn and Hentschel 1985, Lauterborn and Hentschel 1986, Blake *et al.* 1986, Blake *et al.* 1987, Ilyichev *et al*. 1989, Vogel *et al*. 1989, Phillip and Lauterborn 1998, Pecha and Gompf 2000) have investigated this phenomenon in the past three decades - either theoretically (numerical simulations) or experimentally (high speed photography). During the asymmetric radial motion, the portion of bubble exposed to higher pressure collapses faster than rest of the bubble, which gives rise to the formation of a high speed liquid jet. However, the direction of this jet depends on the characteristics of the solid boundary. For a rigid boundary, the microjet is directed towards the boundary, while for a free boundary, the microjet is directed away from the boundary. The velocity of these microjets has been estimated in the range of 120-150 m/s (Plesset and Chapman 1971, Lauterborn and Hentschel 1985, Lauterborn and Hentschel 1986, Blake *et al.* 1986, Blake *et al.* 1987, Ilyichev *et al*. 1989, Vogel *et al*. 1989, Phillip and Lauterborn 1998, Pecha and Gompf 2000). In case of rigid boundaries, these jets can cause severe damage at the point of impact and can erode the surface.

2.8 Objectives of the present study

Lignocellulosic biomass has emerged as potential cheap substrate for bioethanol production. Ethanol production by lignocellulosic biomass involves biomass pretreatment, enzymatic hydrolysis of pretreated biomass and fermentation of sugar. The economy of bioethanol production depends mainly on availability and

cost of the substrate. Moreover, the efficiency of enzymatic hydrolysis of biomass, pretreatment and fermentation also plays an important role in bioethanol production. In view of this, the thesis mainly focused on development, optimization and intensification of significant steps in bioethanol production process.

Considering these objectives, a natural cellulase producing strain *Bacillus amyloliquefaciens* SS35 was isolated from rhinoceros dung and enzyme production from the isolate was optimized by statistical design. The enzyme was purified, characterized and subsequently used for hydrolysis of *Parthenium hysterophorus* (carrot grass) biomass. Also, biomass pretreatment and delignification methods were optimized and intensified prior to subsequent step of enzymatic hydrolysis. Various pretreatment methods, *viz*. physical, chemical and physicochemical, were screened and the selected one was optimized. Delignification of pretreated *P. hysterophorus* biomass was attempted by ultrasound-assisted alkaline treatment and the mechanism of the process was suggested on the basis of simulations of cavitation bubble dynamics. Enzymatic hydrolysis of pretreated and delignified *P. hysterophorus* biomass was also optimized by statistical method. The efficiency of the hydrolysis process was enhanced by applying ultrasound and the effect on kinetic parameters was investigated. Fermentation was then carried out separately by utilizing enzyme hydrolysate as sugar source for *Saccharomyces cerevisiae* MTCC170. The fermentation was carried out under the influence of ultrasound and the effect on yeast growth and other process parameters were investigated. Further, separate hydrolysis and fermentation (SHF) processes were coupled as simultaneous saccharification and fermentation (SSF) and the effect of sonication on SSF was

investigated. The experimental results from both the processes were fitted in a mathematical model and the effects of ultrasonic irradiation on various parameters related to kinetics of fermentation were studied.

References

Ahamed, A. and Vermette, P. (2009) Effect of culture medium composition on *Trichoderma reesei*'s morphology and cellulase production. Bioresource Technology, 100, 5979-5987.

Akhtar, N., Sharma, A., Deka, D., Jawed, M., Goyal, D. and Goyal A. (2013) Characterization of cellulase producing *Bacillus* sp. for effective degradation of leaf litter biomass. Environmental Progress and Sustainable Energy, 32, 1195-1201.

Akinosho, H., Yee, K., Close, D. and Ragauskas, A. (2008) The emergence of Clostridium thermocellum as a high utility candidate for consolidated bioprocessing applications. Frontiers in Chemistry, 2, 66.

Alvo, P. and Belkacemi, K. (1997) Enzymatic saccharification of milled timothy (*Phleum pretense* L.) and alfalfa (*Medicago sativa* L.). Bioresource Technology, 61, 185-198.

Apiraksakorn, J., Nitisinprasert, S. and Levin, R. E. (2008) Grass degrading β-1,3-1,4-D-glucanases from *Bacillus subtilis* GN156: Purification and characterization of glucanase J1 and pJ2 possessing extremely acidic pI. Applied Biochemistry and Biotechnology, 149, 53-66.

Ariffin, H., Abdullah, N., Kalsom, M. S. U., Shirai, Y. and Hassan, M. A. (2006) Production and characterization of cellulase by *Bacillus pumilus* EB3. International Journal of Engineering and Technology, 3, 47-53.

Ariffin, H., Abdullah, N., Umikalsom, M. S., Shirai, Y. and Hassan, M. A. (2008) Production of bacterial endoglucanase from pretreated oil palm empty fruit

bunch by *Bacillus pumilus* EB3. Journal of Bioscience and Bioengineering, 106, 231-236.

Ash, C., Farrow, J. A. E., Wallbanks, S. and Collins, M. D. (1991) Phylogenetic heterogeneity of the genus *Bacillus* revealed by comparative analysis of small-subunit-ribosomal RNA sequences. Letters in Applied Microbiology, 13, 202-206.

Asha, B. M. and Sakthivel, N. (2014) Production, purification and characterization of a new cellulase from *Bacillus subtilis* that exhibit halophilic, alkalophilic and solvent-tolerant properties. Annals of Microbiology, 64, 1839-1848.

Ayeni, A. O., Banerjee, S., Omoleye, J. A., Hymore, F. K., Giri, B. S., Deshmukh, S. C., Pandey, R. A. and Mudliar, S. N. (2013) Optimization of pretreatment conditions using full factorial design and enzymatic convertibility of shea tree sawdust. Biomass Bioenergy, 48, 130-138.

Ayeni, A. O., Banerjee, S., Omoleye, J. A., Hymore, F. K., Giri, B. S., Deshmukh, S. C., Pandey, R. A. and Mudliar, S. N. (2013) Optimization of pretreatment conditions using full factorial design and enzymatic convertibility of shea tree sawdust. Biomass Bioenergy, 48, 130-138.

Azzeddine, B., Abdelaziz, M., Estelle, C., Mouloud, K., Nawel, B., Nabila, B., Francis, D. and Said, B. (2013) Optimization and partial characterization of endoglucanase produced by *Streptomyces* sp. B-PNG23. Archives of Biological Sciences, Belgrade, 65, 549-558.

Bajaj, B. K., Pangotra, H., Wani, M. A., Sharma, P. and Sharma, A. (2009) Partial purification and characterization of a highly thermostable and pH stable

endoglucanase from a newly isolated *Bacillus* strain M-9. Indian Journal of Chemical Technology, 16, 382-387.

Bak, J. S., Ko, J. K., Han, Y. H., Choi, I. G. and Kim, K. H. (2009) Improved enzymatic hydrolysis yield ofrice straw using electron beam irradiation pretreatment. Bioresource Technology, 100, 1285-1290.

Baker, R. A. and Wicker, L. (1996) Current and potential applications of enzyme infusion in the food industry. Trends in Food Science and Technology, 7, 279-284.

Balan, V., Bals, B., Chundawat, S. P., Marshall, D. and Dale, B. (2009) Lignocellulosic biomass pretreatment using AFEX. Methods in Molecular Biology 581, 61-77.

Ballesteros, I., Negro, M. J., Oliva, J. M., Cabanas, A., Manzanares, P. and Ballesteros, M. (2006) Ethanol production from steam-explosion pretreated wheat straw. Applied Biochemistry and Biotechnology, 129-132, 496-508.

Bals, B., Rogers, C., Jin, M., Balan, V. and Dale, B. (2010) Evaluation of ammonia fibre expansion (AFEX) pretreatment for enzymatic hydrolysis of switchgrass harvested in different seasons and locations. Biotechnology for Biofuels, 3, 1.

Bamforth, C. W. (2009) Current perspectives on the role of enzymes in brewing. Journal of Cereal Science, 50, 353-357.

Baxi, P. B. and Pandit, A. B. (2012) Using cavitation for delignification of wood. Bioresource Technology 110, 697-700.

Bayer, E. A., Chanzy, H., Lamed R. and Shoham, Y. (1998) Cellulose, cellulases and

cellulosomes. Current Opinion in Structural Biology, 8, 548-557.

Bayer, E. A., Shoham, Y. and Lamed, R. (2006) Cellulose decomposing bacteria and their enzyme systems. Prokaryotes, 2, 578-617.

Bhat, M. K. (2000) Cellulases and related enzymes in biotechnology. Biotechnology Advances, 18, 355-358.

Binod, P., Sindhu, R., Singhania, R. R., Vikram, S., Devi, L., Nagalakshmi, S., Kurien, N., Sukumaran, R. K. and Pandey, A. (2010) Bioethanol production from rice straw: An overview. Bioresource Technology, 101, 4767-4774.

Blake, J. R., Taib, B. B. and Doherty, G. (1986) Transient cavities near boundaries. Part I. Rigid boundary. Journal of Fluid Mechanics, 170, 479-497.

Blake, J. R., Taib, B. B. and Doherty, G. (1987) Transient cavities near boundaries. Part II. Free surface. Journal of Fluid Mechanics, 181, 197-212.

Box, G. E. P. and Wilson, K. B. (1951) On the experimental attainment of optimum conditions. Journal of Royal Statistical Society, 13, 1-45.

Brenner, M., Hilgenfeldt, S. and Lohse, D. (2002) Single-bubble sonoluminescence. Reviews of Modern Physics, 74, 425-484.

Bussemaker, M. J. and Zhang, D. (2013) Effect of ultrasound on lignocellulosic biomass as a pretreatment for biorefinery and biofuels applications. Industrial and Engineering Chemistry Research, 52, 3563-3580.

Cadoche, L. and Lopez, G. D. (1989) Assessment of size reduction as a preliminary step in the production of ethanol from lignocellulosic wastes. Biological Wastes, 30, 153-157.

Caldini, C., Bonomi, F., Pifferi, P. G., Lanzarini, G. and Galante ,Y. M. (1994)

Kinetic and immobilization studies on fungal glycosidases for aroma enhancement in wine. Enzyme and Microbial Technology, 16, 286-291.

Canilha, L., Chandel, A. K., Milessi, T. S. S., Antunes, F. A. F., Freitas, W. L. C., Felipe, M. D. G. A. and da Silva, S. S. (2012) Bioconversion of sugarcane biomass into ethanol: an overview about composition, pretreatment methods, detoxification of hydrolysates, enzymatic saccharification and ethanol fermentation. Journal of Biomedicine and Biotechnology, Article ID 989572,15 pages.

Cardona, C. A. and Sanchez, O. J. (2007) Fuel ethanol production: Process design trends and integration opportunities. Bioresource Technology, 98, 2415-2457.

Chandel, A. K., Kapoor, R. K., Singh, A. and Kuhad, R. C. (2007) Detoxification of sugarcane bagasse hydrolysate improves ethanol production by *Candida shehatae* NCIM 3501. Bioresource Technology, 98, 1947-1950.

Chandel, A. K., Singh, O. V., Narasu, M. L. and Rao, L. V. (2011) Bioconversion of *Saccharum spontaneum* (wild sugarcane) hemicellulosic hydrolysate into ethanol by mono and co-cultures of Pichia stipitis NCIM3498 and thermotolerant *Saccharomyces cerevisiae*-VS3. New Biotechnology, 28, 593-599.

Chang, V. S. and Holtzapple, M. (2000) Fundamentals factors affecting biomass reactivity. Applied Biochemistry and Biotechnology, 84-86, 5-37.

Chen, H. (2014) Biotechnology of Lignocellulose: Theory and Practice. Chemical Industry Press, Springer.

Chen, H. (2014) Biotechnology of Lignocellulose: Theory and Practice. Chemical Industry Press, Springer.

Chen, M., Zhao, J. and Xia, L. (2008) Enzymatic hydrolysis of maize straw polysaccharides for the production of reducing sugars. Carbohydrate Polymers, 71, 411-415.

Chun, J. and Bae, K. S. (2000) Phylogenetic analysis of *Bacillus subtilis* and related taxa based on partial *gyr*A gene sequences. Antonie van Leeuwenhoek, 78, 123-127.

Cinar, I. (2005) Effects of cellulase and pectinase concentrations on the colour yield of enzyme extracted plant carotenoids. Process Biochemistry, 40, 945-949.

Claassen, P. A. M., van Lier, J. B., Lopez Contreras, A. M., van Niel, E. W. J., Sijtsma, L., Stams, A. J. M., de Vries, S. S. and Weusthuis, R. A. (1999) Utilisation of biomass for the supply of energy carriers. Applied Microbiology and Biotechnology, 52, 741-755.

Colussi, A. J. and Hoffmann, M. R. (1999) Vapor supersaturation in collapsing bubbles: relevance to mechanisms of sonochemistry and sonoluminescence. The Journal of Physical Chemistry A, 103, 11336-11339.

Colussi, A. J., Weavers, L. K. and Hoffmann, M. R. (1998) Chemical bubble dynamics and quantitative sonochemistry. The Journal of Physical Chemistry A, 102, 6927-6934.

Cowan, W. D. (1996) Animal feed. Industrial Enzymology, T. Godfrey and S. West, Eds., pp. 360-371, Macmillan Press, London, UK, 2nd edition.

da Silva, A. S., Inoue, H., Endo, T., Yano, S. and Bon, E. P. (2010) Milling

pretreatment of sugarcane bagasse and straw for enzymatic hydrolysis and ethanol fermentation. Bioresource Technology, 101, 7402-7409.

Dadi, A. P., Schall, C. A. and Varanasi, S. (2007) Mitigation of cellulose recalcitrance to enzymatic hydrolyis by ionic liquid pretreatment. Applied Biochemistry and Biotechnology, 137, 407-421.

Das, S. P., Ghosh, A., Gupta, A., Goyal, A. and Das, D. (2013) Lignocellulosic fermentation of wild grass employing recombinant hydrolytic enzymes and fermentative microbes with effective bioethanol recovery. BioMed Research International, Article ID 386063, 14 pages.

de Bari I., Nanna, F. and Braccio, G. (2007) SO_2-catalyzed steam fractionation of aspen chips for bioethahnol production: Optimization of the catalyst impregnation. Industrial and Engineering Chemistry Research. 46, 7711-7720.

de Carvalho, L. M. J., de Castro, I. M. and da Silva, C. A. B. (2008) A study of retention of sugars in the process of clarification of pineapple juice (Ananas comosus, L. Merril) bymicro- and ultra-filtration. Journal of Food Engineering, 87, 447-454.

Deka, D., Bhargavi, P., Sharma, A., Goyal, D., Jawed, M. and Goyal, A. (2011) Enhancement of cellulase activity from a new strain of *Bacillus subtilis* by medium optimisation and analysis with various cellulosic substrates. Enzyme Research, Article ID 151656, 8 pages.

Deka, D., Das, S. P., Sahoo, N., Das, D., Jawed, M., Goyal, D. and Goyal, A. (2013b) Enhanced cellulase production from *Bacillus subtilis* by optimizing

physical parameters for bioethanol production. ISRN Biotechnology, doi:10.5402/2013/965310.

Deka, D., Jawed, M. and Goyal, A. (2013a) Purification and characterization of an alkaline cellulase produced by *Bacillus subtilis* (AS3). Preparative Biochemistry and Biotechnology, 43, 256-270.

Deshpande, S. K., Bhotmange, M. G., Chakrabarti, T. and Shastri, P. N. (2008) Production of cellulase and xylanase by *Trichoderma reesie* (QM 1494 mutant), Aspergillus niger and mixed culture by solid state fermentation (SSF) of water hyacinth (*Eichhornia crassipes*). Indian Journal of Chemical Technology, 15, 449-456.

Dias, P. V. S., Ramos, K. O., Padilha, I. Q. M., Araujob, D. A. M., Santos, S. F. M. and Silva, F. L. H. (2014) Optimization of cellulase production by *Bacillus* sp. isolated from sugarcane cultivated soil. Chemical Engineering Transactions, 38, 277-282.

Dien, B. S., Jung, H. G., Vogel, K. P., Casler, M. D., Lamb, J. F. S., Iten, L., Mitchell, R. B. and Sarath, G. (2006) Chemical composition and response to dilute-acid pretreatment and enzymatic saccharification of alfalfa, reed canarygrass and switchgrass. Biomass and Bioenergy, 30, 880-891.

Dumitrache, A., Wolfaardt, G. M., Allen, D. G., Liss, S. N. and Lynd L. R. (2013) Tracking the cellulolytic activity of *Clostridium thermocellum* biofilms. Biotechnology for Biofuels, 6, 175.

Dwivedi, P., Vivekanand, V., Ganguly, R. and Singh, R. P. (2009) *Parthenium* sp. as a plant biomass for the production of alkalitolerant xylanase from mutant

Penicillium oxalicum SAU_E-3.510 in submerged fermentation. Biomass Bioenergy, 33, 581-588.

Eames, I. W., Marr, N. J. and Sabir, H. (1997) The evaporation coefficient of water: a review. International Journal of Heat and Mass Transfer, 40, 2963-2973.

Eliana, C., Jorge, R., Juan, P. and Luis, R. (2014) Effects of the pretreatment method on enzymatic hydrolysis and ethanol fermentability of the cellulosic fraction from elephant grass. Fuel, 118, 41-47.

Fang, H., Zhao, C. and Song, X. Y. (2010) Optimization of enzymatic hydrolysis of steam-exploded corn stover by two approaches: Response surface methodology or using cellulase from mixed cultures of *Trichoderma reesei* RUT-C30 and *Aspergillus niger* NL02. Bioresource Technology, 101, 4111-4119.

Flynn, H. G. (1975) Cavitation dynamics I. A mathematical formulation. Journal of Acoustic Society of America. 57, 1379-1396.

Fontes, C. M. G. A., Ponte, P. I. P., Reis, T. C., Soares, M. C., Gama, L. T., Dias, F. M. V. Ferreira, L. M. A. (2004) A carbohydrate-binding module potentiates the efficiency of a recombinant xylanase used to supplement cereal based diets for poultry. British Poultry Science, 45, 648-656.

Fox, G. E., Wisotzkey, J. D. and Jurtshuk, P. (1992) How close is close: 16S rRNA sequence identity may not be sufficient to guarantee species identity. International Journal of Systematic Bacteriology, 42, 166-170.

Galante, Y. M., De Conti, A. and Monteverdi, R. (1998) Application of *Trichoderma* enzymes in textile industry. In: Harman, G. F. and Kubicek, C. P. (Eds.)

Trichoderma and *Gliocladium*-Enzymes, biological control and commercial applications. Taylor & Francis, London, vol 2, pp 311-326.

Gao, J., Weng, H., Zhu, D., Yuan, M., Guan, F. and Xi, Y. (2008) Production and characterization of cellulolytic enzymes from the thermoacidophilic fungal *Aspergillus terreus* M11 under solid-state cultivation of corn stover. Bioresource Technology, 99, 7623-7629.

Ghosh, P. and Ghose, T. K. (2003) Bioethanol in India: recent past and emerging future. Advances in Biochemical Engineering/Biotechnology, 85, 1-27.

Ghosh, S., Haldar, S., Ganguly, A. and Chatterjee, P. K. (2013) Investigations on the kinetics and thermodynamics of dilute acid hydrolysis of *Parthenium hysterophorus* L. substrate. Chemical Engineering Journal, 229, 111-117.

Gilmore, F. R. (1954) Hydrodynamic laboratory report, 26-4. California Institute of Technology, Pasadena.

Gong, C. and Hart, D. P. (1998) Ultrasound induced cavitation and sonochemical yields. Journal of Acoustic Society of America, 104, 2675-2682.

Guiseppi-Elie, A., Choi, S. H. and Geckeler, K. E. (2009) Ultrasonic processing of enzymes: Effect on enzymatic activity of glucose oxidase. Journal of Molecular Catalysis B: Enzymatic, 58, 118-123.

Guo, F., Fang, Z., Xu, C. C. and Smith Jr, R. L. (2012) Solid acid mediated hydrolysis of biomass for producing biofuels. Progress in Energy and Combustion Science, 38, 672-690.

Gupta, R., Khasa, Y. P. and Kuhad, R. C. (2011) Evaluation of pretreatment methods in improving the enzymatic saccharification of cellulosic materials.

Carbohydrate Polymers, 84, 1103-1109.

Gupta, R., Kumar, S., Gomes, J. and Kuhad, R. C. (2012) Kinetic study of batch and fed-batch enzymatic saccharification of pretreated substrate and subsequent fermentation to ethanol. Biotechnology for Biofuels, 5, 16.

Gupta, R., Sharma, K. K. and Kuhad, R. C. (2009) Separate hydrolysis and fermentation (SHF) of *Prosopis juliflora*, a woody substrate, for the production of cellulosic ethanol by *Saccharomyces cerevisiae* and *Pichia stipitis*-NCIM 3498. Bioresource Technology, 100, 1214-1220.

Hamberg, Y., Ruimy-Israeli, V., Dassa, B., Barak, Y., Lamed, R., Cameron, K., Fontes, C. M. G. A., Bayer, E. A. and Fried, D. B. (2014) Elaborate cellulosome architecture of *Acetivibrio cellulolyticus* revealed by selective screening of cohesin-dockerin interactions. Peer Journal, doi: 10.7717/peerj.636.

Handelsman J. (2005) Sorting out metagenome. Nature Biotechnology, 23, 38-39.

He, M. X., Qin, H., Yin, X. B., Ruan, Z. Y., Tan, F. R., Wu, B., Shui, Z. X., Dai, L. C. and Hu, Q. C. (2014) Direct ethanol production from dextran industrial waste water by *Zymomonas mobilis*. Korean Journal of Chemical Engineering, 11, 2003-2007.

Heinze, T., Schwikal, K., Barthel, S. (2005) Ionic liquids as reaction medium in cellulose functionalization. Macromolecular Bioscience, 5, 520-525.

Hideno, A., Inoue, H., Tsukahara, K., Fujimoto, S., Minowa, T., Inoue, S., Endo, T. and Sawayama, S. (2009) Wet disc milling pretreatment without sulfuric acid for enzymatic hydrolysis of rice straw. Bioresource Technology, 100,

2706-2711.

Hilgenfeldt, S., Lohse, D. and Brenner, M. P. (1996) Phase diagrams for sonoluminescing bubbles. Physics of Fluids 8, 2808-2826.

Holtzapple, M. T., Lundeen, J. E., Sturgis, R., *et al.* (1992) Pretreatment of lignocellulosic municipal solid-waste by ammonia fiber explosion (AFEX). Applied Biochemistry and Biotechnology, 34, 5-21.

Hsu, C. L., Chang, K. S., Lai, M. Z., Chang, T. C., Chang, Y. H., Jang, H. D. (2011) Pretreatment and hydrolysis of cellulosic agricultural wastes with a cellulase-producing *Streptomyces* for bioethanol production. Biomass and Bioenergy, 35, 1878-1884.

Hu, Z. and Wen, Z. (2008) Enhancing enzymatic digestibility of switchgrass by microwave-assisted alkali pretreatment. Biochemical Engineering Journal, 38, 369-378.

Hua, I., Hochemer, R. H. and Hoffmann, M. R. (1995) Sonochemical degradation of p-Nitrophenol in a parallel plate near field acoustic processor. Environmental Science and Technology, 29, 2790-2796.

Hua, I., Hochemer, R. H. and Hoffmann, M. R. (1995) Sonochemical degradation of *p*-Nitrophenol in a parallel plate near field acoustic processor. Environmental Science and Technology, 29, 2790-2796.

Huang, J., Chen, D., Wei, Y., Wang, Q. Li, Z. Chen, Y. and Huang, R. (2014) Direct ethanol production from lignocellulosic sugars and sugarcane bagasse by a recombinant *Trichoderma reesei* strain HJ48. The Scientific World Journal, 2014, Article ID 798683, 8 pages.

Ibrahim, M. M., El-Zawawy, W. K., Abdel-Fattah, Y. R., Soliman, N. A. and Agblevor, F. A. (2011) Comparison of alkaline pulping with steam explosion for glucose production from rice straw. Carbohydrate Polymer, 83, 720-726.

Ilyichev, V. I., Koretz, V. L. and Melnokov, N. P. (1989) Spectral characteristics of acoustic cavitation. Ultrasonics, 27, 357-361.

Imai, M., Ikari, K. and Suzuki, I. (2004) High-performance hydrolysis of cellulose using mixed cellulase species and ultrasonication pretreatment. Biochemical Engineering Journal, 17, 79-83.

Immanuel, G., Dhanusha, R., Prema, P. and Palavesam, A. (2006) Effect of different growth parameters on endoglucanase enzyme activity by bacteria isolated from coir retting effluents of estuarine environment. International Journal of Environmental Science and Technology, 3, 25-34.

Irfan, M., Nadeem, M. and Syed, Q. (2012) Influence of Nutritional Conditions for Endoglucanase Production by *Trichoderma viride* in SSF. Global Journal of Biotechnology and Biochemistry, 7, 7-12.

Itelima, J., Ogbonna, A., Pandukur, S., Egbere, J. and Salami A. (2013) Simultaneous saccharification and fermentation of corn cobs to bio-ethanol by co-culture of *Aspergillus niger* and *Saccharomyces cerevisiae*. International Journal of Environmental Science and Development, 4, 239-242.

Ivanen, D. R., Rongjina, N. L., Shishlyannikov, S. M., Litviakova, G. I., Isaeva-Ivanova, L. S., Shabalin, K. A. and Kulminskaya, A. A. (2009) Novel precipitated fluorescent substrates for the screening of cellulolytic

microorganisms. Journal of Microbiological Methods, 76, 295-300.

Jamaludin, S. I. S., Kadir, S. A. S. A., Krishnan, J. and Safri, N. H. M. (2013) Optimization of enzymatic hydrolysis of kitchen waste using response surface methodology (rsm) for reducing sugar production. IEEE Business Engineering and Industrial Applications Colloquium (BEIAC).

Jaradat, Z., Dawagreh, A., Ababneh, Q. and Saadoun, I. (2008) Influence of culture conditions on cellulase production by *Streptomyces* sp. (strain J2). Jordan Journal of Biological Sciences, 1, 141-146.

Jiang, X., Geng, A., He, N. and Li, Q. (2011) New isolate of *Trichoderma viride* strain for enhanced cellulolytic enzyme complex production. Journal of Bioscience and Bioengineering, 111, 121-127.

Jindou, S., Xu, Q., Kenig, R., Shulman, M., Shoham, Y., Bayer, E. A. and Lamed, R. (2006) Novel architecture of family-9 glycoside hydrolases identified in cellulosomal enzymes of *Acetivibrio cellulolyticus* and *Clostridium thermocellum*. FEMS Microbiology Letters, 254, 308-316.

Jorgensen, H., Kristensen, J. B. and Felby, C (2007) Enzymatic conversion of lignocellulose into fermentable sugars: Challenges and opportunities. Biofuels, Bioproducts and Biorefining, 1, 119-134.

Jourdier, E., Chaabane, F. B., Poughon, L., Larroche, C., Monot, F. (2012) Simple kinetic model of cellulase production by *Trichoderma reesei* for productivity or yield maximization. Chemical Engineering Transactions, 27, 313-318.

Kaar, W. E. and Holtzapple, M. T. (2000) Using lime pretreatment to facilitate the

enzymic hydrolysis of corn stover. Biomass and Bioenergy, 18, 189-199.

Kadar, Zs., Szengyel, Zs. and Reczey, K. (2004) Simultaneous saccharification and fermentation (SSF) of industrial wastes for the production of ethanol. Industrial Crops and Products, 20, 103-110.

Kamath, V., Prosperetti, A. and Egolfopoulos, F. N. (1993) A theoretical study of sonoluminescence. Journal of Acoustic Society of America, 94, 248-260.

Karmakar, M. and Ray, R. R. (2011) Current trends in research and application of microbial cellulases. Research Journal of Microbiology, 6, 41-53.

Kasana, R. C., Salwan, R., Dhar, H., Dutt, S. and Gulati, A. (2008) A rapid and easy method for the detection of microbial cellulases on agar plates using gram's iodine. Current Microbiology, 57, 503-507.

Kataria, R. and Ghosh, S. (2011) Saccharification of Kans grass using enzyme mixture from *Trichoderma reesei* for bioethanol production. Bioresource Technology, 102, 9970-9975.

Kazlauskas, R. J. and Bornschcucr U. T. (2009) Finding better protein engineering strategies. Nature Chemical Biology, 5, 526-529.

Keller, J. B. and Kolodner, I. I. (1956) Damping of underwater explosion bubble oscillations. Journal of Applied Physics, 27, 1152-1161.

Keller, J. B. and Miksis, M. J. (1980) Bubble oscillations of large amplitude. Journal of Acoustic Society of America, 68, 628-633.

Khan, F. A. B. A. and Husaini, A. A. S. A. (2006) Enhancing *α*-amylase and cellulase *in vivo* enzyme expressions on sago pith residue using *Bacillus amyloliquefaciens* UMAS 1002. Biotechnology, 5, 391-403.

Khanna, S., Jaiswal, S., Goyal, A. and Moholkar, V. S. (2013) Mechanistic investigation of ultrasonic enhancement of glycerol bioconversion by immobilized *Clostridium pasteurianum* on silica support. Biotechnology and Bioengineering, 110, 1637-1645.

Kim, B. J., Lee, S. H., Lyu, M. A., Kim, S. J., Bai, G. H., Kim, S. J., Chae, G. T., Kim, E. C., Cha, C. Y. and Kook, Y. H. (1999) Identification of mycobacterial species by comparative sequence analysis of the RNA polymerase gene (*rpo*B). Journal of Clinical Microbiology, 37, 1714-1720.

Kim, B. K., Lee, B. H., Lee, Y. J., Jin, I. H. Chung, C. H. and Lee, J. W. (2009) Purification and characterization of carboxymethylcellulase isolated from a marine bacterium, *Bacillus subtilis* subsp. subtilis A-53. Enzyme and Microbial Technology, 44, 411-416.

Kim, H. J., Kim, S. B. and Kim, C. J. (2007) The effects of nonionic surfactants on the pretreatment and enzymatic hydrolysis of recycled newspaper. Biotechnology and Bioprocess Engineering, 12, 147-151.

Kim, J. S., Lee, Y. Y. and Park, A. C. (2000) Pretreatment of wastepaper and pulp mill sludge by aqueous ammonia and hydrogen peroxide. Applied Biochemistry and Biotechnology, 84-86, 129-139.

Kim, J. S., Um, B. H. and Park, A. C. (2001) Effect of pretreatment reagent and hydrogen peroxide on enzymatic hydrolysis of oak in percolation process. Applied Biochemistry and Biotechnology, 91-93, 81-94.

Kim, S. B. and Chun, J. W. (2004) Enhancement of enzymatic digestibility of recycled newspaper by addition of surfactant in ammonia-hydrogen

peroxide pretreatment. Applied Biochemistry and Biotechnology, 113-116, 1023-1031.

Kim, T. H., Kim, J. S., Sunwoo, C. and Lee, Y. Y. (2003) Pretreatment of corn stover by aqueous ammonia. Bioresource Technology, 90, 39-47.

Kirkwood, J. G. and Bethe, H. A. (1942) The pressure wave produced by an under water explosion. Office of Science Research and Development, Report 558.

Knutsen, J. S. and Davis, R. H. (2004) Cellulase retention and sugar removal by membrane ultrafiltration during lignocellulosic biomass hydrolysis. Applied Biochemistry and Biotechnology, 113-116, 585-599.

Ko, J. K., Bak, J. S., Jung, M. W., Lee, H. J., Choi, I. G., Kim, T. H. and Kim K. H. (2009) Ethanol production from rice straw using optimized aqueous-ammonia soaking pretreatment and simultaneous saccharification and fermentation processes. Bioresource Technology, 100, 4374-4380.

Kolb, J. and Nyborg, W. L. (1956) Small scale acoustic streaming in liquids. Journal of Acoustic Society of America, 28, 1237-1242.

Kootstra, A. M. J., Beeftink, H. H., Scott, E. L. and Sanders, J. P. M. (2009) Optimization of the dilute maleic acid pretreatment of wheat straw. Biotechnology for Biofuels, 2, 31.

Koppram, R., Nielsen, F., Albers, E., Lambert, A., Wännström, S. Welin, L., Zacchi, G. and Olsson, L. (2013) Simultaneous saccharification and co-fermentation for bioethanol production using corncobs at lab, PDU and demo scales. Biotechnology for Biofuels, 6, 2.

Kaullas, D. P., Christakopoulos, P., Kekos, D., Macris, B. J. and Koukios, E. G.

(1992) Correlating the effect of pretreatment on the enzymatic hydrolysis of straw. Biotechnology and Bioengineering, 39,113-116.

Krassig, H. H. (1992) Cellulose, Structure, Accessibility and Reactivity. Switzerland, USA: Gordon and Breach Science Publishers.

Krishnan, S. J., Dwivedi, P. and Moholkar, V. S. (2006) Numerical investigation into the chemistry induced by hydrodynamic cavitation. Industrial and Engineering Chemistry Research, 45, 1493-1504.

Kuhad, R. C., Gupta, R. and Khasa, Y. P. (2010a) Bioethanol production from lignocellulosic biomass: an overview. Wealth from Waste, B. Lal, Ed., Teri Press, New Delhi, India.

Kuhad, R. C., Gupta, R. and Singh, A. (2011) Microbial Cellulases and Their Industrial Applications. Enzyme Research, Volume 2011, Article ID 280696,10 pages.

Kuhad, R. C., Gupta, R., Khasa, Y. P. and Singh, A. (2010b) Bioethanol production from *Lantana camara* (red sage): Pretreatment, saccharification and fermentation. Bioresource Technology, 101, 8348-8354.

Kumar, A., Singh, L. K. and Ghosh, S. (2009) Bioconversion of lignocellulosic fraction of water-hyacinth (*Eichhornia crassipes*) hemicellulose acid hydrolysate to ethanol by *Pichia stipitis*. Bioresource Technology, 100, 3293-3297.

Kunamneni, A. and Singh,S. (2005) Response surface optimization of enzymatic hydrolysis of maize starch for higher glucose production. Biochemical Engineering Journal, 27, 179-190.

Kuo, C. H. and Lee, C. K. (2009) Enhanced enzymatic hydrolysis of sugarcane bagasse by N-methylmorpholine-N-oxide pretreatment. Bioresource Technology, 100, 866-871.

Kurakake, M., Ooshima, H., Kato, J. and Harano, Y. (1994) Pretreatment of bagasse by nonionic surfactant for the enzymatic-hydrolysis. Bioresource Technology, 49, 247-251.

Laser, M., Schulman, D., Allen, S. G., Lichwa, J., Antal, M. J. Jr and Lynd, L. R. (2002) A comparison of liquid hot water and steam pretreatments of sugar cane bagasse for bioconversion to ethanol. Bioresource Technology, 81, 33-44.

Lauterborn, W. and Hentschel, W. (1985) Cavitation bubble dynamics studied by high speed photography and holography: part one. Ultrasonics,23, 260-268.

Lauterborn, W. and Hentschel, W. (1986) Cavitation bubble dynamics studied by high speed photography and holography: part two. Ultrasonics, 24, 59-65.

Lee, B. H., Kim, B. K., Lee, Y. J., Chung, C. H. and Lee, J. W. (2010) Industrial scale of optimization for the production of carboxymethylcellulase from rice bran by a marine bacterium, *Bacillus subtilis* subsp. subtilis A-53. Enzyme and Microbial Technology, 46, 38-42.

Lee, Y. J., Kim, B. K., Lee, B. H., Jo, K. I., Lee, N. K., Chung, C. H., Lee, Y. C. and Lee, J. W. (2008) Purification and characterization of cellulase produced by *Bacillus amyloliquefaciens* DL-3 utilizing rice hull. Bioresource Technology, 99, 378-386.

Leighton, T. G. (1994) The acoustic bubble. Academic Press, San Diego.

Lewin, M. and Pearce, E. M. (1998) Handbook of Fiber Chemistry. New York: Marcel Dekker.

Li, Q., Ji, G. S., Tang, Y. B., Gu, X. D., Fei, J. J. and Jiang, H. Q. (2012) Ultrasound-assisted compatible in situ hydrolysis of sugarcane bagasse in cellulase-aqueous-N-methylmorpholine-N-oxide system for improved saccharification. Bioresource Technology, 107, 251-257.

Li S., Yang X., Yang S., Zhu M., Wang X. (2012) Technology prospecting on enzymes: application, marketing and engineering. Computational and Structural Biotechnology Journal, 2, 1-11.

Lim, W. S., Kim, J. Y., Kim, H. Y., Choi, J. W., Choi, I. G. and Lee, J. W. (2013) Structural properties of pretreated biomass from different acid pretreatments and their effects on simultaneous saccharification and ethanol fermentation. Bioresource Technology, 139, 214-219.

Lin, L., Kan, X., Yan, H. and Wang, D. (2012) Characterization of extracellular cellulose-degrading enzymes from *Bacillus thuringiensis* strains. Electronic Journal of Biotechnology, 15, 7 pages.

Lunelli, F. C., Sfalcin, P., Souza, M., Zimmermann, E., Pra, V. D., Foletto, E. L., Jahn, S. L., Kuhn, R. C. and Mazutti, M. A. (2014) Ultrasound-assisted enzymatic hydrolysis of sugarcane bagasse for the production of fermentable sugars. Biosystems Engineering, 124, 24-28.

Lynd, L. R. van Zyl, W. H., McBride, J. E. and Laser, M. (2005) Consolidated bioprocessing of cellulosic biomass: an update. Current Opinion in Biotechnology, 16, 577-583.

Lynd, L. R., Weimer, P. J., Van, Z. W. H. and Pretorius, I. S. (2002) Microbial cellulose utilization: fundamentals and biotechnology. Microbiology and Molecular Biology Reviews, 66, 506-577.

Lynd, L. R., Wyman, C. E. and Gerngross T. U. (1999) Biocommodity engineering. Biotechnology Progress, 15, 777-793.

Lynd, L.R. (1996) Overview and evaluation of fuel ethanol from cellulosic biomass: technology, economics, the environment, and policy. Annual Review of Energy and the Environment, 21, 403-465.

Ma, H., Liu, W. W., Chen, X., Wu, Y. J. and Yu, Z. L. (2009) Enhanced enzymatic saccharification of rice straw by microwave pretreatment. Bioresource Technology, 100, 1279-1284.

Maki, M. L., Armstrong, L. Leung, K. T. and Qin, W. (2013) Increased expression of *β*-glucosidase A in *Clostridium thermocellum* 27405 significantly increases cellulase activity. Bioengineered, 4, 15-20.

Maki, M., Leung, K. T. and Qin, W. (2009) The prospects of cellulase-producing bacteria for the bioconversion of lignocellulosic biomass. International Journal of Biological Sciences, 5, 500-516.

Marcos, M., García-Cubero, M. T., González-Benito, G., Coca, M., Bolado, S. and Lucas, S. (2013) Optimization of the enzymatic hydrolysis conditions of steam-exploded wheat straw for maximum glucose and xylose recovery. Journal of Chemical Technology and Biotechnology, 88, 237-246.

Mason, T. J. and Lorimer, J. P. (2002) Applied sonochemistry: the uses of power ultrasound in chemistry and processing. Wiley-VCH, Coventry

Mather, R. R. and Wardman, R. H. (2011) The Chemistry of Textile fibres. Cambridge: RSC Publishing.

Mawadza, C., Hatti-Kaul, R., Zvauya, R. and Mattiason, B. (2000) Purification and characterization of cellulases produced by *Bacillus* strain. Journal of Biotechnology, 83, 177-187.

McMillan, J. D. (1997) Bioethanol production: status and prospects. Renewable Energy, 10, 295-302.

Millet, M. A., Baker, A. J. and Scatter, L. D. (1976) Physical and chemical pretreatment for enhancing cellulose saccharification. Biotechnology and Bioengineering Symposium, 6, 125-153.

Moholkar, V. S., Choudhury, H. A., Singh, S., Khanna, S., Ranjan, A., Chakma, S. and Bhasarkar, J. (2014) Physical and chemical mechanisms of ultrasound in biofuel synthesis. Production of Biofuels and Chemicals with Ultrasound: Editors, Fang, Z., Smith Jr., R. L. and Qi, X., Springer.

Mollet, C., Drancourt, M. and Raoult, D. (1997) *rpo*B sequence analysis as a novel basis for bacterial identification. Molecular Microbiology, 26, 1005-1011.

Mosier, N., Hendrickson, R., Ho, N., Sedlak, M. and Ladisch, M. R. (2005) Optimization of pH controlled liquid hot water pretreatment of corn stover. Bioresource Technology, 96, 1986-1993.

Moss, W. C., Young, D. A., Harte, J. A., Levalin, J. L., Rozsnyai, B. F., Zimmerman, G. B. and Zimmerman, I. H. (1999) Computed optical emissions from sonoluminescing bubbles. Physical Review E, 59, 2986-2992.

Nakamura, L. K., Roberts, M. S. and Cohan, F. M. (1999) Relationship of *Bacillus*

subtilis clades associated with strains 168 and W23: a proposal for *Bacillus subtilis* subsp. *subtilis* subsp. nov. and *Bacillus subtilis* subsp. *spizizenii* subsp. nov. International Journal of Systematic Bacteriology, 49, 1211-1215.

Nanda, S., Dalai, A. K. and Kozinski, J. A. (2014) Butanol and ethanol production from lignocellulosic feedstock: biomass pretreatment and bioconversion. Energy Science and Engineering, 2, 138-148.

Narra, M., Dixit, G., Divecha, J., Madamwar, D. and Shah, A. R. (2012) Production of cellulases by solid state fermentation with *Aspergillus terreus* and enzymatic hydrolysis of mild alkali-treated rice straw. Bioresource Technology, 121, 355-361.

Nathan, V. K., Rani, M. E., Rathinasamy, G., Dhiraviam, K. N. and Jayavel, S. (2014) Process optimization and production kinetics for cellulase production by *Trichoderma viride* VKF3, SpringerPlus, 3, 92.

Nigam, P. and Pandey, A. (2009) Eds.; Biotechnology for Agro-Industrial Residues Utilisation; Springer Science Business Media B.V., pp. 1-466.

Nitayavardhana, S., Rakshit, S K, Grewell, D., van Leevan, J. H. and Khanal, S. K. (2008) Ultrasound pretreatment of cassava chip slurry to enhance sugar release for subsequent ethanol production. Biotechnology and Bioengineering, 101, 487-496.

Noltingk, B. E. and Neppiras, E. A. (1950) Cavitation produced by ultrasonics. Proceedings of the Physical Society, B63, 674-685.

Nyborg, W. L. (1958) Acoustic streaming near a boundary. Journal of Acoustic

Society of America, 30, 329-339.

Olofsson, K., Palmqvist, B. and Liden, G. (2010) Improving simultaneous saccharification and co-fermentation of pretreated wheat straw using both enzyme and substrate feeding. Biotechnology for Biofuels, 3, 17.

Olsson, L. and Hahn-Hagerdal, B. (1996) Fermentation of lignocellulosic hydrolysates for ethanol production. Enzyme and Microbial Technology, 18, 312-331.

Onofre, S. B., Bonfante, T., dos Santos, Z. M. Q. de Moura, M. C., Cardoso, A. F. (2014) Cellulase production by endophytic strains of *Trichoderma reesei* from *Baccharis dracunculifolia* D. C. (Asteraceae). Advances in Microbiology, 2014, 4, 275-283

Pandiyan, K., Tiwari, R., Rana, S., Arora, A., Singh, S., Saxena, A. K. and Nain, L. (2014) Comparative efficiency of different pretreatment methods on enzymatic digestibility of *Parthenium* sp. World Journal of Microbiology and Biotechnology, 30, 55-64.

Patagundi, B. I., Shivasharan, C. T. and Kaliwal, B. B. (2014) Isolation and characterization of cellulase producing bacteria from soil. International Journal of Current Microbiology and Applied Sciences, 3, 59-69.

Patel, S. (2011) Harmful and beneficial aspects of *Parthenium hysterophorus*: an update 3 Biotech, 1, 1-9.

Pecha, R. and Gompf, B. (2000) Microimplosions: cavitation collapse and shock wave emission on a nanosecond time scale. Physical Review Letters, 84, 1328-1330.

Phillip, A. and Lauterborn, W. (1998) Cavitation erosion by single laser-produced bubbles. Journal of Fluid Mechanics, 361, 75-116.

Plackett, R. L. and Burman, J. P. (1946) The design of optimum multifactorial experiments. Biometrika, 33, 305-325.

Plesset, M. S. (1949) Dynamics of cavitation bubbles. Journal of Applied Mechanics: ASME DC, 16, 277-282.

Plesset, M. S. and Chapman, R. B. (1971) Collapse of an initially spherical vapour cavity in the neighbourhood of a solid boundary. Journal of Fluid Mechanics, 47, 283-290.

Poritsky, H. (1952) The collapse or growth of a spherical bubble or cavity in a viscous fluid. In: Sternberg E (ed) Proceedings of the 1st US national congress on applied mechanics, 813-821.

Prasad Naidu, D. V., Rajan, R., Kumar, R., Gandhi, K. S., Arakeri, V. H. and Chandrasekaran, S. (1994) Modeling of a batch sonochemical reactor. Chemical Engineering Science 49, 877-888.

Prosperetti, A. and Lezzi, A. (1986) Bubble dynamics in a compressible liquid. Part 1. First order theory. Journal of Fluid Mechanics, 168, 457-477.

Purkarthofer, H., Sinner, M. and Steiner, W. (1993) Effect of shear rate and culture pH on the production of xylanase by *Thermomyces lanuginosus*. Biotechnology Letters, 15, 405-410.

Rabelo, S. C., Filho, R. M. and Costa, A. C. (2013) Lime pretreatment and fermentation of enzymatically hydrolyzed sugarcane bagasse. Applied Biochemistry and Biotechnology, 169, 1696-1712.

Ramon, A. P., Taschetto, L., Lunelli, F., Mezadri, E. T., Souza, M., Foletto, E. L., Jahn, S. L., Kuhnn, R. C. and Mazutti, M. A. (2014) Ultrasound-assisted acid and enzymatic hydrolysis of Yam (*Dioscorea* sp.) for the production of fermentable sugars. Biocatalysis and Agricultural Biotechnology, http://dx.doi.org/10.1016/j.bcab.2014.11.001.

Rana, S., Tiwari, R., Arora, A., Singh, S., Kaushik, R., Saxena, A. K., Dutta, S. C. and Nain, L. (2013) Prospecting *Parthenium* sp. pretreated with Trametes hirsuta, as a potential bioethanol feedstock. Biocatalysis and Agricultural Biotechnology, 2, 152-158.

Ranjan, A. and Moholkar, V. S. (2013) Comparative study of various pretreatment techniques for rice straw saccharification for the production of alcoholic biofuels. Fuel, 112, 567-571.

Rastogi, G., Bhalla, A., Adhikari, A., Bischoff, K. M., Hughes, S. R., Christopher, L. P. and Sani, R. K. (2010) Characterization of thermostable cellulases produced by *Bacillus* and *Geobacillus* strains. Bioresource Technology, 101, 8798-8806.

Rayleigh, L. (1917) On the pressure developed in a liquid during the collapse of spherical cavity. Philosophical Magazine 34, 94-98.

Rocha, E. G. A., da Costa, A. C. and Aznar, M. (2014) Use of protic ionic liquids as biomass pretreatment for lignocellulosic ethanol production. Chemical Engineering Transactions, 37, 397-402.

Rodhe, V., Sateesh, L., Sridevi, J., Venkateswarlu, B., Rao, L. V. (2011) Enzymatic hydrolysis of sorghum straw using native cellulase produced by *T. reesei*

NCIM 992 under solid state fermentation using rice straw. 3 Biotech, 1, 207-215.

Rogalinski, T., Ingram, T. and Brunner, G. J. (2008) Hydrolysis of lignocellulosic biomass in water under elevated temperatures and pressures. Journal of Supercritical Fluids, 47, 54-63.

Sadhu, S., Ghosh, P. K., Aditya, G. and Maiti, T. K. (2014) Optimization and strain improvement by mutation for enhanced cellulase production by *Bacillus* sp. (MTCC10046) isolated from cow dung. Journal of King Saud University - Science, 26, 323-332.

Sadhu, S., Saha, P., Sen, S. K., Mayilraj, S. and Maiti, T. K. (2013) Production, purification and characterization of a novel thermotolerant endoglucanase (CMCase) from *Bacillus* strain isolated from cow dung. SpringerPlus, 2, 10.

Saha, B. C. and Cott, M. A. (2008) Lime pretreatment, enzymatic saccharification and fermentation of rice hulls to ethanol. Biomass and Bioenergy, 32, 971-977.

Saha, B. C. and Cotta, M. A (2007) Enzymatic hydrolysis and fermentation of lime pretreated wheat straw to ethanol. Journal of Chemical Technology and Biotechnology, 82, 913-919.

Saha, B. C. and Cotta, M. A. (2006) Ethanol production from alkaline peroxide pretreated enzymatically saccharified wheat straw. Biotechnology Progress, 22, 449-453.

Saha, B. C., Iten, L. B., Cotta, M. A. and Wu, Y. V. (2005) Dilute acid pretreatment, enzymatic saccharification, and fermentation of rice hulls to ethanol.

Biotechnology Progress, 21, 816-822.

Sanchez, O. J. and Cardona, C. A. (2008) Trends in biotechnological production of fuel ethanol from different feedstocks. Bioresource Technology, 99, 5270-5295.

Sarkar, N. and Aikat, K. (2012) Alkali pretreatment of rice straw and enhanced cellulase production by a locally isolated fungus *Aspergillus fumigatus* NITDGPKA3. Journal of Microbiology and Biotechnology Research, 2, 717-726.

Satyanagalakshmi, K., Sindhu, R., Binod, P., Janu, K. U., Sukumaran, R. K. and Pandey, A. (2011) Bioethanol production from acid pretreated water hyacinth by separate hydrolysis and fermentation. Journal of Scientific and Industrial Research, 70, 156-161.

Saxena, A., Garg, S. K. and Verma, J. (1992) Simultaneous saccharification and fermentation of waste newspaper to ethanol. Bioresource Technology, 42, 13-15.

Sethi, S., Datta, A., Gupta, B. L. and Gupta, S. (2013) Optimization of cellulase production from bacteria isolated from soil. ISRN Biotechnology, Volume 2013, Article ID 985685, 7 pages.

Shabeb, M. S. A., Younis, M. A. M., Hezayen, F. F. and Noureldein, M. A. (2010) Production of cellulase in low-cost medium by *Bacillus subtilis* KO strain. World Applied Sciences Journal, 8, 35-42.

Shah, Y. T., Pandit, A. B. and Moholkar, V. S. (1999) Cavitation reaction engineering. Plenum Press, New York.

Sharma, R., Kocher, G. S., Bhogal, R. S., Oberoi, H. S. (2014) Cellulolytic and xylanolytic enzymes from thermophilic *Aspergillus terreus* RWY. Journal of Basic Microbiology, 54, 1-11.

Sindhu, R., Kuttiraja, M., Binod, P. Janu, K. U., Sukumaran, R. K. and Pandey, A. (2011) Dilute acid pretreatment and enzymatic saccharification of sugarcane tops for bioethanol production. Bioresource Technology, 102, 10915-10921.

Sindhu, R., Kuttiraja, M., Binod, P., Sukumaran, R. K. and Pandey, A. (2014) Physicochemical characterization of alkali pretreated sugarcane tops and optimization of enzymatic saccharification using response surface methodology. Renewable Energy, 62, 362-368.

Singh, J., Batra, N. and Sobti, R. C. (2001) A highly thermostable, alkaline CMCase produced by a newly isolated *Bacillus* sp. VG1. World Journal of Microbiology and Biotechnology, 17, 761-765.

Singh, K., Richa, K., Bose, H., Karthik, L., Kumar, G., Rao, K. V. B. (2014b) Statistical media optimization and cellulase production from marine *Bacillus* VITRKHB. 3 Biotech, 4, 591-598.

Singh, R. K., Kumar, S., Kumar, S. and Kumar, A. (2008) Development of *Parthenium* based activated carbon and its utilization for adsorptive removal of *p*-cresol from aqueous solution. Journal of Hazardous Material, 155, 523-535.

Singh, S., Dikshit P. K., Moholkar V. S. and Goyal, A. (2014c) Purification and characterization of acidic cellulase from *Bacillus amyloliquefaciens* SS35 for hydrolyzing *Parthenium hysterophorus* biomass. Environmental

Progress and Sustainable Energy. doi: 10.1002/ep.12046.

Singh, S., du Preez, J. C., Pillay, B. and Prior, B. A. (2000) The production of hemicellulases by *Thermomyces lanuginosus* strain SSBP: influence of agitation and dissolved oxygen tension. Applied Microbiology and Biotechnology, 54, 698-704.

Singh, S., Khanna, S., Moholkar, V. S. and Goyal, A. (2014d) Screening and optimization of pretreatments for *Parthenium hysterophorus* as feedstock for alcoholic biofuels. Applied Energy, 129, 195-206.

Singh, S., Moholkar, V. S. and Goyal, A. (2014a) Optimization of carboxymethylcellulase production from *Bacillus amyloliquefaciens* SS35. 3 Biotech, 4, 411-424.

Singhania, R. R., Sukumaran, R. K. and Pandey, A. (2007) Improved cellulase production by *Trichoderma reesei* RUT C30 under SSF through process optimization. Applied Biochemistry and Biotechnology, 142, 60-70.

Sochard, S., Wilhelm, A. M. and Delmas, H. (1997) Modeling of free radicals production in a collapsing gas-vapor bubble. Ultrasonics Sonochemistry, 4, 77-84.

Souza, M., Mezadri, E. T., Zimmerman, E., Leaes, E. X., Bassaco, M. M., Prá, V. D., Foletto, E., Cancellier, A., Terra, L. M., Jahn S. L. and Mazutti, M. A. (2013) Evaluation of activity of a commercial amylase under ultrasound-assisted irradiation. Ultrasonics Sonochemistry, 20, 89-94.

Sreenath, H. K., Shah, A. B., Yang, V. W., Gharia, M. M. and Jeffries, T. W. Enzymatic polishing of jute/cotton blended fabrics. Journal of Fermentation

and Bioengineering, 81, 18-20.

Stenberg, K., Bollok, M., Reczey, K., Galbe, M. and Zacchi, G. (2000) Effect of substrate and cellulase concentration on simultaneous saccharification and fermentation of steam-pretreated softwood for ethanol production. Biotechnology and Bioengineering, 68, 2, 204-210.

Storey, B. D. and Szeri, A. J. (2000) Water vapor, sonoluminescence and sonochemistry. Proceedings of the Royal Society of London, Series A, 456, 1685-1709.

Storey, B. D. and Szeri, A. J. (2001) A reduced model of cavitation physics for use in sonochemistry. Proceedings of the Royal Society of London, Series A, 457, 1685-1700.

Subhedar, P. B. and Gogate, P. R. (2014) Alkaline and ultrasound assisted alkaline pretreatment for intensification of delignification process from sustainable raw-material. Ultrasonics Sonochemistry, 21, 216-225.

Subhedar, P. B., Babu, N. R. and Gogate, P. R. (2015) Intensification of enzymatic hydrolysis of waste newspaper using ultrasound for fermentable sugar production. Ultrasonics Sonochemistry, 22, 326-332.

Sulaiman, A. Z., Ajit, A. Yunus, R. M. and Chisti, Y. (2011) Ultrasound-assisted fermentation enhances bioethanol productivity. Biochemical Engineering Journal, 54, 141-150.

Sun, J., Wen, F., Si, T., Xu, J. H. and Zhao, H. (2012) Direct conversion of xylan to ethanol by recombinant *Saccharomyces cerevisiae* strains displaying an

engineered minihemicellulosome. Applied and Environmentsl Microbiology, 78, 3837-3845.

Sun, R. C. and Tomkinson, J. (2002) Characterization of hemicelluloses obtained by classical and ultrasonically assisted extractions from wheat straw. Carbohydrate Polymers, 50, 263-271.

Sun, W. L. and Tao, W. Y. (2013) Simultaneous saccharification and fermentation of rice straw pretreated by a sequence of dilute acid and dilute alkali at high dry matter content. Energy Source, Part A, 35, 741-752.

Sun, Y. and Cheng, J. (2002) Hydrolysis of lignocellulosic materials for ethanol production: a review. Bioresource Technology, 83, 1-11.

Suresh, K., Ranjan, A., Singh, S. and Moholkar, V. S. (2014) Mechanistic investigations in sono-hybrid techniques for rice straw pretreatment. Ultrasonics Sonochemistry, 21, 200-207.

Suwannarangsee, S., Bunterngsook, B., Arnthong, J., Paemanee, A., Thamchaipenet, A., Eurwilaichitr, L., Laosiripojana, N. and Champreda, V. (2012) Optimisation of synergistic biomass-degrading enzyme systems for efficient rice straw hydrolysis using an experimental mixture design. Bioresource Technology, 119, 252-261.

Taherzadeh, M. J. and Karimi, K. (2007) Enzyme-based hydrolysis processes for ethanol form lignocellulosic materials: A review. Bioresources, 2, 707-738.

Talebnia F. and Taherzadeh, M. J. (2006) In-situ detoxification and continuous cultivation of dilute-acid hydrolysate to ethanol by encapsulated *Saccharomyces cerevisiae*. Journal of Biotechnology, 125, 377-384.

Talebnia, F., Karakashev, D. and Angelidaki, I. (2010) Production of bioethanol from wheat straw: An overview on pretreatment, hydrolysis and fermentation. Bioresource Technology, 101, 4744-4753.

Teather, R. M. and Wood, P. J. (1982) Use of Congo red-polysaccharide interactions in enumeration and characterization of cellulolytic bacteria from the bovine rumen. Applied and Environmental Microbiology, 43, 777-780.

Thompson, D. N. and Chen H. C. (1992) Comparison of pretreatment methods on the basis of available surface area. Bioresource Technology, 39, 155-163.

Thongkheaw, S. and Pitiyont, B. (2011) Enzymatic hydrolysis of acid-pretreated sugarcane shoot. World Academy of Science, Engineering and Technology, 60.

Toegel, R., Gompf, B., Pecha, R. and Lohse, D. (2000) Does water vapor prevent upscaling sonoluminescence? Physical Review Letters, 85, 3165-3168.

Trivedi, N., Gupta, V., Kumar, M., Kumari, P., Reddy, C. R. K. and Jha, B. (2011) An alkali-halotolerant cellulase from *Bacillus flexus* isolated from green seaweed *Ulva lactuca*. Carbohydrate Polymers, 83, 891-897.

Um, B. H., Karim, M. N. and Henk, L. L. (2003) Effect of sulfuric and phosphoric acid pretreatments on enzymatic hydrolysis of corn stover. Applied Biochemistry and Biotechnology, 105-108, 115-125.

Vasudeo, Z. and Lew, C. (2011) Optimization of culture conditions for production of cellulase by a thermophilic *Bacillus* strain. Journal of Chemistry and Chemical Engineering, 5, 521-527.

Velmurugan, R. and Muthukumar, K. (2012) Ultrasound-assisted alkaline

pretreatment of sugarcane bagasse for fermentable sugar production: Optimization through response surface methodology. Bioresource Technology, 112, 293-299.

Vijayaraghavan, P. and Vincent, S. G. P. (2012) Purification and characterization of carboxymethyl cellulase from *Bacillus* sp. isolated from a paddy field. Polish Journal of Microbiology, 61, 51-55.

Vintila, T., Croitoriu, V., Dragomirescu, M. and Nica, D. (2010) The effects of bioprocess parameters on cellulase production with *Trichoderma viride* CMIT35. Scientific Papers: Animal Science and Biotechnologies, 43 , 337-340.

Vishwanatha, K. S., Appu Rao, A. G. and Singh S. A. (2010) Acid protease production by solid-state fermentation using *Aspergillus oryzae* MTCC 5341: optimization of process parameters. Journal of Industrial Microbiology and Biotechnology, 37, 129-138.

Vogel, A., Lauterborn, W. and Timm, R. (1989) Optical and acoustic investigations of the dynamics of laser-produced cavitation bubbles near a solid boundary. Journal of Fluid Mechanics, 206, 299-338.

Vyas, A., Vyas, D. and Vyas, K. M. (2005). Production and optimization of cellulases on pretreated groundnut shell by *Aspergillus terreus* AV49. Journal of Scientific and Industrial Research, 64, 281-286.

Wang, H. C., Chen, Y. C. and Hseu, R. S. (2014) Purification and characterization of a cellulolytic multienzyme complex produced by *Neocallimastix patriciarum* J11. Biochemical and Biophysical Research Communications,

451, 190-195.

Wang, T. Y., Chen, H. L., Lu, M. Y. J., Chen, Y. C., Sung, H. M., Mao, C. T., Cho, H. Y., Ke, H. M., Hwa, T. Y., Ruan, S. K., Hung, K. Y., Chen, C. K., Li, J. Y., Wu, Y. C., Chen, Y. H., Chou, S. P., Tsai, Y. W., Chu, T. C., Shih, C. C. A., Li, W. H. and Shih, M. C. (2011) Functional characterization of cellulases identified from the cow rumen fungus *Neocallimastix patriciarum* W5 by transcriptomic and secretomic analyses. Biotechnology for Biofuels, 4, 24.

Wi, S. G., Choi, I. S., Kim, K. H., Kim H. M. and Bae, H. J. (2013) Bioethanol production from rice straw by popping pretreatment. Biotechnology for Biofuels, 6, 166.

Wiselogel, A., Tyson, S. and Johnson, D. (1996) Biomass feedstock resources and composition. In: Wyman, C.E. (Ed.), Handbook on Bioethanol: Production and Utilization. Taylor & Francis, Washington, DC, 105-118.

Wood, B. E., Aldrich, H. C. and Ingram, L. O. (1997) Ultrasound stimulates ethanol production during the simultaneous saccharification and fermentation of mixed waste office paper. Biotechnology Progress, 13, 232−237.

Wyman, C. E. (1994) Ethanol from lignocellulosic biomass: technology, economics, and opportunities. Bioresource Technology, 50, 3-16.

Xu, Q., Bayer, E. A., Goldman, M., Kenig, R., Shoham, Y. and Lamed, R. (2004) Architecture of the *Bacteroides cellulosolvens* cellulosome: Description of a cell surface-anchoring scaffoldin and a Family 48 Cellulase. Journal of Bacteriology, 186, 968-977.

Xu, Q., Gao, W., Ding, S. Y., Kenig, R., Shoham, Y., Bayer, E. A. and Lamed, R. (2003) The cellulosome system of *Acetivibrio cellulolyticus* includes a novel type of adaptor protein and a cell surface anchoring protein. Journal of Bacteriology, 185, 4548-4557.

Yamada, R., Nakatani, Y., Ogino, C. and Kondo, A. (2013) Efficient direct ethanol production from cellulose by cellulase- and cellodextrin transporter-co-expressing *Saccharomyces cerevisiae*. AMB Express, 3, 34.

Yamamoto, S., Bouvet, P. J. and Harayama, S. (1999) Phylogenetic structures of the genus *Acinetobacter* based on *gyr*B sequences: comparison with the grouping by DNA-DNA hybridization. International Journal of Systematic Bacteriology, 49, 87-95.

Yamashita, Y., Kurosumi, A., Sasaki, C. and Nakamura, Y. (2008) Ethanol production from paper sludge by immobilized *Zymomonas mobilis*. Biochemical Engineering Journal, 42, 314-319.

Yang, C., Shen, Z., Yu, G. and Wang, J. (2008) Effect and after effect of gamma radiation pretreatment on enzymatic hydrolysis of wheat straw. Bioresource Technology, 99, 6240-6245.

Yassien, M. A. M., Jiman-Fatani, A. A. M. and Asfour, H. Z. (2014) Production, purification and characterization of cellulase from *Streptomyces* sp. African Journal of Microbiology Research, 8, 348-354.

Yasui, K. (1997a) Alternative model for single-bubble sonoluminescence. Physical Review E, 56, 6750-6760.

Yasui, K. (1997b) Chemical reactions in a sonoluminescing bubble. Journal of the

Physical Society of Japan, 66, 2911-2920.

Youn, K. S., Hong, J. H., Bae, D. H., Kim, S. J. and Kim, S. D. (2004) Effective clarifying process of reconstituted apple juice using membrane filtration with filter-aid pretreatment. Journal of Membrane Science, 228, 179-186.

Young, F. R. (1989) Cavitation. McGraw Hill, London.

Yu, Q., Zhuang, X., Yuan, Z., Wang, Q., Qi, W., Wang, W. Zhang, Y., Xu, J., Xu, H. (2010) Two-step liquid hot water pretreatment of *Eucalyptus grandis* to enhance sugar recovery and enzymatic digestibility of cellulose. Bioresource Technology, 101, 4895-4899.

Yuan, T. Q., Xu, F., He, J. and Sun, R. C. (2010) Structural and physico-chemical characterization of hemicelluloses from ultrasound-assisted extractions of partially delignified fast-growing poplar wood through organic solvent and alkaline solutions. Biotechnology Advances, 28, 583-593.

Zaldivar, J., Roca, C., Caroline, L.F., Hahn-Ha¨gerdal, B., Olsson, L., 2005. Ethanolic fermentation of acid pre-treated starch industry effluents by recombinant *Saccharomyces cerevisiae* strains. Bioresour. Technol. 96, 1670-1676.

Zhang, H., Wu, J., Zhang, J. and He, J. S. (2005) 1-Allyl-3-methylimidazolium chloride room temperature ionic liquid: A new and powerful non derivatizing solvent for cellulose. Macromolecules, 38, 8272-8277.

Zhang, Y. H. P. and Lynd L. R. (2004) Toward an aggregated understanding of enzymatic hydrolysis of cellulose: Noncomplexed cellulase systems. Biotechnology and Bioengineering, 88, 797-824.

Zhao, L., Cao, G. L., Wang, A. J., Ren, H. Y., Xu, C. J. and Ren, N. Q. (2013) Enzymatic saccharification of cornstalk by onsite cellulases produced by *Trichoderma viride* for enhanced biohydrogen production. GCB Bioenergy, 5, 591-598.

Zheng, Y., Lin, H. M., Wen, J., Cao, N., Yu, X. and Sao, G. T. (1995) Supercritical carbon dioxide explosion as a pretreatment for cellulose hydrolysis. Biotechnology Letters, 17, 845-850.

Zheng, Y., Pan, Z. and Zhang, R. (2009) Overview of biomass pretreatment for cellulosic ethanol production. International Journal of Agriculture and Biological Engineering, 2, 51-68.

Zuroff, T. R., Xiques, S. B. and Curtis, W. R. (2013) Consortia-mediated bioprocessing of cellulose to ethanol with a symbiotic *Clostridium phytofermentans*/yeast co-culture. Biotechnology for Biofuels, 6, 59.

Chapter 3

Isolation, screening, identification and characterization of cellulolytic *Bacillus amyloliquefaciens* SS35

3.1 Introduction

Cellulose, a structural carbohydrate of the plant cell wall, is an abundant and ubiquitous polymer. The use of cellulose for the second generation biofuel production involves the hydrolysis of cellulosic biomass, that is, saccharification, to form simple sugar monomers to ferment into bioethanol (Sun and Cheng 2002; Martin *et al*. 2006; Sanchez and Cardona 2008). Cellulases are the group of enzymes involved in the conversion of cellulosic substrates to fermentable sugars. Main members of this group include endoglucanase (EC 3.2.1.4), exoglucanase or cellobiohydrolase (EC 3.2.1.91) and *β*-glucosidase (EC 3.2.1.21) (Bayer *et al*. 2007). The endoglucanase hydrolyses *β*-(1→4) bonds in cellulose molecule, whereas exoglucanase cleaves the ends to release cellobiose and *β*-glucosidase converts cellobiose to glucose (Bhat and Bhat 1997). Several cellulase producing fungi such as *Aspergillus*, *Rhizopus* and *Trichoderma* species (Murashima *et al*. 2002; Saito *et al*. 2003) and bacteria such as *Bacillus*, *Clostridium*, *Cellulomonas*,

Thermomonospora, *Ruminococcus*, *Bacteroides*, *Erwinia* and *Acetivibrio* species (Roboson and Chambliss 1989; Lee *et al*. 2008; Kim *et al*. 2009) have been identified. However, the isolation and characterization of novel cellulose hydrolyzing enzymes from bacteria are still a highly active research area, because bacteria have a higher growth rate than fungi, leading to greater production of enzymes (Lynd *et al*. 2002). Also, the habitat of bacteria covers different environmental niches, which favors the existence of versatile strains such as thermophiles (Maki *et al*. 2009), psychrophiles, alkaliphiles and acidophiles. The culturable cellulase producing bacteria have been isolated from the variety of sources such as composting heaps, decaying agricultural wastes, the feces of cow (Akhtar *et al*. 2013) and elephant, gastrointestinal tract of buffalo and horse (Wahyudi *et al*. 2010), soil and extreme environments like hot springs (Doi 2008). Cellulose degrading bacteria play an important role in energy supply for forage animals. Wahyudi *et al*. (2010) and Varga and Kovler (1997) reported that the feed fibers were not completely converted to animal product in intensive animal farming and a large portion of undigested cellulose passed out with feces. The crude fiber degradation in gut is not optimal and the fiber content of feces is still high which can be efficiently utilized by microbes present in the feces of herbivores (Krause *et al*. 2003). The herbivores, in their natural habitats are considered to have an efficient system for cellulose digestion. In this study, the dung of a pachyderm, Rhinoceros, from Kaziranga National Park, Assam (India), was used as the source of cellulolytic bacteria. The primary food of rhinoceros, wild grasses, primarily contains 30-50% (w/w) cellulose (Sun and Cheng 2002; Das *et al*. 2013).

In the present study most efficient cellulose degrading isolate was identified as *Bacillus amyloliquefaciens* by conventional morphological and biochemical studies and the identity was confirmed by phylogenetic analyses. *B. amyloliquefaciens* was first proposed by Fukumoto (1943a, b) to accommodate *B. subtilis* like strains with higher α-amylase activity. Priest *et al*. (1987) included this taxon in the approved lists of bacterial names (Skerman *et al*. 1980). The closely related taxa of *Bacillus,* such as *B. subtilis, B. atrophaeus, B. mojavensis, B. amyloliquefaciens* and *B. vallismortis* can be differentiated by using fatty acid composition, restriction digest analysis, genetic transformation and DNA-DNA hybridization data and not only by phenotypic and biochemical properties (Chun and Bae 2000). Moreover, these organisms have almost identical 16S rRNA gene sequences with 99.2-99.6% sequence similarity (Ash *et al*. 1991; Nakamura *et al*. 1999). Therefore, the identification of *B. subtilis* like organisms has become difficult. On the other hand, it has been explained in several studies (Mollet *et al*. 1997; Kim *et al*. 1999; Yamamoto *et al*. 1999) that protein coding genes exhibit much higher genetic variation, which can be used for classification and identification of closely related taxa. Therefore, in this study partial gyrase A gene sequencing was also carried out along with 16S rRNA gene sequencing for phylogenetic characterization of the isolate.

3.2 Materials and Methods

3.2.1 Substrate and chemicals

Carboxymethylcellulose (CMC) (low viscosity, 50-200 cP) was procured from Sigma Aldrich, USA. Medium components, congo red, carbohydrate discs and antibiotic discs were procured from HiMedia Pvt. Ltd., India. Chemicals used for reagent preparation for sugar estimation were purchased from Fisher Scientific, India.

3.2.2 Sample collection

The dung sample of one-horned Indian Rhinoceros (*Rhinoceros unicornis*) was collected from its natural habitat, Kaziranga National Park, Assam, India. Presterilized spatula and plastic bags were used for sample collection and before bacterial isolation, the samples were stored at 4°C in icebox for approximately, 12 h.

3.2.3 Isolation of cellulolytic bacteria

Dung sample (0.5 g) was suspended in 50 mL of 0.85% (w/v) sterile NaCl solution in a 250 mL conical flask and incubated at 37°C and at 180 rpm for 1 h. This solution was further serially diluted upto 10^{-7} dilution using sterilized NaCl solution. An aliquot of 100 µL of each dilution was spread plated onto Bushnell Haas (BH) medium (Bushnell and Haas 1941) agar plates supplemented with carboxymethylcellulose (CMC) (pH 7.0) containing (g/L) CMC (10.0), K_2HPO_4 (1.0), KH_2PO_4 (1.0), $MgSO_4 \cdot 7H_2O$ (0.2), NH_4NO_3 (1.0), $FeCl_3 \cdot 6H_2O$ (0.05), $CaCl_2$ (0.02) and agar (20.0) (Atlas 2004). The plates were incubated at 37°C for 96 h.

3.2.4 Qualitative screening of cellulolytic bacteria by plate staining method

Morphologically dissimilar and discrete colonies were picked from different dilution plates and streaked on separate BHM-CMC plate with grids drawn over it and incubated at 37^{o}C for 96 h. The replica plates were also prepared separately for staining (Ruijssenaars and Hartmans 2001). The replica plates were flooded with 0.3% (w/v) congo red for 20 min. The stain was poured off and the plates were washed with 1 M NaCl (Teather and Wood 1982). The isolates showing clear zone around the colonies were picked from master plate and further used for the enzyme production in liquid medium. The selected cultures were maintained on nutrient agar slants containing (g/L) peptone (5.0), beef extract (1.0), yeast extract (2.0), NaCl (5.0) and agar (20.0). The culture slants were stored at 4°C and sub-cultured every 2 weeks.

3.2.5 Quantitative determination of extracellular carboxymethylcellulase (CMCase) production

The isolates, selected on the basis of plate staining method, were grown in 50 mL enzyme production medium (pH 7.0) containing the following components (g/L): CMC (10.0), K_2HPO_4 (1.0), KH_2PO_4 (1.0), $MgSO_4 \cdot 7H_2O$ (0.2), NH_4NO_3 (1.0), $FeCl_3 \cdot 6H_2O$ (0.05), $CaCl_2$ (0.02) and yeast extract (5.0). This medium is the same as the Bushnell Haas medium (Bushnell and Haas 1941) used during isolation, with the only difference of addition of yeast extract. This addition is to provide additional nitrogen source and enhance the growth rate. 50 mL medium (containing 2%, v/v inoculum) was taken in 250 mL Erlenmeyer flask and incubated at 37°C and at 180

rpm for 72 h. After every 6 h, 100 µL samples were withdrawn and the culture was centrifuged at 12000g for 20 min at 4°C. The cell-free supernatant containing the crude enzyme was used for estimation of CMCase activity. Based on the higher CMCase activity (as described later in Results and discussion section), an isolate SS35 (named after author and its colony number) was selected for further characterization and identification. The CMCase production and growth of the isolate SS35 were recorded with time, the growth was monitored by measuring the absorbance at 600 nm using UV-visible spectrophotometer (Perkin Elmer, Lambda-45).

3.2.6 CMCase activity assay

The CMCase activity (U/mL) was measured by estimation of reducing sugar liberated from CMC. The enzyme assay was carried out by incubating the enzyme with CMC at 37°C for 15 min. The reaction mixture (100 µL) contained 50 µL of enzyme and 1.0% (w/v) final concentration of CMC in 50 mM phosphate buffer (pH 7.0). The reducing sugar was estimated by the method of Nelson (1944) and Somogyi (1945). The reaction was stopped by adding 100 µL of reagent D (described later in Section 3.2.7) and the tubes were boiled using a boiling water bath for 20 min. The tubes were cooled at 30^{o}C and 100 µL of reagent C (described later in Section 3.2.7) was added to each tube. Volume was made up to 1 mL by adding 700 µL of distilled water. The absorbance was measured at 500 nm using a UV-Visible spectrophotometer (Perkin Elmer, Lambda-45) against a blank with D-glucose as

standard. One unit (U) of cellulase activity is defined as the amount of enzyme that liberates 1 µmol of reducing sugar (glucose) in 1 min at 37^{o}C and pH 7.0.

3.2.7 Reagents for enzyme activity assay

Composition of the reagents used in CMCase activity assay is as follows (Nelson 1944, Somogyi 1945):

Reagent A

Sodium carbonate (2.5 g), potassium sodium tartrate tetrahydrate (2.5 g), sodium bicarbonate (2.0 g) and sodium sulphate (20.0 g) dissolved in 100 mL distilled water.

Reagent B

Copper sulphate pentahydrate (4.5 g) and conc. sulphuric acid (1-2 drops) in 30 mL of distilled water.

Reagent C

Ammonium molybdate tetrahydrate (2.5 g) and conc. sulphuric acid (2.1 mL) were added to 45 mL of distilled water. Solution of sodium arsenate heptahydrate (0.3 g) in 2.5 mL of distilled water was mixed to it and stored in an amber bottle at 37^{o}C for 24 h prior to use.

Reagent D

Mixture of reagents A and B in a ratio of 25:1.

3.2.8 Calculation of CMCase activity

One unit (U) of CMCase activity is defined as the amount of enzyme that liberates 1 µmole of reducing sugar per min at 37°C in 50 mM sodium phosphate buffer (pH 7.0). The carboxymethylcellulase activity was calculated as:

$$\text{Enzyme activity}\left(\text{U/mL}\right)=\frac{\Delta A_{500}\times C\times V}{180\times t\times v}=\left(\mu\text{mole/min/mL}\right)$$

ΔA_{500} = change in absorbance at 500 nm
C = 1 OD equivalent glucose concentration (mg/mL) from standard plot
V = volume of the reaction mixture (mL)
t = time of reaction (min)
180 = molecular weight of glucose
v = volume of the enzyme source (mL) for reducing sugar estimation

3.2.9 Morphological and biochemical characterizations of the isolate SS35

All the morphological and biochemical properties of the isolate were compared with the characteristics of the bacteria described in Bergey's Manual of Systematic Bacteriology (Boone *et al*. 2001). The colony morphology was observed under a colony counter (Digital S, Gen Labs). The cell morphology of the selected isolate was observed under scanning electron microscope (SEM) (Leo 1430 VP, Leo Electron Microscopy Ltd., Cambridge, UK). The sample was prepared by centrifuging 1 mL of 18 h old culture at 8,000 rpm for 10 min. The cell pellet was washed twice with deionized water and was suspended in 5 mL of 2.5% glutaraldehyde and incubated at 4^{o}C for 4 h. The cell suspension was centrifuged at 10000***g*** for 10 min to get cell pellet. The pellet was washed three times with deionized water and subsequently dissolved in 30% (v/v) acetone followed by dehydrating it through 45, 55, 65, 75, 85, 95 and 100% (v/v) acetone, 10 min each (Glauert 1965). The dried sample was spread on the double sided carbon tape placed

over the surface of SEM stub and was coated with 10 nm gold in a sputter coater (SCH 620, Leo). The sample was viewed in electron microscope (Leo1330 VP) operated at 14.0 kV.

Gram staining and endospore staining were done as per standard protocols in Bergey's Manual of Systematic Bacteriology (Vos *et al*. 2011). For endospore staining the culture was first heat fixed on a glass slide and then flooded with 0.5% (w/v) aqueous solution of malachite green. The slide was then heated over a boiling water bath for 5 min. The malachite green stain was washed with water and the sample was counterstained with safranine for 30 sec. Both the slides with Gram staining and endospore staining were observed under a 100x immersion oil objective lens of the bright field microscope (Nikon Eclipse E200). Urease test was done as per standard protocol (Cappuccino and Sherman 2004). The bacterial strain was grown in urea broth containing phenol red as pH indicator. Urease after the hydrolysis of urea, forms ammonia which creates an alkaline environment that causes phenol red to turn deep pink. No change in color indicates negative reaction (Krishna *et al*. 2008). The catalase activity was determined adding few drops of 3% (v/v) H_2O_2 to 5 mL of 18 h grown culture (Kannan 2002). Catalase test was performed to determine the ability of microorganisms to produce catalase which will degrade hydrogen peroxide to evolve oxygen gas. The nitrate agar slants (M072, HiMedia Pvt. Ltd.) were used to test nitrate reducing property of the isolate SS35. The hydrogen sulphide production property of the isolate SS35 was examined by using triple sugar iron slants (M021I, HiMedia Pvt. Ltd.) which contains sodium thiosulphate and ferric citrate. Thiosulphate is reduced to hydrogen sulphide by several species of bacteria and H_2S

combines with ferric ions of ferric salt to produce the insoluble black precipitate of ferrous sulphide resulting to blackening of butt of the tube. The amylase activity of the isolate was tested by growing it on a BHM-Agar plate supplemented with 1% (w/v) starch. After 96 h of incubation at 37ºC the plate was flooded with Lugol's iodine which was the aqueous solution of I_2 (1%, w/v) and KI (2%, w/v) (Boone *et al*. 2001). The temperature tolerance test was performed by growing the isolate in 100 mL nutrient broth using 250 mL Erlenmeyer flask and incubating at the temperatures ranging 20-60°C. Samples (2 mL) were withdrawn at a regular interval and the cell growth was measured at an absorbance of 600 nm using UV-visible spectrophotometer (Perkin Elmer, Lambda-45). Acid production after carbohydrate fermentation was observed by placing different carbohydrate discs (HiMedia Pvt. Ltd.) onto BHM agar plates with phenol red indicator (0.01%, w/v).

3.2.10 Antibiotic sensitivity pattern of isolate SS35

Antibiotic sensitivity and resistance of isolate SS35 was determined by disc diffusion method (Bauer *et al*. 1966). Briefly, cells were prepared by growing in nutrient broth for 18 h at 37ºC. 2% (v/v) inoculum was mixed with nutrient agar (0.7% agar) when temperature reached approximately 40ºC and then was poured on the plates and allowed to dry for 10 min. Different standard antibiotic discs (Octadisc, HiMedia Pvt. Ltd.) were placed on the surface of the plates and incubated for 24 h at 37ºC. After incubation isolate SS35 was observed as sensitive, moderate or resistant to an antibiotic according to the diameter of inhibition zone.

3.2.11 Identification of isolate SS35 on the basis of 16S ribosomal RNA (rRNA) and partial Gyrase A (*gyr*A) gene sequence analyses

The bacterial culture was grown in agar slant and sent to Xcelris Labs Limited, Ahmedabad, India, for identification by 16S ribosomal RNA (rRNA) and partial gyrase A (*gyr*A) gene amplification and sequencing.

3.2.11.1 Amplification of 16S rRNA and partial gyrA gene segments

The genomic DNA of the isolate SS35 was extracted, purified and amplified by Xcelris Labs Limited. The genomic DNA extraction was carried out using Qiagen DNA extraction kit and purified by QIAamp DNA Purification Kit (Qiagen). The universal 16S rRNA primer 8F (5'AGAGTTTGATCCTGGCTCAG3') and 1492R (5'ACGGCTACCTTGTTACGACTT3') were used for amplification of genomic DNA by polymerase chain reaction (PCR). The *gyr*A region was amplified using the primers, p-*gyr*A-F (5'CAGTCAGGAAATGCGTACGTCCTT 3') and p-*gyr*A-R (5'CAAGGTAATGCTCCAGGCATTGCT3') (Chun and Bae 2000). The concentration of each primer in 25 µL PCR reaction mixture was 10 pmol and 1x PCR master mix (MBI Fermentas). The PCR reaction was run for 30 cycles in a Thermal Cycler (Eppendorf) and the thermal profile used for the PCR was as follows: initial denaturation at 95°C for 2 min, final denaturation at 94°C for 30 s, primer annealing at 52°C for 30 s and extension at 72°C for 90 s. Full extension of the products was ensured by running a final cycle that included extension for 10 min at 72°C. PCR product of 5 µL from each tube was mixed with 1 µL of 6x gel loading

dye and this mixture was subjected to electrophoresis on 1.2% agarose gel to confirm the targeted PCR amplification.

3.2.11.2 Sequencing of 16S rRNA and partial gyrA gene segments

Sequencing reactions of both, 16S rRNA and partial *gyr*A gene segments was carried out by Xcelris Labs Ltd. The amplified product was excised from the gel and purified using QIAamp DNA Purification Kit (Qiagen). The purified DNA was subjected to automated DNA sequencing on ABI 3730xl Genetic Analyzer (Applied Biosystems, USA). The cycle sequencing was carried out using BigDye Terminator v3.1 Cycle sequencing kit following manufacturer's instructions. The cycle sequencing was carried out in a final reaction volume of 20 µL using 200 µL capacity PCR tube. The cycling protocol was designed for 25 cycles as follows: denaturation at 96°C for 10 s, annealing at 52°C for 5 s and extension at 60°C for 4 min. After cycling, the extension products were purified and mixed well in 10 µL of Hi-Di formamide. Eluted products were placed in a sample plate, heated at 95°C for 5 min, chilled and loaded into auto-sampler of the instrument.

3.2.11.3 Sequence analyses of 16S rRNA and partial gyrA gene segments

Sequences from forward and reverse sequencing reactions for both 16S rRNA and partial *gyr*A genes were provided by Xcelris Labs Ltd., Ahmedabad, India. The consensus sequences for 16S rRNA and partial *gyr*A genes were generated using aligner software and the resulted sequences were used to carry out Basic Local Alignment Search Tool (BLAST) with non-redundant database of NCBI GenBank

using MEGABLAST algorithm. Multiple sequence alignment was performed by using CLUSTAL W (Thompson *et al*. 1994) and evolutionary history was inferred using the neighbor-joining method (Saitou and Nei 1987). The evolutionary distances were computed using the Kimura 2-parameters method (Kimura 1980) and phylogenetic analysis was carried out with MEGA4 (Tamura *et al*. 2007).

3.3 Results and Discussion

3.3.1 Isolation and screening of cellulolytic bacteria by plate staining method

After 96 h of incubation colonies were observed on BHM-agar plates (Fig. 3.3.1). Total 36 discrete colonies were picked from different dilution plates and streaked on fresh BHM-agar medium supplemented with CMC.

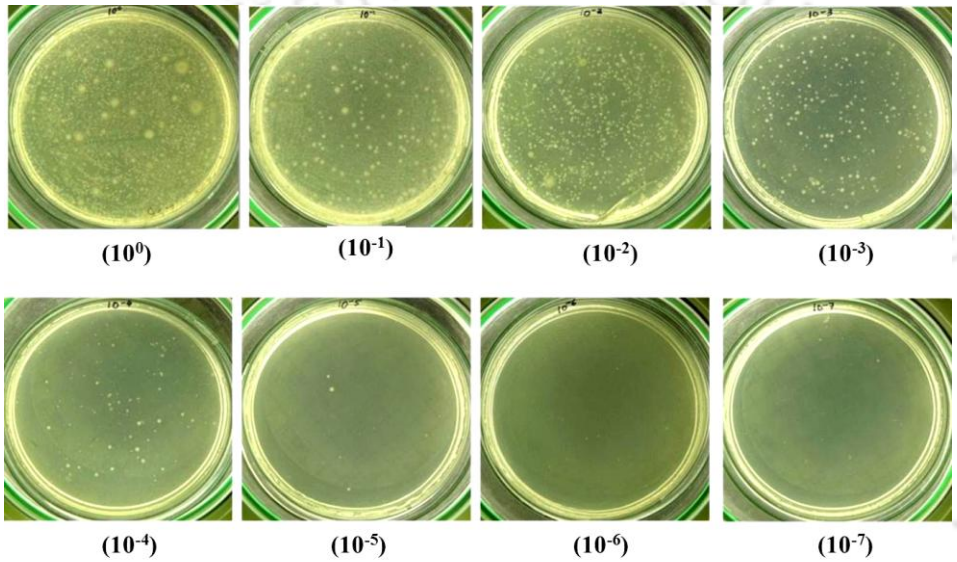

Fig. 3.3.1 BHM agar plates supplemented with 1% (w/v) carboxymethyl cellulose (CMC) showing growth of bacteria from different dilutions ranging from 10^0 to 10^{-7}.

Plate staining method revealed that among 36 isolates, 9 were cellulose hydrolysing strains. The isolates (no. 21, 24, 25, 28, 31, 32, 34, 35 and 36) showed clear zone around colonies after staining the plates with congo red and destaining with 1 M NaCl as shown in Fig. 3.3.2 (A1-C2). However, plate-screening method is not quantitative because of poor correlation between enzyme activity and colony to clear zone ratio (Maki *et al*. 2009). The colonies showing halo zones of yellow color

were picked from replica plate and further screened on the basis of CMCase production in liquid medium.

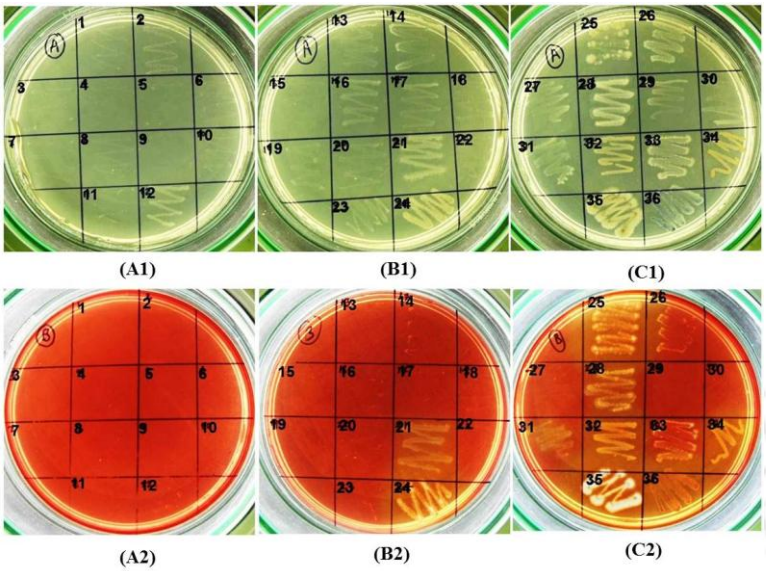

Fig. 3.3.2 Petri plates containing 1% (w/v) CMC agar incubated at 37°C for 96 h. (A1), (B1) and (C1) colonies before staining; (A2), (B2) and (C2) colonies after staining with 0.3% (w/v) congo red.

Out of 9 isolates, isolate no. 35 exhibited maximum CMCase activity of 0.079 U/mL (Table 3.3.1). This value was higher than activity of CMCase produced from some known natural isolates (expressed per mL of cell-free supernatant), for example, *Cellulomonas* sp. (0.0336 U/mL, isolated from coir retting effluents) (Immanuel *et al*. 2006), *Micrococcus* sp. (0.0152 U/mL, isolated from coir retting effluents) (Immanuel *et al*. 2006), *Bacillus* sp. (0.0197 U/mL, isolated from coir retting effluents) (Immanuel *et al*. 2006), *Brevibacillus* sp. JXL (0.02 U/mL, isolated from swine waste) (Liang *et al*. 2009), *Brevibacillus* sp. DUSELG12 (0.02 U/mL, isolated from goldmine) (Rastogi *et al*. 2009), *Geobacillus* sp. DUSELR7 (0.058 U/mL, isolated from goldmine) (Rastogi *et al*. 2009), *Geobacillus* sp. (0.0113 U/mL,

isolated from sugar refinery waste water) (Tai *et al*. 2004) and *Bacillus subtilis* AS3 (0.07 U/mL, isolated from cow dung) (Deka *et al*. 2011). Ariffin *et al*. (2006) reported maximum CMCase activity of 0.079 U/mL by *Bacillus pumilus* EB3 produced in a 2 L stirred tank reactor, which was equal to the CMCase activity of the isolate in this study. Thus, the isolate no. 35 was an efficient CMCase producing species and was designated as SS35.

Table 3.3.1 CMCase activity (U/mL) of cellulase producing isolates (after 48 h at 37°C, 180 rpm and medium pH 7.0).

Isolate no.	CMCase activity (U/mL)*
21	0.063 ± 0.008
24	0.059 ±0.003
25	0.072 ± 0.010
28	0.073 ± 0.008
31	0.071 ± 0.006
32	0.067 ± 0.007
34	0.057 ± 0.004
35	0.079 ± 0.002
36	0.049 ± 0.003

** values are mean ± SE (n = 3)*

This strain was further characterized for growth curve along with CMCase production profile (Fig. 3.3.3). This study revealed that the CMCase production was associated with cell growth and growth reached stationary phase after 48 h of incubation. The CMCase production reached at the maximum at the late log phase or early stationary phase of cell growth with a CMCase activity of 0.079 U/mL. Growth associated CMCase production from *Bacillus* spp. has been reported in various studies (Ariffin *et al*. 2006; Vijayaraghavan and Vincent 2012). Slight reduction in enzyme activity after 48 h could be a consequence of the denaturation of the enzyme at 37°C.

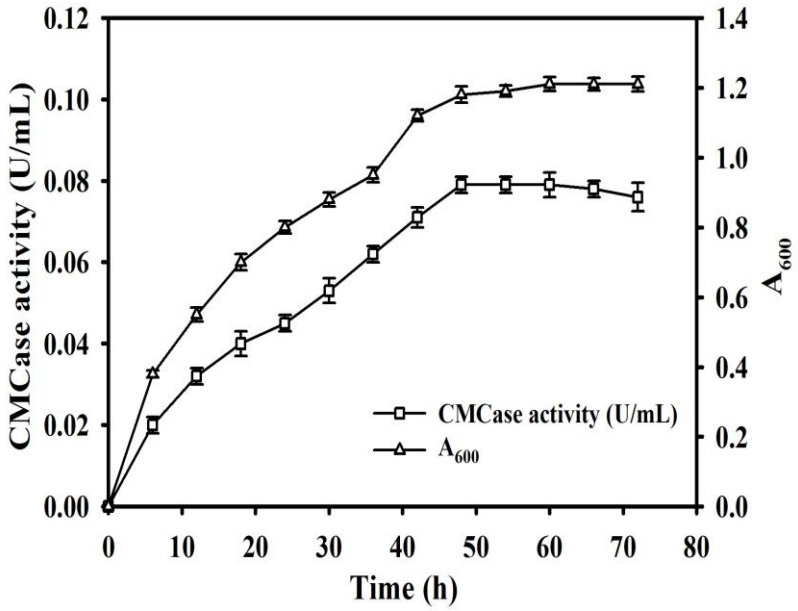

Fig. 3.3.3 Enzyme production profile and growth curve of isolate SS35 grown in enzyme production medium at 37°C and 180 rpm for 72 h.

3.3.2 Morphological and biochemical characterization of the isolate SS35

The colony morphology of the isolate SS35 on nutrient agar plate was observed to be circular, 4-5 mm in diameter, creamish appearance with undulated edges (Fig. 3.3.4A). The isolate was found to be rod-shaped cells with a width and length of 0.5-0.6 µm and 1.5-1.6 µm, respectively, as observed under scanning electron microscope (Fig. 3.3.4B). The isolate was Gram-positive (Fig. 3.3.4C), spore forming bacterium (Fig. 3.3.4D). It gave positive test for catalase which was indicated by appearance of bubbles of free oxygen gas (Fig. 3.3.4E) and nitrate reduction (Fig. 3.3.4F), whereas negative test for urease (Fig. 3.3.4G) as well as for hydrogen sulphide (Fig. 3.3.4H) production. The clear zone on the BHM-starch agar plate (Fig. 3.3.4I) showed that the bacterium hydrolysed starch by producing α-amylase. The temperature tolerance test revealed that the isolate was able to grow at a wide temperature range 20-50°C (Fig. 3.3.5) with an optimum growth at 40°C.

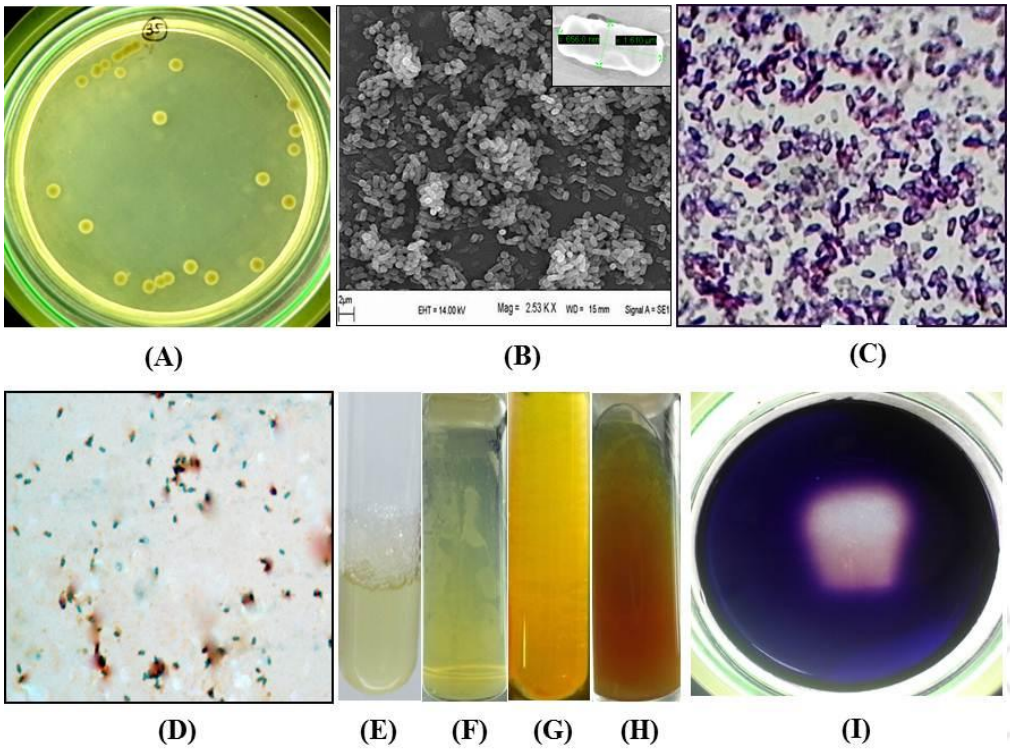

Fig. 3.3.4 Different morphological, biochemical and physiological properties of isolate SS35 (A) Colonies on nutrient agar plate (B) SEM image of the isolate with a single cell in inset (C) Gram staining of the isolate (D) Green colored endospores (E) Catalase test (F) Nitrate reduction test (G) Urease test (H) H_2S production test (I) Amylase test.

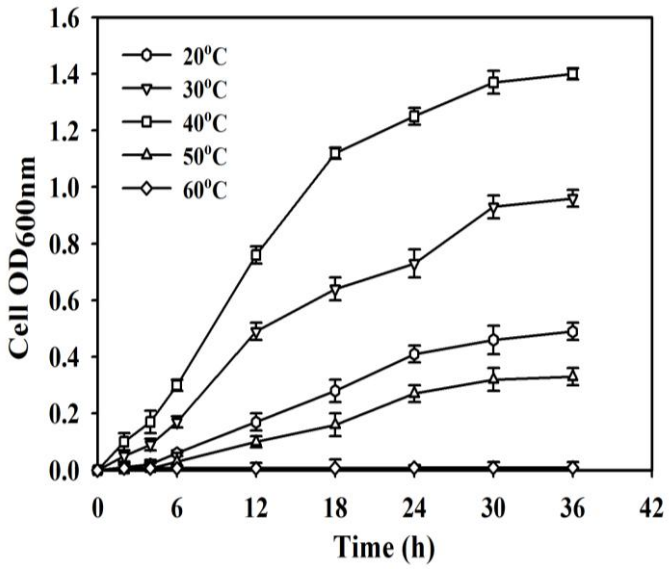

Fig. 3.3.5 Growth of isolate SS35 in nutrient broth at different temperatures, 180 rpm and initial medium pH 7.0.

Acid production after carbohydrate fermentation was detected by yellow zones around the carbohydrate discs (Fig. 3.3.6 B-H), which was because of change in pH after acid production from fermentation, indicated that the bacterium was able to ferment the sugars cellobiose, dextrose, fructose, maltose, mannitol, rhamnose, sucrose, xylose, salicin, arabinose, inositol, trehalose, mannose and has not fermented the sugars adonitol, raffinose, dulcitol, galactose, melibiose, sorbitol, inulin, lactose (Table 3.3.2).

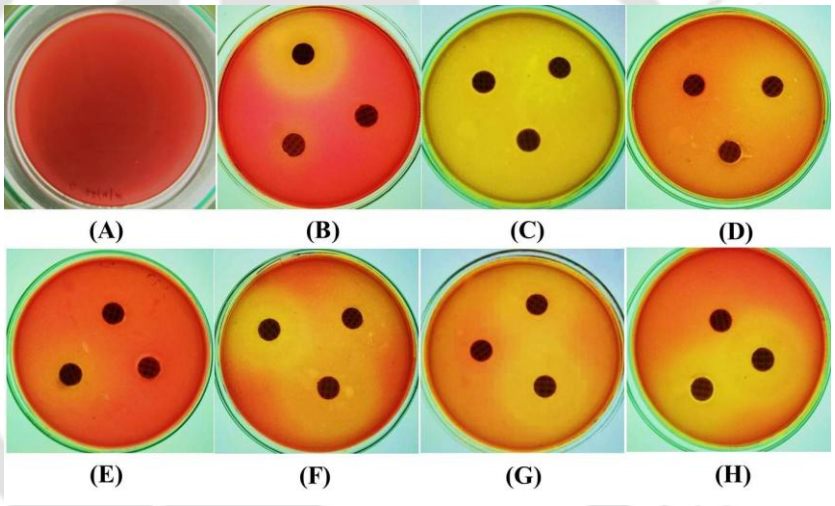

Fig. 3.3.6 BHM agar plates (A) negative control without any carbohydrate and inoculum, (B-H) with isolate SS35 culture and different carbohydrate discs.

The acid production specifically from salicin, mannose, maltose, arabinose and xylose suggested that the isolate was closer to *B. subtilis* and *B. subtilis* like species (Vos *et al*. 2011). Though the exact identification could not be ensured on the basis of morphological and biochemical properties. All these characteristics have been summarized in Table 3.3.2.

Table 3.3.2 Morphological and biochemical characteristics of isolate SS35.

Characteristic/biochemical test	Observation
Colony Diameter	4-5 mm
Colony shape and edges	Circular and undulate
Colony color	Creamish
Cell shape	Rod
Cell size	0.5-0.6 µm × 1.5-1.6 µm
Gram reaction	+
Endospore formation	+
Acid production from:	
Cellobiose (Ce)	+
Dextrose (De)	+
Fructose (Fc)	+
Maltose (Ma)	+
Mannitol (Mn)	+
Rhamnose (Rh)	+
Sucrose (Su)	+
Xylose (Xy)	+
Salicin (Sa)	+
Sorbitol (Sb)	-
Inulin (In)	-
Arabinose (Ar)	+
Lactose (La)	-
Inositol (Is)	+
Adonitol (Ad)	-
Mannose (Mo)	+
Raffinose (Rf)	-
Dulcitol (Du)	-
Galactose (Ga)	-
Melibiose (Mb)	-
Trehalose (Te)	+
Catalase test	+
Urease test	-
NO_3 reduction into NO_2	+
H_2S production	-
Growth between 20-50°C	+
Starch hydrolysis	+

+, positive reaction; -, negative reaction

3.3.3 Antibiotic sensitivity pattern of isolate SS35

The isolate was further tested for response towards different classes of antibiotics. All the antibiotics tested in this study inhibited the growth of the isolate

to some extent (Fig. 3.3.7 C-H), except few from the class Penicillin (penicillin, ampicillin, carbenicillin and ticarcillin) and cephalosporin. On the basis of extent of antibiotic action the isolate was characterized under three categories *viz*., resistant, moderate and sensitive which has been summarized in Table 3.3.3.

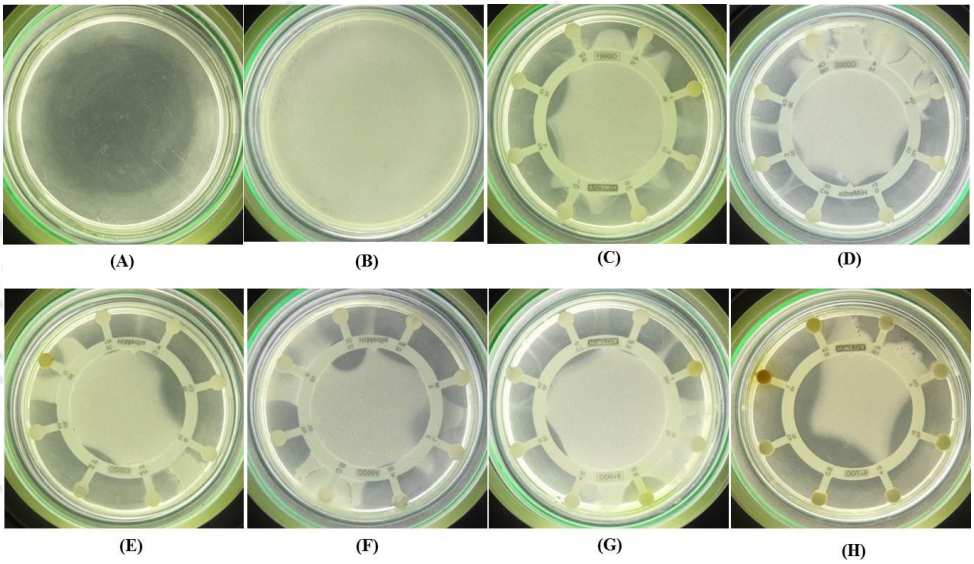

Fig. 3.3.7 Antibiogram of isolate SS35 towards different antibiotics using antibiotic octadiscs on nutrient agar plates (A) plate without culture as negative control, (B) plate with culture and without any antibiotic as positive control and (C-H) antibiotic octadisc on isolate SS35 culture plates.

Resistance of isolate SS35 towards penicillin has been shown by few studies earlier (Dias *et al*. 1986; Parker and Collier 1990). Resistance towards penicillin, ampicillin and cephalosporin may also be the result of the production of a broad spectrum of *β*-lactamase (Vos *et al*. 2011).

Table 3.3.3 Effect of different antibiotics on growth of isolate SS35.

Antibiotic	Concentration (mg)	Radius of clear zone (cm)	Response
Carbenicillin (Cb)	100	-	R
Cephatotaxime (Ce)	30	1.2	M
Chloramphenicol (C)	30	1.3	M
Co-Trimazine (Cm)	25	2	S
Gentamicin (G)	10	1.8	S
Oxacillin (Ox)	5	1.1	M
Cephalexin (Cp)	10	1.2	M
Ciprofloxacin (Cf)	10	2.2	S
Clindamycin (Cd)	2	1.9	S
Cloxacillin (Cx)	1	1.1	M
Co-trimoxazole (Co)	25	1.3	M
Erythromycin (E)	15	1.3	M
Amoxiclav (Ac)	10	0.9	M
Amoxycillin (Am)	10	1.2	M
Bacitracin (B)	10	0.6	M
Cephalothin (Ch)	10 units	2.4	S
Novobiocin (Nv)	30	1.5	M
Oxytetracyclin (O)	30	0.8	M
Vancomycin (Va)	30	1.4	M
Amikacin (Ak)	10 mcg	1.9	S
Kanamycin (K)	30	1.7	S
Linomycin (L)	2	1.2	M
Methicillin (M)	5	1.2	M
Oleandomycin (Ol)	15	1.3	M
Penicillin G (P)	10 units	-	R
Tobramycin (Tb)	10	1.5	M
Cephaloridin (Cr)	30	-	R
Ampicillin (A)	25	-	R
Nitrofurantoin (Nf)	50	1	M
Ticarcillin (Ti)	75	-	R
Tetracyclin (T)	100	1.5	M
Nalidixic acid (Na)	30	1.4	M
Trimethoprim (Tr)	2.5	1.2	M
Sulphamethoxazole (Sx)	50	1.2	M
Gentamicin (G)	10	1.8	S
Norfloxacin (Nx)	10	2.3	S
Cefixime (Cfx)	5	-	R
Piperacillin (Pc)	100	1	M
Ceftazidime (Ca)	30	0.8	M
Imipenam (I)	10	2.4	S
Cefoperazone (Cs)	75	0.5	R
Cefaclor (Cj)	30	2.7	S

R (resistant): 0-0.5 cm, M (moderate): 0.6-1.5 cm, S (sensitive): 1.6-2.7 cm.

3.3.4 Identification of isolate SS35 on the basis of phylogenetic analyses

3.3.4.1 Amplification and sequencing of 16S ribosomal RNA (rRNA) and partial Gyrase A (gyrA) gene segments

The 16S ribosomal RNA **(**rRNA) and partial gyrase A (*gyr*A) gene segments were amplified and sequenced by Xcelris Labs Limited, Ahmedabad, India. Discrete PCR amplicons of 1.5 kbp and 1 kbp for 16S rRNA and partial *gyr*A gene, respectively, were obtained (Fig. 3.3.8A and B).

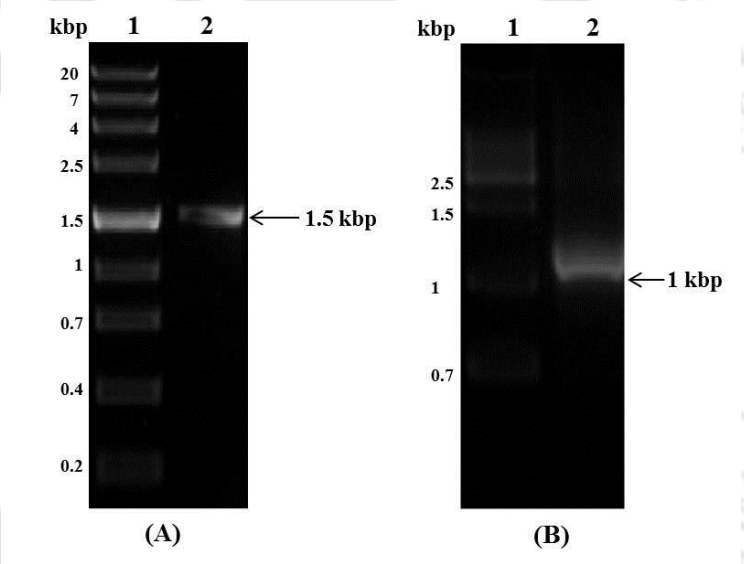

Fig. 3.3.8 The amplicons resolved on 1.2% agarose gel (A) 16S rRNA gene of isolate SS35 (1.5 kbp); Lane 1: DNA Ladder, Lane 2: amplified product of full length 16S rRNA gene. (B) partial gyrase A gene of isolate SS35 (1 kbp); Lane 1: DNA Ladder, Lane 2: amplified product of partial gyrase A gene.

3.3.4.2 Analyses of 16S ribosomal RNA (rRNA) and partial Gyrase A (gyrA) gene sequences

Consensus sequences of 1380 bp and 948 bp of 16S rRNA and partial *gyr*A amplicons, respectively, were generated from forward and reverse sequences using the aligner software.

16S rRNA consensus sequence (1380 bp)

GACAGATGGGAGCTTGCTCCCTGATGTTAGCGGCGGACGGGTGAGTAACACGTGGGTAACCTGCCTG
TAAGACTGGGATAACTCCGGGAAACCGGGGCTAATACCGGATGGTTGTTTGAACCGCATGGTTCAGA
CATAAAAGGTGGCTTCGGCTACCACTTACAGATGGACCCGCGGCGCATTAGCTAGTTGGTGAGGTAAC
GGCTCACCAAGGCGACGATGCGTAGCCGACCTGAGAGGGTGATCGGCCACACTGGGACTGAGACAC
GGCCCAGACTCCTACGGGAGGCAGCAGTAGGGAATCTTCCGCAATGGACGAAAGTCTGACGGAGCA
ACGCCGCGTGAGTGATGAAGGTTTTCGGATCGTAAAGCTCTGTTGTTAGGGAAGAACAAGTGCCGTT
CAAATAGGGCGGCACCTTGACGGTACCTAACCAGAAAGCCACGGCTAACTACGTGCCAGCAGCCGC
GGTAATACGTAGGTGGCAAGCGTTGTCCGGAATTATTGGGCGTAAAGGGCTCGCAGGCGGTTTCTTAA
GTCTGATGTGAAAGCCCCCGGCTCAACCGGGGAGGGTCATTGGAAACTGGGGAACTTGAGTGCAGA
AGAGGAGAGTGGAATTCCACGTGTAGCGGTGAAATGCGTAGAGATGTGGAGGAACACCAGTGGCGA
AGGCGACTCTCTGGTCTGTAACTGACGCTGAGGAGCGAAAGCGTGGGGAGCGAACAGGATTAGATA
CCCTGGTAGTCCACGCCGTAAACGATGAGTGCTAAGTGTTAGGGGGTTTCCGCCCCTTAGTGCTGCAG
CTAACGCATTAAGCACTCCGCCTGGGGAGTACGGTCGCAAGACTGAAACTCAAAGGAATTGACGGG
GGCCCGCACAAGCGGTGGAGCATGTGGTTTAATTCGAAGCAACGCGAAGAACCTTACCAGGTCTTGA
CATCCTCTGACAATCCTAGAGATAGGACGTCCCCTTCGGGGGCAGAGTGACAGGTGGTGCATGGTTG
TCGTCAGCTCGTGTCGTGAGATGTTGGGTTAAGTCCCGCAACGAGCGCAACCCTTGATCTTAGTTGCC
AGCATTCAGTTGGGCACTCTAAGGTGACTGCCGGTGACAAACCGGAGGAAGGTGGGGATGACGTCA
AATCATCATGCCCCTTATGACCTGGGCTACACACGTGCTACAATGGACAGAACAAAGGGCAGCGAAA
CCGCGAGGTTAAGCCAATCCCACAAATCTGTTCTCAGTTCGGATCGCAGTCTGCAACTCGACTGCGT
GAAGCTGGAATCGCTAGTAATCGCGGATCAGCATGCCGCGGTGAATACGTTCCCGGGCCTTGTACACA
CCGCCCGTCACACCACGAGAGTTTGTAACACCCGAAGTCGGTG

Gyrase A consensus sequence (948bp)

GCAATGAGCGTTATCGTATCCCGGGCGCTTCCGGATGTGCGTGACGGTCTGAAGCCGGTTCACAGAC
GGATTTTGTACGCAATGAATGATTTAGGCATGACCAGTGACAAACCATATAAAAAATCTGCCCGTATCG
TCGGTGAAGTTATCGGTAAGTACCATCCGCACGGTGACTCAGCGGTTTACGAATCAATGGTCAGAATG
GCGCAGGATTTTAACTACCGCTACATGCTTGTTGACGGACACGGCAACTTCGGTTCGGTTGACGGCG
ACTCAGCGGCCGCGATGCGTTACACAGAAGCGAGAATGTCAAAAATCGCAATGGAAATTCTGCGTGA
CATTACGAAAGATACGATTGATTATCAAGATAACTATGACGGCGCAGAAAGAGAACCTGTCGTCATGC
CTTCGAGATTTCCGAATCTGCTCGTAAACGGAGCTGCCGGTATTGCGGTCGGAATGGCGACAAATATT
CCTCCGCATCAGCTTGGGGAAGTCATTGAAGGCGTGCTTGCCGTAAGTGAGAATCCTGAGATTACAA
ACCAGGAGCTGATGGAATACATTCCGGGCCCGGATTTTCCGACTGCTGGTCAGATTTTGGGCCGGAG
CGGCATCCGCAAGGCATATGAATCCGGACGGGGATCAATCACAATCCGGGCTAAGGCTGAAATCGAA
GAGACATCATCAGGAAAAGAAAGAATTATTGTTACGGAACTTCCTTATCAGGTGAACAAAGCGAGAT
TAATTGAAAAAATCGCAGATCTTGTCCGAGACAAAAAAATCGAAGGAATTACCGACCTGCGAGACGA
ATCCGACCGTAACGGAATGAGAATCGTCATTGAGATCCGCCGTGACGCCAATGCTCACGTCATTTTGA
ATAACCTGTACAAACAAACGGCCCTGCAGACGTCTTTCGGAATCAACCTGCTGGCGCTCGTTGACGG
ACAG

The phylogenetic tree generated using 16S rRNA gene sequences of the isolate SS35 showed that the bacterium has the highest homology with *Bacillus amyloliquefaciens* NBRC 3035 (Gen-Bank accession no.: AB679994.1) (Fig. 3.3.9).

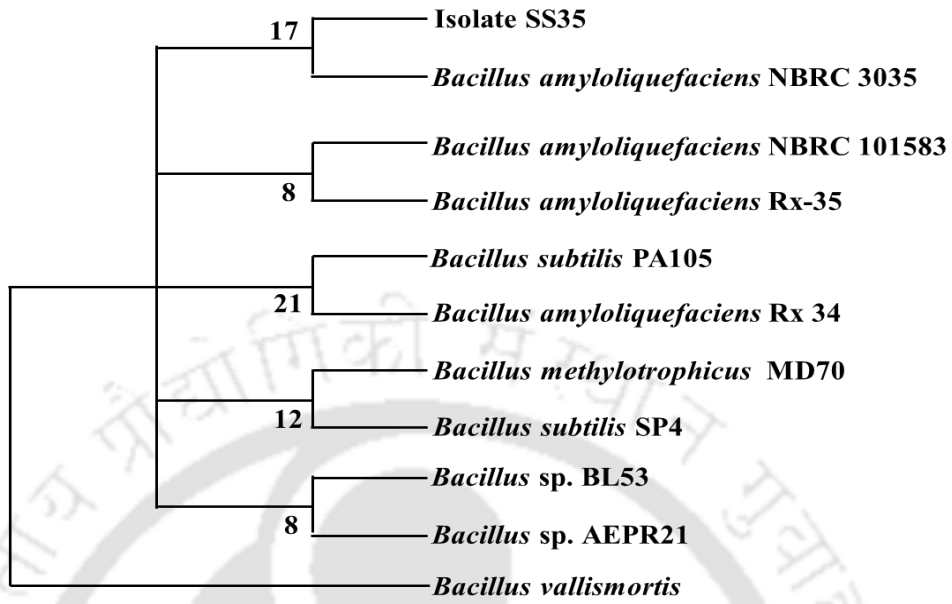

Fig. 3.3.9 Neighbor-joining tree based on 16S rRNA gene sequences of *B. amyloliquefaciens* SS35. Numbers at nodes of the tree are indications of the levels of bootstrap support based on a neighbour-joining analysis of 500 resampled datasets.

The bacterial identification using 16S rRNA gene sequence is a widely practiced technique, although with limitations for the members of closely related taxa (Fox *et al*. 1992). To overcome this limitation, several studies have been done, which concluded that some protein-coding genes such as RNA polymerase (*rpo*B) gene (Kim *et al*. 1999), RNA polymerase sigma factor (*rpo*D) gene, gyrase B (*gyr*B) gene (Yamamoto and Harayama, 1998) and gyrase A (*gyr*A) gene (Chun and Bae, 2000) can be used for the identification of closely related taxa, because the genetic variation in protein-coding genes are much higher.

Chun and Bae (2000) demonstrated that the *gyr*A sequences coding for DNA gyrase subunit A, can be used for accurate identification of *Bacillus amyloliquefaciens* and related taxa including *Bacillus subtilis*, *Bacillus vallismortis*,

Bacillus mojavensis, *Bacillus atrophaeus* and *Bacillus licheniformis*. Therefore, in this study, partial *gyr*A gene sequences have been used for the confirmation of the result obtained from 16S rRNA sequence analysis. The phylogenetic analysis using partial *gyr*A gene sequences also revealed that the isolate SS35 has the highest homology with *Bacillus amyloliquefaciens* FZB45 (GenBank accession no.: FN662840.1) (Idriss *et al*. 2002), as shown in Fig. 3.3.10.

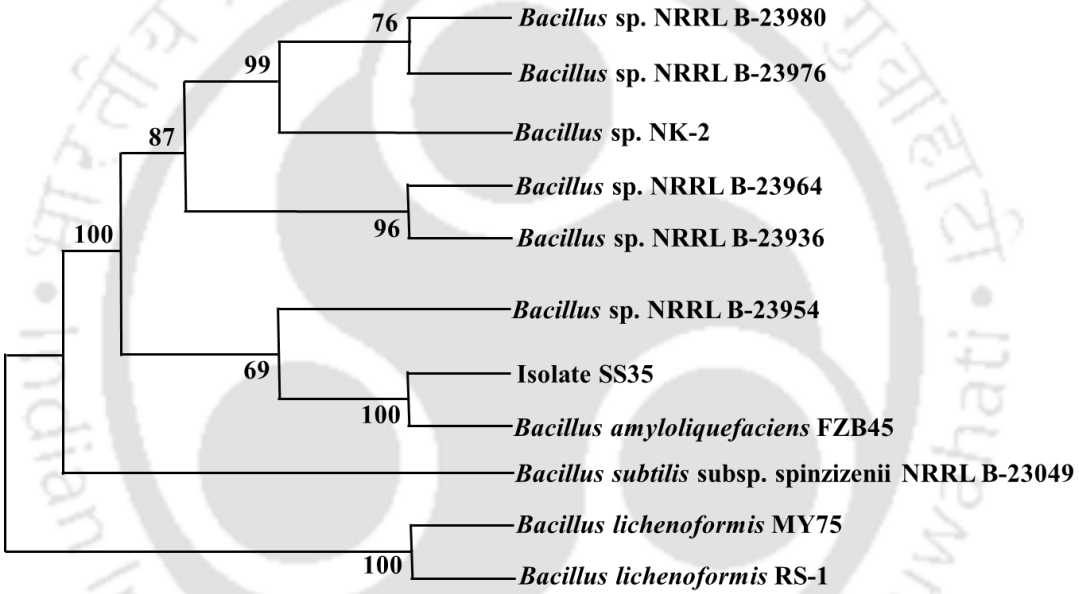

Fig. 3.3.10 Neighbor-joining tree based on partial *gyr*A gene sequences of *B. amyloliquefaciens* SS35. Numbers at nodes of the tree are indications of the levels of bootstrap support based on a neighbour-joining analysis of 1000 resampled datasets.

The isolate SS35 was identified as *Bacillus amyloliquefaciens* and designated as *Bacillus amyloliquefaciens* SS35. The 16S rRNA and *gyr*A gene sequences of the isolate *B. amyloliquefaciens* SS35 have been deposited in the NCBI nucleotide sequence database under the accession numbers JX674030 and KF019284, respectively.

3.4 Conclusions

Cellulose hydrolytic bacteria were isolated from rhinoceros dung and screened on the basis of plate staining method and CMCase production in liquid medium. Among all cellulolytic bacteria, isolate no. 35 exhibited maximum enzyme activity of 0.079 U/mL at 37ºC, 180 rpm and initial medium pH 7.0, therefore it was selected for further identification and characterization. The CMCase production was cell growth associated displaying maxima at the late exponential phase of growth. Morphological, physiological and biochemical characteristics of isolate SS35 revealed that it is a rod-shaped, Gram positive and spore forming bacterium. SEM analysis showed that the dimension of a single cell of isolate SS35 was 0.5-0.6 µm × 1.5-1.6 µm. Isolate SS35 showed positive results for catalase and nitrate tests and negative results for urease and H_2S production. Amylase production by isolate SS35 was indicated by the hydrolysis of starch on the agar plate. The isolate SS35 displayed significant growth within a range of 20-50ºC and was not able to ferment adonitol, raffinose, dulcitol, galactose, melibiose, sorbitol, inulin and lactose. The antibiotic test revealed that the isolate SS35 was resistant to penicillin, cephaloridin, ampicillin, ticarcillin, cefixime and cefoperazone, a prominent attribute of genus *Bacillus*. The isolate was identified as *Bacillus amyloliquefaciens* SS35 on the basis of 16S rRNA gene (GenBank accession no.: JX674030) and partial gyrase A gene sequence (GenBank accession no.: KF019284) analyses. The isolate *B. amyloliquefaciens* SS35 was found to be a potential candidate for CMCase production which can be utilized for cellulase assisted hydrolysis of lignocellulosic wastes and subsequently for bioethanol production.

References

Akhtar, N., Sharma, A., Deka, D., Jawed, M., Goyal, D. and Goyal, A. (2013) Characterization of cellulase producing *Bacillus* sp. for effective degradation of leaf litter biomass. Environmental Progress and Sustainable Energy, 32, 1195-1201.

Ariffin, H., Abdullah, N., Kalsom, M. S. U., Shirai, Y. and Hassan, M. A. (2006) Production and characterization of cellulase by *Bacillus pumilus* EB3. International Journal of Engineering and Technology, 3, 47-53.

Ash, C., Farrow, J. A. E., Wallbanks, S. and Collins, M. D. (1991) Phylogenetic heterogeneity of the genus *Bacillus* revealed by comparative analysis of small-subunit-ribosomal RNA sequences. Letters in Applied Microbiology, 13, 202-206.

Atlas, R. M. (2004) Handbook of Microbiological Media, CRC Press, Boca Raton, Fla, USA, 3rd edition.

Bauer, A. W., Kirby, W. M. M., Sherris, J. C. and Tuck, M. (1966) Antibiotics susceptibility testing by a standardized single disc method. American Journal of Clinical Pathology, 45, 493-496.

Bayer, E. A., Lamed, R. and Himmel M. E. (2007) The potential of cellulases and cellulosomes for cellulosic waste management. Current Opinion in Biotechnology, 18, 237-245.

Bhat, M. K. and Bhat, S. (1997) Cellulose degrading enzymes and their potential industrial application. Biotechnology Advances, 15, 583-620.

Boone, D. R., Garrity, G. M., Castenholz, R. W., Brenner, D. J., Krieg, N. R. and Staley, J. T. (2001) Genus *Bacillus* in Bergey's manual of systematic bacteriology: The Firmicutes, Springer, NewYork, NY, USA, 2nd edition, 3, 21-128.

Bushnell, D. L. and Haas, H. F. (1941) The utilization of certain hydrocarbons by microorganisms. Kansas Agricultural Experiment Station, 199, 653-673.

Cappuccino, J. C. and Sherman, N. (2004) Microbiology—A laboratory manual, Pearson Education Publication, New Delhi, India, 7th edition.

Chun, J. and Bae, K. S. (2000) Phylogenetic analysis of *Bacillus subtilis* and related taxa based on partial *gyr*A gene sequences. Antonie van Leeuwenhoek, 78, 123-127.

Das, S. P., Ghosh, A., Gupta, A., Goyal, A. and Das, D. (2013) Lignocellulosic fermentation of wild grass employing recombinant hydrolytic enzymes and fermentative microbes with effective bioethanol recovery. BioMed Research International, Article ID 386063, 14 pages.

Deka, D., Bhargavi, P., Sharma, A., Goyal, D., Jawed, M. and Goyal, A. (2011) Enhancement of cellulase activity from a new strain of *Bacillus subtilis* by medium optimisation and analysis with various cellulosic substrates. Enzyme Research, Article ID 151656, 8 pages.

Dias, F. F., Shaikh, M. K. G., Bhatt, Y. B., Modi, D. C. and Subramanyan, V. R. (1986) Tunicamycin resistant mutants of *Bacillus amyloliquefaciens* are deficient in amylase, protease and penicillinase synthesis and have altered

sensitivity to antibiotics and autolysis. Journal of Applied Bacteriology 60, 271-275.

Doi, R. H. (2008) Cellulases of mesophilic microorganisms: cellulosome and noncellulosome producers. Annals of the New York Academy of Sciences, 1125, 267-279.

Fox, G. E., Wisotzkey, J. D. and Jurtshuk, P. (1992) How close is close: 16S rRNA sequence identity may not be sufficient to guarantee species identity. International Journal of Systematic Bacteriology, 42, 166-170.

Fukumoto, J. (1943a) Studies on the production of bacterial amylase. I. Isolation of bacteria secreting potent amylase and their distribution. Journal of Agricultural Chemical Society of Japan, 19, 487-503.

Fukumoto, J. (1943b) Studies on the production of bacterial amylase. II. Bacterial and physiological nature. Journal of Agricultural Chemical Society of Japan,19, 643-650.

Glauert, A. M. (1965) The Fixation and embedding of biological tissues, In: Desmond, H. K. (ed) Techniques for electron microscopy, 2nd edn. Davis FA Co., Philadelphia.

Idriss, E. E., Makarewicz, O., Farouk A. *et al*. (2002) Extracellular phytase activity of *Bacillus amyloliquefaciens* FZB45 contributes to its plant-growth-promoting effect. Microbiology, 148, 2097-2109.

Immanuel, G., Dhanusha, R., Prema, P. and Palavesam, A. (2006) Effect of different growth parameters on endoglucanase enzyme activity by bacteria isolated

from coir retting effluents of estuarine environment. International Journal of Environmental Science and Technology, 3, 25-34.

Kannan, N. (2002) Laboratory Manual in General Microbiology, Panima Publishing Corporation, New Delhi, India.

Kim, B. J., Lee, S. H., Lyu, M. A., Kim, S. J., Bai, G. H., Kim, S. J., Chae, G. T., Kim, E. C., Cha, C. Y., and Kook, Y. H. (1999) Identification of mycobacterial species by comparative sequence analysis of the RNA polymerase gene (*rpo*B). Journal of Clinical Microbiology, 37, 1714-1720.

Kim, B. K., Lee, B. H., Lee, Y. J., Jin, I. H. Chung, C. H. and Lee, J. W. (2009) Purification and characterization of carboxymethylcellulase isolated from a marine bacterium, *Bacillus subtilis* subsp. subtilis A-53. Enzyme and Microbial Technology, 44, 411-416.

Kimura, M. (1980) A simple method for estimating evolutionary rates of base substitutions through comparative studies of nucleotide sequences. Journal of Molecular Evolution, 16, 111-120.

Krause, D. O., Denman, S. E., Mackie R. I. *et al*. (2003) Opportunities to improve fiber degradation in the rumen: microbiology, ecology and genomics. FEMS Microbiology Reviews, 27, 663-693.

Krishna, P., Arora, A. and Reddy, M. S. (2008) An alkaliphilic and xylanolytic strain of actinomycetes *Kocuria* sp. RM1 isolated from extremely alkaline bauxite residue sites. World Journal of Microbiology and Biotechnology, 24, 3079-3085.

Lee, Y. J., Kim, B. K., Lee, B. H., Jo, K. I., Lee, N. K., Chung, C. H., Lee, Y. C. and Lee, J. W. (2008) Purification and characterization of cellulase produced by *Bacillus amyloliquefaciens* DL-3 utilizing rice hull. Bioresource Technology, 99, 378-386.

Liang, Y., Yesuf, J., Schmitt, S., Bender, K. and Bozzola, J. (2009) Study of cellulases from a newly isolated thermophilic and cellulolytic *Brevibacillus* sp. strain JXL. Journal of Industrial Microbiology and Biotechnology, 36, 961-970.

Lynd, L. R., Weimer, P. J., Van Zyl, W. H. and Pretorius, I. S. (2002) Microbial cellulose utilization: Fundamentals and biotechnology. Microbiology and Molecular Biology Reviews, 66, 506-577.

Maki, M., Leung, K. T. and Qin, W. (2009) The prospects of cellulase-producing bacteria for the bioconversion of lignocellulosic biomass. International Journal of Biological Sciences, 5, 500-516.

Martin, C., Lopez, Y., Plasencia, Y. and Hernandez, E. (2006) Characterisation of agricultural and agro-industrial residues as raw materials for ethanol production. Chemical and Biochemical Engineering Quarterly, 20, 443-447.

Mollet, C., Drancourt, M. and Raoult, D. (1997) *rpo*B sequence analysis as a novel basis for bacterial identification. Molecular Microbiology, 26, 1005-1011.

Murashima, K., Nishimura, T., Nakamura Y. *et al*. (2002) Purification and characterization of new endo-1,4-β-D-glucanases from *Rhizopus oryzae*. Enzyme and Microbial Technology, 30, 319-326.

Nakamura, L. K., Roberts, M. S. and Cohan, F. M. (1999) Relationship of *Bacillus subtilis* clades associated with strains 168 and W23: a proposal for *Bacillus subtilis* subsp. Subtilis subsp. nov. and *Bacillus subtilis* subsp. *spizizenii* subsp. nov. International Journal of Systematic Bacteriology, 49, 1211-1215.

Nelson, N. (1944) A photometric adaptation of the Somogyi method for the determination of glucose. Journal of Biological Chemistry, 153, 375-380.

Parker, M. T. and Collier, L. H. (1990) Principles of bacteriology, virology and immunity. 7th. Ed., vol. 2. D. C. Decker, Philadelphia.

Priest, F. G., Goodfellow, M., Shute, L. A. and Berkeley, R. C. W. (1987) *Bacillus amyloliquefaciens* sp. nov., nom. rev. International Journal of Systematic Bacteriology, 37, 69-71.

Rastogi, G., Muppidi, G. L., Gurram R. N. *et al*. (2009) Isolation and characterization of cellulose-degrading bacteria from the deep subsurface of the Homestake gold mine, Lead, South Dakota, USA. Journal of Industrial Microbiology and Biotechnology, 36, 585-598.

Roboson, L. M. and Chambliss, G. H. (1989) Cellulases of bacterial origin. Enzyme and Microbial Technology, 11, 626-644.

Ruijssenaars, H. J. and Hartmans, S. (2001) Plate screening methods for the detection of polysaccharase-producing microorganisms. Applied Microbiology and Biotechnology, 55, 143-149.

Saito, K., Kawamura, Y. and Oda Y. (2003) Role of the pectinolytic enzyme in the lactic acid fermentation of potato pulp by *Rhizopus oryzae*. Journal of Industrial Microbiology and Biotechnology, 30, 440-444.

Saitou, N. and Nei, M. (1987) The neighbor-joining method: a new method for reconstructing phylogenetic trees. Molecular biology and Evolution, 4, 406-425.

Sanchez, O. J. and Cardona, C. A. (2008) Trends in biotechnological production of fuel ethanol from different feedstocks. Bioresource Technology, 99, 5270-5295.

Skerman, V. B. D., McGowan, V. and Sneath, P. H. A. (1980) Approved lists of bacterial names. International Journal of Systematic Bacteriology, 30, 225-420.

Somogyi, M. (1945) A new reagent for the determination of sugars. Journal of Biological Chemistry, 160, 61-68.

Sun, Y. and Cheng, J. (2002) Hydrolysis of lignocellulosic materials for ethanol production: a review. Bioresource Technology, 83, 1-11.

Tai, S. K., Lin, H. P. P., Kuo, J. and Liu, J. K. (2004) Isolation and characterization of a cellulolytic *Geobacillus thermoleovorans* T4 strain from sugar refinery wastewater. Extremophiles, 8, 345-349.

Tamura, K., Dudley, J., Nei, M. and Kumar, S. (2007) MEGA4:Molecular Evolutionary Genetics Analysis (MEGA) software version 4.0. Molecular Biology and Evolution, 24, 1596-1599.

Teather, R. M. and Wood, P. J. (1982) Use of Congo red-polysaccharide interactions in enumeration and characterization of cellulolytic bacteria from the bovine rumen. Applied and Environmental Microbiology, 43, 777-780.

Thompson, J. D., Higgins, D. G. and Gibson, T. J. (1994) CLUSTAL W: improving the sensitivity of progressive multiple sequence alignment through sequence weighting, position-specific gap penalties and weight matrix choice. Nucleic Acids Research, 22, 4673-4680.

Varga, G. A. and Kovler, E. S. (1997) Microbial and animal limitation to fiber digestion and utilization. Journal of Nutrition, 127, 819-823.

Vijayaraghavan, P. and Vincent, S. G. P. (2012) Purification and characterization of carboxymethyl cellulase from *Bacillus* sp. isolated from a paddy field. Polish Journal of Microbiology, 61, 51-55.

Vos, P. D., Boone, D. R., Garrity, G. M., Castenholz, R. W., Brenner, D. J., Krieg, N. R. and Staley, J. T. (2011) Bergey's manual of systematic bacteriology: The Firmicutes, vol. 3, Springer.

Wahyudi, A., Cahyanto, M. N., Soejono, M. and Bachruddin, Z. (2010) Potency of lignocellulose degrading bacteria isolated from Buffalo and horse gastrointestinal tract and elephant dung for feed fiber degradation. Journal of the Indonesian Tropical Animal and Agriculture, 35, 34-41.

Yamamoto, S. and Harayama, S. (1998) Phylogenetic relationships of *Pseudomonas putida* strains deduced from the nucleotide sequences of *gyr*B, *rpo*D and 16S rRNA genes. International Journal of Systematic Bacteriology, 48, 813-819.

Yamamoto, S., Bouvet, P. J. and Harayama, S. (1999) Phylogenetic structures of the genus *Acinetobacter* based on *gyr*B sequences: comparison with the grouping by DNA-DNA hybridization. International Journal of Systematic Bacteriology, 49, 87–95.

Chapter 4

Optimization of carboxymethylcellulase production from *Bacillus amyloliquefaciens* SS35 by response surface methodology

4.1 Introduction

Cellulases, which essentially are the suite of enzymes that act synergistically for complete hydrolysis of cellulose to glucose, include: endoglucanases (carboxymethylcellulase), exoglucanases (avicelase) and cellobiases (*β*-glucosidase) (Lynd *et al*. 2002). Among cellulase enzymes, carboxymethylcellulase (CMCase) has been predominantly used in the process of ethanol production (Ballesteros *et al*. 2004, Zheng *et al*. 2009, Singh and Bishnoi 2012). Commercial cellulases are produced by fungi *viz*. *Aspergillus niger* and *Trichoderma reesei*. Bacteria have been also considered and used as robust and versatile enzyme producers because of their high growth rate, stability under extreme conditions and existence as multi-enzyme complexes. Among these, *Bacillus* spp. are more popular extracellular enzyme producer (Singh *et al*. 2001, Pason *et al*. 2006, Khan and Husaini 2006, Lee *et al*. 2008, Van Dyk *et al*. 2009, Kim *et al*. 2009). Enzymatic hydrolysis of cellulosic biomass is an important step in the production of bioethanol. Enzyme being an expensive component of this process, the economical production of cellulase is an

important aspect for bioethanol production. The extent of enzyme production by a microbial culture is a function of fermentation parameters and medium components. In this study, the medium composition and fermentation parameters of *Bacillus amyloliquefaciens* SS35 culture was optimized for CMCase production using statistical design of experiments. The conventional optimization technique is one-variable-at-a-time (OVAT) method; however, this method has limitations in which it is not able to identify the combined or interactive effect of different factors. Statistical experimental designs such as central composite design fitted with second-order model can be applied to overcome this limitation. In this study, we have addressed the matter of optimization of medium as well as fermentation parameters for the *B. amyloliquefaciens* SS35 to have enhanced enzyme production. A two-stage methodology was employed for the optimization of medium composition, considering large number of medium components. The initial screening of medium components was done by using Plackett-Burman design to identify the components having most significant influence on response variable, i.e. CMCase activity. This is followed by a central composite design for identification of optimum values of the significant components identified earlier for enhanced CMCase activity. The regression coefficients and ANOVA of the second-order model also help in identifying the interaction between significant medium components. The CCD design preceded by OVAT method was used for optimization of fermentation parameters.

4.2 Materials and Methods

4.2.1 Materials

Carboxymethylcellulose (CMC) (low viscosity, 50-200 cP) was procured from Sigma-Aldrich (St. Louis, USA) and medium components (listed in section 4.2.2) were procured from HiMedia Pvt. Ltd., India.

4.2.2 Microorganism and culture conditions

The bacterium used in this study, *B. amyloliquefaciens* SS35 was isolated from rhinoceros dung (Chapter 3, Section 3.2.3) (Singh *et al*. 2013) and the bacterial culture was maintained on nutrient agar slants. The basic medium used for CMCase production under unoptimized conditions, contained (g/L): CMC-Na (10.0), yeast extract (5.0), peptone (5.0), K_2HPO_4 (1.0), $MgSO_4 \cdot 7H_2O$ (0.2) and NaCl (1.0). The unoptimized fermentation conditions were, incubation temperature 37^oC, initial medium pH 7.0, shaking speed 180 rpm and inoculum size 2 %, v/v (Optical density at 600 nm = 1.0). The cell growth was monitored by taking OD at 600 nm using UV-visible spectrophotometer (Perkin Elmer, Lambda-45).

4.2.3 Medium optimization for enhancing enzyme activity

The culture was grown in enzyme production medium (pH 7.0) containing following six components: CMC-Na, yeast extract, peptone, K_2HPO_4, $MgSO_4 \cdot 7H_2O$ and NaCl. These medium components were selected on the basis on published literature on CMCase production from different *Bacillus* spp. (Apun *et al*. 2000; Singh *et al*.2001; Lee *et al*. 2008; Kim *et al*. 2009; Rastogi *et al*. 2009; Deka *et al*.

2011). Two levels of concentrations of each of these components (again based on the published literature) were selected for Plackett-Burman analysis. The total number of experiments, with permutation-combination of different components and their levels, were 20 (Table 4.3.1). In each of these 20 experiments, three trial runs were taken to assess the reproducibility of results.

In each experiment, 100 mL medium containing 2%, v/v (A_{600} = 1.0) inoculum was taken in a 250 mL Erlenmeyer flask and incubated at 37^{o}C with shaking at 180 rpm for 72 h in a shaking incubator (Orbitek, Scigenics Biotech). After every 6 h, 500 µL of broth was taken out and centrifuged at 12,000***g*** for 20 min at 4^{o}C. The cell-free supernatant containing the crude enzyme was used for estimation of CMCase activity. It was observed that the CMCase activity showed maxima after 48 h of incubation and a reduction in activity was seen thereafter. In view of this, the enzyme activity at 48 h was considered for analysis.

4.2.4 Fermentation parameters optimization

The optimization parameters in this category were: (1) incubation temperature (^{o}C), (2) initial pH of the medium, (3) shaking speed (rpm) and (4) inoculum size (%, v/v). The optimized medium (subsequently defined) was used for further optimization of fermentation parameters and the initial pH of the medium was adjusted to the selected range (pH 4.5-11.0) in different sets of experiments using 2 N HCl and NaOH. In this case, the CCD experimental design was adopted after OVAT analysis to determine the levels of these parameters. The CCD experimental

design and its analysis are based on these levels. The experimental design employed is described in Table 4.3.3.

4.2.5 CMCase assay

The response variable of the statistical experiments is CMCase activity (U/mL), which was quantified by measurement of total reducing sugar liberated after incubation of enzyme with CMC. The enzyme assay was carried out as described in Chapter 3, Section 3.2.6. The total reducing sugar was quantified using method of Nelson and Somogyi (Nelson 1944; Somogyi 1945). A_{500} was measured using a UV-visible spectrophotometer (Perkin Elmer, Lambda-45) against a blank with D-glucose as standard in a range of concentration 0-500 µg/mL.

4.2.6 Experimental designs for medium optimization

4.2.6.1 Plackett-Burman design

As stated earlier, the Plackett-Burman experimental design was used for initial screening of medium components to short-list components having significant effect on CMCase production. This experimental design was devised using statistical software package MINITAB (Release 15.1, PA, USA, Trial Version). Plackett-Burman factorial design is a two-level fractional design that follows first-order polynomial model:

$$Y = \beta_o + \sum_{i=1}^{n} \beta_i X_i \qquad \text{(eq. 4.1)}$$

Notations: Y - response variable (CMCase activity), β_o - model intercept, β_i - linear

coefficient and X_i - level of independent variable. Total six medium components (or factors) have been examined at two levels each, *viz*. -1 and +1, indicating low and high level, respectively (Plackett and Burman 1946). These components and their coded as well as actual values (given in parentheses) are shown in Table 4.3.1. This experimental design comprised a total of 20 sets of experiments (with each experiment conducted in triplicate to assess reproducibility). The average CMCase activity in each experiment was considered as the response. The regression analysis of Plackett-Burman design revealed the significant variables (or medium components) influencing CMCase activity, with significance level ≥ 95 % and *p*-value < 0.05 (Table 4.3.2A). This result was further corroborated with central composite design (CCD) of experiments.

4.2.6.2 Central composite design

The central composite experimental design is commonly employed for processes with significant interaction effects between variables. This design essentially fits a second-order polynomial model. A three-factor, five-level design was used in which five coded levels (-α, -1, 0, +1, +α) were assigned to each factor. α is the extended level with value of $(2)^{3/4}$ =1.682. A 2^3 full-factorial CCD experimental design with three significant medium constituents *viz*. CMC, yeast extract and peptone at five coded levels was generated by Minitab statistical software (Release 15, Trial Version). This experimental design comprised 20 individual experiments ($=2^k + 2k + n_o$), where '*k*' is the number of independent variables and n_o

is the number of replicate runs at center point of the variables. This design is described in Table 4.3.3.

4.2.6.3 Statistical analysis and model fitting

The experimental data (Table 4.3.1) were analyzed by the regression procedure to fit the following second-order polynomial equation:

$$Y = \beta_o + \sum_{i=1}^{k} \beta_i X_i + \sum_{i=1}^{k} \beta_{ii} X_i^2 + \sum_{i \neq j} \sum_{i} \beta_{ij} X_i X_j \qquad \text{(eq. 4.2)}$$

Notation: Y - response (CMCase activity), k - number of factors or medium components, β_o - regression constant, β_i - linear coefficient, β_{ii} - quadratic coefficient and β_{ij} - interaction coefficient. The following equation (eq. 4.3) was used for coding (in the range of -1 to +1) the actual experimental values (given in the parentheses in the table) of the factors:

$$x_i = X_i - X_o/\Delta X_i, \qquad i = 1, 2, 3,..., k \qquad \text{(eq. 4.3)}$$

Where, x_i is the dimensionless value of an independent variable, X_i is the real value of an independent variable, X_o is the value of X_i at the center point and ΔX_i is the step change. The analysis of variance (ANOVA) was also done to determine the significance of each factor in fitted model (eq. 4.2) and also to determine the goodness of fit. For this purpose, the software Design Expert 7.0 (trial version) has been used. Graphical representation of the fitted polynomial eq. 4.2 was given in the form of contour plots. ANOVA of the linear, quadratic and interaction regression

coefficients (i.e., *F* value and *p* value) are given in Table 4.3.2A. The *F* and *p* values essentially exhibit the individual and interactive effects of the independent variables.

4.2.7 Experimental design for optimization of fermentation parameters

4.2.7.1 Central composite design

A 2^4 full-factorial CCD experimental design with four parameters (*viz.* incubation temperature, initial medium pH, rpm or speed of orbital shaking and inoculum size) at five coded levels was generated by Minitab statistical software (Release 15, Trial Version) (Table 4.3.6). In this 4-factor, 5-level design, five coded levels ($-\alpha$, -1, 0, +1, $+\alpha$) were assigned to each factor, where $\alpha = (2)^{4/4} = 2$. This experimental design comprised 31 individual experiments ($= 2^k + 2k + n_o$), where k is the number of independent variables (4) and n_o is the number of replicate runs (7) at center point of the variables.

4.2.7.2 Experimental validation of optimization

Experiments were conducted in two steps with optimized medium composition and optimized fermentation parameters predicted by statistical analysis to assess the accuracy of the models. Initially, validation of optimization of medium composition was carried out using results of CCD experimental design. After that, validation of optimum fermentation parameters was carried out using optimum medium composition. All validation experiments were performed in triplicate to assess the reproducibility.

4.3 Results and Discussion

The optimization of CMCase production by the bacterium *B. amyloliquefaciens* SS35 was carried out in two stages, first, optimization of the medium composition and secondly, the optimization of fermentation parameters.

4.3.1 Optimization of fermentation medium

4.3.1.1 Plackett-Burman design for screening of significant medium components

The results of initial screening of medium components using Plackett-Burman design are given in Table 4.3.1. The experimental and predicted values of CMCase activity matched quite well. The CMCase activity in the cell-free supernatant of *B. amyloliquefaciens* SS35 varied from 0.132 to 0.528 U/mL. As stated in section 4.2.3, this is the maximum activity attained after 48 h of incubation.

The statistical analysis of the Plackett-Burman design is given in Table 4.3.2A and B. The values of the first-order model coefficients for all six variables along with *t* value, *p* value and confidence levels are depicted in Table 4.3.2A, while the ANOVA of the model is given in Table 4.3.2B. The model variable is termed to be significant if the *t* value is greater than *p* value. As seen from Table 4.3.2A, this condition is satisfied by three variables, *viz*. CMC, yeast extract and peptone. The significance of these variables is also corroborated by results of Table 4.3.2B, which shows high *F* value and zero *p* value for these variables.

Table 4.3.1 Plackett-Burman design in coded units and the real values (in parenthesis) in g/L for six variables along with the CMCase activity.

Run order	CMC (X_1)	Yeast extract (X_2)	Peptone (X_3)	K_2HPO_4 (X_4)	$MgSO_4 \cdot 7H_2O$ (X_5)	NaCl (X_6)	CMCase activity (U/mL)*	
							Experimental	Predicted
1	-1 (10)	+1 (16)	+1 (10)	-1 (1)	-1 (0.1)	-1 (1)	0.263 ± 0.030	0.281
2	+1 (26)	-1 (8)	-1 (2)	-1 (1)	-1 (0.1)	+1 (4)	0.366 ± 0.032	0.391
3	-1 (10)	+1 (16)	+1 (10)	+1 (4)	+1 (0.4)	-1 (1)	0.272 ± 0.014	0.274
4	-1 (10)	-1 (8)	-1 (2)	+1 (4)	-1 (0.1)	+1 (4)	0.155 ± 0.013	0.174
5	-1 (10)	+1 (16)	-1 (2)	+1 (4)	-1 (0.1)	+1 (4)	0.241 ± 0.012	0.258
6	+1 (26)	+1 (16)	-1 (2)	-1 (1)	+1 (0.4)	+1 (4)	0.478 ± 0.017	0.453
7	+1 (26)	+1 (16)	-1 (2)	-1 (1)	-1 (0.1)	-1 (1)	0.499 ± 0.027	0.460
8	-1 (10)	+1 (16)	+1 (10)	-1 (1)	+1 (0.4)	+1 (4)	0.267 ± 0.021	0.274
9	+1 (26)	-1 (8)	-1 (2)	+1 (4)	+1 (0.4)	-1 (1)	0.372 ± 0.023	0.369
10	+1 (26)	-1 (8)	+1 (10)	+1 (4)	-1 (0.1)	-1 (1)	0.431 ± 0.019	0.445
11	-1 (10)	-1 (8)	-1 (2)	-1 (1)	+1 (0.4)	-1 (1)	0.132 ± 0.018	0.121
12	+1 (26)	-1 (8)	+1 (10)	-1 (1)	+1 (0.4)	+1 (4)	0.413 ± 0.025	0.422
13	+1 (26)	-1 (8)	+1 (10)	+1 (4)	+1 (0.4)	+1 (4)	0.425 ± 0.023	0.438
14	-1 (10)	+1 (16)	-1 (2)	+1 (4)	+1 (0.4)	+1 (4)	0.223 ± 0.016	0.236
15	+1 (26)	+1 (16)	-1 (2)	+1 (4)	+1 (0.4)	-1 (1)	0.461 ± 0.023	0.453
16	-1 (10)	-1 (8)	+1 (10)	-1 (1)	+1 (0.4)	-1 (1)	0.173 ± 0.011	0.175
17	-1 (10)	-1 (8)	-1 (2)	-1 (1)	-1 (0.1)	-1 (1)	0.132 ± 0.012	0.143
18	+1 (26)	+1 (16)	+1 (10)	-1 (1)	-1 (0.1)	+1 (4)	0.528 ± 0.017	0.529
19	-1 (10)	-1 (8)	+1 (10)	+1 (4)	-1 (0.1)	+1 (4)	0.306 ± 0.022	0.227
20	+1 (26)	+1 (16)	+1 (10)	+1 (4)	-1 (0.1)	-1 (1)	0.516 ± 0.009	0.529

**Experimental values are mean ± SE (n = 3)*

Table 4.3.2 Statistical analysis of results from Plackett-Burman experimental design.

(A) Coefficient values, *t*-and *p*-value for each variable.

Model term	Coefficient Estimate	Computed *t*-value	*p*-value	Confidence level (%)
Intercept	0.33265	51.00	0.000*	100
CMC (X_1)	0.11625	17.82	0.000*	100
Yeast extract (X_2)	0.04215	6.46	0.000*	100
Peptone (X_3)	0.02675	4.10	0.001*	99.9
K_2HPO_4 (X_4)	0.00755	1.16	0.268	73.2
$MgSO_4 \cdot 7H_2O$ (X_5)	-0.01105	-1.69	0.114	88.6
NaCl (X_6)	0.00755	1.16	0.268	73.2

*Significant *p* values, $p \leq 0.05$; $R^2 = 0.9671$; Predicted $R^2 = 0.9220$; Adjusted $R^2 = 0.9519$

(B) ANOVA for the model.

Variable	SS	DF	MS	*F*-value	*p*-value Prob > *F*
Constant	0.325	6	0.0541	63.62	0.000
CMC (X_1)	0.27	1	0.27	317.59	0.000
Yeast extract (X_2)	0.0355	1	0.0355	41.75	0.000
Peptone (X_3)	0.0143	1	0.0143	16.82	0.001
K_2HPO_4 (X_4)	0.00114	1	0.00114	1.34	0.268
$MgSO_4$. $7H_2O$ (X_5)	0.00244	1	0.00244	2.87	0.114
NaCl (X_6)	0.00114	1	0.00114	1.16	0.268
Residual	0.0111	13	0.000851	1.34	
Total	0.336	19			

DF - degrees of freedom; SS - sum of squares; MS - mean square

The *t* value limit for this analysis is 2.16 (as shown in Fig. 4.3.1). The *t* value for CMC, yeast extract and peptone are higher than this limit, which points towards their significance. Moreover, $MgSO_4 \cdot 7H_2O$ has shown a negative effect on the CMCase activity as indicated by the negative Plackett-Burman model coefficient.

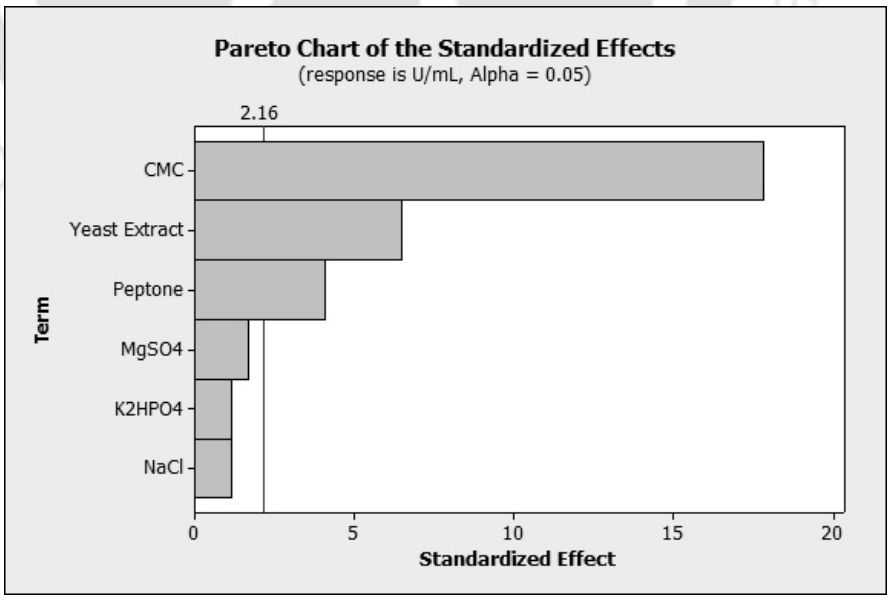

Fig. 4.3.1 Pareto plot for Plackett-Burman analysis.

Another measure of significance level of variables is the confidence level, which is ~100% for CMC, yeast extract and peptone. The overall regression coefficient for the Plackett-Burman design is $R^2 = 0.9671$, with adjusted $R^2 = 0.9519$ shows the model fits very well to the data. Neglecting the insignificant variables, the model equation for CMCase activity could be written as:

$$Y_{activity} = 0.33265 + 0.11625\ X_1 + 0.04215\ X_2 + 0.02675\ X_3 \quad \text{(eq. 4.4)}$$

Among the significant variables CMC acts as carbon source, while yeast extract and peptone are the nitrogen sources. Earlier studies by Li *et al*. (2008) and Deka *et al*. (2011) reported significant role played by these components on cellulase production by *Bacillus* spp. The inorganic salts have been found to have insignificant effect on CMCase production. This is rather an anomaly as potassium phosphate is known for the production of microbial polysaccharides and also act as an ingredient in buffer solutions that enhances the cell growth (Lee *et al*.2008; Jin *et al*. 2011; Gao *et al*. 2012). Sodium chloride as well as magnesium sulphate in the medium also play important role in cell growth (Gao *et al*. 2012). This anomaly was explained in terms of differences in the phases of cell life cycle in which the cell growth and enzyme production occur. The maximum CMCase production was observed at late log phase or early stationary phase of life cycle of *B. amyloliquefaciens* SS35 (Singh *et al*. 2013).

4.3.1.2 Optimization by central composite experimental design

The central composite design (CCD) was based on the results of Plackett-Burman design, which revealed that three factors, *viz.* CMC, yeast extract and

peptone had significant influence on CMCase production. The full factorial CCD matrix of these variables is given in Table 4.3.3 which also shows the CMCase activity obtained in each experiment and the standard deviation. The results of second-order response model fitted to the coded data are given in Table 4.3.4A.

Table 4.3.3 Full factorial central composite design matrix of three medium components in coded and actual (in parentheses, g/L) values and the response of CMCase activity.

Run order	CMC (X_1)	Yeast extract (X_2)	Peptone (X_3)	CMCase activity (U/mL)*	
				Experimental	Predicted
1	0 (18)	0 (12)	0 (6)	0.456 ± 0.031	0.444
2	+1 (22.75)	+1 (14.37)	+1 (8.37)	0.500 ± 0.042	0.510
3	0 (18)	-α (8)	0 (6)	0.456 ± 0.031	0.444
4	0 (18)	0 (12)	0 (6)	0.456 ± 0.031	0.444
5	0 (18)	0 (12)	0 (6)	0.410 ± 0.073	0.419
6	0 (18)	0 (12)	+α (10)	0.425 ± 0.064	0.414
7	-1 (13.24)	+1 (14.37)	-1 (3.62)	0.430 ± 0.048	0.428
8	0 (18)	0 (12)	0 (6)	0.411 ± 0.056	0.424
9	0 (18)	0 (12)	0 (6)	0.431 ± 0.054	0.443
10	+α (26)	0 (12)	0 (6)	0.268 ± 0.036	0.260
11	+1 (22.75)	-1 (9.62)	-1 (3.62)	0.484 ± 0.062	0.461
12	0 (18)	0 (12)	-α (2)	0.148 ± 0.024	0.168
13	-1 (13.24)	-1 (9.62)	-1 (3.62)	0.530 ± 0.051	0.517
14	-1(13.24)	+1 (14.37)	+1 (8.37)	0.412 ± 0.046	0.395
15	-α (10)	0 (12)	0 (6)	0.431 ± 0.041	0.444
16	-1 (13.24)	-1 (9.62)	+1 (8.37)	0.457 ± 0.083	0.477
17	+1 (22.75)	+1 (14.37)	-1 (3.62)	0.431 ± 0.075	0.444
18	0 (18)	0 (12)	0 (6)	0.431 ± 0.061	0.443
19	0 (18)	+α (16)	0 (6)	0.500 ± 0.086	0.513
20	+1 (22.75)	-1 (9.62)	+1 (8.37)	0.431 ± 0.078	0.444

**Experimental values are mean ± SE (n = 3)*

The second-order regression equation fitted to this data is as follows:

$$Y_{activity} = 0.443596 + 0.087215\ X_1 - 0.028983\ X_2 - 0.008664\ X_3 - 0.045706\ X_1^2 + 0.008741\ X_2^2 - 0.011942\ X_3^2 + 0.0175\ X_1X_2 + 0.02175\ X_1X_3 + 0.02975\ X_2X_3 \quad \text{(eq. 4.5)}$$

The notations used in equation 4.5 are same as that for Plackett-Burman design. The overall model had regression coefficient of 0.9776 with adjusted coefficient of

R^2 = 0.9575. The predicted R^2 of 0.8642 is also in reasonable agreement with adjusted R^2 of 0.9575. This essentially indicated that the model fits very well to the experimental data. This is also corroborated by the predicted CMCase activity values which matched well with the experimental values (Table 4.3.3). The ANOVA of the fitted model is described in Table 4.3.4B. The lack of fit *F* value of 2.99 implies that lack of fit is not significantly related to pure error. The *p* value of 0.127 for lack of fit implies that there is 12.7% chance that a 'lack of fit *F* value' this large could occur due to noise.

Table 4.3.4 Results of statistical (CCD) analysis for medium optimization.

(A) Values of coefficients for second order regression model.

Model term	Coefficient estimate	Computed *t*-value	*p*-value Prob > *F*
Intercept	0.443596	56.21	0.000*
CMC (X_1)	0.087215	16.657	0.000*
Yeast extract (X_2)	-0.028983	-5.535	0.000*
Peptone (X_3)	-0.008664	-1.655	0.129
CMC × CMC (X_1^2)	-0.045706	-8.967	0.000*
Yeast extract × Yeast extract (X_2^2)	0.008741	1.715	0.117
Peptone × Peptone (X_3^2)	-0.011942	-2.343	0.041*
CMC × Yeast extract ($X_1 \times X_2$)	0.0175	2.558	0.028*
CMC × Peptone ($X_1 \times X_3$)	0.02175	3.179	0.010*
Yeast extract × Peptone ($X_2 \times X_3$)	0.02975	4.349	0.001*

*Significant *p* values, $p \leq 0.05$; R^2 = 0.9776; Predicted R^2 = 0.8642; Adjusted R^2 = 0.9575

(B) ANOVA for quadratic model.

Source	DF	SS	MS	*F*-value	*p*-value Prob > *F*
Regression	9	0.163	0.0182	48.51	0.000
Linear	3	0.116	0.0388	103.61	0.000
Square	3	0.0338	0.0113	30.05	0.000
Interaction	3	0.0133	0.00444	11.85	0.001
Residual (Error)	10	0.00374	0.000374		
Lack of fit	5	0.00281	0.000561	2.99	0.127
Pure Error	5	0.000938	0.000188		
Total	19	0.167			

DF - degrees of freedom; SS - sum of squares; MS - mean square

Another yardstick for fitness of model is Adequate Precision value that measures the signal-to-noise ratio. A ratio >4 is desirable. The ratio obtained for the present analysis is 25.538, which represents adequacy of the signal. The *p* value of the linear, square and interaction coefficients, all are zero, pointing their significance. An interesting trend is in the *F* values of the coefficients. The *F* value for linear coefficients is higher (10 fold) than the value for interaction coefficients. This essentially means that effects of CMC, yeast extract and peptone on the CMCase production are predominantly independent. The optimum value of concentration of medium components as revealed by the statistical analysis and quadratic model for maximum CMCase production are CMC = 19.05 g/L, yeast extract = 8.0 g/L and peptone = 2.0 g/L. These have been depicted in the desirability function plot shown in Fig. 4.3.2.

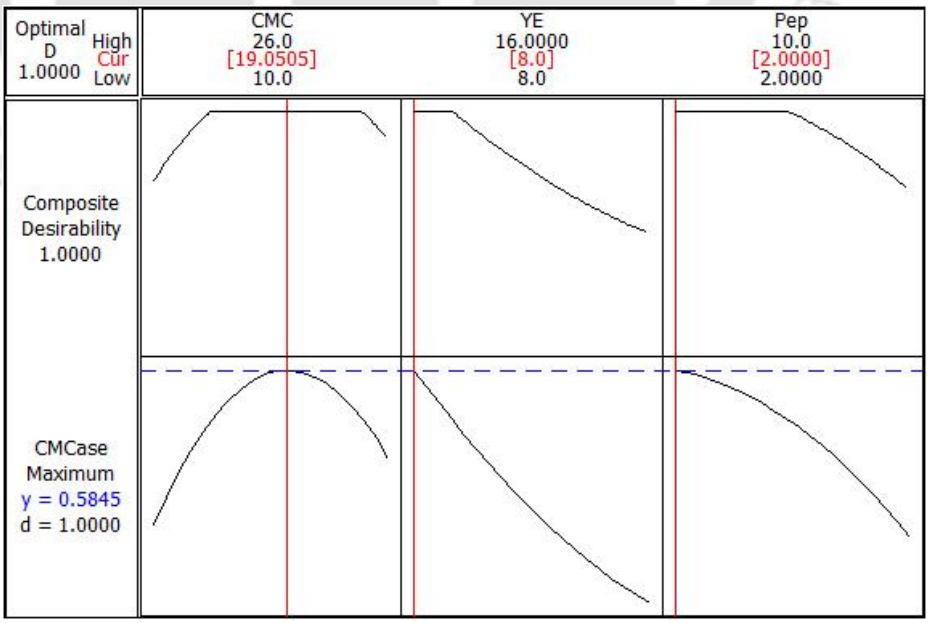

Fig. 4.3.2 Desirability function plot showing the optimum levels of medium components.

The maximum CMCase activity for these parameters the model predicts 0.585 U/mL. The experiments were conducted to validate these predictions and the CMCase activity for the optimum medium composition was found to be 0.553 ± 0.021 U/mL, which is in close agreement with predicted result of CCD. The CMCase activity under un-optimized conditions (as mentioned in section 4.2.2) was 0.161 ± 0.014 U/mL. Thus, the enhancement in enzyme activity after medium optimization was 3-fold.

4.3.1.3 Interaction effects of medium components

The interactive effects between medium components have been assessed using contour plots shown in Fig. 4.3.3 (A-C). Following trends in interactive effect can be identified: (1) for smaller concentration of both yeast extract and CMC, the enzyme activity increases with concentration. However, as the CMC concentration crosses 16 g/L, the highest enzyme activity is seen for low concentration of yeast extract ~8 g/L. (2) The highest enzyme activity is observed for the yeast extract concentration of 8 g/L and peptone concentration range of 3-6 g/L. With concentration of peptone and yeast extract increasing beyond this range, the enzyme activity decreases. (3) The CMCase activity increases monotonically with the increase of both peptone and CMC concentration.

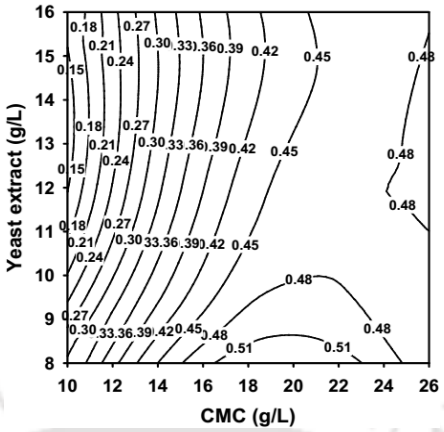

(A)

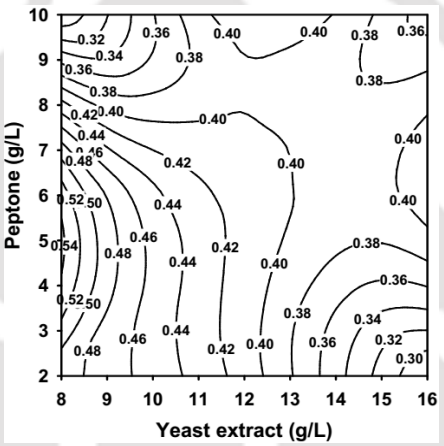

(B)

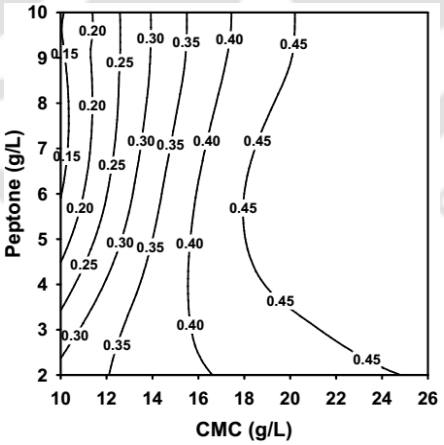

(C)

Fig. 4.3.3 Contour plots for CMCase activity showing the interactive effects of medium components: (A) concentrations of yeast extract and CMC, (B) concentrations of yeast extract and peptone; (C) concentrations of CMC and peptone.

These results can be explained on the basis of amino acid composition of the enzyme CMCase (endoglucanase) given below. On the basis of the methodology given by Unrean and Nguyen (2013), the metabolic and energy requirement to produce one mole of CMCase by *B. amyloliquefaciens* UMAS1002 have been listed in Table 4.3.5. Based on the amino acid composition it could be seen that one mole of CMCase production requires large amount of nitrogen, i.e., 677 mol of ammonia (Fig. 4.3.4). Consequently, both peptone and yeast extract being the nitrogen sources play a vital role in CMCase production. CMC being the main substrate of the metabolic pathway enhances bacterial cell growth and thus, is a significant component of the CMCase production process.

MKRSISIFITCLLIAVLTMGGLLPSPASAAGTKTPVAKNGQLSIKDTQLVNRDGKAVQ
LKGISSHGLQWYGDFVNKDSLKWLRDDWGITVFRAAMYTADGGYIDNPSVKNKV
KEAVEAAKELGIYVIIDWHILNDGNPNQNKEKAKEFFKEMSSLYGNTPNVIYEIANE
PNGDVNWKRDIKPYAEEVISVIRKNDPDNIIIVGTGTWSQDVNDAADDQLKDANVM
YALHFYAGTHGQSLRDKANYALSKGAPIFVTEWGTSDASGNGGVFLDQSREWLNY
LDSKNISWVNWNLSDKQESSSALKPGASKTGGWPLTDLTASGTFARENIRGTKGST
KDGPETPAQDNPTQEKGVSVQYKAGYGRVNSNQIRPQLHMKNNGNTKVDLKGVT
ARYWYNTKNKGQNFDCDYTQIGCGNLTHKFVTLHKPKQDADTYLELGFKTGTLSP
GASTGNIQLRLPMMTGAIMHKATIIPFSNQIHLKQREKSHYISQGKLIWGTEPN

Reference: European Nucleotide Archive, Sequence: AF363635.1
Organism: *Bacillus amyloliquefaciens*, Strain: UMAS1002
(Available on webpage: http://www.ebi.ac.uk/ena/data/view/AAL99668)

Fig. 4.3.4 Amino acid sequence of cellulase (*eng*A gene) of *B. amyloliquefaciens* UMAS 1002.

Table 4.3.5 Metabolic and energy requirements and stoichiometric coefficients to produce one mole of CMCase (Endoglucanase) by *Bacillus amyloliquefaciens* UMAS 1002. The amino acid composition of cellulase was obtained from European Nucleotide Archive (Sequence: AF363635.1).*

Amino acid	Moles	G3P	R5P	E4P	PEP	PYR	ACCOA	AKG	OA	NH_3	ATP	NADH	NADPH	CO_2
Alanine	35	--	--	--	--	35	--	--	--	35	--	--	35	--
Arginine	15	--	--	--	--	--	--	15	--	60	105	-15	60	--
Asparagine	38	--	--	--	--	--	--	--	38	76	114	--	38	--
Asparate	32	--	--	--	--	--	--	--	32	32	--	--	32	--
Cysteine	3	--	--	--	--	--	--	--	--	--	--	--	--	--
Glutamine	22	--	--	--	--	--	--	22	--	44	22	--	22	--
Glutamate	19	--	--	--	--	--	--	19	--	19	--	--	19	--
Glycine	46	46	--	--	--	--	--	--	--	46	--	-46	46	-46
Histidine	10	--	6	--	--	--	--	--	--	30	60	-30	10	10
Isoleucine	32	--	--	--	--	32	--	--	32	32	64	--	160	-32
Leucine	36	--	--	--	--	72	36	--	--	36	--	-36	72	--
Lysine	43	--	--	--	--	43	--	--	43	86	86	--	172	--
Methionine	9	--	--	--	--	--	--	--	9	9	63	--	72	9
Phenylalanine	13	--	13	--	26	--	--	--	--	13	13	--	26	--
Proline	21	--	--	--	--	--	--	21	--	21	21	--	63	--
Serine	34	34	--	--	--	--	--	--	--	34	--	-34	34	--
Threonine	34	--	--	--	--	--	--	--	34	34	68	--	102	--
Tryptophane	13	--	13	13	13	--	--	--	--	26	65	-26	39	--
Tyrosine	18	--	--	18	36	--	--	--	--	18	18	-18	36	--
Valine	26	--	--	--	--	52	--	--	--	26	--	--	52	--
Peptide bonds	498	--	--	--	--	234	36	77	188	--	1096	--	--	--
Stoichiometric coefficient	1	80	32	31	75	139	15	32	72	677	1795	-205	1055	-59

*Adopted in modified form from: Unrean and Nguyen (2013), G3P Glycerol-3-phosphate, R5P Ribose-5-phosphate, E4P erythrose-4-phosphate, PEP phosphoenol pyruvate, PYR pyruvate, ACCoA acetyl coenzyme A, AKG α-ketoglutarate, OAA oxaloacetate.

4.3.2 Optimization of fermentation parameters

The optimization of fermentation parameters was carried out in two steps: (1) OVAT method and (2) central composite experimental design. As reported in literature (Immanuel *et al*. 2006), the cellulase production is dependent on several parameters such as temperature, initial pH of the medium and inoculum size. The OVAT experiments helped in elucidating individual effect of the fermentation parameters, as well as in deciding the levels of these parameters for a CCD design. The results of OVAT experiment are depicted in Fig. 4.3.5 (A-D).

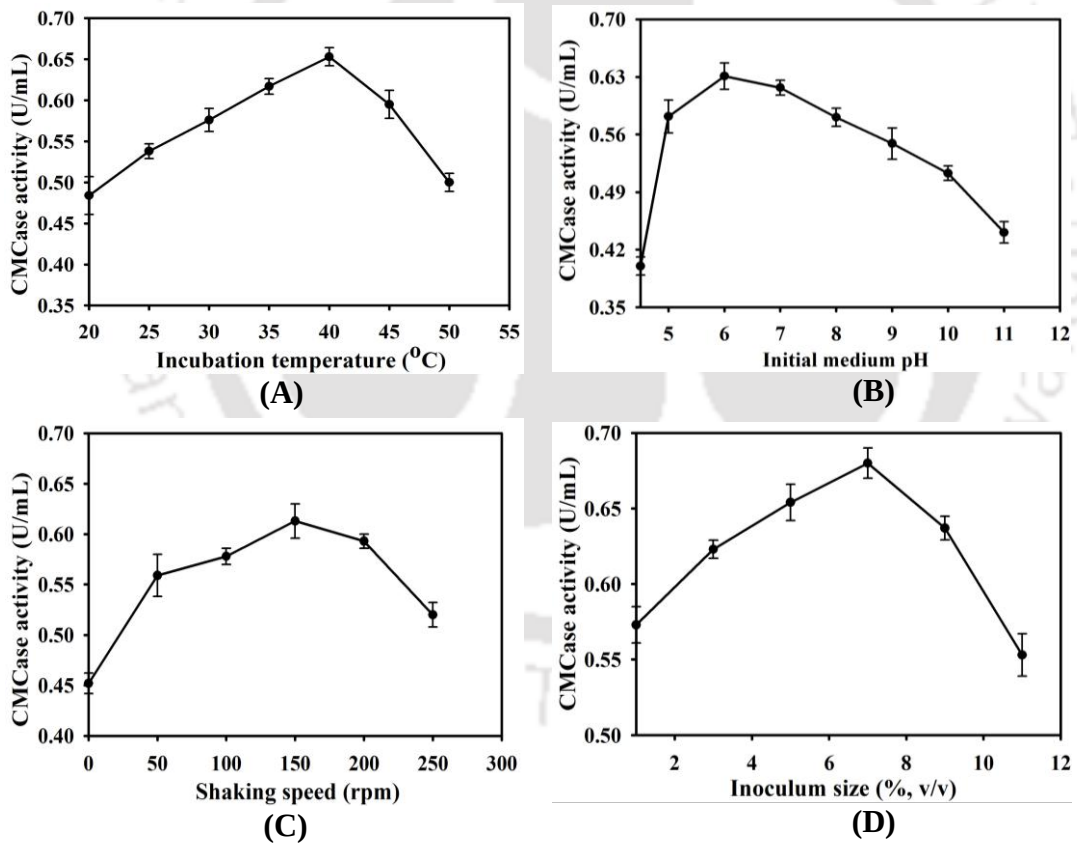

Fig. 4.3.5 Evaluation of individual effect of fermentation parameters on CMCase production (OVAT method): (A) Effect on temperature at medium pH = 7.0, shaking speed = 180 rpm, inoculum size = 2% v/v; (B) Effect of initial medium pH at temperature = 37°C, shaking speed = 180 rpm, inoculum size = 2% v/v; (C) Effect of shaking speed at medium pH = 7.0, temperature = 37°C, inoculum size = 2% v/v; (D) Effect of inoculum size at temperature = 37°C, shaking speed = 180 rpm, medium pH = 7.0.

The results showed that each of the parameter gave optima at which maximum CMCase activity was observed. The values of these parameters are (1) temperature = 40^{o}C, (2) initial pH of medium = 6.0, (3) shaking speed = 150 rpm and (4) inoculum volume = 6% (v/v).

4.3.2.1 Optimization of fermentation parameters by CCD

The CCD experimental matrix with the actual and coded values of the above parameters is given in Table 4.3.6, along with the values of response, the CMCase activity for each experiment with different combination of parameters.

The results of second-order response model fitted to the coded data and ANOVA of the model is given in Table 4.3.7A and B, respectively. The model equation for response variable is as follows:

$$Y_{activity} = 0.637714 + 0.008208\ X_1 - 0.021208\ X_2 - 0.006125\ X_3 - 0.004958\ X_4 - 0.028564\ X_1^2 - 0.007314\ X_2^2 + 0.008811\ X_3^2 - 0.002689\ X_4^2 + 0.003563\ X_1X_2 - 0.007438\ X_1X_3 + 0.005938\ X_1X_4 + 0.001X_2X_3 + 0.000313\ X_2X_4 + 0.000063\ X_3X_4 \quad \text{(eq. 4.6)}$$

It was seen that all coefficients (linear/quadratic/interaction) are at least one to three orders of magnitude smaller than the intercept value. The analysis of coefficients presented in Table 4.3.7A shows that most of linear and quadratic coefficients are significant (as indicated by p <0.05), while most of interaction coefficients are insignificant. The overall model fitted very well to the data as seen

from R^2 value of 0.9704 and fairly matched with value of R^2 = 0.8494. ANOVA of the model presented in Table 4.3.7B shows all regression coefficients as significant. But relative magnitude of F values of these coefficients indicated that individual influence of parameters is much higher than interactive effect.

Table 4.3.6 Full factorial central composite design matrix of 4 fermentation parameters in coded and actual (in parentheses) values and the response of CMCase activity.

Run order	Temperature (^oC) (X_1)	Medium pH (X_2)	Shaking speed (rpm) (X_3)	Inoculum size (%, v/v) (X_4)	CMCase activity (U/mL)*	
					Experimental	Predicted
1	0 (37.5)	-α (5)	0 (185)	0 (5)	0.643 ± 0.041	0.651
2	0 (37.5)	0 (7.5)	0 (185)	0 (5)	0.642 ± 0.035	0.638
3	+1 (43.75)	+1 (8.75)	+1 (217.5)	-1 (3.5)	0.581± 0.056	0.575
4	0 (37.5)	0 (7.5)	0 (185)	0 (5)	0.637 ± 0.062	0.638
5	-1 (31.25)	+1 (8.75)	+1 (217.5)	-1 (3.5)	0.576 ± 0.047	0.578
6	0 (37.5)	0 (7.5)	0 (185)	-α (2)	0.612 ± 0.047	0.617
7	+1 (43.75)	+1 (8.75)	-1 (152.5)	-1 (3.5)	0.603 ± 0.029	0.600
8	0 (37.5)	0 (7.5)	-α (120)	0 (5)	0.678 ± 0.031	0.685
9	-α (25)	0(7.5)	0 (185)	0 (5)	0.514 ± 0.037	0.507
10	0 (37.5)	0 (7.5)	0 (185)	0 (5)	0.627 ± 0.045	0.638
11	+1 (43.75)	-1 (6.25)	-1 (152.5)	+1 (6.5)	0.673 ± 0.052	0.659
12	0 (37.5)	0 (7.5)	+α (250)	0 (5)	0.658 ± 0.082	0.661
13	0 (37.5)	0 (7.5)	0 (185)	0 (5)	0.634 ± 0.059	0.638
14	-1 (31.25)	-1 (6.25)	+1 (217.5)	+1 (6.5)	0.632 ± 0.081	0.623
15	+1 (43.75)	+1 (8.75)	+1 (217.5)	+1 (6.5)	0.604 ± 0.091	0.597
16	0 (37.5)	0 (7.5)	0 (185)	0 (5)	0.638 ± 0.038	0.638
17	+α (50)	0 (7.5)	0(185)	0 (5)	0.523 ± 0.082	0.54
18	-1 (31.25)	-1 (6.25)	+1 (217.5)	-1 (3.5)	0.621 ± 0.081	0.626
19	0 (37.5)	0 (7.5)	0 (185)	+α (8)	0.632 ± 0.067	0.637
20	+1 (43.75)	-1 (6.25)	-1 (152.5)	-1 (3.5)	0.642 ± 0.083	0.638
21	+1 (43.75)	-1 (6.25)	+1 (217.5)	-1 (3.5)	0.617 ± 0.079	0.608
22	-1 (31.25)	+1 (8.75)	-1 (152.5)	+1 (6.5)	0.575 ± 0.060	0.572
23	-1 (31.25)	+1 (8.75)	-1 (152.5)	-1 (3.5)	0.573 ± 0.058	0.573
24	-1 (31.25)	-1 (6.25)	-1 (152.5)	-1 (3.5)	0.631 ± 0.092	0.626
25	-1 (31.25)	+1 (8.75)	+1 (217.5)	+1 (6.5)	0.571 ± 0.067	0.577
26	+1 (43.75)	+1 (8.75)	-1 (152.5)	+1 (6.5)	0.625 ± 0.092	0.622
27	-1 (31.25)	-1 (6.25)	-1 (152.5)	+1 (6.5)	0.615 ± 0.054	0.623
28	+1 (43.75)	-1 (6.25)	+1 (217.5)	+1 (6.5)	0.628 ± 0.072	0.630
29	0 (37.5)	0 (7.5)	0 (185)	0 (5)	0.643 ± 0.081	0.638
30	0 (37.5)	0 (7.5)	0 (185)	0 (5)	0.643 ± 0.072	0.638
31	0 (37.5)	+α (10)	0 (185)	0 (5)	0.564 ± 0.052	0.566

**Experimental values are mean ± SE (n = 3)*

Table 4.3.7 Results of statistical (CCD) analysis for optimization of fermentation parameters.

(A) Values of coefficients for second order regression model.

Model term	Coefficient Estimate	Computed *t*-value	*p*-value
Intercept	0.637714	184.607	0.000*
Temperature (X_1)	0.008208	4.4	0.000*
Medium pH (X_2)	-0.021208	-11.368	0.000*
Shaking (X_3)	-0.006125	-3.283	0.005*
Inoculum size (X_4)	0.004958	2.658	0.017*
Temperature × Temperature (X_1^2)	-0.028564	-16.713	0.000*
pH × pH (X_2^2)	-0.007314	-4.279	0.001*
Shaking × Shaking (X_3^2)	0.008811	5.155	0.000*
Inoculum size × Inoculum size (X_4^2)	-0.002689	-1.573	0.135
Temperature × Medium pH ($X_1 \times X_2$)	0.003563	1.559	0.139
Temperature × Shaking ($X_1 \times X_3$)	-0.007438	-3.255	0.005*
Temperature × Inoculum size ($X_1 \times X_4$)	0.005938	2.599	0.019*
Medium pH × Shaking ($X_2 \times X_3$)	0.001187	0.520	0.610
Medium × Inoculum size pH ($X_2 \times X_4$)	0.000313	0.137	0.893
Shaking × Inoculum size ($X_3 \times X_4$)	0.000063	0.027	0.979

*Significant p values, $p \leq 0.05$; $R^2 = 0.9701$; Predicted $R^2 = 0.9422$; Adjusted $R^2 = 0.8473$

(B) ANOVA for quadratic model.

Source	DF	SS	MS	*F*-value	*p*-value, Prob > *F*
Regression	14	0.043830	0.003131	37.48	0.000
Linear	4	0.013903	0.003476	41.61	0.000
Square	4	0.028251	0.007063	84.55	0.000
Interaction	6	0.001676	0.000279	3.34	0.025
Residual (Error)	16	0.001337	0.000084		
Lack of fit	10	0.001133	0.000113	3.34	0.077
Pure Error	6	0.000203	0.000034		
Total	30	0.045167			

DF - degrees of freedom; SS - sum of squares; MS - mean square

4.3.2.2 Interaction effects of fermentation parameters

The interaction between the fermentation parameters has been explained with the help of contour plots of the regression model, shown in Fig. 4.3.6A-F. The highest CMCase activity is seen for temperature range of 35-45^{o}C within pH range of

5.0-7.0. At a given temperature, even two fold increase of shaking speed did not give any significant increase in the enzyme activity. Similarly, in the optimum pH range of 6.0-7.0, shaking speed did not influence CMCase activity. Same observation was true for variation of CMCase activity with inoculum size and pH. The maxima of CMCase activity was in the range of pH 6.0-7.0 and 40-45^{o}C. The enzyme activity rapidly decreased as either of these variables shifted away from the optimum range. The optimum values of the four variables could be deduced from the desirability function plot as shown in Fig. 4.3.7, which were temperature = 40^{o}C, pH 5.65, shaking speed = 120 rpm and inoculum size = 6.9% (v/v). The predicted enzyme activity under these conditions was 0.710 U/mL. Validation of these results was done using shake flask experiments at the optimum values of these parameters. The experimental enzyme activity was observed to be 0.693 ± 0.043 U/mL, which is an excellent agreement with the predicted value. Quite interestingly these values matched fairly well with the values obtained from OVAT analysis.

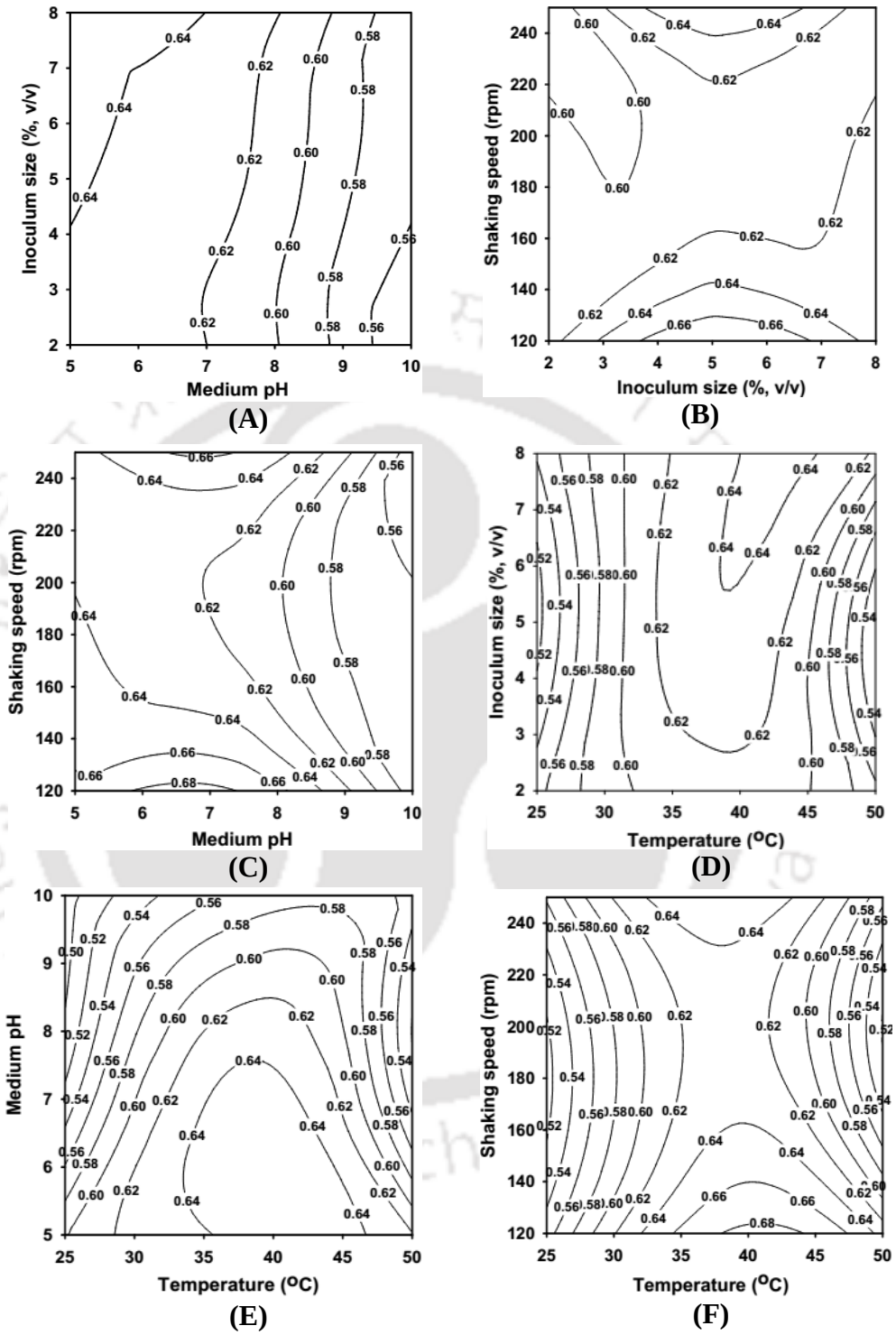

Fig. 4.3.6 Contour plot for CMCase activity (U/mL) showing the interactive effects of fermentation parameters: (A) medium pH and inoculum size; (B) shaking speed and inoculum size; (C) shaking speed and medium pH; (D) temperature and inoculum size (E) temperature and medium pH; (F) temperature and shaking speed.

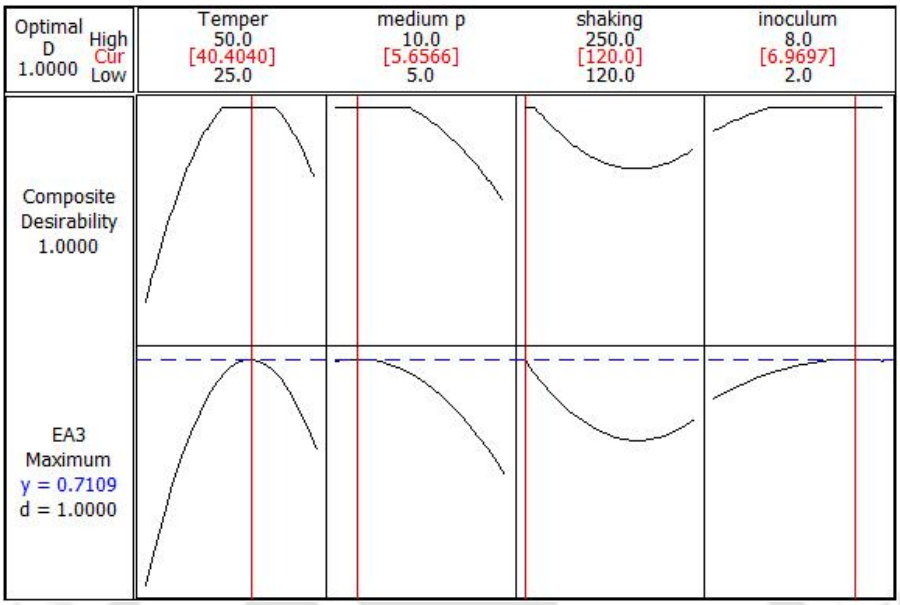

Fig. 4.3.7 Desirability function plot showing the optimum levels of fermentation parameters.

4.3.3 Overall analysis of optimization of CMCase production

The CMCase activity for the optimum medium composition was found to be 0.553 ± 0.021 U/mL and was 0.693 ± 0.043 U/mL after both medium and fermentation parameters optimization (Table 4.3.8). Thus the observed enhancement of CMCase activity after complete optimization (i.e., medium composition and fermentation parameters) was approximately four fold as compared with the CMCase activity (0.161 ± 0.014 U/mL) under unoptimized conditions. However, the increment in activity after optimization of medium composition alone was three fold and further optimization of fermentation parameters yielded only one fold increment. Thus, it can be concluded that the concentration of major medium components is the principal governing factor for CMCase production.

Table 4.3.8 CMCase production at different steps of optimization

Optimization Step	CMCase activity (U/mL)	Enhanced CMCase activity (Fold)
Without optimization	0.161 ± 0.014	-
Fermentation medium	0.553 ± 0.021	3
Fermentation medium + physical parameters	0.693 ± 0.043	4

4.3.4 Comparative assessment of results with published literature

The conclusion of this study is also supported by the outcome of the study by Deka *et al*. (2013), where overall optimization of medium composition and fermentation parameters resulted in eight-fold enhancement in CMCase activity from *Bacillus* sp. and the contribution of medium optimization alone was six fold. A comparative account of optimization of medium as well as optimization of fermentation parameters is given in Table 4.3.9A and B. The enzyme activity reported by Lee *et al*. (2008) and Lee *et al*. (2010) for *Bacillus* sp. is significantly higher (i.e., 137 and 153 U/mL) than that reported in this study as well as several other studies cited in Table 4.3.9A. However, it should be noted that the Lee *et al*. (2008) and Lee *et al*. (2010) determined the enzyme activity at bioreactor scale as compared with shake flask scale in present study, which has better controlled system in terms of operating parameters. Moreover, the carbon source for all species reported in Table 4.3.9A is different from each other, which influences the activity of the enzyme. For example, Sethi *et al*. (2013) used glucose as the sole carbon source, while Shabeb *et al*. (2010) used dual carbon source in the form of molasses and cellulose. It was observed that microorganisms, producing cellulase activity within a similar range as *B. amyloliquefaciens* SS35, were able to hydrolyze several lignocellulosic biomasses significantly. For example: (1) Sago pith waste hydrolysis

by *B. amyloliquefaciens* UMAS 1002 with CMCase activity 0.63 U/mL (Apun *et al*. 2000); (2) enzymatic hydrolysis of sugarcane bagasse for bioethanol production using cellulase with 0.112 and 0.902 U/mL produced by *Trichoderma longibrachiatum* PTCC 5140 and *Aspergillus niger*, respectively (Shaibani *et al*. 2011); (3) Wild grass (*Achnatherum hymenoides*) hydrolysis by *B. subtilis* AS3 with 0.57 U/mL CMCase activity (Deka *et al*. 2013).

It was proven with rigorous study of numerous commercial enzyme preparations (from suppliers such as Novozymes, Dyadic, Genencor, Rhodia-Danisco, Lyven) comprising cellulase, cellobiase and xylanases that the enzyme activities predicted by standard assays using commercially available substrates do not really reflect the actual activity of the enzyme on plant (lignocellulosic) materials (Kabel *et al*. 2006). The enzyme showing lower activity with commercial substrates can do efficient hydrolysis with a lignocellulosic substrate. In the study by Kabel *et al*. (2006), xylanase activity analyzed in the standard xylanase assay did not present a high correlation with the degradation of xylan-rich fractions of wheat bran and grass. A remarkable example is the comparison of the standard activity of Cellubrix (107 U/mL) and Cellulase 2000L (568 U/mL) with the degradation of xylan to xylose of Cellubrix (only 50-60%) and Cellulase 2000L (only 18-20%). The enzyme activity towards the cellulose- and xylan-enriched fractions from grass and wheat bran was revealed to be markedly different than that found with standard assays. Therefore, the actual degradation of the xylan- and cellulose-rich fractions from wheat bran and grass could not be correlated with the (relatively low) activity of enzymes as indicated by standard assays. Therefore, in general, the choice of most suitable

enzyme preparation is dependent on the substrate characteristics also other than on standard enzyme activities measured.

Table 4.3.9 Comparison of various optima reported in literature for CMCase production by *Bacillus* spp.

(A) Representative literature review on optimization of medium components.

***Bacillus* sp.**	**Source**	**Medium Component**	**Method**	**Optimum Conc. (g/L)**	**Scale**	**Cellulase activity (U/mL)**	**Reference**
Bacillus sp. VG1	Hot spring soil	CMC Tryptone	OVAT	10.0 5.0	Shake flask	0.63	Singh *et al*. 2001
B. pumilus EB3	Oil palm empty fruit bunch	CMC Yeast extract $(NH_4)_2SO_4$	OVAT	10.0 2.5 2.5	Shake flask	0.076	Ariffin *et al*. 2008
B. amyloliquefaciens DL3	Soil	Rice hull Peptone $(NH_4)_2SO_4$	OVAT	20.0 2.5 0.6	7 L Bioreactor	153.0	Lee *et al*. 2008
B. subtilis subsp. *subtilis* A-53	Sea water	Rice bran Yeast extract	OVAT	20.0 2.5	7 L Bioreactor	137.0	Lee *et al*. 2010
B. subtilis KO	Sugar factory product	Molasses + Cellulose $(NH_4)_2PO_4$/tryptone	OVAT	1.0 2.0	Shake flask	35.0	Shabeb *et al*. 2010
B. subtilis AS3	Cow dung	CMC Yeast extract Peptone	Plackett-Burman and CCD	18.0 4.79 8.0	Shake flask	0.43	Deka *et al*. 2011
B. subtilis	Soil	Glucose $(NH_4)_2SO_4$	OVAT	50.0 5.0	Shake flask	1.0	Sethi *et al*. 2013
B. amyloliquefaciens SS35	Rhino-ceros dung	CMC Yeast extract Peptone	Plackett-Burman and CCD	19.05 8.0 2.0	Shake flask	0.55	This study (Singh *et al*. 2014)

(B) Representative literature review for optimization of fermentation parameters.

***Bacillus* sp.**	**Source**	**Optimization Parameter**	**Method**	**Optimum value**	**Scale**	**Cellulase activity (U/mL)**	**Reference**
B. amyloliquefaciens UMAS1002	Sago pith waste	pH	OVAT	6.0	Shake flask	9.38	Khan and Hussaini 2006
		Temperature (°C)		40			
		Inoculum size (%, v/v)		4			
		Shaking speed (rpm)		100			
Bacillus sp.	Coir retting effluent	pH	OVAT	7.0	Shake flask	0.02	Immanuel *et al*. 2006
		Temperature (°C)		40			
		Inoculum size (%, v/v)		ND			
		Shaking speed (rpm)		ND			
B. amyloliquefaciens DL3	Soil	pH	OVAT	6.8	7 L Bioreactor	367	Lee *et al*. 2008
		Temperature (°C)		37			
		Inoculum size (%, v/v)		ND			
		Shaking speed (rpm)		ND			
B. subtilis subsp. *subtilis* A-53	Sea water	pH	OVAT	6.8	7 L Bioreactor	137	Lee *et al*. 2010
		Temperature (°C)		30			
		Inoculum size (%, v/v)		ND			
		Shaking speed (rpm)		ND			
B. amyloliquefaciens UNPDV-22	Hot spring	pH	CCD	5.25	Shake flask	13	Vasudeo and Lew 2011
		Temperature (°C)		42.24			
		Inoculum size (%, v/v)		4.95			
		Shaking speed (rpm)		ND			
B. subtilis AS3	Cow dung	pH	CCD	7.2	Shake flask	0.56	Deka *et al*. 2013
		Temperature (°C)		39			
		Inoculum size (%, v/v)		ND			
		Shaking speed (rpm)		121			
B. subtilis	Soil	pH	OVAT	10.0	Shake flask	0.9	Sethi *et al*. 2013
		Temperature (°C)		40			
		Inoculum size (%, v/v)		ND			
		Shaking speed (rpm)		ND			
B. amyloliquefaciens SS35	Rhino-ceros dung	pH	CCD	5.65	Shake flask	0.69	This study (Singh *et al*. 2014)
		Temperature (°C)		40.4			
		Inoculum size (%, v/v)		6.96			
		Shaking speed (rpm)		120			

ND - not determined

4.4 Conclusions

The optimization of the medium components and fermentation parameters for enhancing CMCase activity by *B. amyloliquefaciens* SS35 was carried out. The statistical experimental designs were applied in two steps *viz*. medium optimization and optimization of fermentation parameters. For medium optimization, Plackett-Burman design followed by central composite design was used, while for optimization of fermentation parameters one-variable-at-a-time method followed by central composite design was used. In case of medium optimization Plackett-Burman factorial design revealed that carbon and nitrogen sources in the medium were the significant factors for enzyme production. The results from a 2^3-central composite design were fit in a second-order polynomial model which showed a good agreement between predicted and adjusted coefficient of determination values with R^2 = 0.8642 and 0.9575, respectively. At the concentration of 18.05 g/L CMC, 8.0 g/L yeast extract and 2.0 g/L peptone, the CMCase activity was found to be 0.553 ± 0.021 U/mL, after experimental validation of the model predicted value (0.553 U/mL). The inorganic salts played relatively subordinate role. In optimization of fermentation parameters the results from a 2^4-central composite design were fit in a second-order polynomial model which showed an agreement between predicted and adjusted coefficient of determination values with R^2 = 0.9422 and 0.8473, respectively. The optimum fermentation parameters for optimized medium were: initial medium pH 5.65, incubation temperature 40^{o}C, shaking speed 120 rpm and inoculum size 6.96%, v/v. After experimental validation of the model with predicted CMCase activity of 0.710 U/mL under optimized conditions, CMCase activity was found to be 0.693 ±

0.043 U/mL. Thus the fold enhancement in CMCase activity was 3-fold after medium optimization and 4-fold after both medium and fermentation parameters optimization. The optimization study of fermentation parameters reveals independent influence of the fermentation parameters and overall, even the individual influence is only marginal, as compared to the effect of medium composition. The CMCase production by *B. amyloliquefaciens* SS35 is predominantly influenced by the medium components in comparison to fermentation parameters.

References

Apun, K., Jong, B. C. and Salleh, M. A. (2000) Screening and isolation of a cellulolytic and amylolytic *Bacillus* from sago pith waste. Journal of General and Applied Microbiology, 46, 263-267.

Ariffin, H., Abdullah, N., Umikalsom, M. S., Shirai, Y. and Hassan, M. A. (2008) Production of bacterial endoglucanase from pretreated oil palm empty fruit bunch by *Bacillus pumilus* EB3. Journal of Bioscience and Bioengineering, 106, 231-236.

Ballesteros, M., Oliva, J. M., Negro, M. J., Manzanares, P. and Ballesteros, J. (2004) Ethanol from lignocellulosic materials by a simultaneous saccharification and fermentation process (SSF) with *Kluyveromyces marxianus* CECT 10875. Process Biochemistry, 39, 1843-1848.

Deka, D., Bhargavi, P., Sharma, A., Goyal, D., Jawed, M. and Goyal, A. (2011) Enhancement of cellulase activity from a new strain of *Bacillus subtilis* by medium optimisation and analysis with various cellulosic substrates. Enzyme Research, volume 201, Article ID 151656, 8 pages.

Deka, D., Das, S. P., Sahoo, N., Das, D., Jawed, M., Goyal, D. and Goyal, A. (2013) Enhanced cellulase production from *Bacillus subtilis* by optimizing physical parameters for bioethanol production. ISRN Biotechnology, doi:10.5402/2013/965310.

Gao, W., Lee, E. J., Lee, S. U., Li, J., Chung, C. H. and Lee, J. W. (2012) Enhanced carboxymethylcellulase production by a newly isolated marine bacterium

Cellulophaga lytica LBH-14 using rice bran. Journal of Microbiology and Biotechnology, 22, 1412-1422.

Immanuel, G., Dhanusha, R., Prema, P. and Palavesam, A. (2006) Effect of different growth parameters on endoglucanase enzyme activity by bacteria isolated from coir retting effluents of estuarine environment. International Journal of Environmental Science and Technology, 3, 25-34.

Jin, I. H., Jing, D. Y., Son, C. W., Kim, S. K., Gao, W., Chung, C. H. and Lee, J. W. (2011) Enhanced production of heteropolysaccharide-7 by *Beijerinkia indica* HS-2001 in repeated batch culture with optimized substitution of culture medium. Biotechnology and Bioprocess Engineering, 16, 245-255.

Kabel, M. A., van der Maarel, M. J. E. C., Klip, G., Voragen, A. G. J. and Schols, H. A. (2006) Standard assays do not predict the efficiency of commercial cellulase preparations towards plant materials. Biotechnology and Bioengineering, 93, 56-63.

Khan, F. A. B. A. and Husaini, A. A. S. A. (2006) Enhancing *α*-amylase and cellulase *in vivo* enzyme expressions on sago pith residue using *Bacillus amyloliquefaciens* UMAS 1002. Biotechnology, 5, 391-403.

Kim, B. K., Lee B. H., Lee, Y. J., Jin I. H., Chung C. H. and Lee, J. W. (2009) Purification and characterization of carboxymethylcellulase isolated from a marine bacterium *Bacillus subtilis* sub sp. subtilis A-53. Enzyme and Microbial Technology, 44, 411-416

Lee, B. H., Kim, B. K., Lee, Y. J., Chung, C. H. and Lee, J. W. (2010) Industrial scale of optimization for the production of carboxymethylcellulase from rice

bran by a marine bacterium, *Bacillus subtilis* subsp. subtilis A-53. Enzyme and Microbial Technology, 46, 38-42.

Lee, Y. J., Kim, B. K., Lee, B. H., Jo, K. I., Lee, N. K., Chung, C. H., Lee, Y. C. and Lee, J. W. (2008) Purification and characterization of cellulase produced by *Bacillus amyloliquefaciens* DL-3 utilizing rice hull. Bioresource Technology, 99, 378-386.

Li, W., Zhang, W. W., Yang, M. M. and Chen, Y. L. (2008) Cloning of the thermostable cellulase gene from newly isolated *Bacillus subtilis* and its expression in *Escherichia coli*. Molecular Biotechnology, 40, 195-201.

Lynd, L. R., Weimer, P. J., van Zyl, W. H. and Pretorius, I. S. (2002) Microbial cellulose utilization: fundamentals and biotechnology. Microbiology and Molecular Biology Reviews, 66, 506-577.

Nelson, N. (1944) A photometric adaptation of the Somogyi method for the determination of glucose. Journal of Biological Chemistry, 153, 375-380.

Pason, P., Kyu, K. L. and Ratanakhanokchai, K. (2006) *Paenibacillus curdlanolyticus* strain B-6 xylanolytic-cellulolytic enzyme system that degrades insoluble polysaccharides. Applied and Environmental Microbiology, 72, 2483-2490.

Plackett, R. L. and Burman, J. P. (1946) The design of optimum multifactorial experiments. Biometrika, 33, 305-325.

Rastogi, G., Muppidi, G. L., Gurram, R. N., Adhikari, A., Bischoff, K. M., Hughes, S. R., Apel, W. A., Bang, S. S., Dixon, D. J. and Sani, R. K. (2009) Isolation and characterization of cellulose-degrading bacteria from the deep subsurface

of the Homestake gold mine, Lead, South Dakota, USA. Journal of Industrial Microbiology and Biotechnology, 36, 585-598.

Sethi, S., Datta, A., Gupta, B. L. and Gupta, S. (2013) Optimization of cellulase production from bacteria isolated from soil. ISRN Biotechnology, Volume 2013, Article ID 985685, 7 pages.

Shabeb, M. S. A., Younis, M. A. M., Hezayen, F. F. and Noureldein, M. A. (2010) Production of cellulase in low-cost medium by *Bacillus subtilis* KO strain. World Applied Sciences Journal, 8, 35-42.

Shaibani, N., Ghazvini, S. Andalibi, M. R. and Yaghmaei, S. (2011) Ethanol production from sugarcane bagasse by means of enzymes produced by solid state fermentation method. World Academy of Science Engineering and Technology, 59, 1836-1839.

Singh, A. and Bishnoi, N. R. (2012) Enzymatic hydrolysis optimization of microwave alkali pretreated wheat straw and ethanol production by yeast. Bioresource Technology, 108, 94-101.

Singh, J., Batra, N. and Sobti, R. C. (2001) A highly thermostable, alkaline CMCase produced by a newly isolated *Bacillus* sp. VG1. World Journal of Microbiology and Biotechnology, 17, 761-765.

Singh, S., Moholkar, V. S. and Goyal, A. (2013) Isolation, identification and characterization of a cellulolytic *Bacillus amyloliquefaciens* strain SS35 from rhinoceros dung. ISRN Microbiology, Volume 2013, Article ID 728134, 7 pages.

Singh, S., Moholkar, V. S. and Goyal, A. (2014) Optimization of carboxymethylcellulase production from *Bacillus amyloliquefaciens* SS35. 3Biotech, 4, 411-424.

Somogyi, M. (1945) A new reagent for the determination of sugars. Journal of Biological Chemistry, 160, 61-68.

Unrean, P. and Nguyen, N. H. A. (2013) Metabolic pathway analysis and kinetic studies for production of nattokinase in *Bacillus subtilis*. Bioprocess and Biosystems Engineering, 36, 45-56.

Van Dyk, J. S., Sakka, M., Sakka, K. and Pletschke, B. I. (2009) The cellulolytic and hemi-cellulolytic system of *Bacillus licheniformis* SVD1 and the evidence for production of a large multi-enzyme complex. Enzyme and Microbial Technology, 45, 372-378.

Vasudeo, Z. and Lew, C. (2011) Optimization of culture conditions for production of cellulase by a thermophilic *Bacillus* strain. Journal of Chemistry and Chemical Engineering, 5, 521-527.

Zheng, Y., Pan, Z., Zhang, R. and Wang, D. (2009) Enzymatic saccharification of dilute acid pretreated saline crops for fermentable sugar production. Applied Energy, 86, 2459-2465.

Chapter 5

Purification and characterization of endoglucanase from *Bacillus amyloliquefaciens* SS35

5.1 Introduction

Cellulases have become prominent commercial enzymes in the contemporary market because of their ubiquitous applications in diverse fields. In the present day context of fossil fuel scarcity, the most important application of cellulases is in hydrolysis of lignocellulosic biomass to fermentable sugars, which could be used for bioalcohol (bioethanol or biobutanol) production (Bhatt 2000; Ranjan *et al*. 2013), which are potential alternate liquid transportation fuels. Aerobic mesophilic bacteria such as *Cellulomonas* spp. (Saratale *et al*. 2010; Yin *et al*. 2010), *Bacillus* spp. (Jiang 2006; Lee *et al*. 2008; Kim *et al*. 2009) and thermophilic anaerobic bacteria such as *Acetivibrio cellulolyticus*, *Bacteroides cellulosolvens* and *Clostridium thermocellum* (Clarke *et al*. 1996) as well as actinomycetes such as *Microbispora bispora* (Eida *et al*. 2012) and *Thermomonospora* sp. (Spiridonov and Wilson 1998) have been reported to produce active cellulases. Some efficient cellulase producers of the genus *Bacillus* include *Bacillus* sp. KSM-S237 (Hakamada *et al*. 1997), *Bacillus amyloliquefaciens* (Lee *et al*. 2008), *Bacillus subtilis* (Kim *et al*. 2009; Deka *et al*.

2013) and *Bacillus megaterium* (Shobharani *et al*. 2013). The purification of extracellular carboxymethylcellulase (CMCase) from *Bacillus* spp. by ammonium sulphate fractionation followed by ion exchange chromatography has been reported (Lee *et al*. 2008; Kim *et al*. 2009; Yin *et al*. 2010; Vijayaraghavan and Vincent 2012; Deka *et al*. 2013). Very few reports are available on the production of acidic CMCase from *Bacillus* spp. such as from *Bacillus* sp. M-9 (Bajaj *et al*. 2009) and *Bacillus thuringiensis* (Lin *et al*. 2012). In the present study, the purification and characterization of an extracellular acidic endoglucanase from a mesophilic and facultative acidophilic isolate from rhinoceros dung, is reported. The characterization of the enzyme was done in terms of activity staining for investigating active forms, molecular weight determination by polyacrylamide gel electrophoresis, pH and temperature optima, stability, effect of additives, substrate specificity and kinetic studies. These properties depend on the nature and occurrence of organism from which the enzyme is produced (Wang *et al*. 2009). The properties of the CMCase revealed in this study may be very useful for various processes of bioethanol production by means of enzymatic hydrolysis of lignocellulosic biomass. These processes may be separate hydrolysis and fermentation (SHF) or simultaneous saccharification and fermentation (SSF), the selection of these processes depends on the compatibilities of the enzyme used and the properties of fermenting microorganisms.

5.2 Materials and Methods

5.2.1 Materials

Carboxymethylcellulose (CMC) (low viscosity, 50-200 cP) and other substrates were procured from Sigma Aldrich (St. Louis, USA) except avicel, hydroxyethylcellulose and barley β-glucan which were purchased from Fluka, Biochemika. DEAE-Sepharose CL-6B anion exchange resin was purchased from Sigma Aldrich (St. Louis, USA). All medium components and chemicals used in this study were procured from HiMedia Pvt. Ltd., India.

5.2.2 Microorganism and CMCase production

The bacterium used for extracellular CMCase production, *Bacillus amyloliquefaciens* SS35 was isolated from rhinoceros dung and identified by sequencing of 16S rDNA (GenBank accession no.: JX674030) and gyrase A (GenBank accession no.: KF019284) gene (Singh *et al*. 2013). The medium composition, used for CMCase production was: CMC-Na (19.0 g/L), yeast extract (8 g/L), peptone (2 g/L), K_2HPO_4 (1 g/L), $MgSO_4 \cdot 7H_2O$ (0.2 g/L), NaCl (1 g/L) and the pH of medium was adjusted to 5.6. A 500 mL Erlenmeyer flask containing 200 mL of medium was inoculated with 7% (v/v) culture (A_{600} = 1.0) and incubated at 40°C and 120 rpm (Singh *et al*. 2014a). The culture was grown for 48 h and then centrifuged at 12000***g*** for 20 min at 4°C. The cell free supernatant containing the enzyme was analysed for endoglucanase (CMCase) activity.

5.2.3 CMCase activity assay

The CMCase activity was measured by estimation of glucose liberated from CMC. The enzyme assay was carried out by incubating the enzyme with CMC for 15 min at 55°C as described in Chapter 3, Section 3.2.6. The reaction mixture (100 µL) contained 50 µL of enzyme and 1.0% (w/v) final concentration of CMC in 50 mM sodium acetate buffer (pH 5.0). The activity of enzyme was measured by estimation of reducing sugar following Nelson-Somogyi procedure (Nelson 1944; Somogyi 1945) as described in Chapter 3, Section 3.2.6. The absorbance at 500 nm (A_{500}) was measured using a UV-visible spectrophotometer (Varian, Cary 100) against a blank and CMCase activity was calculated by using a calibration curve for glucose. One unit (U) of CMCase activity is defined as the amount of enzyme that liberates 1 µmole of reducing sugar (glucose) per min under the assay conditions of pH 5.0 and temperature 55^{o}C.

5.2.4 Estimation of protein concentration

The protein concentration was determined by the method of Lowry *et al*. (1951) using bovine serum albumin (BSA) as standard. A concentration range 20-500 µg/mL BSA was used to plot standard curve. To 200 µL of sample containing 10 µL cell free extract, 1.0 mL of reagent C (described below) was added. After 10 min, 100 µL of Folin's reagent (described below) was added and absorbance at 660 nm (A_{660}) was measured after 30 min against a blank. Composition of the reagents used for protein estimation by Lowry method is as follows:

Reagent A

Sodium hydroxide (0.4 g) and sodium carbonate (2.0 g) were dissolved in water and the volume made up to 100 mL.

Reagent B1

Potassium sodium tartrate tetrahydrate (2.0 g) dissolved in 100 mL distilled water.

Reagent B2

Copper sulphate pentahydrate (1.0 g) dissolved in 100 mL distilled water.

Reagent C

Freshly prepared by mixing reagent B1, A and B2 in a ratio of B1:A:B2 = 1:100:1.

Folin's reagent

1 N Folin's reagent.

The concentration of protein was calculated as follows:

$$\text{Protein concentration}\left(\text{mg/mL}\right)=\frac{\Delta A_{660}\times C\times V}{v}$$

ΔA_{660} = change in absorbance of the sample at 660 nm
C = 1 absorbance equivalent BSA concentration (mg/mL) from standard plot
V = total volume (mL)
v = volume of the sample (mL)

5.2.5 Purification of enzyme

5.2.5.1 Ammonium sulphate fractionation method

Ammonium sulfate was added to 200 mL of the cell free supernatant containing crude enzyme with stirring to attain 60% saturation. The precipitated protein in this fraction was separated from supernatant by centrifugation at 12000***g*** at

4°C for 20 min. The ammonium sulphate was further added to the remaining supernatant to attain 90% saturation. The protein was allowed to precipitate for 12 h and then collected by centrifugation at 12000***g*** and at 4°C for 20 min. The pellet was dissolved in 50 mM sodium acetate buffer (pH 5.0) and subsequently, dialyzed using 12 kDa cut-off membrane against the same buffer for 12 h with three changes.

5.2.5.2 Ion exchange chromatography

After dialysis the enzyme was further purified using Fast Protein Liquid Chromatography, FPLC (GE Healthcare). A DEAE-Sepharose column (1.5 cm x 10 cm) was used for anion exchange chromatography. The column was pre-equilibrated with 50 mM sodium acetate buffer pH 6.0 and 10 mL of the enzyme was loaded on it. The column was washed with two bed volume of the same buffer and the bound protein was eluted with a linear gradient of 0-0.6 M NaCl in equilibration buffer at a flow rate of 1 mL/min. Each fraction of 3 mL was collected for estimation of protein (absorbance 280 nm) using a spectrophotometer (Varian, Cary 100) and CMCase activity (U/mL). The fractions exhibiting cellulase activity were further analyzed by sodium dodecyl sulphate polyacrylamide gel electrophoresis (SDS-PAGE), to check the purity of the enzyme and to determine molecular mass of the enzyme. All the purification steps were performed at 4^{o}C.

5.2.6 Molecular mass determination by SDS-PAGE and zymogram analysis

5.2.6.1 Preparation of reagents and buffers

Preparation of 30% (w/v) acrylamide solution

Acrylamide (29.2 g) and bis acrylamide (0.8 g) were dissolved in 100 mL distilled water and the solution was then filtered using Whatman No. 1 filter paper under dark condition. The solution was stored at 4°C in an amber colour bottle.

Tris-HCl (1.5 M, pH 8.8)

54.45 g Tris base (121.14 g/mol) was dissolved in 150 ml of distilled water and pH of solution was adjusted to 8.8. Volume was made up to 300 ml and stored at 4°C.

Tris-HCl (0.5 M, pH 6.8)

6.0 g Tris base (121.14 g/mol) was dissolved in 60 ml of distilled water and pH of solution was adjusted to 6.8. Volume was made up to 100 ml and stored at 4°C.

SDS solution (10%, w/v)

10.0 g SDS was dissolved in 100 mL distilled water.

Sample buffer (5x)

The protein sample buffer (5x) was prepared by mixing the components given in Table 5.2.1. 5x stock solution of sample buffer was mixed with 4 volumes of protein sample to make it to 1x before loading on to the gel.

Table 5.2.1 Composition of 5x sample buffer.

Component	Final concentration
Tris HCl (pH 6.8)	62.5 mM
Glycerol	20% (v/v)
SDS	2% (v/v)
Bromophenol blue	0.025% (w/v)
β-mercaptoethanol	5% (v/v)

Running buffer (5x)

1x Tris-glycine buffer (pH 8.3) was used for running SDS-PAGE gel and was prepared from the 5x stock solution. The composition of 5x Tris glycine buffer (pH 8.3) is given in Table 5.2.2. The 5x running buffer was filtered (Whatman, Filter No. 1) and stored at 4°C.

Table 5.2.2 Composition of 5x running buffer.

Component	Final concentration
Tris base	0.125 M
Glycine	1.25 M
SDS	0.5% (w/v)

5.2.6.2 Preparation of SDS-PAGE gels

The SDS-polyacrylamide gel electrophoresis was performed by using a vertical slab mini gel unit (Mini-PROTEAN®Tetra cell, BioRad, USA) with 1.5 mm thick gels. The composition of resolving gel with 12% (w/v) acrylamide and stacking gel with 4% (w/v) acrylamide is given in Table 5.2.3 and Table 5.2.4, respectively.

Table 5.2.3 Composition of 12% resolving gel.

Component	Volume (mL)
Acrylamide-bisacrylamide solution (30%, w/v)	4.00
SDS solution (10%, w/v)	1.00
1.5 M Tris (pH 8.8)	3.30
APS solution (10%, w/v)	0.10
TEMED	0.01
Deionised water	1.70
Total volume	10.00

Table 5.2.4 Composition of 4% stacking gel.

Component	Volume (mL)
Acrylamide-bisacrylamide solution (30%, w/v)	0.70
SDS solution (10%, w/v)	0.50
0.5 M Tris (pH 6.8)	1.00
APS solution (10%, w/v)	0.05
TEMED	0.01
Deionised water	2.74
Total volume	5.00

5.2.6.3 Staining and destaining solutions

The Coomassie brilliant blue (CBB) staining solution was prepared by dissolving 250 mg of CBB R-250 dye in 50 ml of distilled water. The solution was filtered through Whatman, Filter No. 1. After filtration 40 ml of methanol and 10 ml of glacial acetic acid were added and the solution was stored in amber colour bottle. Destaining solution was prepared by mixing 40 mL methanol (40%, v/v) and 10 mL acetic acid (10%, v/v) in 50 mL distilled water.

5.2.6.4 SDS-PAGE and zymogram analysis

SDS-polyacrylamide gel electrophoresis was performed using 12% resolving gel and 4% stacking gel under denaturing condition following the method described by Laemmli (1970). 0.1% (w/v) CMC was incorporated into the resolving gel for zymogram analysis of CMCase. The protein sample from DEAE-sepharose column chromatography was concentrated by using Lyophilizer (Christ Alpha 1-4 LD Freeze dryer), before loading on the gel. The samples were mixed with 5x loading dye buffer in the ratio of 4:1. The sample mixtures were subjected to heat denaturation for 5 min. The electrophoresis was carried out using 1x running buffer with a current

of 2.5 mA per lane. Molecular mass marker (10-200 kDa), purchased from Fermentas International Inc., was used as standard for SDS-PAGE. After electrophoresis, gel was cut into two parts; one part was subjected to staining with Coomassie brilliant blue (CBB) R-250 and the other to activity staining. Activity of separated bands was detected by renaturing the gel in 2.5% (v/v) Triton X-100 in 50 mM sodium acetate buffer (pH 5.0) for 4 h following the method of van Dyk *et al.* (2010). The gel was then incubated in 50 mM acetate buffer (pH 5.0) at 55°C for 3-4 h. After removal of the buffer, the gel was stained with 0.1% (w/v) Congo red for 15 min and then destained with 1 M NaCl until bands appeared. The zymogram containing gel was then counterstained with 1 M HCl. The molecular mass of the CMCase was estimated by using Hendrick plot (Hendrick and Smith 1968) based on relative mobility of the proteins with respect to standard calibration proteins.

5.2.7 Effect of temperature on CMCase activity and stability

The optimum temperature of purified enzyme was determined by performing assay at temperatures 30, 35, 40, 45, 50, 55, 60 and 65°C. 2 mL (0.08 mg/mL) of purified enzyme was lyophilized and re-dissolved in 400 µL of 50 mM sodium phosphate buffer (pH 7.0) to a final protein concentration of 0.4 mg/mL. The CMCase assay was performed using 10 µL (0.4 mg/mL) enzyme in a 100 µL reaction mixture containing 1% (w/v) final concentration of CMC in 50 mM sodium phosphate buffer (pH 7.0). The reaction mixture was incubated in water bath at various temperatures for 15 min. Thermal stability study of CMCase was performed by incubating 500 µL (0.4 mg/mL) of purified enzyme in 50 mM sodium acetate

buffer (pH 5.0) at temperatures ranging from 20-70°C for 20 h. The samples (10 µL) were withdrawn periodically and residual CMCase activity of each sample was determined, following the CMCase assay method as described in Section 5.2.3.

5.2.8 Effect of pH on CMCase activity and stability

The optimum pH of enzyme assay was determined by using different buffers of pH range 3.5-10.5 with a difference of 0.5 units. 500 µL (0.08 mg/mL) of purified enzyme was lyophilized and re-dissolved in buffers (100 µL) of different pH values to final protein concentration of 0.4 mg/mL. The reaction mixture (100 µL) contained 10 µL (0.4 mg/mL) purified enzyme and 1%, w/v CMC final concentration in different buffers. Buffers used in the reaction were 50 mM sodium acetate pH 3.5-5.5, 50 mM sodium phosphate buffer pH 6.0-8.0 and 50 mM glycine-NaOH pH 8.5-10.5. The reaction mixtures were incubated at 55°C for 15 min and CMCase activity was determined as described in Section 5.2.3. The stability of CMCase at different pH environment was examined by incubating 500 µL (0.4 mg/mL) enzyme in buffers with different pH values ranging from 4.0-10.0 with the difference of 1 unit, at 30^{o}C for 20 h. The samples (10 µL) were withdrawn periodically and assayed in 100 µL reaction mixture containing 1%, w/v CMC final concentration in 50 mM sodium acetate buffer (pH 5.0). Residual CMCase activity was determined by following the CMCase assay described in Section 5.2.3.

5.2.9 Effect of metal ions on enzyme activity

The variation in CMCase activity in presence of various metal ions was

examined by using 1, 5, 10 and 50 mM concentrations of each metal ion *viz*. Co^{+2} ($CoCl_2$), Ca^{+2} ($CaCl_2$), K^+ (KCl), Na^+ (NaCl), Mn^{2+} ($MnCl_2$), Zn^{2+} ($ZnCl_2$), Fe^{3+} ($FeCl_3$) and Hg^{2+} ($HgCl_2$). 500 µL (0.08 mg/mL) of purified enzyme from column was lyophilized and re-dissolved in 100 µL, 50 mM sodium acetate buffer (pH 5.0) giving 0.4 mg/mL final protein concentration. The enzyme was incubated with different concentrations of metal ions at 30°C and pH 5.0 for 1 h before carrying out CMCase activity assay. The CMCase assay was performed using 10 µL sample in 100 µL reaction mixture containing 1%, w/v CMC final concentration in 50 mM sodium acetate buffer (pH 5.0) at 55°C. Residual CMCase activity was determined by following the CMCase assay described in Section 5.2.3.

5.2.10 Substrate specificity of purified enzyme

The substrate specificity of the purified enzyme was determined by incubating the enzyme with CMC, *β*-D-Glucan (barley), lichenan, hydroxyethylcellulose, avicel, starch, *p*NPG (4-nitrophenyl *β*-D-glucopyranoside), birch wood xylan, beech wood xylan and oat spelt xylan for 15 min at 55°C. The reaction mixture (100 µL) contained 10 µL of enzyme (0.4 mg/mL) and 90 µL (1.0% w/v, final concentration) of each of different substrates in 50 mM sodium acetate buffer (pH 5.0). The hydrolysis of different substrates was measured with estimation of the liberated reducing sugar following Nelson-Somogyi procedure (Nelson 1944; Somogyi 1945). The A_{500} was measured against a blank with D-glucose and D-xylose (for xylans) as standard. For determination of *p*NPG hydrolysis the amount of released *p*-nitrophenol (*p*NP) was measured at A_{405}. 2 mM stock solutions of *p*NPG was

prepared by dissolving 6.3 mg of *p*NPG in 50-75 µl of dimethyl sulphoxide (DMSO) and then making up the final volume to 10 ml with 50 mM sodium acetate buffer (pH 5.0). The reaction mixture containing 1 mL *p*NPG solution and 50 µL of enzyme (0.08 mg/mL) was incubated at 55^{o}C for 15 min. The reaction was stopped by the adding 0.5 mL of 1 M Na_2CO_3. The released *p*NP was quantified using the molar extinction coefficient (ε) of 1819 M^{-1} cm^{-1} as reported by Yang et al. (2008).

5.2.11 Determination of kinetic parameters of CMCase

The kinetics of CMCase was characterized in terms of Michaelis-Menten kinetic parameters (K_m and V_{max}) (Michaelis and Menten 1913) using the Lineweaver-Burk double reciprocal plot (Lineweaver and Burk 1934). The CMCase was assayed in CMC concentration range from 0.1 mg/mL to 10.0 mg/mL in 50 mM sodium acetate buffer (pH 5.0) at 55°C for 15 min. The data were analyzed using linear regression (Fig. 5.3.8) and the value of kinetic constants was calculated from the best fit.

5.2.12 Enzymatic hydrolysis of *Parthenium hysterophorus* biomass

P. hysterophorus biomass was collected from IIT Guwahati campus. After washing, drying and grinding the biomass was subjected to pretreatment employing a physicochemical method (1%, v/v H_2SO_4 + 30 min autoclaving and ultrasound assisted alkali treatment for lignin removal) as described in Chapter 6 (Section 6.3.3 and 6.3.3.1, respectively) and also published (Singh *et al*. 2014b, Singh *et al*. 2014c). Pretreated *P. hysterophorus* biomass was subjected to enzymatic hydrolysis using

CMCase, produced by *B. amyloliquefaciens* SS35. The partially purified CMCase (60-90% ammonium sulphate precipitated CMCase) was used for making the enzymatic hydrolysis process economical. The experiments were performed with 0.5% w/v pretreated biomass loading in aqueous solution containing sodium acetate buffer (0.05 M, pH 5.0). This solution was supplemented with CMCase (concentration 200 U/g biomass). The reactions were carried out in 150 mL Erlenmeyer flask with total reaction volume of 20 mL. 0.005%, w/v sodium azide was added to the reaction mixture to avoid contamination. The flask was incubated at 30^{o}C and 150 rpm in an incubator shaker (Orbitek, Scigenics Biotech). The temperature of incubation was 30^{o}C instead of 55^{o}C (which was optimum for CMCase activity, Fig. 5.3.4) assuming the use of enzyme further in an SSF process, because the most of the wild type fermenting organisms are true mesophiles. Moreover, the thermo-stability profile (Fig. 5.3.5) of enzyme indicated the unstability of the enzyme at temperature above 55^{o}C. 100 µL sample was withdrawn at regular interval and analysed for total reducing sugar (TRS) following the method given by Nelson (1944) and Somogyi (1945).

5.3 Results and Discussion

5.3.1 Purification of CMCase

The precipitation of CMCase from cell-free supernatant was carried out by ammonium sulphate fractionation method followed by ion exchange chromatography using DEAE-Sepharose. The crude enzyme obtained as a cell free supernatant had specific activity of 0.216 U/mg, (calculated from 0.70 U/mL and 3.1 mg/mL) (Table 5.3.1). The proteins present in crude extract were precipitated with addition of ammonium sulphate and maximum CMCase activity was observed in fractions precipitated at 60-90% saturation. After ammonium sulphate precipitation, 1.0 U/mg specific activity was observed with 4.6-fold purification (as compared with crude extract) with 12.4% yield (Table 5.3.1). The enzyme was further purified by DEAE-Sepharose column chromatography. Fraction number 19-27 (each 3 mL fraction size) obtained after ion exchange chromatography showed high protein content (A_{280}) and were selected for determination of CMCase activity (Fig. 5.3.1). Among these, fraction numbers 19-21 showed higher CMCase activities, hence were pooled and selected for further work. The purified enzyme showed specific activity of 4.0 U/mg with 18.5 fold purification and a final yield of 2.1% (Table 5.3.1).

Table 5.3.1 Purification of CMCase enzyme from *B. amyloliquefaciens* SS35.

Purification step	Volume (mL)	Enzyme activity (U/mL)	Total activity (U)	Protein (mg/mL)	Total protein (mg)	Specific activity (U/mg)	Yield (%)	Purification fold
Culture supernatant	200	0.70	138.6	3.1	620	0.22	-	-
60-90% $(NH_4)_2SO_4$ precipitation	10	1.72	17.2	1.7	17	1.0	12.4	4.6
Ion-exchange chromatography	9	0.32	2.9	0.08	0.72	4.0	2.1	18.5

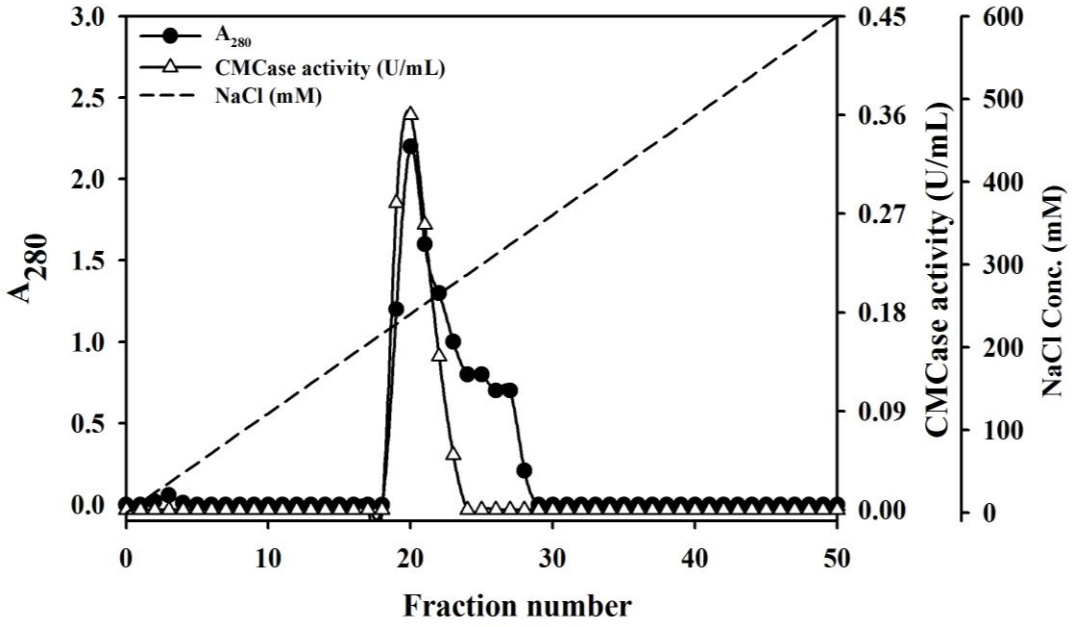

Fig. 5.3.1 Elution profile of CMCase given by DEAE-sepharose column equilibrated with 50 mM sodium acetate buffer pH (6.0) and eluted with linear gradient of 0-600 mM NaCl.

5.3.2 Molecular weight determination and zymogram analysis

In the SDS-PAGE denaturing gel, lane M showed standard proteins as molecular mass marker, lane 1 was precipitated enzyme after ammonium sulphate fractionation (60-90%) and lane 2 was CMCase active fraction by DEAE-Sepharose column chromatography (Fig. 5.3.2). Zymogram analysis of purified CMCase confirmed the single CMCase activity band (Fig. 5.3.2, lane 3). Molecular mass of the enzyme was found to be 37 kDa as estimated by Hendrick plot (Hendrick and Smith 1968) based on relative mobility of the proteins with respect to standard proteins (Fig. 5.3.3). The molecular mass of 37 kDa of CMCase in this study is closer or similar to the molecular weight of cellulase from *Bacillus* sp. PDV (33 kDa) (Sharma *et al*. 1990), *Bacillus* sp. CH43 (40 kDa) (Mawadza *et al*. 2000), *Bacillus* sp. HR68 (40 kDa) (Mawadza *et al*. 2000), *B. licheniformis* (37 kDa) (Bischoff *et al*.

2006), *B. subtilis* GN156 (25 kDa) (Apiraksakorn *et al*. 2008), *B. subtilis* YJ1 (32.5 kDa) (Yin *et al* 2010) and *B. subtilis* AS3 (30 kDa) (Deka *et al*. 2013) (Table 5.3.4).

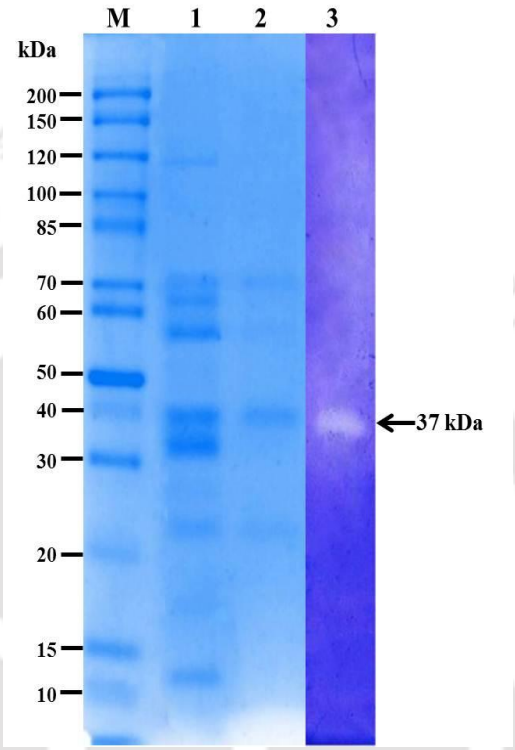

Fig. 5.3.2 SDS-PAGE showing the purification steps and zymogram of CMCase from *B. amyloliquefaciens* SS35 using 12% acrylamide gel. Lane M: molecular mass marker (10-200 kDa), Lane 1: cell-free supernatant precipitated by ammonium sulphate fractionation (60-90%) method, Lane 2: active fraction after DEAE-Sepharose chromatography and Lane 3: zymogram of purified CMCase stained with 0.3% (w/v) congo red, destained with 1 M NaCl and counter stained with 1 N HCl.

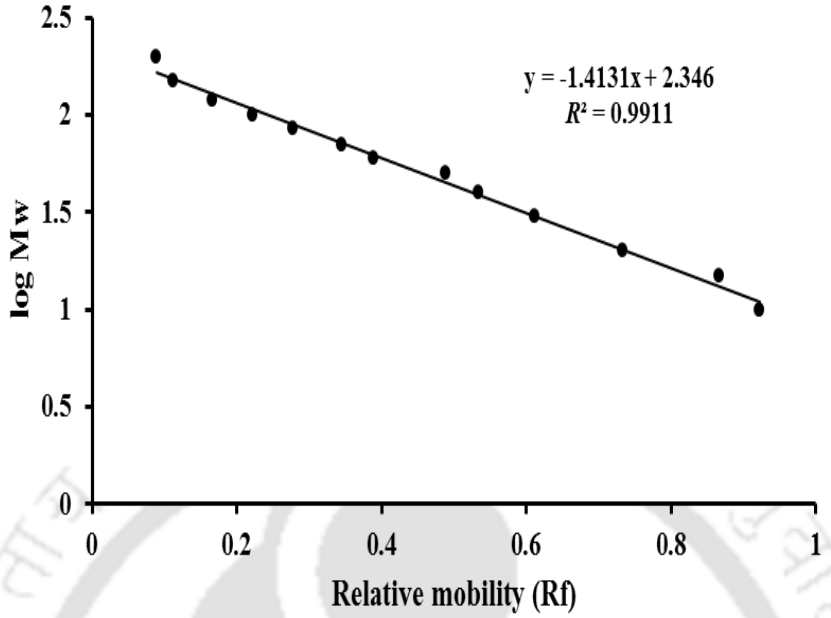

Fig. 5.3.3 Hendricks plot for determination of molecular weight (M_w) of an unknown protein by SDS-PAGE. Plot showing relative mobility (R_f) versus log M_w to determine molecular weight of the purified CMCase from *B. amyloliquefaciens* SS35.

5.3.3 Effect of temperature on enzyme activity and stability

The optimum temperature for CMCase activity was found to be 55°C and more than 60% of the relative CMCase activity was observed at the range of 30-60^{o}C (Fig. 5.3.4). The optimum temperature of CMCase produced by *B. amyloliquefaciens* SS35 is higher than that produced by *B. amyloliquefaciens* DL-3 (50^{o}C) (Lee *et al*. 2008), *B. subtilis* subsp. *subtilis* A-53 (50^{o}C) (Kim *et al*. 2009), *B. thuringiensis* (40^{o}C) (Lin *et al*. 2012), *Bacillus* sp. (50^{o}C) (Vijayaraghavan and Vincent 2012), *B. subtilis* AS3 (45^{o}C) (Deka *et al*. 2013) and *Bacillus* sp. (50^{o}C) (Sadhu *et al*. 2013) and lower than that cellulase produced by *B. subtilis* GN156 (60^{o}C) (Apiraksakorn *et al*. 2008), *Bacillus* sp. M-9 (60^{o}C) (Bajaj *et al*. 2009) and *Bacillus* sp. DUSELR13 (75^{o}C) (Rastogi *et al*. 2010) (Table 5.3.4).

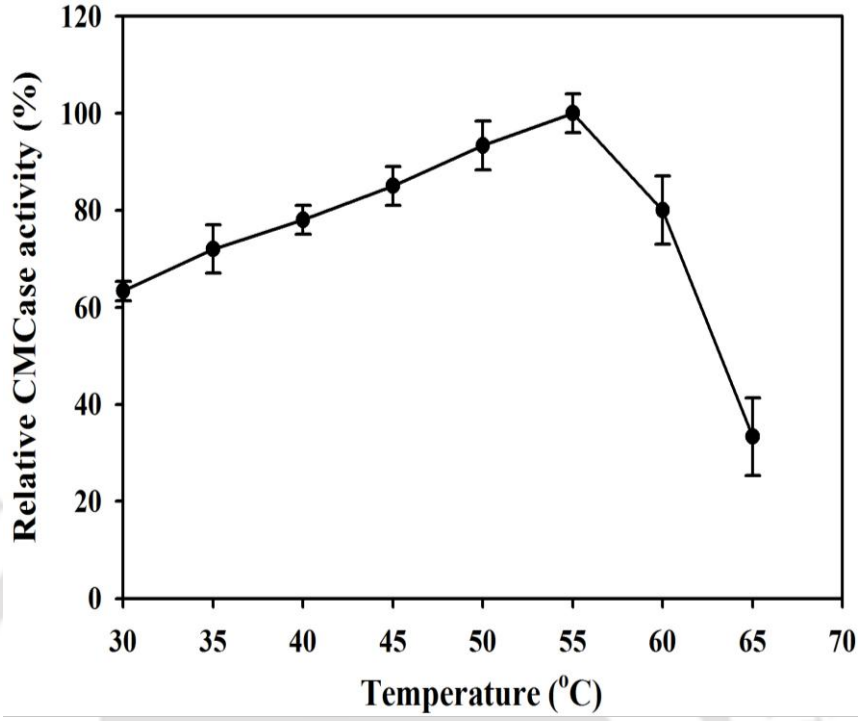

Fig. 5.3.4 Effect of temperature on activity of purified CMCase from *B. amyloliquefaciens* SS35. The CMCase assays were performed in a range of temperature 30-65°C and pH 7.0.

Thermostability studies of purified CMCase revealed that the enzyme retained more than 80% of the initial CMCase activity at temperatures ranging from 20-40°C and was most stable at 30°C after 20 h. At 50°C after 1 h of incubation the residual activity was above 80% (Fig. 5.3.5), whereas at 60-70°C CMCase activity dropped to less than 40% after 30 min. Similar outcome of thermostability study was observed for CMCase produced by a marine bacterium *B. subtilis* subsp. *subtilis* A-53 (Kim *et al*. 2009). Whereas in some other studies CMCase from *B. amyloliquefaciens* DL-3 (Lee *et al*. 2008) and *B. subtilis* YJ1 (Yin *et al* 2010) was stable at the temperature above 40°C.

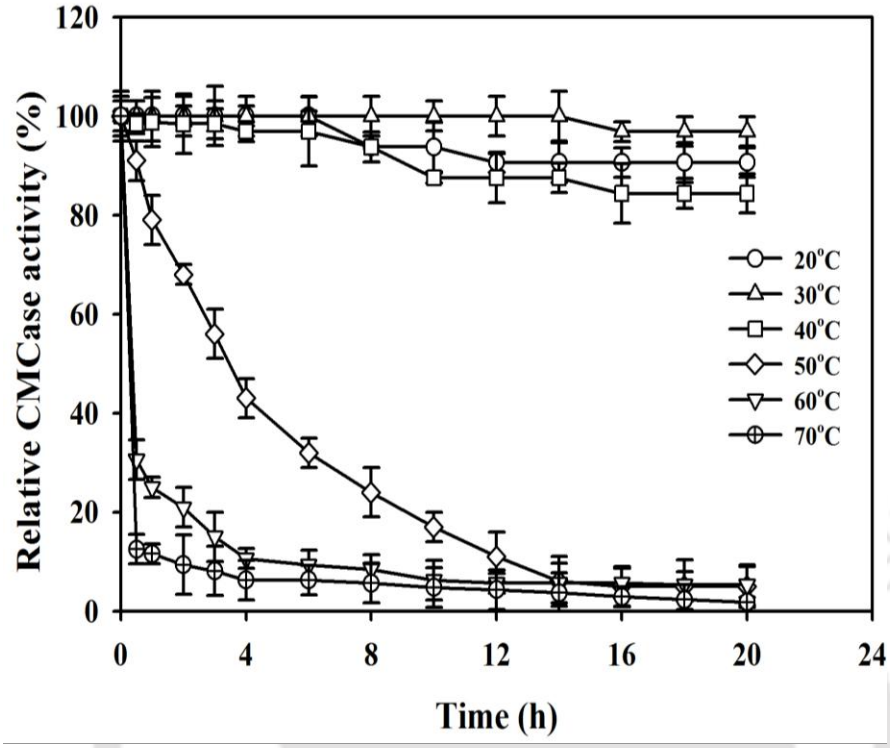

Fig. 5.3.5 Effect of temperature on stability of purified CMCase from *B. amyloliquefaciens* SS35. The enzyme was incubated at a temperature range 20-70°C and CMCase assays were performed at 55°C and pH 5.0.

5.3.4 Effect of pH on CMCase activity and stability

Relative CMCase activity was higher (more than 80%) at a pH range 4.5-6.5. However, as evident from Fig. 5.3.6, the CMCase activity was relatively lower (less than 60%) at pH 3.5 and 6.5-10.5. The optimum pH for CMCase activity was found to be 5.0 which is similar to the pH optima for cellulases produced by other *Bacillus* spp. (Table 5.3.4) such as cellulase from *Bacillus* sp. PDV (Sharma *et al*. 1990), *Bacillus* sp. CH43, *Bacillus* sp. HR68 (Mawadza *et al*. 2000), *Bacillus* sp. M-9 (Bajaj *et al*. 2009) and *Bacillus* sp. DUSELR13 (Rastogi *et al*. 2010). This optimal pH value is higher than that for the cellulase from *B. thuringiensis* (optimal pH 4.0) (Lin *et al*. 2012) and lower than the optimal pH for the cellulases produced by *B. licheniformis*

(pH 6.0) (Bischoff *et al*. 2006), *B. subtilis* GN156 (pH 6.0-6.5) (Apiraksakorn *et al*. 2008), *B. amyloliquefaciens* DL-3 (optimum pH 7.0) (Lee *et al*. 2008) and *B. subtilis* subsp. *subtilis* A-53 (optimum pH 6.5) (Kim *et al*. 2009).

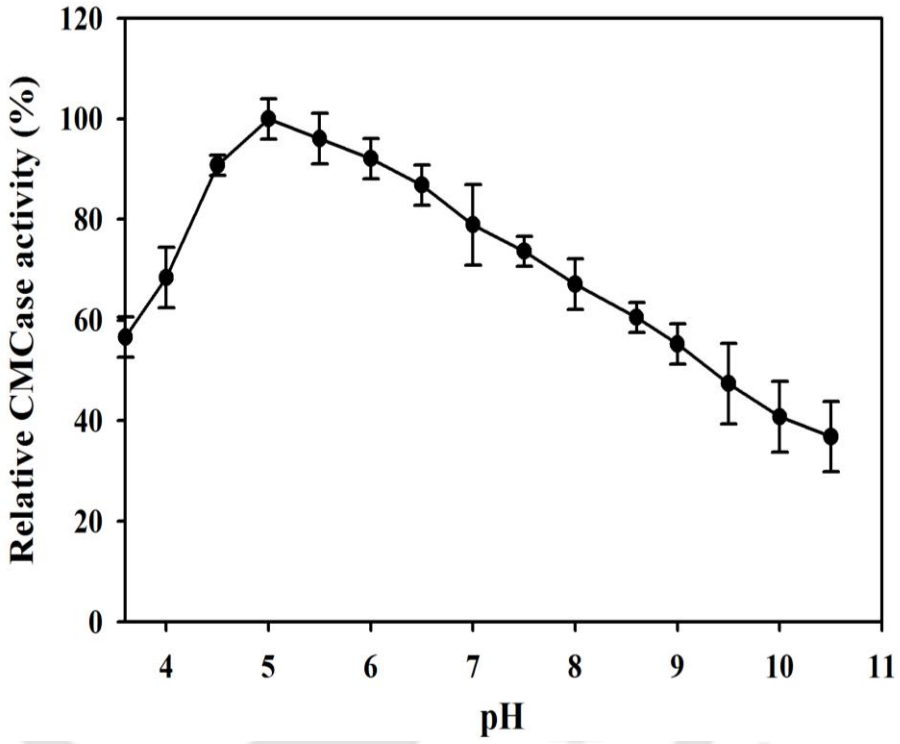

Fig. 5.3.6 Effect of pH on activity of purified CMCase from *B. amyloliquefaciens* SS35. The CMCase assay was performed at a pH range 3.6-10.5 and temperature 55^{o}C.

The stability study of enzyme at different pH revealed that more than 80% activity was retained at a pH range 5.0-9.0 and more than 70% activity was retained at pH 10.0 after 20 h. This is a common characteristic of endoglucanases produced by various *Bacillus* spp. for e.g. CMCase produced by *B. subtilis* subsp. *subtilis* A-53 retained more than 40% CMCase activity at a range of pH 6.5-8.0 after 12 h and more than 80% CMCase activity at pH 7.0 and 8.0 for 1 h (Kim *et al*. (2009).

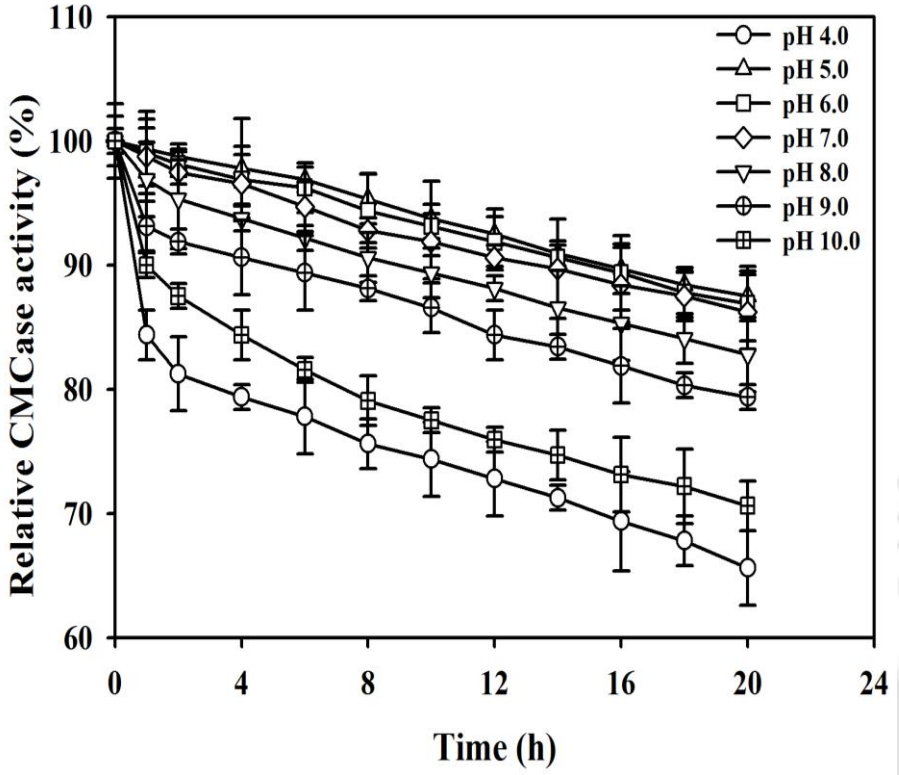

Fig. 5.3.7 Effect of pH on stability of purified CMCase from *B. amyloliquefaciens* SS35. The enzyme was incubated at a pH range 4.0-10.0 and CMCase assays were performed at 55^{o}C and pH 5.0.

In this study the CMCase from *B. amyloliquefaciens* SS35 retained more than 65% of the initial CMCase activity at broad pH range of 4.0-10.0 for 20 h (Fig. 5.3.7). The property of this enzyme, that is an acidic pH 5.0 optimum for CMCase activity and stability, attributed it as a significant component in the process of simultaneous saccharification and fermentation where the most of the fermenting microorganisms require an acidic pH to grow and in that environment the CMCase will be most active and stable.

5.3.6 Effect of metal ions on enzyme activity

The relative change in CMCase activity in presence of various metal ions was studied and it was found that CMCase activity was enhanced by Co^{2+}, Ca^{2+}, K^{+}, Na^{+} and Mn^{2+} ions and the relative activities obtained were 120, 118, 116, 115 and 115%, respectively. Zn^{2+}, Fe^{3+} and Hg^{2+} inhibited the CMCase activity and the relative activities were 72, 54 and 0% (Table 5.3.2). These results matched fairly well with some already studied characteristics of CMCase from *Bacillus* spp. such as *Bacillus* sp. VG1 (Singh *et al*. 2004) and *B. flexus* NT (Trivedi *et al*. 2011). However a study on endoglucanases from *B. subtilis* GN156 showed the inhibition effect on enzyme activity by Co^{2+} and Mn^{2+} ions (Apiraksakorn *et al*. 2008).

Table 5.3.2 Effect of various ions on activity of CMCase produced by *B. amyloliquefaciens* SS35.

Ion	Concentration	Relative activity (%)
Control*	-	100.0
Co^{2+} ($CoCl_2$)	1.0 mM	120.0
Ca^{2+} ($CaCl_2$)	1.0 mM	118.0
K^{+} (KCl)	50 mM	116.0
Na^{+} (NaCl)	50 mM	115.0
Mn^{2+} ($MnCl_2$)	1.0 mM	115.0
Zn^{2+} ($ZnCl_2$)	1.0 mM	72.0
Fe^{3+} ($FeCl_3$)	1.0 mM	54.0
Hg^{2+} ($HgCl_2$)	1.0 mM	0.0

**CMCase enzyme without any ion added*

5.3.7 Substrate specificity of purified enzyme

The enzyme activity with various substrates, *viz.* carboxymethylcellulose (4.0 U/mg), barley *β*-D-Glucan (7.68 U/mg), lichenan (7.14 U/mg), hydroxyethylcellulose (HEC) (2.0 U/mg), avicel (0.0 U/mg), starch (1.5 U/mg) and xylans (for oat spelt, birchwood and beechwood the activities were 0.16, 0.16 and 0.06 U/mg,

respectively) are listed in Table 5.3.3. In comparison to CMC the activity of enzyme with barley *β*-D-glucan and lichenan was significantly higher than the activity towards HEC, starch and xylans (Table 5.3.3). All the substrates have *β*-1,4-linked sugar monomers, whereas barley *β*-D-Glucan and lichenan has mixed *β*-1,3 and *β*-1,4 linkages. These results indicated that the enzyme is a *β*-1,3-1,4-glucanase or endoglucanase (EC 3.2.1.4).

Table 5.3.3 Specificity of the enzyme with different substrates assayed at 55^{o}C and pH 5.0.

Substrate	*Specific activity (U/mg)
Carboxymethylcellulose	4.00 ± 0.05
β-D-Glucan (barley)	7.7 ± 0.08
Lichenan	7.1 ± 0.04
Hydroxyethylcellulose	2.0 ± 0.07
Avicel	0.0
*p*NPG	0.0
Starch	1.5 ± 0.05
Xylan (birchwood)	0.16 ± 0.03
Xylan (oat spelt)	0.16 ± 0.02
Xylan (beechwood)	0.06 ± 0.01

**values are mean ± SE (n=3)*

There was no detectable activity with avicel and *p*NPG, which indicated the absence of exoglucanase or *β*-glucosidase (cellobiase) activities. These properties were similar to the cellulases produced by other *Bacillus* sp. such as enzyme from *B. amyloliquefaciens* DL-3 hydrolyzed CMC, avicel, barley *β*-D-glucan and xylan but not *p*NPG (Lee *et al*. 2008). In another study by Kim *et al*. (2009), avicel and *p*NPG were not hydrolyzed by the enzyme produced by *B. subtilis* subsp. *subtilis* A-53. Endoglucanase from *B. subtilis* AS3 showed 3.3, 6.7 and 7.0 U/mg specific activity towards CMC, lichenan and barley *β*-D-glucan, respectively (Deka et al. 2013).

5.3.8 Determination of kinetic parameters of CMCase

The Michaelis-Menten parameters, K_m and V_{max} of purified CMCase were calculated by using Linewaever-Burk reciprocal plot (Fig. 5.3.8). K_m and V_{max} values for CMCase produced by *B. amyloliquefaciens* SS35 were 0.33 mg/mL and 4.19 µmoles/mg/min, respectively. A lower K_m and higher V_{max} value is desirable for an enzyme to show higher affinity towards a specific substrate.

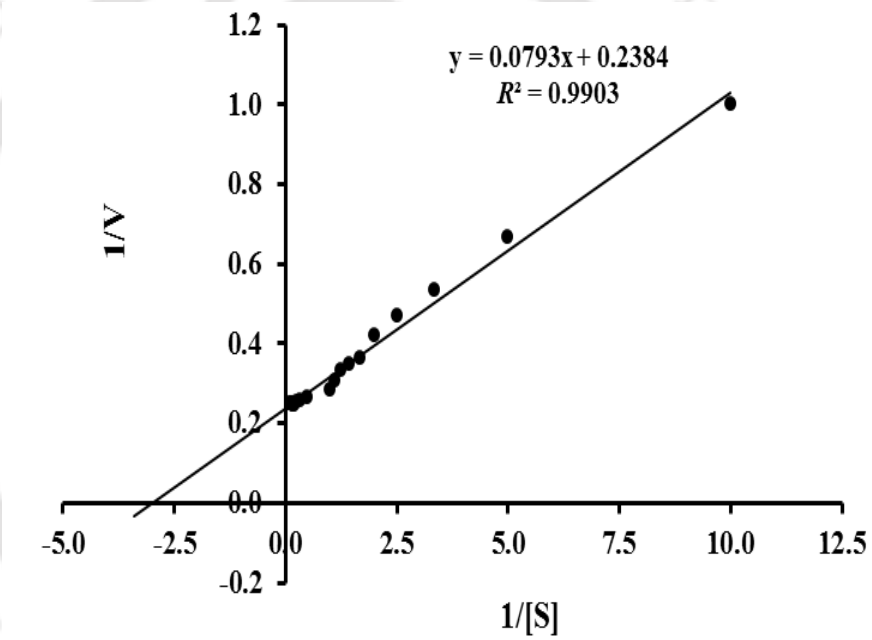

Fig. 5.3.8 Linewaever-Burk plot for determination of kinetic parameters of purified CMCase from *B. amyloliquefaciens* SS35.

The K_m value of 0.33 mg/mL was lower than that obtained with CMCase produced by *Bacillus sp.* PDV (0.588 mg/mL) (Sharma *et al*. 1990), *Bacillus sp.* CH43 (1.5 mg/mL) (Mawadza *et al*. 2000), *Bacillus* sp. HR68 (1.7 mg/mL) (Mawadza *et al*. 2000), *B. subtilis* GN156 (1.53 mg/mL) (Apiraksakorn *et al*. 2008), *Bacillus* sp. DUSELR13 (3.11 mg/mL) (Rastogi *et al*. 2010) and *B. flexus* NT (6.18 mg/mL) (Trivedi *et al*. 2011) and was higher than that obtained with CMCase

produced by *B. subtilis* AS3 (0.13 mg/mL) (Deka *et al*. 2013), *Bacillus* sp. (0.25 mg/mL) (Sadhu *et al*. 2013) (Table 5.3.4).

Table 5.3.4 Comparison of characteristics of cellulases from different *Bacillus* spp.

Strain	Molecular mass (kDa)	K_m (mg/ml)	V_{max}*	Optimal Temperature (^oC)	Optimal pH	Reference
Bacillus sp. PDV	33	0.588	ND	60	5.0	Sharma *et al*. 1990
Bacillus sp. HR68	40	1.7	0.0017	70	5-6.5	Mawadza *et al*. 2000
Bacillus sp. CH43	40	1.5	0.00093	65	5-6.5	Mawadza *et al*. 2000
B. licheniformis	37	ND	ND	65	6.0	Bischoff *et al*. 2006
B. subtilis GN156	25	1.53	0.0085**	60	6-6.5	Apiraksakorn *et al*. 2008
B. amyloliquefaciens DL-3	54	ND	ND	50	7.0	Lee *et al*. 2008
Bacillus sp. M-9	54	ND	ND	60	5.0	Bajaj *et al*. 2009
B. subtilis subsp. *subtilis* A-53	56	ND	ND	50	6.5	Kim *et al*. 2009
Bacillus sp. DUSELR13	ND	3.11	0.56**	75	5.0	Rastogi *et al*. 2010
B. subtilis YJ1	32.5	ND	ND	50-60	6.0	Yin *et al* 2010
B. flexus NT	97	6.18	370.17	45	10.0	Trivedi *et al*. 2011
B. thuringiensis	ND	ND	ND	40	4.0	Lin *et al*. 2012
Bacillus sp.	58	ND	ND	50	6.0	Vijayaraghavan and Vincent 2012
B. subtilis AS3	30	0.13	3.38	45	9.2	Deka *et al*. 2013
Bacillus sp.	97	0.25	ND	50	7.0	Sadhu *et al*. 2013
B. amyloliquefaciens SS35	37	0.33	4.19	55	5.0	This study

*ND, not determined; *unit of V_{max} in µmoles/mg/min; **Values were given in U/mL*

The value of V_{max} (4.19 µmoles/mg/min) obtained in this study was higher than that showed by CMCase produced from *Bacillus* sp. CH43 (0.00093 µmoles/mg/min) (Mawadza *et al*. 2000), *Bacillus* sp. HR68 (0.0017 µmoles/mg/min) (Mawadza *et al*. 2000), *B. subtilis* AS3 (3.38 µmoles/mg/min) (Deka *et al*. 2013) and was lower than CMCase from *B. flexus* NT (370.17 µmoles/mg/min) (Trivedi *et al*. 2011) (Table 5.3.4).

5.3.9 Enzymatic hydrolysis of pretreated *Parthenium hysterophorus*

The CMCase enzyme characterized in this study was analysed for its application in hydrolyzing a cellulosic biomass for the release of reducing sugar. The maximum TRS concentration obtained was 1.36 ± 0.10 g/L with a TRS yield of 271.5 mg/g pretreated biomass after 120 h of hydrolysis (Fig. 5.3.9). The TRS yield of the present study was higher than the other reports such as the reducing sugar yield of 197.0, 201.0 and 207.0 mg/g biomass after enzymatic hydrolysis of dilute acid pretreated reed canary grass, alfa–alfa and switch grass, respectively (Dien *et al*. 2006). In another study TRS yield of 209.0 mg/g biomass was obtained after enzymatic hydrolysis of microwave assisted alkali pretreated switch grass (Hu and Wen, 2008).

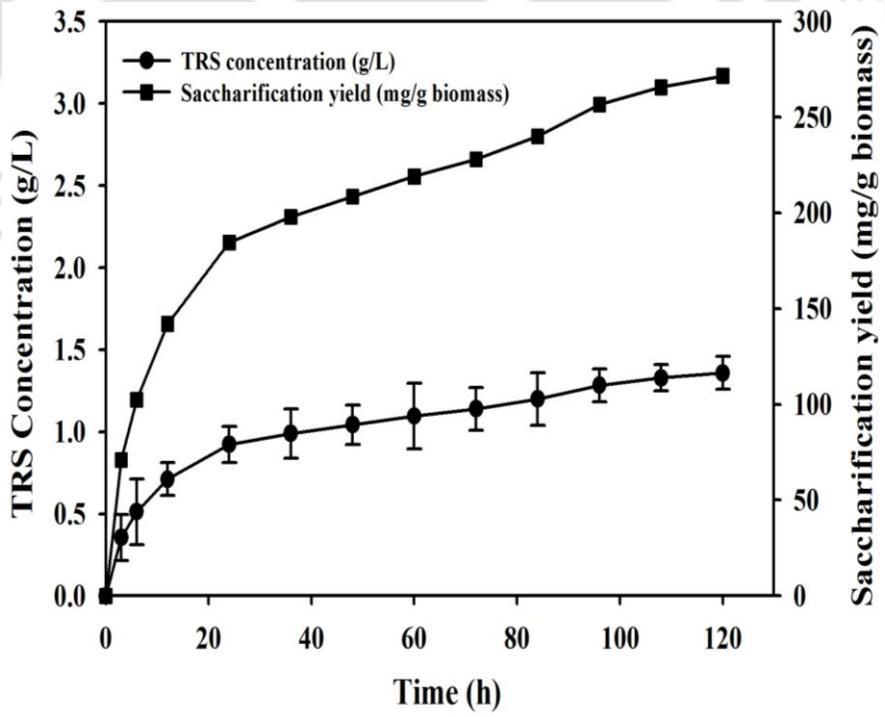

Fig. 5.3.9 Enzymatic hydrolysis of pretreated and delignified biomass of *Parthenium hysterophorus* using CMCase from *Bacillus amyloliquefaciens* SS35.

5.4 Conclusions

This study focused on the purification and characterization of an acidic endoglucanase (carboxymethylcellulase) produced by *B. amyloliquefaciens* SS35. The purification of CMCase was carried out by ammonium sulphate fractionation method and anion exchange chromatography using DEAE-Sepharose which resulted in yield of 12.4 and 2.1%, respectively and both the purification steps showed the purification fold of 4.6 and 18.5, respectively. The molecular weight of the CMCase was approximately, 37 kDa as determined by SDS-polyacrylamide gel electrophoresis and zymogram analysis. The optimal temperature for CMCase activity was 55°C and the pH was 5.0. The enzyme was highly stable in the temperature range of 20-40°C and pH range of 5.0-9.0 for more than 20 h with significant residual CMCase activity of 80%. Endoglucanase activity at pH 5.0 and stability at 30^{o}C reflected the significance of the enzyme in the SSF process of ethanol production using lignocellulosic biomass, since most of the ethanol fermenting organisms are truly mesophilic and acidophilic. The CMCase activity was significantly inhibited by Fe^{3+}, Zn^{2+}, Hg^{2+} ions and enhanced by Co^{2+}, Ca^{2+}, K^{+}, Na^{+} and Mn^{2+} ions. The study of effect of various ions on CMCase activity may be helpful in selecting or excluding the same ions in an SSF process as medium component for the microorganism. The purified CMCase hydrolyzed carboxymethylcellulose (CMC), barley-*β*-D-Glucan, lichenan, hydroxyethylcellulose, starch and xylan. These observations showed that the enzyme was able to hydrolyze *β*-1,3 and *β*-1,4 glucosidic bonds preferably, making it a good candidate for hydrolysis of cellulosic biomass. However, no detectable activities were observed

with avicel and *p*NPG indicating that the enzyme lacks exoglucanase and cellobiase (*β*-glucosidase) activities, respectively. The kinetic parameters *viz*. K_m and V_{max} for CMCase were 0.33 mg/mL and 4.19 μmoles/mg/min, respectively, using CMC. The asset of the enzyme was checked by hydrolysing *Parthenium hysterophorus*, a noxious weed and a maximum total reducing sugar (TRS) yield of 271.5 mg/g of biomass was obtained. These results indicated that the CMCase isolated and purified in this study has high potential for application in enzymatic hydrolysis of lignocellulosic biomass, which is an important step in synthesis of bioalcohols through fermentation.

References

Apiraksakorn, J., Nitisinprasert, S. and Levin, R. E. (2008) Grass degrading *β*-1,3-1,4-D-glucanases from *Bacillus subtilis* GN156: Purification and characterization of glucanase J1 and pJ2 possessing extremely acidic pI. Applied Biochemistry and Biotechnology, 149, 53-66.

Bajaj, B. K., Pangotra, H., Wani, M. A., Sharma, P. and Sharma, A. (2009) Partial purification and characterization of a highly thermostable and pH stable endoglucanase from a newly isolated *Bacillus* strain M-9. Indian Journal of Chemical Technology, 16, 382-387.

Bhatt, M. K. (2000) Cellulases and related enzymes in biotechnology. Biotechnology Advances, 18, 355-383.

Bischoff, K. M., Rooney, A. P., Li, X. L., Liu, S. and Hughes, S. R. (2006) Purification and characterization of a family 5 endoglucanase from a moderately thermophilic strain of *Bacillus licheniformis*. Biotechnology Letters, 28, 1761-1765.

Clarke, J. H., Davidson, K., Gilbert, H. J., Fontes, C. M. G. A. and Hazlewood, G. P. (1996) A modular xylanase from mesophilic *Cellulomonas fimi* contains the same cellulose-binding and thermostabilizing domains as xylanases from thermophilic bacteria. FEMS Microbiology Letters, 139, 27-35.

Deka, D., Bhargavi, P., Sharma, A., Goyal, D., Jawed, M. and Goyal, A. (2011) Enhancement of cellulase activity from a new strain of *Bacillus subtilis* by medium optimization and analysis with various cellulosic substrates. Enzyme Research, Article ID 151656, 8 pages.

Deka, D., Jawed, M. and Goyal, A. (2013) Purification and characterization of an alkaline cellulase produced by *Bacillus subtilis* (AS3). Preparative Biochemistry and Biotechnology, 43, 256-270.

Dien, B. S., Jung, H. G., Vogel, K. P., Casler, M. D., Lamb, J. F. S., Iten, L., Mitchell, R. B. and Sarath G. (2006) Chemical composition and response to dilute-acid pretreatment and enzymatic saccharification of alfalfa, reed canarygrass, and switchgrass. Biomass and Bioenergy, 30, 880-891.

Eida, F. M., Nagaoka, T., Wasaki, J. and Kouno K. (2012) Isolation and characterization of cellulose-decomposing bacteria inhabiting sawdust and coffee residue composts. Microbes and Environments, 27, 226-233.

Hakamada, Y., Koike, K., Yoshimatsu, T., Mori, H., Kobayashi, T. and Ito, S. (1997) Thermostable alkaline cellulase from an alkaliphilic isolate, *Bacillus* sp. KSM-S237. Extremophiles, 1, 151-156.

Hendrick, J. L. and Smith, A. J. (1968) Size and charge isomer separation and estimation of molecular weights of proteins by disc gel electrophoresis. Archives of Biochemistry and Biophysics, 126, 155-164.

Hu, Z. and Wen, Z. (2008) Enhancing enzymatic digestibility of switchgrass by microwave-assisted alkali pretreatment. Biochemical Engineering Journal, 38, 369-378.

Jiang, Z., Wei, Y., Li, D., Li, L., Chai, P. and Kusakabe, I. (2006) High-level production, purification and characterization of a thermostable β-mannanase from the newly isolated *Bacillus subtilis* WY34. Carbohydrate Polymers, 66, 88-96.

Kim, B., Lee, B., Lee, Y., Jina, I., Chunga, C. and Lee, J. (2009) Purification and characterization of carboxymethylcellulase isolated from a marine bacterium, *Bacillus subtilis* subsp. *subtilis* A-53. Enzyme and Microbial Technology, 44, 411-416.

Laemmli, U. K. (1970) Cleavage of structural proteins during the assembly of the head of bacteriophage T4. Nature, 227, 680-685.

Lee, Y. J., Kim, B. K., Lee, B. H., Jo, K. I., Lee, N. K., Chung, C. H., Lee, Y. C. and Lee, J. W. (2008) Purification and characterization of cellulase produced by *Bacillus amyloliquefaciens* DL-3 utilizing rice hull. Bioresource Technology, 99, 378-386.

Lin, L., Kan, X., Yan, H. and Wang, D. (2012) Characterization of extracellular cellulose-degrading enzymes from *Bacillus thuringiensis* strains. Electronic Journal of Biotechnology, 15, 1.

Lineweaver, H. and Burk, D. (1934) The determination of enzyme dissociation constants. Journal of the American Chemical Society, 5, 658-666.

Lowry, O. H., Rosebrough, N. J., Farr, A. L. and Randall, R. J. (1951) Protein measurement with the Folin phenol reagent. The Journal of Biological Chemistry, 193, 265-275.

Mawadza, C., Hatti-Kaul, R., Zvauya, R. and Mattiason, B. (2000) Purification and characterization of cellulases produced by two *Bacillus* strains. Journal of Biotechnology, 83, 177-187.

Michaelis, L. and Menten, M. L. (1913) Die kinetic der invertinwirkung. Biochemical Journal, 49, 334-336.

Nelson, N. (1944) A photometric adaptation of the Somogyi method for the determination of glucose. The Journal of Biological Chemistry, 153, 375-380.

Ranjan, A., Khanna, S. and Moholkar, V. S. (2013) Feasibility of rice straw as alternate substrate for biobutanol production. Applied Energy, 103, 32-38. (Also refer: Moholkar, V. S. and Singh, S. (2014) A Corrigendum to 'Feasibility of rice straw as alternative substrate for biobutanol production by Ranjan et al.' [Appl Energy, 103 (2013) 32-38]. Applied Energy, 116, 436-438.

Rastogi, G., Bhalla, A., Adhikari, A., Bischoff, K. M., Hughes, S. R., Christopher, L. P. and Sani, R. K. (2010) Characterisation of thermostable cellulases produced by *Bacillus* and *Geobacillus* strains. Bioresource Technology, 22, 8798-8806.

Sadhu, S., Saha, P., Sen, S. K., Mayilraj, S. and Maiti, T. K. (2013) Production, purification and characterization of a novel thermotolerant endoglucanase (CMCase) from *Bacillus* strain isolated from cow dung. SpringerPlus, 2, 10.

Saratale, G. D., Saratale, R. G., Lo, Y. C. and Chang, J. S. (2010) Multicomponent cellulase production by *Cellulomonas biazotea* NCIM-2550 and its applications for cellulosic biohydrogen production. Biotechnology Progress, 26, 406-416.

Sharma, P., Gupta, J. K. and Vadehra, D. V. (1990) Purification and properties of an endoglucanase from a *Bacillus* isolate. Enzyme and Microbial Technology, 12, 132-137.

Shobharani, P., Yogesh, D., Halami, P. M. and Sachindra, N. M. (2013) Potential of cellulase from *Bacillus megaterium* for hydrolysis of sargassum. Journal of Aquatic Food Product Technology, 22, 520-535.

Singh, J., Batra, N. and Sobti, R. C. (2004) A highly thermostable, alkaline CMCase produced by a newly isolated *Bacillus* sp. VG1. Journal of Industrial Microbiology and Biotechnology, 31, 51-56.

Singh, S., Moholkar, V. S. and Goyal, A. (2013) Isolation, identification and characterization of a cellulolytic *Bacillus amyloliquefaciens* strain SS35 from rhinoceros dung, ISRN Microbiology, Article ID 728134, 7 pages.

Singh, S., Moholkar, V. S. and Goyal, A. (2014a) Optimization of carboxymethylcellulase production from *Bacillus amyloliquefaciens* SS35. 3Biotech, 4, 411-424.

Singh, S., Khanna, S., Moholkar, V. S. and Goyal, A. (2014b) Screening and optimization of pretreatments for *Parthenium* hysterophorus as feedstock for alcoholic biofuels. Applied Energy, 129, 195-206.

Singh, S., Bharadwaja, S. T. P., Yadav, P. K., Moholkar, V. S. and Goyal, A. (2014c) Mechanistic investigation in ultrasound–assisted (alkaline) delignification of *Parthenium hysterophorus* biomass. Industrial and Engineering Chemistry Research, 53, 14241-14252.

Somogyi, M. (1945) A new reagent for the determination of sugars. The Journal of Biological Chemistry, 160, 61-68.

Spiridonov, N. A. and Wilson, D. B. (1998) Regulation of biosynthesis of individual cellulases in *Thermomonospora fusca*. Journal of Bacteriology, 180, 3529-

3532.

Trivedi, N., Gupta, V., Kumar, M., Kumari, P., Reddy, C. R. K. and Jha, B. (2011) An alkali halotolerant cellulase from *Bacillus flexus* isolated from green seaweed Ulva lactuca. Carbohydrate Polymers, 83, 891-897.

van Dyk, J. S., Sakka, M., Sakka, K. and Pletschke, B. I. (2010) Identification of endoglucanases, xylanases, pectinases and mannanases in the multi-enzyme complex of *Bacillus licheniformis* SVD1. Enzyme and Microbial Technology, 47, 112-118.

Vijayaraghavan, P. and Vincent, S. G. P. (2012) Purification and characterization of carboxymethyl cellulase from *Bacillus* sp. isolated from a paddy field. Polish Journal of Microbiology, 61, 51-55.

Yang, S., Jiang Z., Yan Q. and Zhu H. (2008) Characterization of a thermostable extracellular *β*-glucosidase with activities of exoglucanase and transglycosilation from *Paecilomyces thermophila*. Journal of Agricultural and Food Chemistry, 56, 602-608.

Yin, L. J., Lin, H. H. and Xiao, Z. R. (2010) Purification and characterization of a cellulase from *Bacillus subtilis* YJ1. Journal of Marine Science and Technology, 18, 466-471.

Chapter 6

Screening, optimization of pretreatment and ultrasound assisted delignification of *Parthenium hysterophorus*

6.1 Introduction

Fast depletion of global fossil fuel reserves, highly fluctuating prices of crude oil as well as concerns of global warming have led to immense research in the area of alternate sources of liquid transportation biofuels, which are not only renewable but also carbon neutral. Biofuels offer viable solution to both problems of energy security and climate change risks. The economy of production of biofuels (mainly as liquid transportation fuels) is a major function of cost of the substrate (Yan and Lin 2009) and hence, biofuels from cheaper feedstock have been extensively investigated in recent years (Chisti and Yan 2011, Santori *et al*. 2012, Ho *et al*. 2012, Rizzo *et al*. 2013, Cabanelas *et al*. 2013). Moreover, the biomass pretreatment is also a cost intensive component of biofuel production process and has significant implications on the economics of biofuel production (Kumar *et al*. 2012). Optimization of the pretreatment of biomass minimizes total energy requirement of biofuels manufacture and thus reduces the total cost of the process (Ranjan and Moholkar 2013, Ranjan *et*

al. 2013). Among several alcoholic biofuels that have been investigated, bioethanol has emerged as a potential fuel. It is also being used for blending with petroleum as oxygenate instead of conventional MTBE (methyl tertiary butyl ether) (Dias *et al*. 2012, Fraioli *et al*. 2104). Lignocellulosic biomass, available mainly in the form of agricultural and forest residues or thorough plantations on arid/un-used land, is potential cheap substrate for alcoholic biofuel production (Tian *et al*. 2009, Kuhad *et al*. 2010, Talebnia *et al*. 2010, Zhao *et al*. 2010, Chandra *et al*. 2012, Lima *et al*. 2013, Caspeta *et al*. 2014). These lignocellulosic biomasses are essentially made up of three major constituents, *viz.* cellulose, hemicellulose and lignin. Among these, the important components for ethanol production are cellulose and hemicellulose, as these are made up of the sugar monomers. The physical, chemical and structural composition of any lignocellulosic biomass is resistant to the direct action of enzymatic hydrolysis. This is due to high crystallinity of cellulose and also presence of other components, which reduce exposure of the cellulose fraction of biomass to enzyme action and hydrolysis reaction. This necessitates pretreatment of raw biomass prior to ethanol production via fermentation. The main objectives of pretreatment are: reducing the crystallinity of cellulose, increasing the porosity and surface area of biomass and removal of the lignin stratum around cellulose entangled with other two components (Kumar *et al*. 2009a). All of these effects lead to higher and faster hydrolysis of cellulose, thus maximizing the extent of saccharification and yield of fermentable sugars. Several pretreatment methods have been practiced for various lignocellulosic biomasses prior to enzymatic hydrolysis. These methods are of physical, chemical or physicochemical nature (Kumar *et al*. 2009a, Zheng *et al*.

2009). In this study the optimization of pretreatment of a ubiquitous and abundant lignocellulosic waste biomass, i.e. the weed *Parthenium hysterophorus* (carrot grass) was done. *P. hysterophorus* is a native of north-east Mexico and is endemic in America. Recently, this has been included in the world's seven most devastating and hazardous weeds. A single plant of *P. hysterophorus* can produce 10,000 to 15,000 seeds and these seeds can germinate to yield innumerable plants. This is currently widespread in India and an estimated two million hectares of land have been covered with this weed (Patel 2011). The potential of *P. hysterophorus* as a feedstock for biofuels production has not been explored in depth yet. Very few studies have been published in recent past (Ghosh *et al*. 2013, Rana *et al*. 2013, Pandiyan *et al*. 2014) on pretreatment of *P. hysterophorus*. Ghosh *et al*. (2013) have studied the kinetics and thermodynamics of dilute acid hydrolysis of *P. hysterophorus*. In present study, the potential of *P. hysterophorus* as feedstock for biofuels was attempted to explore with far more rigor and meticulousness. Pretreatment of *P. hysterophorus* using as many as 17 physical, chemical and physicochemical techniques was done. The parameters of treatment such as concentration of acid and alkali and time of treatment were optimized. Other techniques such as addition of oxidizing agents and surfactants were also attempted. The enzymatic hydrolysis of pretreated biomass was carried out using carboxymethylcellulase (CMCase) produced by an isolate *Bacillus amyloliquefaciens* SS35 (Chapter 3) and *β*-glucosidase (Novozyme 188). The sugar release after pretreatment as well as enzymatic hydrolysis was determined. Thus, this study revealed the complete potential of *P. hysterophorus* for biofuels production. It is necessary to extract maximum amount of sugar monomers from raw

lignocellulosic biomass for efficient and economic alcoholic biofuels production. Pentose sugars are usually obtained after hydrolysis of hemicellulose during dilute acid pretreatment of biomass. The hexose sugars are obtained from enzymatic hydrolysis of the acid pretreated biomass (which mainly contains lignin and cellulose). Lignin content in the biomass acts as a barrier and hinders the accessibility of enzyme to cellulose and the latter's hydrolysis to hexose sugars (Alvira *et al*. 2010, Barakat *et al*. 2013). This necessitates lignin removal of pretreated biomass. Lignin is derived from three monomer units, *viz.* trans-coniferyl, trans-sinapyl and trans-*p*-coumeryl alcohols. These units are linked randomly mostly via ether linkages at α and β positions to construct the lignin macromolecule. The reactive sites in lignin are mainly the ether linkages and functional groups, since the carbon-carbon linkages are generally resistant to chemical attack. The areas of lignin susceptible to chemical attack are the hydrolysable ether linkages (α-aryl, α-alkyl and β-aryl), phenolic and aliphatic hydroxyl groups, ester groups, methoxyl groups, the unsaturated groups and uncondensed units. Lignin is amorphous and tends to form hydrogen bonds influencing the accessibility of the groups, which in turn affects the levels of reactivity. The delignification process is generally carried out under acidic, alkaline or oxidative conditions (Bussemaker and Zhang 2013). NaOH is a widely used reagent for delignification under alkaline conditions (Sun *et al*. 2002). The main chemical mechanism for degradation of lignin in alkaline and alkaline-oxidative environment is through the cleavage of the α- and β-aryl ether linkages to yield fragmentation units.

Recently, many researchers have employed ultrasound for intensification of delignification under alkaline treatment (Sun *et al*. 2002, Sun and Tomkinson 2002, Yuan *et al*. 2010, Baxi and Pandit 2012, Li *et al*. 2012, Velmurugan and Muthukumar 2012, Subhedar and Gogate 2014). Despite these efforts, the exact physical mechanism of the ultrasound assisted delignification is not established yet. Ultrasound and its secondary effect, cavitation, have physical and chemical effects on the reaction system. The physical effect is in terms of generation of strong micro-turbulence in the system through micro-convection generated by transient bubble motion and micro-streaming (i.e. small amplitude oscillatory motion of liquid elements induced by passage of ultrasound wave) generated by ultrasound wave (Young 1989, Leighton 1994, Shah *et al*. 1999). The chemical effect of cavitation is production of highly reactive radical species such as $^{\bullet}OH$, $^{\bullet}O$ and $HO_2^{\bullet}$ generated through thermal dissociation of vapor molecules entrapped in the bubble during transient collapse (Hart and Henglein 1985, Hart and Henglein 1987, Suslick 1990). These radicals may induce chemical reactions that lead to degradation of lignin through different mechanisms (Bussemaker and Zhang 2013, Bussemaker *et al*. 2013). Relative contributions of the physical and chemical effects of ultrasound in enhancement of delignification process needs to be identified for effective use of ultrasound energy for delignification. In this study, this issue was treated with approach of coupling experiments with simulations of cavitation bubble dynamics at the conditions of the experiments. Concurrent analysis of experimental and simulations results has revealed interesting mechanistic facets of the delignification process, as outlined in the subsequent sections.

6.2 Materials and Methods

6.2.1 Biomass collection and processing

P. hysterophorus biomass was collected from the campus of IIT Guwahati. Whole plant body, except roots, was used as substrate for pretreatment. Biomass was chopped, washed with water and dried at 60 ± 3^{o}C for 24 h. Ground biomass (particle size ~ 1 mm), obtained from first physical pretreatment i.e. mechanical comminution, was used as starting material in all pretreatment methods. However, solid residue of biomass obtained after best method of pretreatment was used in delignification experiments.

6.2.2 Chemicals and enzymes

All components of fermentation media and sodium hydroxide pellets were purchased from HiMedia Pvt. Ltd., India. Other chemicals were procured from Fischer Scientific, India. Carboxymethylcellulase (CMCase) was produced by *Bacillus amyloliquefaciens* SS35 (Chapter 4) (Singh *et al*. 2014a) and prepared as described in Section 5.2.5.1 of Chapter 5 (Singh *et al*. 2014b). *β*-glucosidase from *Aspergillus niger* (Novozyme 188) was procured from Sigma Aldrich, USA.

6.2.3 Analysis of composition of *P. hysterophorus* biomass

The moisture content of raw biomass and cellulose, hemicellulose, lignin contents of raw, pretreated and delignified *P. hysterophorus* biomass were analyzed according to the TAPPI's protocols (TAPPI, 1992). Since TAPPI procedure involves stepwise inclusion of biomass samples for holocellulose, cellulose and hemicellulose

analysis, the other protocols mentioned below were used for individual determination of these components wherever required. In case of cellulose estimation anthrone method (Updegraff, 1969) was used and hemicellulose estimation was done by the method given by Goering and Van Soest (1970). The results from these methods were compared with those obtained from TAPPI's protocols for testing the validity of the methods and similarity in results corroborated the validity of the methods.

6.2.3.1 Moisture content of biomass

An empty silica crucible was dried at 105^{o}C in an oven and was weighed on an analytical balance. Two gram raw biomass was placed in the crucible and reweighed. The sample was dried at 105°C for three hours. Then the crucible was placed in the desiccator for cooling before weighing. The dried biomass was weighed and the moisture content was calculated by using the formula:

$$\text{Moisture content (\%)} = \frac{\text{Initial weight of biomass} - \text{Final weight of biomass}}{\text{Initial weight of biomass}} \times 100$$

6.2.3.2 Determination of holocellulose content

Two gram of raw biomass was mixed in 100 mL water taken in a 250 mL Erlenmeyer flask. The flask was kept at 70^{o}C in a water bath and 1.5 g sodium chlorite and 5 mL of 10% acetic acid were added to it. The mixture was stirred at every 10 min and 5 mL of 10% (v/v) acetic acid was added after 30 min. 1.5 g sodium chlorite and 5 mL acetic acid were added for 4 h at a time interval of 1 h. The

mixture was cooled at 10^{o}C and was poured into a sintered glass crucible. Residue was washed with water followed by acetone and air-dried to make it acetone free.

6.2.3.3 Determination of cellulose content

***6.2.3.3.1 TAPPI's protocol*:** Residue obtained in previous section (Section 6.2.3.2) was used for determination of cellulose. Two gram biomass residue was transferred in a 250 mL glass beaker kept at 20^{o}C in a water bath. Different volumes of 17.5% (~ 4.4 N) NaOH solution were added periodically (15 mL, 10 mL, 10 mL, 35 mL and 10 mL at the intervals of 0 min, 1 min, 45 sec, 15 sec and 3 min, respectively) and mixed intermittently using a glass rod. The mixture was left at 20^{o}C for 30 min then 100 mL of distilled water was added. After 40 min the mixture was poured into a sintered glass crucible for filtration using suction. The residue was washed with 25 mL of 8.3% (~ 2 N) NaOH solution at 20°C and transferred to a pre-weighed crucible. The residue was washed with approximately, 800 mL of distilled water at 20°C under suction. Suction was removed temporarily and the crucible was filled with 2 N acetic acid for 5 min. Then acetic acid was removed by reapplying suction. The residue was washed with distilled water till neutral pH was achieved. The crucible was placed in the oven at 50°C and dried to constant weight. Cellulose was calculated as a percentage based on oven dry sample.

6.2.3.3.2 Anthrone method: The estimation of cellulose content in biomass samples was done following the method given by Updegraff (1969).

Reagents: Acetic/nitric reagent was the mixture of 150 mL of 80% acetic acid (13.3 N) and 15 mL of conc. nitric acid (16 N). Anthrone reagent was freshly prepared by dissolving 0.2 g of anthrone in 100 mL of ice cold conc. H_2SO_4 (37 N) The reagent was stored at 4^oC for 2 h before use.

Method: 0.1 g of raw biomass was taken in a test tube and 5 mL of acetic/nitric reagent was added to it. After a thorough mixing the tube was placed at 100^oC in a water bath for 30 min. The content was cooled and centrifuged at 5000***g*** for 20 min. Supernatant was discarded and the residue was washed with distilled water and dissolved in 10 mL of 67% (~ 13.7 N) H_2SO_4. The mixture was allowed to stand for 1 h. Then 1 mL of the solution was diluted to 100 mL. 10 mL of anthrone reagent was added to 1 mL of diluted solution. The mixture was boiled for 10 min using a boiling water bath. The mixture was cooled and absorbance at 630 nm was recorded using a spectrophotometer (Varian, Cary 100). A calibration curve was drawn using carboxymethylcellulose (CMC) and amount of cellulose in sample was estimated.

6.2.3.4 Determination of hemicellulose content

Hemicellulose content in biomass samples was estimated by following the method of Goering and Van Soest (1970). Neutral detergent fiber (NDF) and acid detergent fiber (ADF) were estimated separately to determine hemicellulose content using the formula:

$$\text{Hemicellulose} = \text{NDF} - \text{ADF}$$

Reagents: Neutral detergent solution was prepared by dissolving 18.61 g of disodium ethylene diamine tetra acetate dihydrate (EDTA) and 6.81 g of sodium borate decahydrate in 800 mL distilled water by heating. 30 g sodium lauryl sulphate and 10 mL of 2-ethoxy ethanol were added to the solution followed by addition of 4.5 g disodium hydrogen phosphate. The pH of the solution was adjusted to 7.0 and volume was made up to 1 L. Acid detergent solution was prepared by dissolving 20 g of cetyl trimethyl ammonium bromide (CTAB) in 1 L of 1 N H_2SO_4. Both neutral and acid detergent solutions were used for estimation of neutral and acid detergent fibers, respectively.

Neutral detergent fiber (NDF) estimation: 1 g of biomass sample was taken in a refluxing flask and 100 mL of cold neutral detergent solution was added to it. 2 mL of decahydronaphthalene and 0.5 g of sodium sulphite was added to the solution. The solution was refluxed for 1 h. The solution was transferred to a pre-weighed sintered glass crucible and filtered by applying suction. The residue was washed with hot water followed by acetone and dried at 100^{o}C till constant weight was achieved.

Acid detergent fiber (ADF) estimation: 1 g of raw biomass was transferred to a refluxing flask and 100 mL of cold acid detergent solution was added to it. The solution was refluxed and processed similarly as described above in case of NDF.

6.2.3.5 Determination of lignin content

TAPPI Standard protocol (TAPPI, 1992) was followed for lignin estimation. 1 g of raw biomass was kept in a 50 mL beaker and 10 mL of 72% (~ 14.7 N) sulphuric acid was added to it. The mixture was transferred to a 500 mL round bottom flask

and diluted with distilled water to make final volume 300 mL. The solution was refluxed for 3 h and then transferred to a pre-weighed sintered glass crucible. The biomass was washed with 300 mL of hot distilled water. The residue was dried at 105^{o}C till constant weight was achieved. The residue was the lignin present in biomass sample and was expressed as weight percentage of raw biomass.

6.2.4 Pretreatment methods

6.2.4.1 Physical pretreatment

The physical treatment involved mainly mechanical comminution and uncatalyzed autoclaving or autohydrolysis at neutral pH in absence of any added chemicals. In mechanical comminution, the dried biomass was ground using a mixer grinder (Khaitan, India) and passed through a sieve of mesh size 1 mm. In the autoclaving (auto-hydrolysis) pretreatment protocol, 10 g of biomass soaked in water (the solid/liquid ratio of 1/10) was subjected to autoclaving for 20 min at 15 psi pressure and 121^{o}C temperature in an autoclave (Equitron). After treatment, the pressure in the autoclave was swiftly released to induce expansion of the biomass. The sugar content released from the biomass (mainly due to hydrolysis of hemicellulosic fraction) was dissolved in 100 mL lukewarm water.

6.2.4.2 Chemical pretreatments

In this category, the biomass was treated with different chemicals. The effect of variation in conditions of pretreatment, i.e. concentration of the chemicals in biomass solution, was examined. 10% (w/v) powdered biomass in aqueous solution was taken

in each chemical pretreatment process. After the treatment, biomass was filtered using double-layered muslin cloth and was repeatedly washed with water till neutral pH of wash water was obtained confirming no residual chemicals left on the biomass surface. The biomass residue was then dried at 60^{o}C in hot air oven for 24 h and used for further enzymatic hydrolysis. The filtrate was analyzed for sugar release during pretreatment.

***6.2.4.2.1 Acid treatment*:** The biomass was subjected to dilute sulphuric acid treatment with concentrations 1%, 3% and 5% (v/v) (which correspond to concentrations of 0.36, 1.08 and 1.8 N, respectively) at a temperature of 120^{o}C for 20 min. Biomass was soaked in acid solution in a 250 mL Erlenmeyer flask.

***6.2.4.2.2 Alkali treatment*:** The biomass was treated with sodium hydroxide using concentrations of 1%, 3%, 5% (w/v) i. e. 0.25 N, 0.75 N and 1.25 N, respectively, at a temperature of 120^{o}C for 20 min.

***6.2.4.2.3 Oxidizing agents*:** In this study alkaline peroxide pretreatment was performed by using 2.15% (v/v) H_2O_2 (0.25 g H_2O_2/g of raw biomass), at pH 11.5 and temperature 35^{o}C for 3 h (Saha and Cotta 2006).

***6.2.4.2.4 Surfactants (SDS and Triton X100)*:** Each surfactant at concentration of 0.5% (w/w) (5 mg/g of dry biomass) was added to 100 mL aqueous solution of biomass in two separate 250 mL Erlenmeyer flasks. These flasks were incubated at 120°C for 20 min. In this pretreatment special care was taken during washing of biomass after filtration to ensure the complete removal of surfactant from biomass surface (this precaution is essential as the surfactant may denature the enzyme).

6.2.4.3 Physicochemical treatments

In this treatment, the physical and chemical methods mentioned above were applied simultaneously as follows:

***6.2.4.3.1 Acid + Autoclaving*:** *P. hysterophorus* was treated with 1% (v/v) H_2SO_4 at 121^oC, 15 psi for 20 min. Impulsive depressurization of autoclave valve was done after completion of the pretreatment.

***6.2.4.3.2 Alkali + Autoclaving*:** The powdered biomass was subjected to alkali catalyzed autoclaving in 1% (v/v) NaOH solution at 121^oC, 15 psi for 20 min. As in previous protocol, the pressure in the autoclave was released swiftly after the pretreatment.

***6.2.4.3.3 Ammonia + autoclaving (Ammonia fiber expansion, AFEX)*:** Ammonia fiber expansion (AFEX) is similar to physical treatment of autoclaving except the use of ammonia. The optimum parameters for this treatment are, liquid ammonia loading of 1-2 kg/kg dry biomass at 90^oC for 30 min as reported by Sun and Cheng (2002). In this study, raw *P. hysterophorus* biomass was reacted with liquid ammonia under autoclaving (15 psi, 121^oC) for 20 min. The loadings (or quantities) of both ammonia and water were 2 g/g of raw biomass, same as used by Bals *et al* (2010) for pretreatment of switchgrass. The pressure in the autoclave was swiftly reduced after treatment as in previous treatments.

***6.2.4.3.4 Oxidizing agent + Autoclaving*:** This treatment was carried out at the same conditions described earlier in chemical treatments (Section 6.2.4.2.3) for the

oxidizing agent (Section 6.2.4.2.3). The only difference has been the application of autoclaving during treatment (121^{o}C temperature, 15 psi pressure) for 20 min.

***6.2.4.3.5 Surfactants + Autoclaving*:** In this process, surfactant treatment (as previously described in Section 6.2.4.2.4) was coupled with concurrent autoclaving as described above in other physicochemical methods.

6.2.5 Enzymatic hydrolysis of pretreated *P. hysterophorus* biomass

P. hysterophorus biomass pretreated with different methodologies described in previous section, was subjected to enzymatic hydrolysis. Two enzymes, *viz.* CMCase produced by *Bacillus amyloliquefaciens* SS35 and *β*-glucosidase from *Aspergillus niger* (Novozyme 188) were used for the hydrolysis. The experiments were performed with 5% (w/v) pretreated biomass in sodium citrate buffer (0.05 M, pH 5.0). This solution was supplemented with CMCase (concentration 10 U/g biomass) and *β*-glucosidase (concentration 5 U/g biomass). In case of enzymatic hydrolysis of delignified biomass, CMCase and *β*-glucosidase concentrations were increased to 200 U/g and 25 U/g, respectively, considering the increased cellulose content in delignified biomass (given subsequently in Section 6.3.1). The reactions were carried out in 150 mL Erlenmeyer flask with reaction volume of 20 mL. Sodium azide (0.005%, w/v) was added to the reaction mixture to avoid contamination. The flasks were incubated at 30^{o}C and 150 rpm in an incubator shaker (Orbitek, Scigenics Biotech).

6.2.6 Parametric investigation and intensification of alkaline delignification process

Parametric investigation of the delignification for both ultrasound assisted and mechanically agitated processes was done for following parameters: (1) alkali concentration, (2) biomass loading or concentration, (3) temperature and (4) reaction time. All experiments were conducted in a 100 mL glass beaker with reaction volume of 80 mL. Sequential investigation was done by assessing effect of variation in one parameter at a time on the extent of delignification while keeping the other parameters constant. The best value of first parameter (corresponding to maximum lignin removal) was used while assessing the effect of next parameter.

6.2.6.1 Effect of NaOH concentration on delignification

The effect of NaOH concentration on delignification was assessed using concentrations from 0.5 to 3% (w/v) i.e. from 0.125 to 0.750 N with values of other parameters as biomass concentration, 3% (w/v), temperature, 30^{o}C and time period of treatment, 15 min.

6.2.6.2 Effect of biomass concentration on delignification

Biomass concentration was varied from 0.5 to 8% (w/v) keeping the other parameters as NaOH concentration, 1.5% w/v (in case of ultrasound assisted process) and 2.5%, w/v (in case of mechanically agitated process), temperature, 30^{o}C and time period of treatment, 15 min.

6.2.6.3 Effect of temperature on delignification

Finally, the temperature of treatment was varied in the range 30°-80°C with values of other parameters as NaOH concentration, 1.5% w/v (in case of ultrasound assisted process) and 2.5% w/v (in case of mechanically agitated process) , biomass concentration, 2% (w/v) and time period of treatment, 15 min.

All experiments were performed in duplicate to check reproducibility of the results. The kinetics of delignification process was measured at the best values of the three parameters obtained in above investigation (mentioned in Section 6.3.3.1). The data obtained from time profiles of delignification with mechanical agitation and ultrasound treatment were analyzed by using pseudo first order kinetics (as an approximation of complex delignification process). The biomass residue after the delignification process was separated by filtration through a double layered muslin cloth. The biomass residue (comprising of cellulose) was washed with hot water several times to remove traces of NaOH and until neutral pH was obtained. This residue was dried for 12 h in hot air oven at 60 ± 3°C and further used for enzymatic hydrolysis.

6.2.6.4 Ultrasound assisted alkali treatment of biomass

A probe type microprocessor based programmable ultrasonic processor (Sonics and Materials, Model: VCX 500, max. power: 500 W, freq.: 20 kHz) was used for sonication of the reaction mixture. The ultrasound probe was made of high grade titanium alloy and had a diameter of 13 mm. The probe was operated at 30% amplitude corresponding to peak theoretical power input of 150 W. The actual

ultrasound power input to the system and the acoustic intensity (in terms of pressure amplitude of the ultrasound wave) was estimated using calorimetric method (Sivasankar *et al*. 2007). The actual power input to the system was determined as 1.045 W using an ultrasound probe with tip diameter of 13 mm, which corresponded to acoustic intensity of 7873 W/cm^2. The pressure amplitude of the ultrasound wave corresponding to this intensity was 1.5 bar. This processor also had facility of automatic frequency tuning and amplitude compensation, which ensures constant power delivery to ultrasound probe and the liquid medium irrespective of the changes occurring in the liquid medium during sonication.

6.2.7 Mathematical model for cavitation bubble dynamics

Simulations of cavitation bubble dynamics were used to get a quantitative estimate of the physical and chemical effects induced by ultrasound and cavitation bubbles under different experimental conditions. The diffusion limited ordinary differential equations (ODE) model (with boundary layer approximation) were used (Table 6.2.1A and B) (Toegel *et al*. 2000) for these simulations. This model is based on the postulate proven by the partial differential equation (PDE) model of Storey and Szeri (2000), which showed that vapor entrapment in the cavitation bubble during its radial motion is essentially a diffusion limited process. Storey and Szeri (2000) showed that not all of the solvent vapor which evaporates into the cavitation bubble during its expansion in the radial motion can escape in the ensuing compression phase. The entrapped vapor is subjected to the extreme conditions of temperature and pressure reached in the bubble during collapse. At these conditions,

the vapor molecules can get dissociated into smaller fragments or chemical species. The main components of the model and relevant thermodynamic data/ boundary conditions have been given in Table 6.2.1B. Greater details of this model are given in our previous papers (Ksishnana *et al*. 2006, Kalva *et al*. 2009, Sivasankar and Moholkar 2009). The main components of the model are set of 4 ordinary differential equations (ODEs) as follows: (1) Keller-Miksis equation for the radial motion of the bubble (Keller and Miksis 1980), (2) Equation for the diffusive flux of solvent vapor through bubble wall (or gas-liquid interface); (3) Equation for heat conduction through bubble wall; (4) Overall energy balance treating the cavitation bubble as an open system (Table 6.2.1A).

Chapman-Enskog theory using Lennard-Jones 12-6 potential has been used to determine the transport parameters for the heat and mass transfer at the bulk temperature of the liquid medium (Hirschfelder *et al*. 1954, Condon and Odishaw 1958, Reid *et al*. 1987). Thermal and diffusive penetration depths are calculated using dimensional analysis. Diffusion of gas across bubble interface is ignored in the present model as the time scale for the diffusion of gases is much higher than the time scale for the radial motion of bubble.

Table 6.2.1 (A) Equations for diffusion limited cavitation bubble dynamics model (Toegel *et al*. 2000).

Model Component	Equation	Initial Value
1. Radial motion of the cavitation bubble	$\left(1-\frac{dR/dt}{c}\right)R\frac{d^2R}{dt^2}+\frac{3}{2}\left(1-\frac{dR/dt}{3c}\right)\left(\frac{dR}{dt}\right)^2 = \frac{1}{\rho_L}\left(1+\frac{dR/dt}{c}\right)(P_i-P_t)+\frac{R}{\rho_L c}\frac{dP_i}{dt}-4\nu\frac{dR/dt}{R}-\frac{2\sigma}{\rho_L R}$ Internal pressure in the bubble: $P_i = \frac{N_{tot}(t)\,kT}{\left[4\pi\left(R^3(t)-h^3\right)/3\right]}$ Pressure in bulk liquid medium: $P_t = P_0 - P_A\sin(2\pi ft)$	At t = 0, $R = R_o$ $dR/dt = 0$
2. Diffusive flux of water molecules	$\frac{dN_W}{dt} = 4\pi R^2 D_W \left.\frac{\partial C_W}{\partial r}\right\|_{r=R} \approx 4\pi R^2 D_W \left(\frac{C_{W,R}-C_W}{l_{diff}}\right)$ Instantaneous diffusive penetration depth: $l_{diff} = \min\left(\sqrt{\frac{RD_w}{\lvert dR/dt\rvert}}, \frac{R}{\pi}\right)$	At t = 0, $N_w = 0$
3. Heat conduction across bubble wall	$\frac{dQ}{dt} = 4\pi R^2\lambda\left.\frac{\partial T}{\partial r}\right\|_{r=R} \approx 4\pi R^2\lambda\left(\frac{T_0-T}{l_{th}}\right)$ Thermal diffusion length: $l_{th} = \min\left(\sqrt{\frac{R\kappa}{\lvert dR/dt\rvert}}, \frac{R}{\pi}\right)$	At t = 0, $Q = 0$
4. Overall energy balance	$C_{V,mix}dT/dt = dQ/dt - P_i dV/dt + (h_W - U_W)dN_W/dt$ Mixture heat capacity: $C_{V,mix} = \sum C_{V,i}N_i$ (i = N_2/O_2/H_2O) Molecular properties of water: Enthalpy: $h_w = 4kT_o$ Internal energy: $U_W = N_W kT\left(3+\sum_{i=1}^{3}\frac{\theta_i/T}{\exp(\theta_i/T)-1}\right)$ Heat capacity of various species (i = N_2/O_2/H_2O): $C_{V,i} = N_i k\left(f_i/2+\sum\left((\theta_i/T)^2\exp(\theta_i/T)\Big/\left(\exp(\theta_i/T)-1\right)^2\right)\right)$	At t = 0, $T = T_0$

R - radius of bubble; dR/dt - bubble wall velocity; c - velocity of sound in bulk liquid medium; ρ_L - density of liquid; ν - kinematic viscosity of liquid; σ - surface tension of liquid; λ - thermal conductivity of bubble contents; κ - thermal diffusivity of bubble contents; θ - characteristic vibrational temperature(s) of species; N_w - number of water molecules in bubble; N_{N2} - number of nitrogen molecules in bubble; N_{O2} - number of oxygen molecules in bubble; t - time, D_w-diffusion coefficient of water vapor; C_w - conc. of water molecules in bubble; $C_{w,R}$ - conc. of water molecules at the bubble wall or gas-liquid interface; Q - heat conducted across bubble wall; T - temperature of bubble contents; T_o - ambient (or bulk liquid medium) temperature; k - Bolzmann constant; h_w - molecular enthalpy of water; U_w - internal energy of water molecules; f_i - translational and rotational degrees of freedom; $C_{V,i}$ - heat capacity at constant volume for species i; N_{tot} - total number of molecules (gas + vapor) in bubble; h - van der Waal's hard core radius; P_o - ambient (bulk) pressure in liquid; P_A - pressure amplitude of ultrasound wave; f - frequency of ultrasound wave.

(B) Thermodynamic data for the model (Hirschfelder *et al*. 1954, Condon and Odishaw 1958, Reid *et al*. 1987).

Species	Degrees of freedom (translational + rotational) (f_i)	Lennard-Jones force constants		Characteristic vibrational temperatures θ (K)
		σ (10^{-10} m)	ε/k (K)	
N_2	5	3.68	92	3350
O_2	5	3.43	113	2273
H_2O	6	2.65	380	2295, 5255, 5400

The set of ODEs in the bubble dynamics model can be solved simultaneously using Runge-Kutta adaptive step size method (Press *et al*. 1992). The liquid medium in the present study was alkaline solution with different NaOH concentrations and temperatures. The physical properties of the liquid medium were obtained either from literature or by experimental measurement. The properties of density, vapor pressure and viscosity of NaOH solutions were obtained from literature (Washburn 1928, SOLVAY 1967). The surface tension of these solutions was measured using tensiometer (K9-Mk1, KRUSS GmbH, Germany). These properties have been listed in Table 6.2.2A and B.

Table 6.2.2. Physical properties of aqueous sodium hydroxide solution.

(A) Properties of NaOH at 30°C.

NaOH conc. (%w/v)	Surface Tension (mN/m)	Viscosity (cP)	Density (kg/m^3)	Vapor Pressure (Pa)
0.5	69.6	0.805	999	4887.6
1.0	68.2	0.830	1006	4868.9
1.5	66.3	0.855	1012	4850.3
2.0	64.2	0.880	1018	4831.6
2.5	66.2	0.905	1024	4812.9
3.0	62.8	0.930	1031	4794.3

(B) Properties of 1.5 % (w/v) NaOH at various temperatures.

Temperature (°C)	Surface Tension (mN/m)	Viscosity (cP)	Density (kg/m^3)	Vapor Pressure (Pa)
30	66.3	0.855	1012	4850.3
40	64.6	0.697	1009	7288.7
50	61.2	0.585	1005	14745.5
60	57.8	0.496	999.3	19771.7
70	48.5	0.430	995	34519.3
80	40.3	0.366	987.6	46836.1

The biomass concentration in the delignification experiments was quite small, i.e. 2% w/v. Therefore, amount of lignin from biomass getting dissolved in solution during process was too small to cause any major change in the physical properties of the solution, which would in turn affect the radial motion of cavitation bubbles. Moreover, the biomass particles are soft (with low elasticity modulus) and of size = 1 mm which is much smaller than the wavelength of ultrasound, i.e. 7.5 cm for 20 kHz frequency. Due to these, the scattering and attenuation effect rendered by the biomass on ultrasound waves is also negligible. It is however possible some re-polymerization and lignin condensation may occur in the bubble-bulk liquid interfacial region (due to reaction between the radicals generated by the bubble and the components of lignin dissolved in the liquid) (discussed later in Section 6.3.3.2). However, the reaction kinetics inside the cavitation bubble will stay unchanged as lignin is unlikely to evaporate into the bubble. Another important parameter in bubble dynamics model is the initial or equilibrium radius of the cavitation bubbles. The bubble population in the liquid medium usually has a wide distribution. In the present simulations the representative value of initial bubble radii was considered as $R_o = 5$.

6.2.8 Quantification of physical and chemical effects of ultrasound and cavitation

6.2.8.1 Micro-streaming due to ultrasound

The small amplitude of yet rapid oscillatory motion of fluid elements as ultrasound wave propagates through the medium is called micro-streaming. This phenomenon gives rise to intense micro-mixing in the medium. The magnitude of the micro-streaming velocity (u) is dependent on the pressure amplitude (P_A) of the ultrasound wave as: $u = P_A/\rho c$. Substituting values of P_A as 1.7×10^5 Pa, ρ = 995 kg/m^3 and c = 1481 m/s, gives u = 0.115 m/s.

6.2.8.2 Chemical effect of cavitation bubbles (*sonochemical effect*)

The diffusion limited mathematical model used in this study can predict the temperature and pressure reached in the cavitation bubble and also the number of gas and solvent molecules present inside the bubble at the moment of transient collapse. Due to very high temperature as well as concentration of species (due to extremely small volume of the bubble) inside the bubble, the kinetics of the reactions among these species is several orders of magnitude higher than the time scale of bubble dynamics (which is same as the period of the acoustic wave i.e. 50 microsecond for 20 kHz frequency) (Krishnan *et al*. 2006, Gong and Hart 1998). Therefore, thermodynamic equilibrium can be assumed to prevail inside the bubble at all times during radial motion. The equilibrium mole fraction of different chemical species in the bubble at the peak conditions reached at transient collapse can be calculated using Gibbs free-energy minimization technique (Sivasankar and Moholkar 2009).

6.2.8.3 Physical effect of cavitation bubbles

As noted earlier, radial motion of cavitation bubbles generates intense convection in the medium through two phenomena, *viz.* micro-convection, shock or acoustic waves. Using time history of radial motion of cavitation bubble (in terms series of radius, R and bubble wall velocity, dR/dt versus time, t) obtained from numerical solution of bubble dynamics model, magnitudes of these entities can be determined as:

Micro-convection velocity (Keller and Miksis 1980):

$$V_{turb}(r,t) = \frac{R^2}{r^2}\left(\frac{dR}{dt}\right)$$

Pressure amplitude of shock waves (*or Acoustic waves*) *(Hirschfelder et al. 1954, Condon and Odishaw 1958, Reid et al. 1987)*:

$$P_{AW}(r,t) = \frac{\rho_L}{4\pi r}\frac{d^2V_b}{dt^2} = \rho_L\frac{R}{r}\left[2\left(\frac{dR}{dt}\right)^2 + R\frac{d^2R}{dt^2}\right]$$

where, V_b is the volume of the bubble. A representative value of r is taken as 1 mm.

6.2.9 Analyses

6.2.9.1 Total reducing sugar (TRS) analysis

The liquid products (or hydrolyzate) obtained from different pretreatment processes were analyzed for sugar release. TRS released after physical, chemical or physicochemical pretreatments was estimated after completion of the treatment following the method given by Nelson (1944) and Somogyi (1945). During enzymatic hydrolysis of pretreated biomass, the samples were withdrawn

periodically and TRS estimation was done using standard method (Nelson 1944, Somogyi 1945). The individual pentose and hexose sugars present in the hydrolyzate were confirmed with HPLC analysis. The HPLC system (Perkin-Elmer, Series 200) comprised a pump, RI (refractive index) detector, a vacuum degasser and a HiPlex-H column (Varian, 300 mm × 5 µm × 4.6 mm). HPLC grade water (deionized water, Milli Q) was used as the mobile phase at a flow rate of 0.4 mL/min.

6.2.9.2 Field emission scanning electron microscopic (FESEM) analysis

The untreated, pretreated and delignified *P. hysterophorus* biomass samples were observed under field emission scanning electron microscope (Zeiss, Sigma). The samples were prepared by drying the biomass at 60^{o}C for 24 h and dried samples were spread on the carbon tape placed over the surface of FESEM stub and were sputtered with 10 nm gold in a sputter coater (SCH 620, Leo).

6.2.9.3 FTIR spectroscopic characterization of biomass samples

The raw, pretreated and delignified *P. hysterophorus* biomass samples were characterized for the change in structural composition using an FTIR spectrophotometer (Perkin-Elmer, Spectrum Two). The samples were prepared by mixing biomass sample (10 mg) and KBr in a ratio (w/w) of 1:100. The mixtures were ground well and the spectra were recorded in the range of 400-4000 cm^{-1} using 200 mg of biomass + KBr mixture in the form of pellets.

6.2.9.4 X-ray diffraction

The effect of different pretreatments on biomass crystallinity was investigated by using an X-ray diffractometer (D8 Advance, Bruker, Germany). The diffractometer was set at 40 KV, 40 mA; radiation was Cu Kα (λ = 1.54 Å). Samples were scanned over the range of 2θ = 5-30^{o} with a step size of 0.05^{o}. The crystallinity index (CrI) of all the samples was calculated as per the formula given by Segal *et al*. (1962):

$$CrI\,(\%) = \frac{I_{crystalline} - I_{amorphous}}{I_{crystalline}} \times 100$$

where, $I_{\text{crystalline}}$ = intensity of the crystalline peak at $2\theta = 22^{o}$ and $I_{\text{amorphous}}$ = intensity of the amorphous peak at $2\theta = 18^{o}$.

6.3 Results and Discussion

6.3.1 Analysis of structural composition of *P. hysterophorus*

The powdered raw biomass of *P. hysterophorus* was found to contain holocellulose (72.1±1.34%, w/w) comprising cellulose (45.2±1.81%, w/w) and pentosans (26.6±1.23%, w/w); lignin (23.6±0.83%, w/w) and moisture (2.31±0.11%, w/w). The presence of 45.2% (w/w) cellulose makes *P. hysterophorus* a potential resource material for bioethanol production. After treatment of biomass under optimum conditions of pretreatment (described in Section 6.3.3), the amount of cellulose, hemicellulose and lignin in treated biomass were be 64.1±2.5% (w/w), 1.02±0.073% (w/w) and 31.6±1.04% (w/w), respectively, which indicated almost complete removal of hemicellulose. Ultrasound-assisted alkaline delignification of pretreated biomass resulted in cellulose content of 96.1±0.94% (w/w) with traces of lignin 3.16±0.07% (w/w) in delignified biomass, where ultrasound assisted alkaline delignification was carried out under best values of parameters (described in Section 6.3.3.1).

6.3.2 Effect of various pretreatment methods on enzyme digestibility

6.3.2.1 Physical pretreatment

***6.3.2.1.1 Mechanical comminution*:** Total reducing sugar yield after mechanical grinding was 5.6 mg/g raw biomass, which is far lesser than 194 mg/g for 5 min ball milling of rice straw as reported by Hideno *et al*. (2009). This is due to the reason that the mechanical grinding applied by domestic kitchen grinder is far less energy intensive than milling (Barakat *et al*. 2013). Enzymatic hydrolysis of comminuted

biomass yielded 17.2 mg sugar/g pretreated biomass which showed the inaccessibility of cellulose for enzyme. However, it was evident from FESEM images of untreated (Fig. 6.3.1A) and treated (Fig. 6.3.1B) biomass that mechanical treatment increased surface area of biomass due to reduction in particle size. Thus, the lesser sugar release in enzymatic hydrolysis may be because this treatment did not remove hemicellulose and lignin from minced biomass, or induce any microscopic effects such as disruption of cellulose crystallinity or reduction in degree of polymerization.

***6.3.2.1.2 Autoclaving (auto-hydrolysis)*:** Autoclaving is the most commonly used method for pretreatment of lignocellulosic biomass (Wright 1998, Ibrahim *et al*. 2011, Das *et al*. 2013). In this method, ground biomass is treated with high-pressure steam and then the pressure is quickly reduced, which makes the materials to endure an explosive decompression. Autoclaving pretreatment can be influenced by the incubation time and temperature. Maximum hemicellulose solubilization and hydrolysis can be achieved by either high temperature and short incubation time or lower temperature and longer incubation time. Recent studies indicate that lower temperature and longer residence time are more favorable (Wright 1998). In this study, autoclaving of powdered biomass at 15 psi pressure at 121^{o}C for 20 min led to sugar yield of only 8.3 mg/g of raw biomass (Table 6.3.1). However, the ensuing enzymatic hydrolysis of pretreated sample resulted in a sugar release of 25.14 mg/g pretreated biomass (Table 6.3.1). This indicated that, in absence of chemicals (i. e. uncatalyzed autoclaving), this technique may have only opened up the complex structure of biomass. However, this technique did not effectively hydrolyze the

carbohydrate components of biomass. The reduction in particle size after the treatment was observed by the FESEM image of pretreated biomass shown in Fig 6.3.1C.

6.3.2.2 Chemical pretreatments

***6.3.2.2.1 Acid treatment*:** Dilute acid hydrolysis is most commonly used pretreatment method for lignocellulosic materials. This treatment yields pentose sugars after hydrolysis of hemicellulosic fraction of biomass (Kuhad *et al*. 2010, Ghosh *et al*. 2013). The dilute acid pretreatment of *P. hysterophorus* using 1, 3 and 5% (v/v) H_2SO_4, at 120^oC for 20 min yielded 75.74, 134.5 and 177.3 mg/g biomass of sugar, respectively. The subsequent enzymatic hydrolysis of pretreated biomass resulted in sugar yield of 133.12, 129.66 and 111.50 mg/g biomass, respectively (Table 6.3.1). An interesting observation in acid pretreatment was that the TRS yield after treatment increased with increasing concentration of acid from 1% to 5%. However, the TRS yield in the ensuing enzymatic hydrolysis reduced with concentration of acid. This anomaly can be attributed to hydrolysis of some of cellulose in the biomass (along with hemicellulose) during acid pretreatment. With increase in the concentration of acid, the fraction of cellulose in biomass undergoing hydrolysis during the pretreatment increases and this leaves lesser cellulose for enzymatic hydrolysis. Thus, the TRS yield per unit biomass in enzymatic hydrolysis reduces with increasing concentration of acid in the pretreatment. Higher temperature in dilute acid treatment shows significantly higher sugar yield as observed by Ghosh *et al*. (2012) and Kuhad *et al*. (2010), however, recently developed dilute acid

hydrolysis processes use less severe conditions, which resulted in high xylan to xylose conversion (Ranjan *et al*. 2013, Zheng *et al*. 2013). Sugar released during this pretreatment can be separately fermented to ethanol. This augments the overall ethanol yield per biomass that has a favorable consequence on process economics. The pentose sugar yield from hemicellulose in dilute acid pretreatment can be enhanced by optimizing acid concentration, incubation time and temperature (Ghosh *et al*. 2013). The FESEM micrographs of acid pretreated biomass showed discrete lignin droplets on its surface (Fig. 6.3.1 E-G). This indicated lignin removal from surface of biomass and similar explanation of this effect has been provided by earlier researchers (Koo *et al*. 2012). The population of surface lignin droplets increased with increase in the acid concentration during pretreatment (Fig. 6.3.1 D-G).

***6.3.2.2.2 Alkali treatment*:** The alkaline pretreatment of *P. hysterophorus* using 1, 3 and 5% (w/v) NaOH at 120^{o}C for 20 min resulted in TRS yield of 10.65, 12.3 and 14.09 mg/g biomass. These values essentially indicated negligible hydrolysis of carbohydrate moieties (in the form of both hemicellulose and cellulose) of biomass during the alkali treatment. These values were almost an order of magnitude smaller than the corresponding values for acid pretreatment. The consequent enzymatic hydrolysis of pretreated biomass resulted in 79.71, 82.01 and 87.86 mg/g biomass of TRS and these yields were also lower than those of the acid pretreatment (Table 6.3.1). These results clearly showed the insignificant overall yield of fermentable sugars in the alkaline pretreatment as well as enzymatic hydrolysis of alkali pretreated biomass. The causes leading to these effects can be explained as follows: main effect of alkali pretreatment of biomass is on its lignin content (Fan *et al*. 1987).

The mechanism of alkaline hydrolysis is believed to be the saponification of intermolecular ester bonds crosslinking xylan hemicelluloses and lignin. Alkaline treatment of lignocellulosic biomass results in swelling of biomass and thus, increased surface area, a decrease in the degree of polymerization, a decrease in crystallinity, separation of structural linkages between lignin and carbohydrates and disruption of the lignin structure (Fan *et al*. 1987). The overall porosity of the lignocellulosic materials also increases during alkali pretreatment. However, alkaline pretreatment does not remove the hemicellulose through hydrolysis (as in case of acid pretreatment). This means that the biomass subjected to enzymatic hydrolysis has significant content of hemicellulose in addition to cellulose. This hemicellulose can possibly hinder the accessibility of enzyme molecules to cellulose leading to lesser hydrolysis. Moreover, the CMCase and β-glucosidase added during enzymatic hydrolysis do not have activity for hemicellulose hydrolysis. Hence, the contribution to overall TRS release from hemicellulose in the entire process of pretreatment and enzymatic hydrolysis is negligible. All of these factors contribute to relatively lower TRS yield as compared to the acid pretreatment. FESEM pictures (Figs. 6.3.1 H-J) of alkali pretreated biomass revealed small holes on the surface of biomass, which probably are left behind after removal of lignin as reported by Kumar *et al*. (2009b). The surface population of these holes is observed to increase with increasing concentration of NaOH during pretreatment.

***6.3.2.2.3 Oxidizing agents*:** An oxidizing agent such as H_2O_2 has significant effect on biomass pretreatment at high pH (> 10) or under alkaline environment. H_2O_2

essentially assists effective solubilization of lignin and hemicellulose. This action makes cellulose more accessible to enzyme action. The TRS yield (15.06 mg/g) after pretreatment shows relatively insignificant hydrolysis, similar to that of alkaline pretreatment (14.09 mg/g). However, after the enzymatic hydrolysis the pretreated biomass showed significantly higher TRS yield (104.29 mg/g) as compared to the alkaline pretreatment alone (with highest TRS yield of 87.86 mg/g) (Table 6.3.1). These results were clear evidence of beneficial action of H_2O_2, as mentioned earlier (Azzam 1989, Saha and Cotta 2006). Oxidizing substances act as swelling agent for cellulosic fibers. Azzam (1989) reported that the pretreatment of sugarcane bagasse with 2% H_2O_2 treatment at 30^{o}C for 8 h resulted in removal of about 50% lignin and most of (~ 100%) hemicellulose and enhanced its degradability by enzymes. The degrading effect of H_2O_2 pretreatment on structure of *P. hysterophorus* biomass is evident from FESEM analysis that showed generation of droplets on biomass surface (Fig. 6.3.1 K) because of removal and migration of lignin.

***6.3.2.2.4 Surfactants* (*SDS and Triton X100*):** Pretreatment of *P. hysterophorus* biomass by SDS and Triton X100 yielded 15.65 and 21.23 mg/g of reducing sugar, respectively. However, enzymatic hydrolysis of *P. hysterophorus* biomass pretreated with SDS and Triton X100 resulted in 97.11 and 97.53 mg/g of sugar, respectively (Table 6.3.1). These results clearly showed that the extent of enzymatic hydrolysis of pretreated biomass was unaltered by the nature of surfactant, whether anionic or nonionic. The effect of surfactants on enzymatic hydrolysis has been investigated in other studies (Eriksson *et al*. 2002, Kim *et al*. 2006), such as SDS was used in the hydrolysis of steam-pretreated spruce (Eriksson *et al*. 2002). FESEM images of both

SDS and Triton pretreated biomass showed similar structures of the biomass surface morphology (Fig. 6.3.1 L and M).

6.3.2.3 The synergy of physicochemical treatments

In the previous section, the effects of various physical and chemical treatments on TRS release and change in biomass structure are reported. In this section, the trends of TRS release in physicochemical techniques have been assessed. An attempt has been made to identify the synergy between the physical and chemical components of these techniques with the yardstick of TRS release during pretreatment and following the enzymatic hydrolysis. The synergy will be positive if the TRS release is more than the sum total of individual techniques. The synergy will be negative if the TRS release is less than the sum total of two techniques, while the synergy will be nil, if the TRS release is equal to the sum total of individual techniques.

***6.3.2.3.1 Acid + Autoclaving*:** The effect of autoclaving of biomass during acid treatment showed marked effect on TRS release due to hemicellulose hydrolysis. The TRS yield increased almost 2-fold with autoclaving as compared to only acid treatment (Table 6.3.1). This result attributed to higher and faster reaction between acid and hemicellulose under elevated pressure and temperature during autoclaving. Thermal expansion of biomass during autoclaving increases the net surface area of biomass, in addition to increasing the accessibility of hemicellulose layer to acid molecules. The FESEM micrographs in Fig. 6.3.1N and O clearly showed the effect

of autoclaving, i.e., disruption of the biomass structure. Acid also has higher diffusivity at higher pressure. A net consequence of these effects is greater extent of hemicellulose hydrolysis. The synergy between acid treatment and autoclaving was thus revealed to be positive.

The TRS yield in the subsequent enzymatic hydrolysis did not show a marked rise. This may be a consequence of some cellulose undergoing hydrolysis during acid treatment with autoclaving, which limits the extent of TRS release in enzymatic treatment. Acid catalyzed autoclaving was proved to be an effective pretreatment of several lignocellulosic materials such as rice straw (Ranjan and Moholkar 2013) and water hyacinth (Satyanagalakshmi *et al*. 2011).

***6.3.2.3.2 Alkali + Autoclaving*:** Autoclaving assisted alkali pretreatment and enzymatic hydrolysis of pretreated biomass resulted 31.83 and 98.11 mg/g of reducing sugar, respectively (Table 6.3.1). The TRS yield under these conditions was found to be much higher than the rest of the alkaline pretreatments. The FESEM image of 1% NaOH pretreated biomass, both without and with autoclaving (Fig. 6.3.1P and Q, respectively), showed that autoclaving increases surface area by rupturing closed structure of the biomass. Fig. 6.3.1R is the enlarged view of Fig. 6.3.1Q, which showed some apertures on the surface of biomass, which may be created because of the migration and removal of lignin as suggested by Ibrahim *et al*. (2011) where similar structures were observed after alkaline pretreatment of rice straw. Using this technique, Sindhu *et al*. (2014) observed ~ 90% removal of lignin after pretreatment and a sugar yield of 0.775 g/g in enzymatic hydrolysis in their study with sugarcane tops.

6.3.2.3.3 Ammonia fiber expansion: In the present study, the AFEX pretreatment and subsequent enzymatic hydrolysis of *P. hysterophorus* biomass yielded TRS of 82.93 and 119.14 mg/g, respectively (Table 6.3.1). FESEM image of AFEX pretreated biomass showed partial lignin removal, as indicated by small droplets on the surface of biomass (Fig. 6.3.1S). AFEX was found to be very efficient for the pretreatment of lignocellulosic materials such as barley straw, corn stover, rice straw (Vlasenko *et al*. 1997) and switchgrass (Reshamwala *et al*. 1995). The AFEX pretreatment does not significantly solubilize hemicellulose compared to acid pretreatment or acid-catalyzed steam explosion as observed by Vlasenko *et al*. (1997).

***6.3.2.3.4 Oxidizing agent + Autoclaving*:** Autoclaving-assisted hydrogen peroxide treatment of biomass resulted in TRS yield of 18.31 mg/g and the ensuing enzymatic hydrolysis yielded 115.69 mg/g of TRS (Table 6.3.1). These yields are not significantly higher than the TRS yields with peroxide treatment in absence of autoclaving (i.e. 15.06 mg/g during pretreatment and 104.29 mg/g during enzymatic hydrolysis of pretreated biomass). The FESEM images of pretreated biomass with and without autoclaving showed almost the same morphology (Fig. 6.3.1K and T). This corroborated the above results that the autoclaving of biomass prior to hydrogen peroxide pretreatment does not contribute to additional TRS release and hence, there was no synergy between these two pretreatment techniques.

***6.3.2.3.5 Surfactants + Autoclaving*:** SDS and Triton treatments with autoclaving resulted in TRS yields of 17.89 and 24.3 mg/g, respectively and yields from subsequent enzymatic hydrolysis were 92.12 and 100.36 mg/g, respectively (Table 6.3.1). Comparison of these values with the yields from only surfactant treatment (without autoclaving) revealed that the effect of additional autoclaving was negligible for surfactant treated biomass. The action of autoclaving is essentially, the thermal expansion of biomass that leads to increase in porosity and the voidage that assists better transport of aqueous medium and dissolved sugar molecules.

The action of surfactant is to reduce surface tension of water, which has two consequences: (1) better and higher wettability of the surface of biomass and (2) effective penetration of water molecules in small micro-sized pores of biomass matrix due to reduced surface tension. Therefore, surfactant solution does not need expansion of biomass for having enhanced transport and thus, effect of autoclaving was almost negligible for surfactant added system. The FESEM images of biomass pretreated with autoclaving-assisted surfactant treatment revealed small disruption of structure (Figs. 6.3.1U and V), while the FESEM images of biomass pretreated without autoclaving (Figs. 6.3.1L and M) did not show any physical disruption.

Table 6.3.1 Results of TRS release during different pretreatments and subsequent enzymatic hydrolysis of *P. hysterophorus* biomass.

Pretreatment method	Conditions	TRS (g/L) released in PTT	TRS yield (mg/g of raw BM)	TRS (g/L) released in EH	TRS yield (mg/g of pretreated BM)
Physical Pretreatment					
Mechanical comminution	Approx. 1 mm particles using a mixture grinder	0.56 ± 0.04	5.60	0.86 ± 0.03	17.20
Autoclaving (Autohydrolysis)	15 psi pressure at 121^{o}C, 20 min	0.83 ± 0.05	8.30	1.25 ± 0.09	25.14
Chemical Pretreatment					
Acid	1% (v/v) (0.36 N) H_2SO_4, 120^{o}C, 20 min	7.57 ± 0.21	75.74	6.65 ± 0.24	133.12
Acid	3% (v/v) (1.08 N) H_2SO_4, 120^{o}C, 20 min	13.45 ± 0.19	134.50	6.48 ± 0.08	129.66
Acid	5% (v/v) (1.80 N) H_2SO_4, 120^{o}C, 20 min	17.73 ± 0.72	177.30	5.57 ± 0.27	111.50
Alkali	1% (w/v) (0.25 N) NaOH, 120^{o}C, 20 min	1.06 ± 0.06	10.65	3.98 ± 0.06	79.71
Alkali	3% (w/v) (0.75 N) NaOH, 120^{o}C, 20 min	1.23 ± 0.04	12.30	4.10 ± 0.29	82.01
Alkali	5% (w/v) (1.25 N) NaOH, 120^{o}C, 20 min	1.40 ± 0.05	14.09	4.39 ± 0.39	87.86
Oxidizing Agent:					
H_2O_2 + NaOH	H_2O_2 (0.25 g/g of biomass), pH 11.5, 35^{o}C, 3 h	1.50 ± 0.09	15.06	5.21 ± 0.42	104.29
Surfactants:					
0.5% (w/w) SDS	120^{o}C, 20 min	1.56 ± 0.10	15.65	4.85 ± 0.05	97.11
0.5% (w/w) Triton X100	120^{o}C, 20 min	2.12 ± 0.13	21.23	4.87 ± 0.05	97.53
Physicochemical Pretreatment					
Acid + Autoclaving	1% (v/v) (0.36 N) H_2SO_4, 20 min	19.86 ± 0.29	198.60	7.64 ± 0.66	152.92
Alkali + Autoclaving	1% (w/v) (0.25 N) NaOH, 20 min	3.18 ± 0.36	31.83	4.90 ± 0.07	98.11
Ammonia + Autoclaving (AFEX)	Ammonia (2 g/g of biomass), 20 min	8.29 ± 0.34	82.93	5.95 ± 0.59	119.14
H_2O_2 + NaOH + Autoclaving	pH 11.5, 20 min	1.83 ± 0.11	18.31	5.78 ± 0.08	115.69
0.5% (w/w) SDS + Autoclaving	20 min	1.78 ± 0.15	17.89	4.60 ± 0.04	92.12
0.5% (w/w) Triton + Autoclaving	20 min	2.18 ± 0.16	24.30	5.01 ± 0.18	100.36

TRS = total reducing sugar; PTT = pretreatment; EH = enzymatic hydrolysis; BM = biomass;
TRS (g/L) values are mean ± standard error (n = 3)

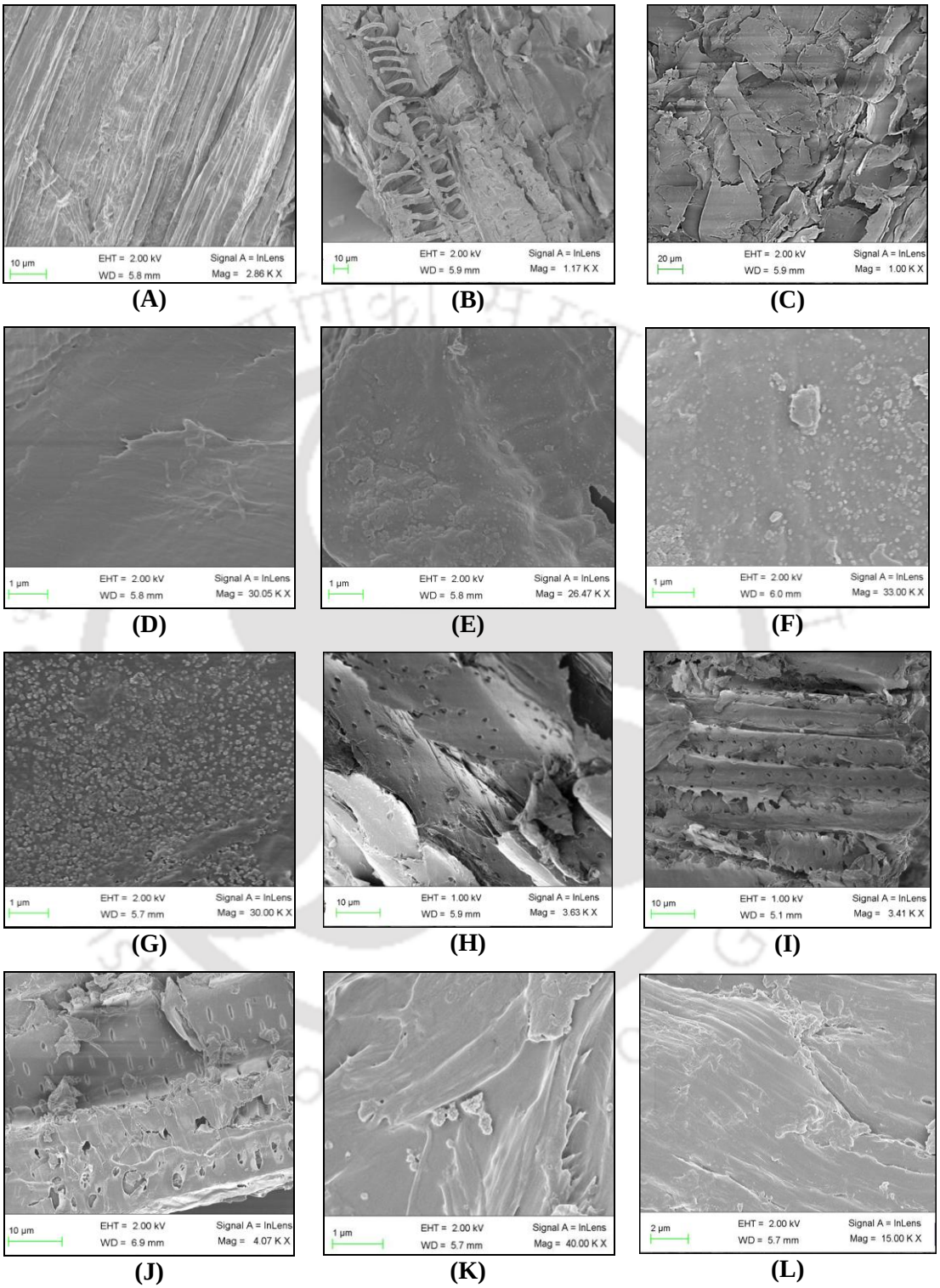

Fig. 6.3.1 FESEM images of untreated and pretreated biomass. (A) intact biomass, (B) mechanical comminution (C) autoclaving (D) untreated biomass (E) 1% H_2SO_4 at 120^oC (F) 3% H_2SO_4 at 120^oC (G) 5% H_2SO_4 at 120^oC (H) 1% NaOH at 120^oC (I) 3% NaOH at 120^oC (J) 5% NaOH at 120^oC (K) H_2O_2 (L) SDS.

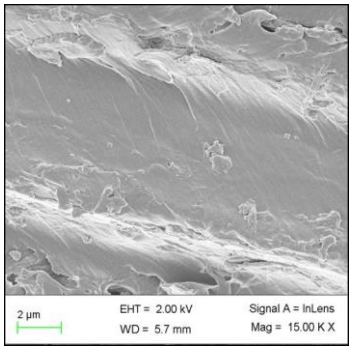

(M)

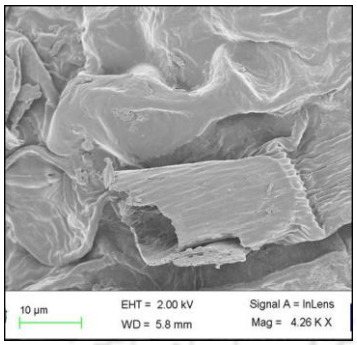

(N)

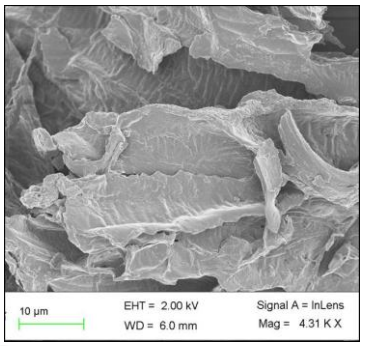

(O)

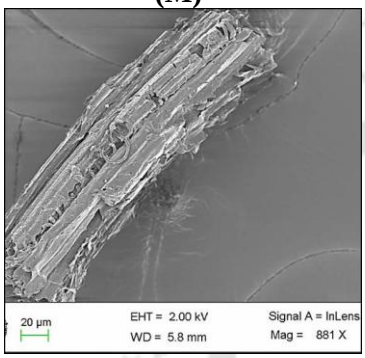

(P)

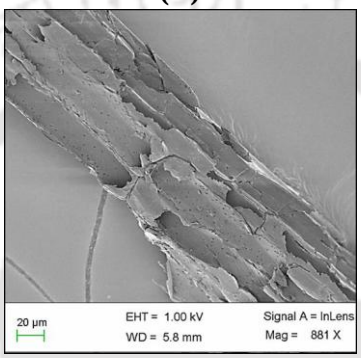

(Q)

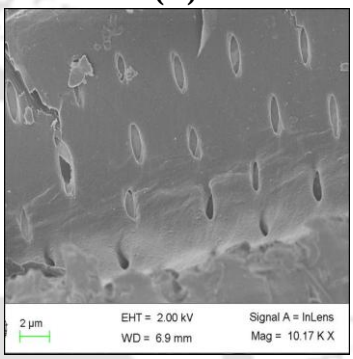

(R)

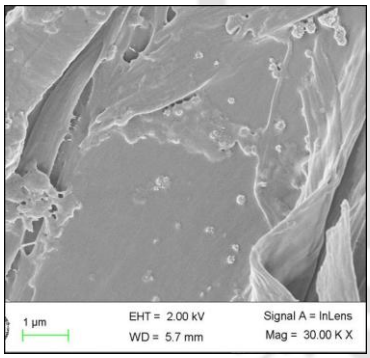

(S)

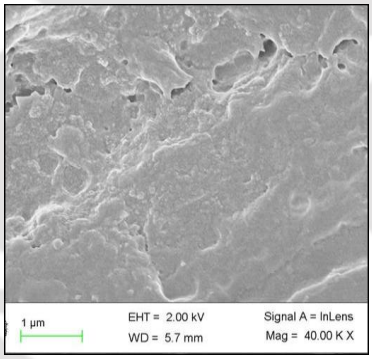

(T)

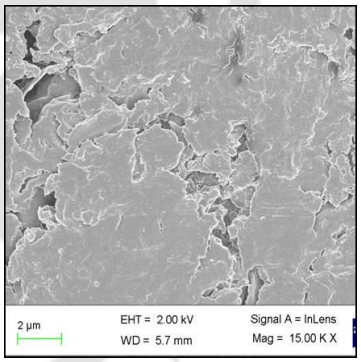

(U)

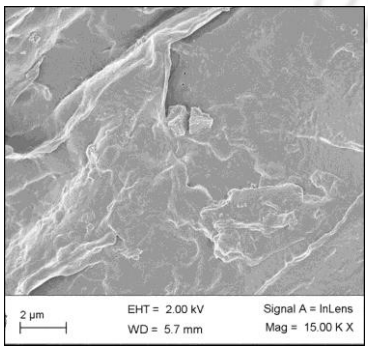

(V)

Fig. 6.3.1 (*Continued*…) FESEM images of untreated and pretreated biomass. (M) Triton X100 (N) 1% H_2SO_4 at 120^oC (O) 1% H_2SO_4 + autoclaving (P) 1% NaOH at 120^oC (Q) 1% NaOH + autoclaving (R) Enlarged 1% NaOH + autoclaving (S) AFEX (T) H_2O_2 + autoclaving (U) SDS + autoclaving (V) Triton X100 + autoclaving.

6.3.3 Optimization of acid pretreatment (secondary optimization)

The results from preliminary screening of pretreatment strategies revealed that acid pretreatment yielded maximum total fermentable sugar (TFS) (i.e. the sum of sugar released during dilute acid pretreatment and obtained from enzymatic hydrolysis). Results of several previous studies also corroborate this result (Satyanagalakshmi *et al*. 2011, Ranjan and Moholkar 2013, Suresh *et al*. 2014). In view of this, the acid pretreatment was further optimized with operational parameters, 1% (v/v) acid + autoclaving for 20, 30 and 40 min and incubation with 5% (v/v) acid at 120^{o}C for 20, 30 and 40 min. TRS yields from pretreatment with 1% acid+autoclaving for 20, 30 and 40 min were 198.6, 285.3 and 199.4 mg/g of raw biomass, respectively; however, 5% (v/v) acid treatment at 120^{o}C for 20, 30 and 40 min resulted TRS yield of 177.3, 184.1 and 194.7 mg/g raw biomass, respectively (Table 6.3.2A). Table 6.3.2B depicts the yields of individual sugars released after different acid pretreatments mentioned in Table 6.3.2A. It could be seen that the hydrolysate was dominated by pentose (xylose and arabinose) sugars rather than glucose. This essentially means that during this pretreatment hemicellulose was hydrolyzed preferentially than cellulose.

Table 6.3.2 Results of optimization of acid pretreatment process (or secondary optimization).

(A) Results of total fermentable sugar release (pretreatment + enzymatic hydrolysis).

Pretreatment (PTT)	TRS* (PTT, g/L)	TRS* (PTT, mg/g of raw BM)	TRS* (EH, g/L)	TRS* (EH, mg/g of pretreated BM)	TRS* (EH, mg/g of raw BM)	TFS yield (g/100 g of raw BM)	Theoretical Ethanol yield (g/100 g of raw BM)§	Theoretical Butanol yield (g/100 g of raw BM)#
1% Acid + Autoclaving, 20 min	19.86 ± 0.42	198.6	7.65 ± 0.03	153.0	91.8	29.04	14.81	11.91
1% Acid + Autoclaving, 30 min	28.53 ± 0.23	285.3	9.37 ± 0.04	187.4	112.4	39.77	20.28	16.31
1% Acid + Autoclaving, 40 min	19.94 ± 0.39	199.4	8.48 ± 0.04	169.6	101.8	30.12	15.36	12.35
5% Acid, 120°C, 20 min	17.73 ± 0.12	177.3	5.58 ± 0.08	111.6	66.0	24.33	12.41	9.98
5% Acid, 120°C, 30 min	18.41 ± 0.31	184.1	5.12 ± 0.02	102.4	61.4	24.55	12.52	10.07
5% Acid, 120°C, 40 min	19.47 ± 0.56	194.7	4.85 ± 0.05	97.0	58.2	25.29	12.89	10.37

TRS = total reducing sugar; PTT = pretreatment; EH = enzymatic hydrolysis; BM = biomass; TFS = total fermentable sugar

*TRS concentration was determined by the method of Nelson (1944) and Somogyi (1945). PTT - TRS release during pretreatment, EH - TRS release during enzymatic hydrolysis. TFS yield = TRS yield after pretreatment + TRS yield after enzymatic hydrolysis. § Maximum theoretical yield for ethanol from hexose as well as pentose sugars is 0.51 g/g sugar. # Maximum theoretical yield for butanol from hexose as well as pentose sugars is 0.41 g/g sugar.

(B) Results of determination of individual sugars in the sugar released during pretreatment.

PTT	Glucose (PTT)**		Xylose (PTT)**		Arabinose (PTT)**	
	g/L	mg/g	g/L	mg/g	g/L	mg/g
1% Acid + Autoclaving, 20 min	1.42 ± 0.04	14.2	13.13 ± 0.21	131.3	2.03 ± 0.01	20.3
1% Acid + Autoclaving, 30 min	1.65 ± 0.03	16.5	21.11 ± 0.27	211.1	3.23 ± 0.02	32.3
1% Acid + Autoclaving, 40 min	1.37 ± 0.01	13.7	10.75 ± 0.03	107.5	2.76 ± 0.01	27.6
5% Acid, 120°C, 20 min	1.23 ± 0.02	12.3	9.13 ± 0.05	91.3	1.96 ± 0.01	19.6
5% Acid, 120°C, 30 min	1.69 ± 0.03	16.9	12.66 ± 0.08	126.6	1.72 ± 0.02	17.2
5% Acid, 120°C, 40 min	1.96 ± 0.02	19.6	14.91 ± 0.08	149.1	1.34 ± 0.01	13.4

**Individual sugar concentrations were determined by HPLC.

Enzymatic hydrolysis of pretreated biomass with 1% acid+autoclaving and 5% acid for 20, 30 and 40 min further yielded reducing sugar of 153.0, 187.4, 169.6, 111.6, 102.4 and 97.0 mg/g pretreated biomass, respectively (Fig. 6.3.2). Thus, the TFS yield was maximum (397.7 mg/g raw biomass) for pretreatment conditions of 1% (v/v) acid + autoclaving for 30 min. The decrease in TFS yield with increased autoclaving of 40 min may be a consequence of formation of sugar degradation products such as furfural due to prolonged incubation in acid solution. These results implied that the technique of simultaneous autoclaving renders acid pretreatment more effective, as it gave larger TFS release at relatively very dilute acid concentrations. This obviates the need for concentrated acid, which also has several other problems such as handling, corrosion of vessels, degradation of released sugar and disposal of used acid.

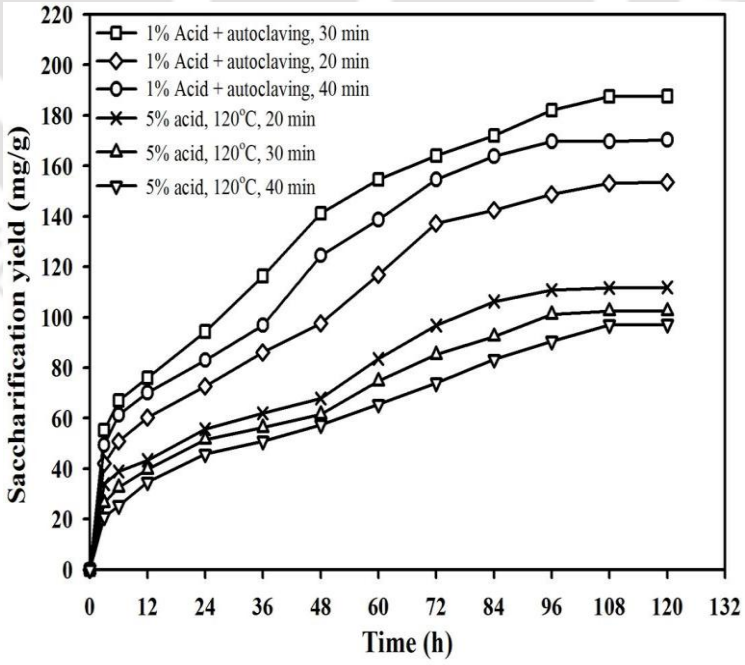

Fig. 6.3.2 Time profile of saccharification during enzymatic hydrolysis of acid pretreated *P. hysterophorus* biomass under different process conditions.

6.3.4 Comparative assessment of pretreatment

6.3.4.1 FTIR analysis

The effect of different pretreatment processes on composition of *P. hysterophorus* biomass was monitored in terms of relative change in intensities at specific band positions. Vibrational frequencies of different functional groups in IR spectrum of biomass are summarized in Table 6.3.3A and spectra of untreated and pretreated samples are shown in Figure 6.3.3. Table 6.3.3B showed the relative percentage change in intensities of various bands after pretreatment, a positive value of which, at a specific band indicates reduction of the particular component assigned to that band, as described by Kumar *et al*. (2009b). The positive values of relative change for most of the bands for all pretreatments indicated removal of biomass components to different extent in various pretreatments. Change in hemicellulose content, represented by the relative intensity change for the band at 1378 cm^{-1}, was maximum for treatment with 1% acid + autoclaving. The band position 1059 cm^{-1} is assigned to the carbohydrate-lignin linkage and intensity at this band was efficiently affected (with a value of > 60%) by 5% alkali (Fig. 6.3.3C) and H_2O_2 treatment (Fig. 6.3.3D), however, the maximum change was seen for 1% acid + autoclaving (Fig. 6.3.3E). This relative change, larger than as in case of 5% acid (Fig. 6.3.3B), was again a corroboration of beneficial effect of autoclaving in terms of reduction in the requirement of concentrated acid during pretreatment. The ratio of relative change in intensities at the band position 1098/900 indicated conversion of crystalline cellulose to amorphous and was found to be positive for all pretreatment with a maximum relative in case of 1% acid + autoclaving pretreatment.

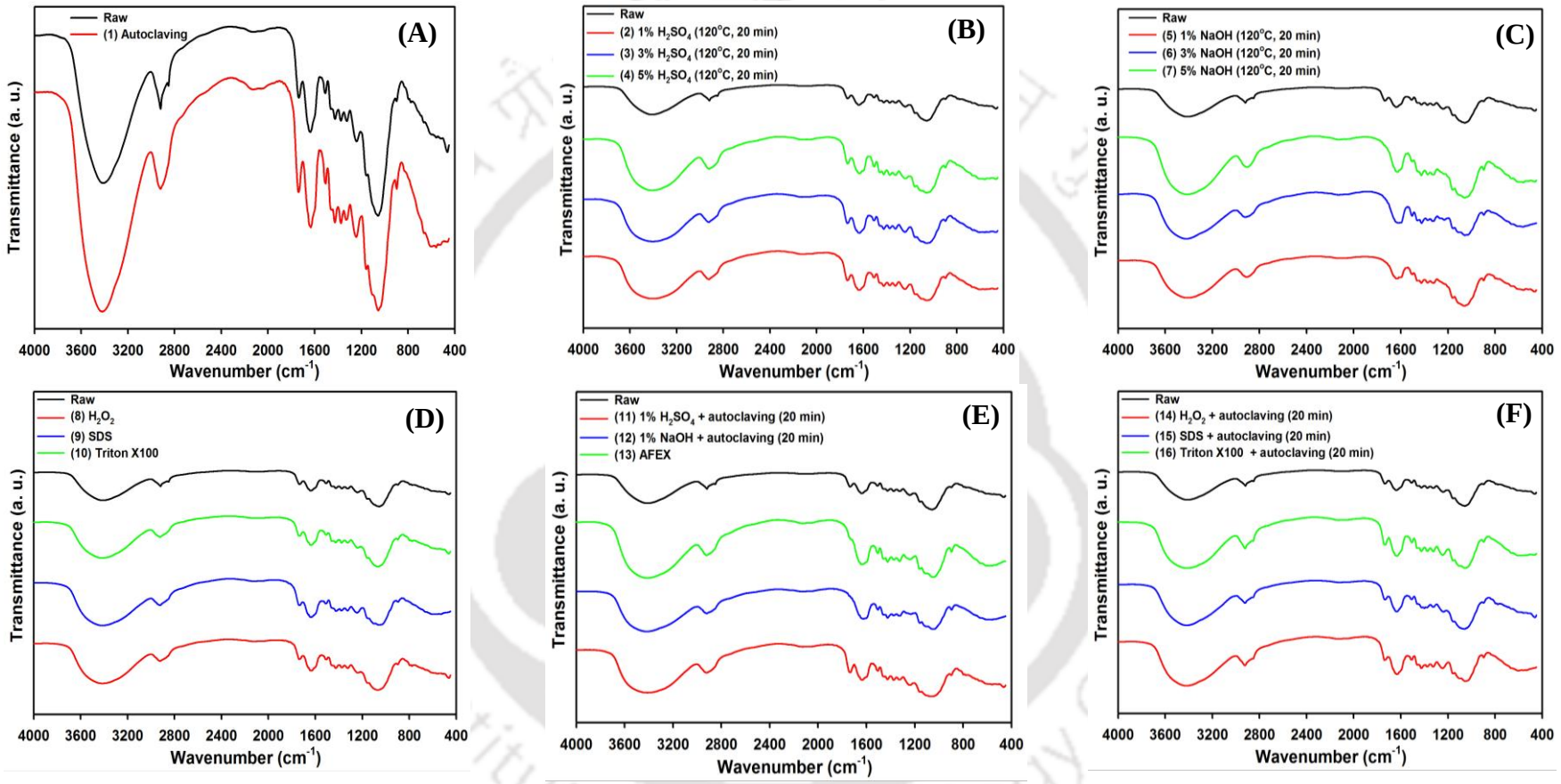

Fig. 6.3.3 FTIR spectra of native (raw) biomass and biomass pretreated with (A) autoclaving (B) 1, 3, 5% H_2SO_4 (120^{o}C, 20 min) (C) 1, 3, 5% NaOH (120^{o}C, 20 min) (D) H_2O_2, SDS and triton X100 (E) 1% H_2SO_4 + autoclaving (20 min), % NaOH + autoclaving (20 min), AFEX and (F) H_2O_2 + autoclaving, SDS + autoclaving, Triton X100 + autoclaving.

Table 6.3.3 Characterization of pretreated biomass by FTIR spectroscopic and XRD analyses.

Band position (cm^{-1})	**Assignment***	1	2	3	4	5	6	7	8	9	10	11	12	13	14	15	16
3348	O-H stretching (related to rupture of cellulose hydrogen bonds)	25.2	57.1	49.3	72.6	11.8	41.1	58.3	51.4	25.5	20.8	77.4	49.0	63.5	58.5	48.9	51.0
2900	C-H stretching (related to rupture of methyl/methylene group of cellulose)	10.6	33.5	27.9	42.1	4.8	24.5	24.6	26.5	54.8	8.6	48.7	34.7	35.1	32.1	23.8	26.1
1745	Carbonyl bonds (related to lignin side chain removal)	11.9	37.3	30.6	31.4	-24.2	-10.5	-16.1	24.1	52.9	8.4	48.8	5.1	4.3	26.8	21.0	25.3
1738	C=O stretching due to carbohydrate linked with lignin	12.1	38.4	30.8	33.8	-25.6	-11.6	-17.3	24.7	51.9	8.4	49.4	4.4	5.4	27.8	21.7	25.8
1720	Carboxylic acids/ester groups	11.1	36.2	30.7	31.9	-16.4	-1.1	-7.1	24.7	54.7	13.7	45.8	12.9	13.0	27.7	22.4	23.8
1595	Aromatic ring stretch (related to lignin removal)	13.8	46.0	43.0	43.5	0.0	31.8	23.1	35.3	41.1	13.7	55.1	40.9	46.1	43.3	31.1	33.9
1508	Aromatic ring vibration (related to lignin removal)	10.7	34.3	28.9	40.5	0.3	23.3	14.4	26.7	54.3	8.2	47.9	30.0	34.3	28.3	22.8	23.3
1458	Aromatic ring vibration (related to lignin removal)	13.5	39.8	32.2	47.1	5.7	26.7	27.7	32.5	48.1	13.3	54.4	34.4	39.7	32.5	25.8	28.5
1428	Band of cellulose	15.1	44.0	36.0	49.3	6.8	29.2	33.4	35.9	43.7	13.4	58.6	38.1	43.7	37.6	30.0	32.2
1378	Band of hemicellulose	15.2	42.6	35.0	50.2	5.7	23.1	30.8	34.3	44.3	13.8	59.6	33.3	39.1	34.3	30.3	32.0
1260	Ester absorbance (related to removal of uronic acid)	13.8	44.7	33.7	52.1	-1.5	14.6	21.8	37.8	42.5	15.2	65.0	24.7	32.9	31.8	31.5	33.4
1245	C=O absorption (resulting from acetyl groups cleavage)	13.7	45.7	34.0	53.8	-1.4	13.9	22.8	39.9	41.4	16.6	67.2	24.0	33.1	31.9	33.1	34.6
1238	Hemicellulose-lignin linkage	13.4	45.2	33.5	54.0	0.1	15.4	24.2	40.4	41.8	17.1	67.2	24.8	33.4	31.2	33.6	33.8
1059	C=O stretching due to carbohydrate-lignin linkage	16.3	56.2	41.8	78.8	24.5	25.2	66.3	67.1	24.2	37.2	87.7	35.0	56.7	40.7	57.6	45.0
1098/900[a]	Amorphous to crystalline cellulose ratio	2.6	30.1	21.9	55.4	14.1	1.6	44.8	48.9	26.2	26.7	69.5	4.1	27.4	17.3	40.1	26.7
900	Band of cellulose	10.0	33.6	24.1	40.6	9.4	19.4	28.1	33.9	56.5	14.5	54.2	28.3	29.4	22.0	27.5	20.2
Crystallinity index (*CrI*)[#] (%)		41.9	53.7	56.9	62.8	50.7	50.8	51.4	51.3	40.2	48.6	63.2	52.8	55.7	55.4	47.5	47.0

*****Assignment of the band positions in IR spectra (Kumar *et al*. 2009b)

[*]%Relative change = 100 x (intensity of untreated solid - intensity of pretreated solid)/ intensity of untreated solid; where positive number indicates reduction;

[a]The ratio of intensity at two band positions. [#]*CrI* of raw biomass (mechanically comminuted) was 50%.

(1) autoclaving (2) 1% H_2SO_4 (120°C, 20 min) (3) 3% H_2SO_4 (120°C, 20 min) (4) 5% H_2SO_4 (120°C, 20 min) (5) 1% NaOH (120°C, 20 min) (6) 3% NaOH (120°C, 20 min) (7) 5% NaOH (120°C, 20 min) (8) H_2O_2 (9) SDS (10) Triton X100 (11) 1% H_2SO_4 + autoclaving (20 min) (12) 1% NaOH + autoclaving (20 min) (13) AFEX (14) H_2O_2 + autoclaving (15) SDS + autoclaving (16) Triton X100 + autoclaving

6.3.4.2 XRD analysis

Crystallinity index (*CrI*) is a measure of extent of removal of non-crystalline or amorphous components of biomass, *viz.* lignin and hemicellulose. An increase in the *CrI* is essentially an indication of the increase in cellulose content of biomass after pretreatment. The *CrI*s for biomass pretreated with different techniques have been listed in Table 6.3.3 and X-ray diffraction patterns of raw and pretreated biomass samples are shown in Figure 6.3.4. XRD analysis revealed significant increase in *CrI* in 1, 3 and 5% acid pretreated and 1% acid + autoclaving pretreated biomass (53.7, 56.9, 62.8 and 63.2%, respectively) in comparison to the *CrI* of untreated biomass which was 50.0%. Increment in crystallinity index after acid treatment was attributed to the hydrolysis of hemicellulose. Relatively smaller increase in *CrI* (55.7 %) was observed after AFEX treatment of biomass, which was due to the partial removal of lignin and hemicellulose as interpreted in a study by Sindhu *et al*. (2014). Increased *CrI* on treatment with 1, 3 and 5% NaOH (*CrI* = 50.7, 50.8 and 51.4 respectively) (Fig. 6.3.4C), 1% NaOH + autoclaving (*CrI* = 52.8%) (Fig. 6.3.4E), oxidizing agent (H_2O_2, *CrI* = 51.3%) (Fig. 6.3.4D) and with oxidizing agent (H_2O_2) + Autoclaving (*CrI* = 55.4%) (Fig. 6.3.4F) indicated the effect of these treatments on amorphous portion was more than the crystalline portion of the biomass. Pretreatments involving surfactants, either in hot aqueous medium or with autoclaving and only autoclaving (SE/Autohydrolysis) of powdered biomass resulted in comparatively lower crystallinity index than that of original biomass (*CrI* = 50%) (Fig. 6.3.4A). The typical values of *CrI* in different protocols in this context are: SDS without autoclaving (*CrI* = 49.2%), Triton X100 without autoclaving (*CrI* = 48.6%), SDS

with autoclaving (*CrI* = 47.5%), Triton X100 with autoclaving (*CrI* = 47%). The crystallinity index obtained after only autoclaving was the lowest (*CrI* = 41.9%). This lowest value of crystallinity index (~ 41.9%) as compared to original biomass (*CrI* = 50%) is attributed to breakage of the linkages between cellulose and lignin, without actual hydrolysis of any component, as indicated by lower sugar yield of 8.3 mg/g biomass.

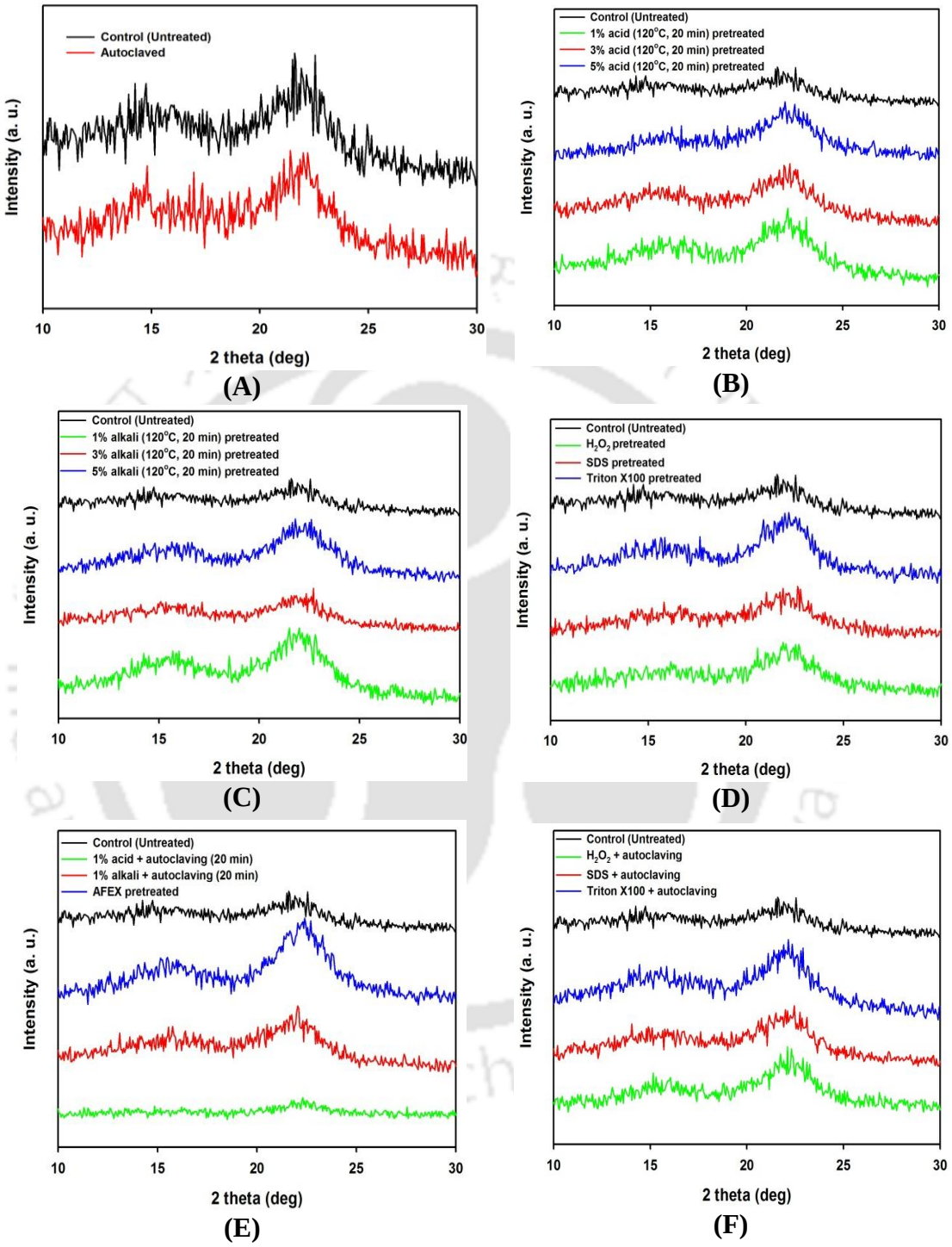

Fig. 6.3.4 Diffractograms of raw biomass and after different pretreatments (A) autoclaved, (B) 1, 3, 5% acid pretreated, (C) 1, 3, 5% alkali pretreated, (D) H_2O_2 and surfactants pretreated (E) 1% acid + autoclaving, 1% alkali + autoclaving and AFEX pretreated and (F) H_2O_2 + autoclaving and surfactants + autoclaving pretreated.

6.3.5 Ultrasound assisted alkaline delignification of pretreated *P. hysterophorus*

The possible mechanisms of lignin degradation with ultrasound under alkaline conditions have been discussed based on the report of Bussemaker and Zhang (2013), before presenting the experimental results. The reactive sites in lignin are mainly the ether linkages and functional groups, since the carbon-carbon linkages are generally resistant to chemical attack. The areas of lignin susceptible to chemical attack are the hydrolysable ether linkages (α-aryl, α-alkyl and β-aryl), phenolic and aliphatic hydroxyl groups, ester groups, methoxyl groups, the unsaturated groups and uncondensed units. In alkaline and alkaline-oxidative environments, lignin degrades through the cleavage of the α- and β-aryl ether linkages to yield fragmentation units. Ultrasound can cause depolymerization and separation of lignin, in addition to degradation of lignin components. Separation of lignin with ultrasound occurs via cleavage of the lignin-hemicellulose linkages. Depolymerization of lignin occurs through homolytic cleavages of the phenyl ether β-O-4 and α-O-4 bonds.

According to Bussemaker and Zhang (2013), hydroxyl radicals produced from transient collapse of cavitation bubble can also induce degradation of lignin. However, this attack usually takes place on aromatic ring. This leads to hydroxylated, demethoxylated and side chain eliminated products. A small extent of hydroxyl radical attack also occurs on the side chains leading to formation of dimers and oxidation of aromatic aldehydes to carboxylic acids. Increase in number of non-conjugated carbonyls also corroborates the hydroxyl radical induced degradation.

In addition to cleavage of inter-unitary bonds within lignin matrix and between lignin-hemicellulose entities, evidence for condensation of lignin in

presence of ultrasound has also been observed. Lignin degradation results in release of low molecular weight phenolic species that are soluble in liquid medium and therefore, get extracted in the medium during sonication. These species (which have phenolic moieties) can accumulate at the bubble interface which essentially is the thin liquid film in contact with bubble surface. This accumulation can enable proton transfer or promote radical scavenging. This liquid film can get heated to moderately high temperatures (400-600 K) during transient collapse of the bubble. Hua *et al*. (1995) have hypothesized that the thin film of liquid near bubble surface can reach supercritical conditions with marked rise in solubility. This further enhances the phenomenon of re-condensation and re-polymerization reactions. The re-polymerized lignin, in the form of small globules or droplets, can get re-deposited on biomass surface. With this preamble the results and analysis of this study have been presented.

6.3.5.1 Parametric investigation of delignification

The results of the experiments for parametric investigation of delignification are presented in Tables 6.3.4 to 6.3.6. From these results the following three definitive trends in delignification with experimental parameters were identified;

1. The lignin removal by ultrasonic treatment at ambient temperature showed the saturation with increasing NaOH concentration, as evident from the results depicted in Table 6.3.4. Beyond 2% (w/v) NaOH, the lignin removal stays practically constant. However, for mechanical agitation, a gradual rise in lignin removal was seen till 2.5% (w/v) NaOH concentration. The percent enhancement

in lignin removal with ultrasound showed maxima at 1.5% (w/v) NaOH concentration.

2. Table 6.3.5 shows the influence of biomass concentration on lignin removal at ambient temperature. In these experiments, the concentration of NaOH has been maintained at the best value of 1.5% (w/v) for ultrasonic treatment based on the results of earlier set of experiments. An interesting trend was seen in these experiments that the lignin removal with ultrasound reduced as the biomass concentration exceeded 2% (w/v). Lignin removal at 8% (w/v) biomass concentration was nearly half of that at 2% (w/v). A similar trend was seen for mechanical agitation however, the effect of lignin reduction with biomass concentration was lower. In the biomass concentration range of 5-8% (w/v), lignin removal by mechanical agitation exceeded that by ultrasound. The best value of biomass concentration with ultrasonic treatment was 2% (w/v) which resulted in maximum enhancement in delignification as compared with mechanical agitation.
3. Table 6.3.6 depicts the effect of temperature on the delignification at the optimum concentration of NaOH and biomass determined earlier. As per these results, the extent of lignin removal with temperature remains practically same for ultrasound in the range 30°-80°C, while for mechanical agitation a 16% increase was seen for the same temperature range. The percent enhancement in lignin removal by ultrasound was highest at 30°C as compared with mechanical agitation and thus this temperature was considered the optimum.

Table 6.3.4 Effect of NaOH concentration on delignification process (Biomass concentration = 3% (w/v), Temperature = 30°C, Time of treatment = 15 min).

NaOH loading (%, w/v)	Lignin content§ in residue (mg/g)		Lignin removal (%)		Enhancement in lignin removal with ultrasound* (%)
	US	MA	US	MA	
0.5	107.3 ± 1.4	134.0 ± 2.8	66.0	57.6	14.6
1.0	104.0 ± 2.5	132.1 ± 1.2	67.1	58.2	15.3
1.5	69.5 ± 2.4	121.2 ± 1.5	78.0	61.7	26.4
2.0	75.2 ± 1.1	108.7 ± 2.3	76.2	65.6	16.2
2.5	74.4 ± 1.8	94.7 ± 1.4	76.5	70.0	9.3
3.0	74.6 ± 2.2	91.0 ± 1.1	76.4	71.2	7.3

US = ultrasound assisted process; MA = mechanically agitated process
* calculated as (US - MA) × 100/MA
§ Lignin content values are: mean ± standard error (n = 2).

Table 6.3.5 Effect of biomass concentration on delignification process (NaOH concentration = 1.5% (w/v) with US and 2.5% (w/v) with MA, Temperature = 30°C, Time of treatment = 15 min)

Biomass loading (%, w/v)	Lignin content§ in residue (mg/g)		Lignin removal (%)		Enhancement in lignin removal with ultrasound (%)
	US	MA	US	MA	
0.5	26.9 ± 1.0	29.4 ± 0.7	91.5	90.7	0.9
2.0	31.6 ± 1.4	43.0 ± 0.5	90.0	86.4	4.2
3.5	83.7 ± 0.7	84.0 ± 1.3	73.5	73.4	0.1
5.0	96.4 ± 1.3	86.49 ± 0.8	69.5	72.6	-4.3
6.5	139.7 ± 1.6	95.25 ± 1.4	55.8	69.9	-20.2
8.0	149.8 ± 2.1	94.7 ± 1.0	52.6	70.0	-24.9

§ Lignin content values are: mean ± standard error (*n* = 2).

Table 6.3.6 Effect of temperature on delignification process (Biomass concentration = 2% w/v, NaOH concentration = 1.5% (w/v) with US and 2.5% (w/v) with MA, Time of treatment = 15 min)

Temperature (°C)	Lignin content§ in residue (mg/g)		Lignin removal (%)		Enhancement in lignin removal with ultrasound (%)
	US	MA	US	MA	
30	31.3 ± 0.75	83.7 ± 0.52	90.1	73.5	22.6
40	30.9 ± 0.52	71.7 ± 0.37	90.2	77.3	16.7
50	30.8 ± 0.42	50.9 ± 1.09	90.3	83.9	7.6
60	30.7 ± 0.59	47.5 ± 0.46	90.3	84.9	6.4
70	30.6 ± 0.25	42.0 ± 0.35	90.3	86.7	4.2
80	21.7 ± 0.43	40.7 ± 0.62	93.1	87.1	6.9

§ Lignin content values are: mean ± standard error (*n* = 2).

Thus, on the basis of these experiments, the set of best values of experimental parameters for ultrasound-assisted delignification were obtained as, temperature, 30°C, NaOH concentration, 1.5% (w/v), biomass concentration, 2% (w/v). Similarly, the set of best values of the parameters for delignification with mechanical agitation were, temperature, 80°C, NaOH concentration, 2.5% (w/v), biomass concentration, 2% (w/v). The ultrasound assisted delignification using best values of the parameters (as mentioned above) for 10 min resulted to the biomass with cellulose and lignin contents of 96.1±0.94% (w/w) and 3.16±0.07% (w/w), respectively.

6.3.5.2 Kinetics of delignification

The time profile of delignification with mechanical agitation and ultrasound treatment is given in Table 6.3.7. These data have been analyzed by using pseudo first order kinetics (as an approximation of the complex delignification process). The graphical plots of pseudo first order kinetic expression fitted to delignification data (Fig. 6.3.5A and B). The kinetic data for ultrasonic treatment show that the extent of delignification remains constant after first 10 min of treatment and after 20 min of treatment in case of mechanical agitation. In view of these observations, the pseudo first order kinetic constant for delignification was calculated as 0.262 min^{-1} using data for 10 min of ultrasound assisted treatment and 0.126 min^{-1} using data for 20 min for mechanically agitated system. The ratio of kinetic constants, determined for both, ultrasound-assisted and mechanically agitated delignification processes, gave a quantitative estimate of the enhancement effect of ultrasound on delignification process. Ultrasound enhanced the kinetics of the process more than 2-fold.

Table 6.3.7 Kinetic analysis of delignification process (Biomass concentration = 2% (w/v), NaOH concentration = 1.5% (w/v) with US and 2.5% (w/v) with MA and Temperature = 30°C with US and 80°C (w/v) with MA).

Time (min)	Lignin content§ in residue (mg/g)		Lignin removal with ultrasound		Lignin removal with mechanical agitation	
	US	MA	% removal	k_{US} (min^{-1})	% removal	k_{MA} (min^{-1})
5	45.2 ± 0.82	84.4 ± 0.76	85.7		73.3	
10	31.6 ± 0.73	60.0 ± 0.68	90.0		81.0	
15	31.3 ± 0.49	42.8 ± 0.46	90.1	0.262	86.4	0.126
20	28.1 ± 0.43	40.7 ± 0.37	91.1		87.1	
25	32.2 ± 0.32	39.6 ± 0.30	89.8		87.5	
30	34.4 ± 0.89	34.4 ± 0.86	89.1		89.1	

k_{US} - pseudo 1st order kinetic constant for lignin removal with ultrasound
k_{MA} - pseudo 1st order kinetic constant for lignin removal with mechanical agitation
Enhancement due to ultrasound: k_{US}/ k_{MA} = 2.08
§ Lignin content values are: mean ± standard error (n = 2).

An interesting observation was that the biomass treated with ultrasound for longer time (30 min) showed higher lignin content as compared to biomass treated for 20 min. This result was attributed to lignin condensation or re-polymerization, which was induced by the radicals generated out of transient cavitation. These radicals are intercepted or scavenged by the soluble lignin moieties present in the interfacial region of the bubble, which gives rise to the formation of phenoxy or similar radicals that induce re-polymerization of lignin. The lignin droplets thus formed can get deposited on the biomass surface. This phenomenon is reflected in higher lignin content of the residual biomass for longer duration of ultrasonic treatment. Garcia *et al*. (2011) also observed recondensation of lignin for longer duration of ultrasound treatment and an effective delignification. The biomass concentration used in their study was much higher (7%, w/v) than used in the present study (2%, w/v) and an effective delignification was observed for treatments of long duration.

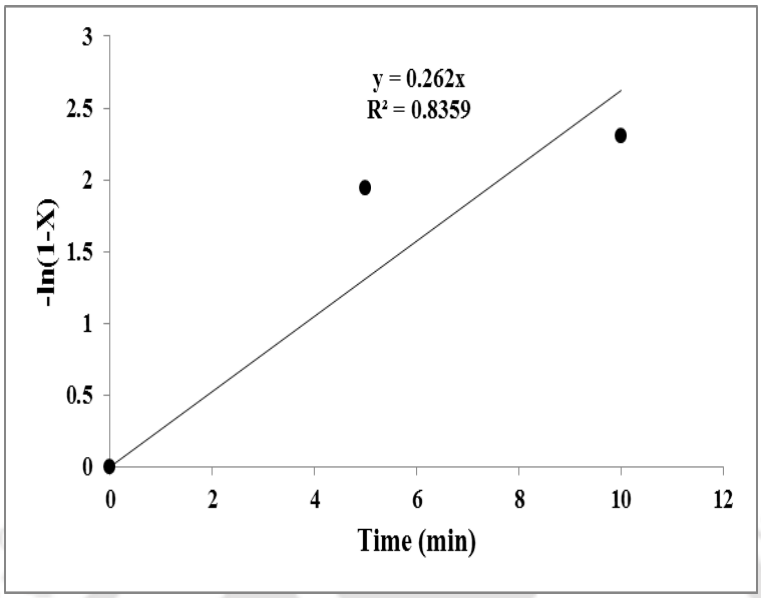

(A)

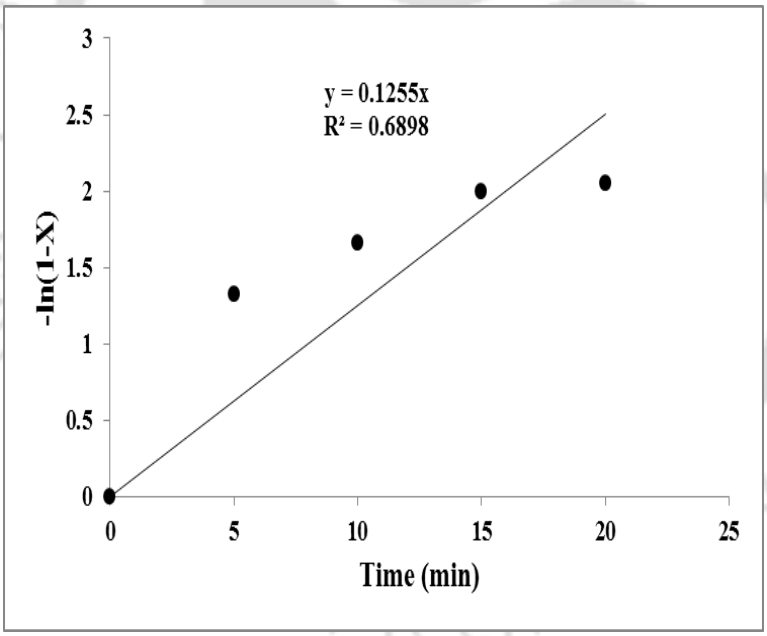

(B)

Fig. 6.3.5 Pseudo kinetic expression fitted to the time profile of delignification. (A) delignification with ultrasound. (B) delignification with mechanical agitation.

6.3.5.3 Results of bubble dynamics simulation

The results of simulations of cavitation bubble dynamics for a 5 µm air bubble are depicted in Table 6.3.8A and B. The table lists the peak temperature and pressure generated in the bubble at the moment of transient collapse, the amount of gas and vapor molecules present in the bubble at the instance of collapse and the equilibrium composition of the species generated from the dissociation of these molecules in the bubble. The graphical simulations results, *viz.* radial dynamics of cavitation bubble along with other effects (i.e. water vapor evaporation in the bubble, variation of temperature and pressure inside the bubble and generation of microturbulence and shock waves), are shown in Figures 6.3.6 and 6.3.7 for a 5 µm air bubble at bulk temperatures of 303 and 353 K. The results given in Table 6.3.8A and B essentially depict influence of two parameters, *viz.* NaOH concentration for the representative values 0.5, 1.5, 3.0% (w/v) and temperature 303, 313, 333 and 353 K, on cavitation bubble dynamics. The simulation results revealed that the temperature and pressure in the cavitation bubble reach extreme values for ambient temperature of 303 K due to which the water vapor molecules entrapped in the bubble are dissociated into oxidative radicals like $^{\bullet}$OH and $^{\bullet}$O. Shock waves of amplitude > 50 bar are also generated. It could be seen that the physical and chemical effects of cavitation bubble remain unaltered by NaOH concentrations. The peak temperature and pressure reached in the bubble and the spectrum of chemical species generated at transient collapse, in addition to the magnitude of the microturbulance velocity and acoustic waves generated by the bubble are practically same for all three concentrations of NaOH. The major oxidizing radical species generated in the bubble are $^{\bullet}$OH and $^{\bullet}$O.

Table 6.3.8 (A) Results of Cavitation Bubble Dynamics Simulations: Effect of NaOH concentration.

Parameters for simulations		
R_o = 5 μm NaOH = 0.5% w/v T = 303 K	R_o = 5 μm NaOH = 1.5% w/v T = 303 K	R_o = 5 μm NaOH = 3.0% w/v T = 303 K
Conditions at the first collapse of the bubble		
T_{max} = 4441 K P_{max} = 9023 atm V_{turb} = 0.0071 m/s P_{AW} = 65.17 atm $N_{N_2} = 1.27\times10^{10}$ $N_{O_2} = 3.39\times10^{9}$ $N_W = 4.32\times10^{9}$	T_{max} = 4444 K P_{max} = 9062 atm V_{turb} = 0.007 m/s P_{AW} = 66.4. atm $N_{N_2} = 1.26\times10^{10}$ $N_{O_2} = 3.35\times10^{9}$ $N_W = 4.22\times10^{9}$	T_{max} = 4443 K P_{max} = 9093 atm V_{turb} = 0.0069 m/s P_{AW} = 67.43 atm $N_{N_2} = 1.25\times10^{10}$ $N_{O_2} = 3.32\times10^{9}$ $N_W = 4.10\times10^{9}$
Species	Equilibrium composition of radical and other oxidizing species in the bubble at collapse (mole fraction)		
N_2	7.09×10^{-1}	7.09×10^{-1}	7.08×10^{-1}
O_2	1.33×10^{-1}	1.33×10^{-1}	1.33×10^{-1}
NO	1.19×10^{-1}	1.20×10^{-1}	1.20×10^{-1}
OH	1.23×10^{-2}	1.23×10^{-2}	1.23×10^{-2}
O	1.23×10^{-2}	1.23×10^{-2}	1.23×10^{-2}
H_2O	9.49×10^{-3}	9.43×10^{-3}	9.40×10^{-3}
NO_2	2.20×10^{-3}	2.21×10^{-3}	2.22×10^{-3}
HO_2	7.12×10^{-4}	7.12×10^{-4}	7.12×10^{-4}
H	6.11×10^{-4}	6.11×10^{-4}	6.07×10^{-4}
N_2O	5.97×10^{-4}	5.99×10^{-4}	6.01×10^{-4}
H_2	3.36×10^{-4}	3.35×10^{-4}	3.32×10^{-4}
HNO	1.06×10^{-4}	1.06×10^{-4}	1.06×10^{-4}
HNO_2	2.06×10^{-4}	1.67×10^{-4}	2.07×10^{-4}
N	6.66×10^{-5}	6.71×10^{-5}	6.67×10^{-5}
O_3	2.96×10^{-5}	2.98×10^{-5}	2.99×10^{-5}
H_2O_2	1.94×10^{-5}	1.94×10^{-5}	1.94×10^{-5}

R_o : initial or equilibrium bubble radius,
T temperature of bubble contents,
T_{max} : maximum ambient (or liquid bulk liquid medium) temperature,
P_{max} : maximum ambient (bulk) pressure in liquid,
V_{turb} : magnitude of oscillatory liquid velocity induced by bubble motion,
P_{AW} : pressure amplitude of acoustic waves emitted by bubble,
N_{N_2} : number of nitrogen molecules in bubble,
N_{O_2} : number of oxygen molecules in bubble,
N_w : number of water molecules in bubble.

Table 6.3.8 (B) Results of Cavitation Bubble Dynamics Simulations: Effect of temperature.

Parameters for simulations		
R_o = 5 μm NaOH = 1.5% w/v T = 313 K	R_o = 5 μm NaOH = 1.5% w/v T = 333 K	R_o = 5 μm NaOH = 1.5% w/v T = 353 K
Conditions at the first collapse of the bubble		
T_{max} = 4253 K P_{max} = 8575 atm V_{turb} = 0.0075 m/s P_{AW} = 62.43 atm $N_{N_2} = 1.21\times10^{10}$ $N_{O_2} = 3.22\times10^{9}$ $N_W = 9.10\times10^{9}$	T_{max} = 3441 K P_{max} = 5310 atm V_{turb} = 0.0142 m/s P_{AW} = 21.15 atm $N_{N_2} = 1.18\times10^{10}$ $N_{O_2} = 2.97\times10^{9}$ $N_W = 6.14\times10^{10}$	T_{max} = 1672 K P_{max} = 195.8 atm V_{turb} = 0.0442 m/s P_{AW} = 1.01 atm $N_{N_2} = 9.95\times10^{10}$ $N_{O_2} = 2.64\times10^{9}$ $N_W = 4.12\times10^{11}$
Species	Equilibrium composition of radical and other oxidizing species in the bubble at collapse (mole fraction)		
N_2	7.14×10^{-1}	7.28×10^{-1}	2.30×10^{-2}
O_2	1.39×10^{-1}	1.63×10^{-1}	6.17×10^{-3}
NO	1.11×10^{-1}	6.66×10^{-2}	8.18×10^{-5}
OH	1.13×10^{-2}	7.41×10^{-3}	1.06×10^{-4}
O	9.46×10^{-3}	2.33×10^{-3}	--
H_2O	1.11×10^{-2}	2.98×10^{-2}	--
NO_2	2.18×10^{-3}	1.64×10^{-3}	--
HO_2	6.78×10^{-4}	4.77×10^{-4}	--
H	4.41×10^{-4}	9.12×10^{-5}	--
N_2O	5.34×10^{-4}	2.43×10^{-4}	--
H_2	2.90×10^{-4}	1.68×10^{-4}	1.31×10^{-5}
HNO	8.79×10^{-5}	3.03×10^{-5}	--
HNO_2	2.08×10^{-4}	1.85×10^{-4}	--
N	3.83×10^{-5}	--	--
O_3	2.62×10^{-5}	--	--
H_2O_2	2.04×10^{-5}	2.43×10^{-5}	2.04×10^{-5}

R_o : initial or equilibrium bubble radius,
T : temperature of bubble contents,
T_{max} : maximum ambient (or liquid bulk liquid medium) temperature,
P_{max} : maximum ambient (bulk) pressure in liquid,
V_{turb} : magnitude of oscillatory liquid velocity induced by bubble motion,
P_{AW} : pressure amplitude of acoustic waves emitted by bubble,
N_{N_2} : number of nitrogen molecules in bubble,
N_{O_2} : number of oxygen molecules in bubble,
N_w : number of water molecules in bubble.

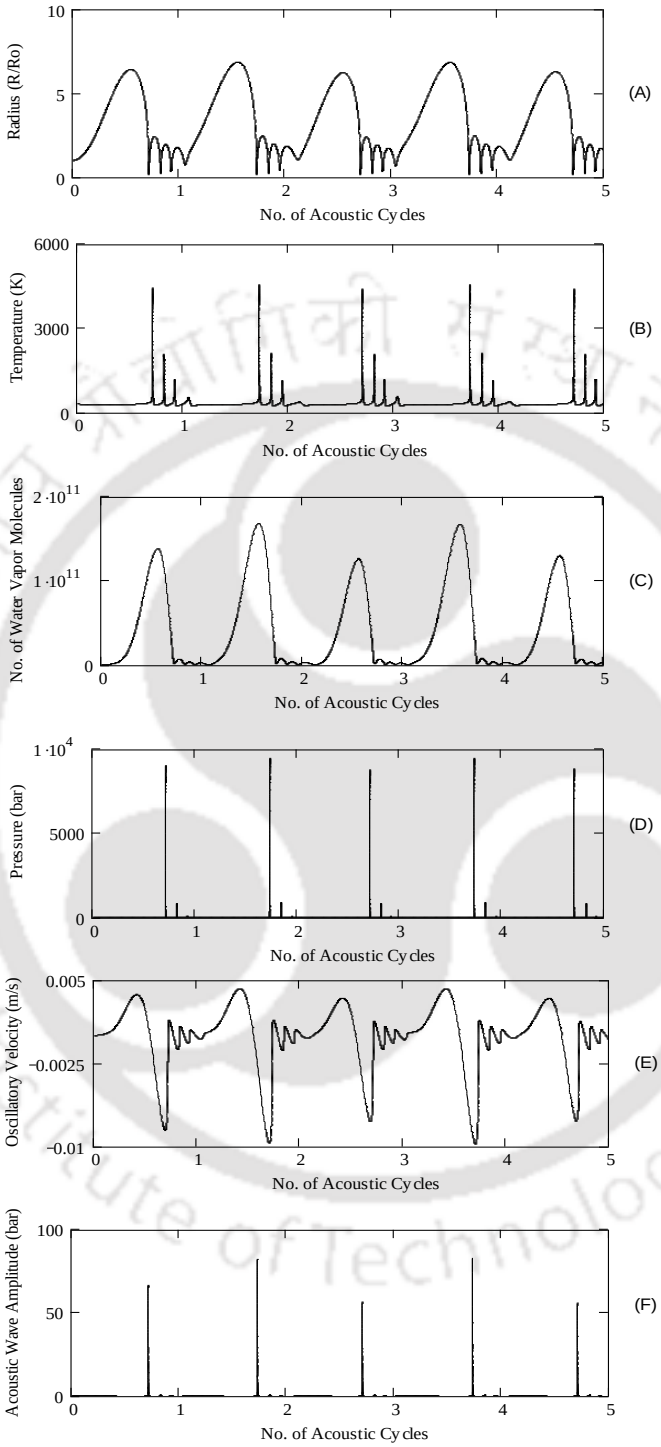

Fig. 6.3.6 Representative simulation results (5 μm air bubble at 303 K, NaOH conc. 1.5% w/v). Time variation of (A) normalized bubble radius (R/R_o); (B) temperature in the bubble; (C) number of water molecules in the bubble; (D) pressure inside the bubble; (E) micro-turbulence generated by the cavitation bubble; (F) acoustic (or shock) waves emitted by the bubble.

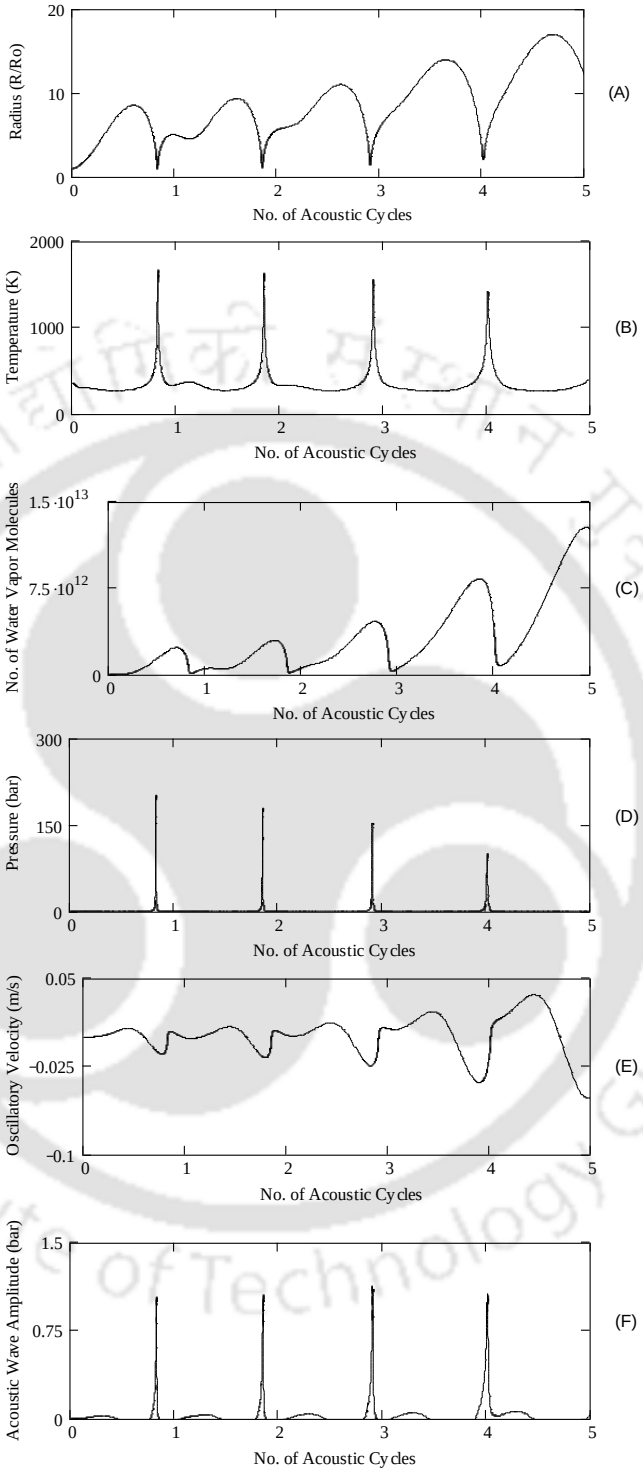

Fig. 6.3.7 Representative simulation results (5 μm air bubble at 353 K, NaOH conc. 1.5% w/v). Time variation of (A) normalized bubble radius (R/R_o); (B) temperature in the bubble; (C) number of water molecules in the bubble; (D) pressure inside the bubble; (E) micro-turbulence generated by the cavitation bubble; (F) acoustic (or shock) waves emitted by the bubble.

6.3.5.4 Explanation for the trends in delignification

The trends in the delignification process seen in the parametric investigation experiments were explained as follows;

(1) Leveling off of the extent of lignin removal by NaOH concentration (Table 6.3.4) could be attributed to switch over of the delignification process from mass transfer limitation to reaction kinetic limitation. Ultrasound and cavitation generate intense turbulence in the system due to which the accessibility of biomass to ions/radicals was enhanced. Bussemaker and Zhang (2014a, 2014b) have also reported the beneficial effect of enhanced turbulence generated in the system by ultrasound. After a certain concentration of NaOH, all biomass is accessible to the delignifying agent and thereafter the process becomes kinetically controlled. Higher concentration of NaOH required in mechanical agitation for saturation of delignification was attributed to lower intensity of convection and lower mass transfer rates.

(2) Reduction in the extent of delignification with ultrasound at higher biomass concentration (Table 6.3.5) was attributed to large scattering and attenuation of ultrasound waves by biomass particles as a result, the pressure amplitude and hence the intensity of transient cavitation bubble collapse driven by these waves decreased. Similar effect in case of system with mechanical agitation can be explained in terms of non-exposure of all biomass to alkaline solution.

(3) As revealed by simulations of cavitation bubble dynamics, the intensity of transient cavitation and its physical/chemical effects reduced with temperature. However, the micro-mixing phenomenon in delignification mixture was also contributed by micro-streaming (i.e. oscillatory motion of fluid elements) due to

ultrasound, which remained unaffected by temperature. Moreover, the intrinsic kinetics of various reactions induced by OH^- ions in delignification process increased with temperature, this rise compensates for the reduction of physical/ chemical effect of transient cavitation due to which the net delignification obtained at different temperature remained constant. Delignification showed gradual rise with temperature in mechanically agitated system, due to higher diffusivity of ions at higher temperature and increased reactivity (Table 6.3.6).

6.3.5.5 Results of enzymatic hydrolysis of delignified biomass

Enzymatic hydrolysis of delignified *P. hysterophorus* biomass resulted in TRS concentration of 15.42±0.33 g/L (308.4 mg/g delignified biomass) after 84 h (Fig. 6.3.8). The TRS yield obtained was equivalent to 164.1 mg/g raw biomass, which was approximately 46% higher than that in case of enzymatic hydrolysis of acid pretreated biomass (112.4 mg/g of raw biomass) (Table 6.3.2).

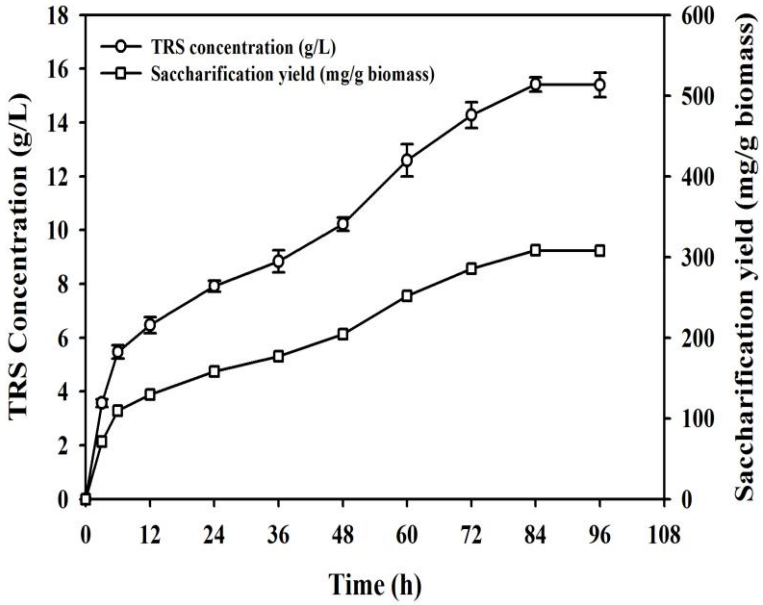

Fig. 6.3.8 Time profile of enzymatic hydrolysis of delignified *P. hysterophorus*.

6.3.5.6 Characterization of delignified biomass

***6.3.5.6.1 FTIR analysis*:** The FTIR spectra of pretreated (acid + autoclaving) and delignified biomass with mechanical agitation and with ultrasound, obtained under best values of experimental parameters as revealed in parametric investigation described earlier: NaOH concentration = 1.5% (w/v), temperature = 30^{o}C and biomass concentration = 2%, (w/v) are depicted in Fig. 6.3.9.

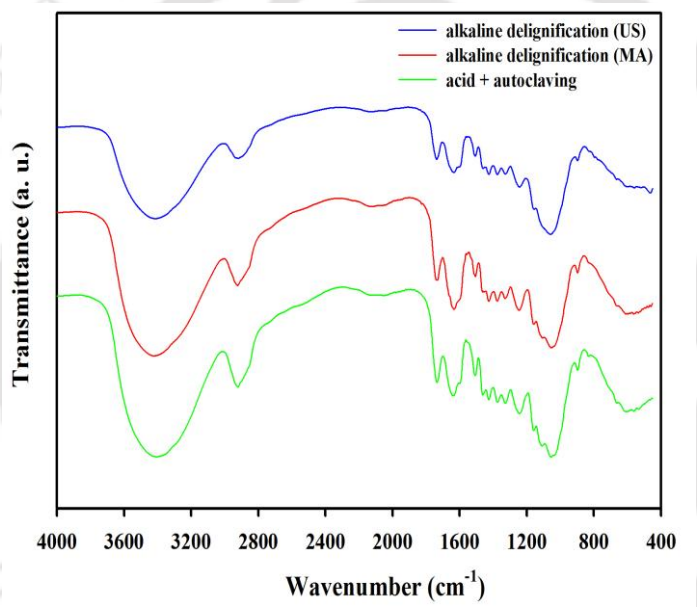

Fig. 6.3.9 FTIR spectra of *P. hysterophorus* biomass after different alkaline treatments, US - ultrasound, MA - mechanical agitation.

The vibrational frequencies (or band positions) in the IR spectrum corresponding to different functional groups of biomass and the percentage change in the intensities of these bands for biomass treated with mechanical agitation and ultrasound are given in Table 6.3.9. The positive relative percentage change of intensity for a specific band corresponding to a component (either functional group or moiety) indicates reduction of that component (Kumar *et al*. 2009b). As seen from

results of Table 6.3.9, the percent relative change is positive for all bands corresponding to lignin removal (along with side chain), rupture of cellulose bonds and carbohydrate-lignin linkages for biomass treated under mechanical agitation and ultrasound irradiation. Comparing between the FTIR spectra for biomass treated under mechanical agitation and ultrasound, the reduction in band intensities corresponding to aromatic ring stretch (1595 cm^{-1}), O-H stretching (3348 cm^{-1}) and cellulose band (1428 cm^{-1}, indicating de-crystallization of cellulose) were found higher for biomass delignified with ultrasound treatment. This essentially indicates enhanced delignification with ultrasound treatment. These results are attributed to the physical and chemical effects of ultrasound and cavitation.

Table. 6.3.9 Characterization of delignified biomass by FTIR spectroscopy.

Band position (cm^{-1})	Assignment*	US	MA
3348	O-H stretching (rupture of cellulose hydrogen bonds)	16.20	-4.85
2900	C-H stretching (rupture of methyl/methylene group of cellulose)	8.71	-0.76
1745	Carbonyl bonds (lignin side chain removal)	10.42	0.92
1738	C=O stretching due to carbohydrate linked with lignin	8.28	0.14
1720	Carboxylic acids/ester groups	7.23	-3.15
1595	Aromatic ring stretch (related to lignin removal)	22.11	7.48
1508	Aromatic ring vibration (related to lignin removal)	9.94	7.18
1458	Aromatic ring vibration (related to lignin removal)	8.79	6.14
1428	Band of cellulose	12.88	5.82
1260	Ester absorbance (related to removal of uronic acid)	9.79	5.58
1245	C=O absorption (resulting from acetyl groups cleavage)	9.65	5.62
1059	C=O stretching due to carbohydrate-lignin linkage	5.95	0.00
900	Band of cellulose	10.91	3.87

*adopted from Kumar *et al*. (2009b)
US - under ultrasound irradiation, MA - under mechanical agitation.
% relative change = 100 × (Intensity of band for untreated solid - Intensity of band for treated solid) / Intensity of band for untreated solid, where positive value of % relative change indicates reduction

The reactive sites in lignin are mainly the ether linkages and functional groups, since the carbon-carbon linkages are generally resistant to chemical attack. In

alkaline and alkaline-oxidative environments, lignin degrades through the cleavage of the α- and β-aryl ether linkages through hydrolysis to yield fragmentation units. Ultrasound can cause depolymerization of the solubilized lignin moieties through homolytic cleavages of the phenyl ether β-O-4 and α-O-4 bonds (Yoshioka *et al*. 2000). Hydroxyl radicals produced from transient collapse of cavitation bubble can also induce degradation of lignin leading to hydroxylated, demethoxylated and side chain eliminated products. A small extent of hydroxyl radical attack also occurs on the side chains leading to formation of dimers and oxidation of aromatic aldehydes to carboxylic acids. In addition to cleavage of inter-unitary bonds within lignin matrix and between lignin-hemicellulose entities, condensation of lignin in presence of ultrasound has also been observed. Lignin degradation results in release of low molecular weight phenolic species that are soluble in the liquid medium and therefore, get extracted in the medium during sonication. These species (which have phenolic moieties) accumulate at the interface of cavitation bubble and can scavenge the radicals released during transient collapse leading to repolymerization. The re-polymerized lignin, in the form of small globules or droplets, can get re-deposited on the biomass surface. In essence, there are two parallel mechanisms leading to delignification of the biomass: first the hydrolysis reactions induced by OH^- ions provided by the delignification agent and secondly, the hydroxylation and oxidation reactions induced by $^{\bullet}OH$ and $^{\bullet}O$ radicals generated by transient cavitation bubbles. The relative contributions of these mechanisms to the overall delignification depend on the reaction conditions.

As revealed in simulations of cavitation bubble dynamics, the intensities of physical as well as chemical effects of cavitation bubbles are the highest for the best temperature of 303 K (~30^{o}C, Table 6.3.6). The biomass particles get drifted in random directions at extremely high velocities in the shock waves generated during transient collapse of the bubbles. During such drifts they can collide with each other and such collisions result in release of high energies (Doktycz and Suslick 1990). The energy released in such collisions can also lead to rupture of bonds in the lignin matrix (such as lignin-carbohydrate linkages) leading to depolymerization of lignin. The interparticle collisions may also cause local heating that can induce reaction and/or accelerate the kinetics of a reaction (in the present context the kinetics of hydrolysis of ether linkages (Reddy *et al*. 2010, Choudhury *et al*. 2013, Goswami *et al*. 2013). In recent studies (Bussemaker *et al*. 2013, Bussemaker and Zhang 2014a, Bussemaker and Zhang 2014b) similar conclusions have been drawn regarding the mechanism of delignification in that the lignin polymers degrade through mechano-acoustic and sonochemical effects of ultrasound from a cumulative effect of hydroxyl radicals, shear forces and degradation of hydrophobic polymers in the interfacial region of transient cavitation bubbles, where the temperatures shoot up to few hundreds of Kelvin at the instance of transient collapse (when the bubble core itself heats up to ~ 5000 K, as noted earlier).

Greater rupture of cellulose-hydrogen bonds and decrystallization of cellulose (which are indications of depolymerization of cellulose matrix) could also be the effect of inter-particle collisions driven by shock waves generated by cavitation bubbles at transient collapse. Greater reduction in aromatic ring stretch and aromatic

ring vibration bands (1595, 1508, 1458 cm^{-1}) for ultrasound treated biomass could be a consequence of hydroxylation/oxidation of aromatic ring by oxidative radicals like $^{\bullet}OH$ and $^{\bullet}O$ produced by cavitation bubbles. Similarly, greater reduction of bond intensities corresponding to lignin side chain removal (1745 cm^{-1}) and carbohydrate-lignin linkages (1738 cm^{-1}) for ultrasound treated biomass can be attributed to physical and chemical effects of cavitation bubbles. Thus, the FTIR spectrum clearly demonstrated the beneficial effects of ultrasound and cavitation on delignification.

***6.3.5.6.2 XRD analysis*:** The XRD spectra of the pretreated and delignified biomass with mechanical agitation or with ultrasound treatment under best values of the parameters have been depicted in Fig. 6.3.10. The pretreated biomass comprises lignin and cellulose and has crystallinity index (*CrI*) = 57.36%. As the amorphous lignin is removed during treatment, one would expect rise in the crystallinity index of biomass due to increase in crystalline cellulose content of residual biomass. However, contrary to this expectation, the crystallinity index was found to decrease for both ultrasonic treatment (*CrI* = 45.9%) and mechanical agitation (*CrI* = 46.9%). This essentially means that cellulose also undergoes partial depolymerization, with scission of β-1-4-glycosidic bonds, giving rise to short chains of glucose monomer units. This effect can be attributed to the interparticle collisions driven by shock waves generated by transient cavitation that cause localized heating at the point of impact inducing chemical reactions.

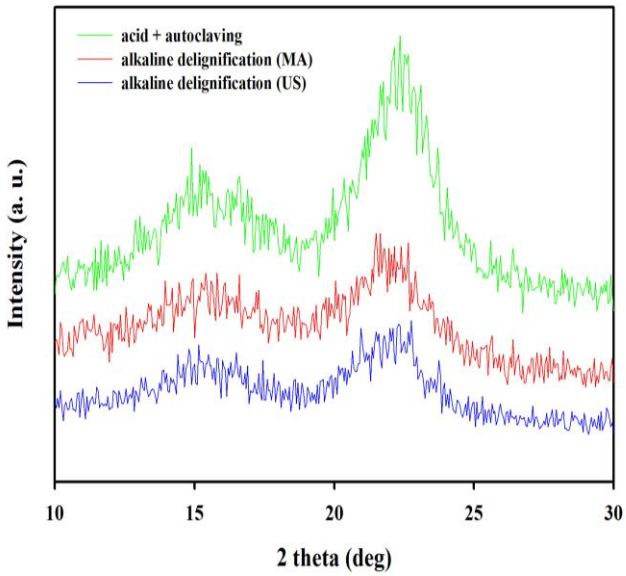

Fig. 6.3.10 X-ray diffractograms of *P. hysterophorus* biomass after different treatments. The crystallinity index of biomasses are determined as: pretreated biomass = 57.36%; delignified biomass with mechanical agitation = 46.9%, delignified biomass with ultrasound = 45.9%.

***6.3.5.6.3 FESEM analysis*:** Fig. 6.3.11 shows the FESEM micrographs of the pretreated and delignified biomass with mechanical agitation or with ultrasound. The pretreated biomass (after acid + autoclaving treatment) clearly shows droplets of lignin that migrate to the surface of biomass (Fig. 6.3.11A). The biomass surface after delignification with either mechanical agitation or ultrasound treatment shows removal of lignin droplets from surface as revealed in Fig. 6.3.11 B and C. However, comparison of surface texture of the two biomasses reveals more surface roughness for ultrasound treated biomass due to erosion or attrition. This erosion is attributed to physical effects of acoustic waves and the micro-turbulence generated by transient cavitation bubbles.

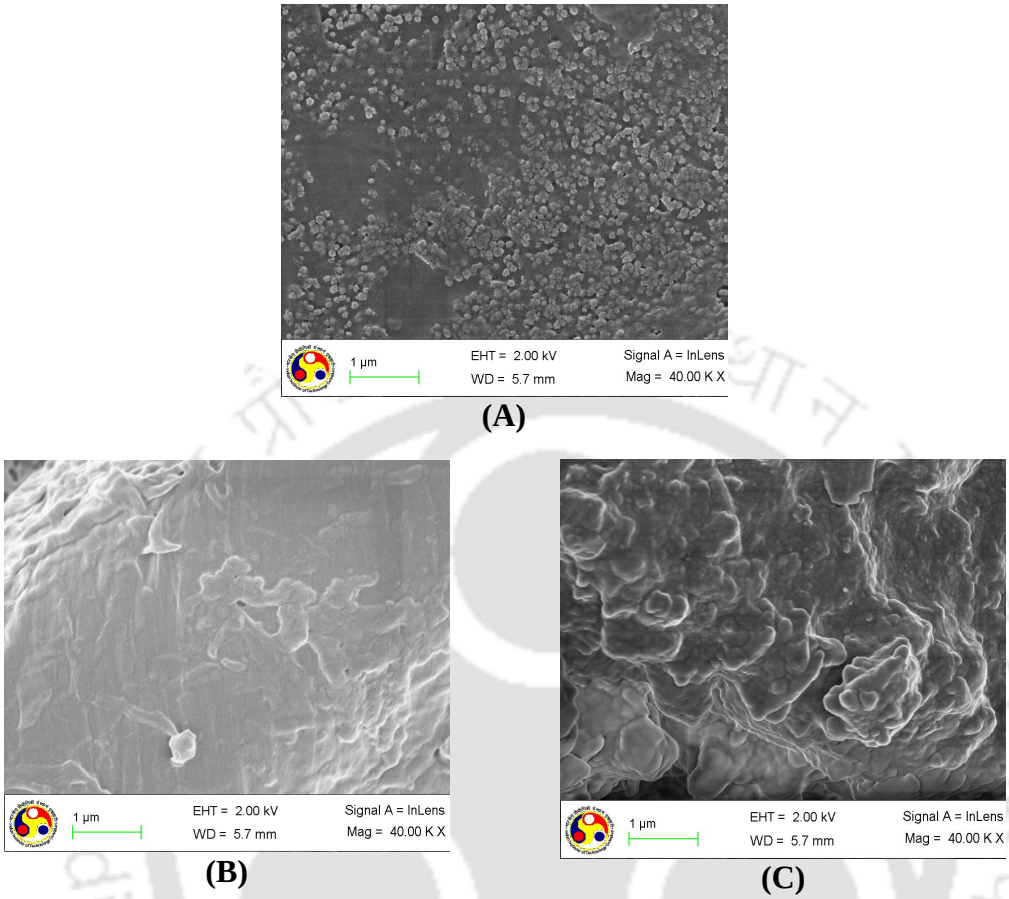

Fig. 6.3.11 FESEM micrographs of *P. hysterophorus* biomass (A) pretreated biomass, (B) delignified biomass with mechanical agitation and (C) delignified biomass with ultrasound.

6.3.6 Comparative assessment of results with published literature

Many lignocellulosic residues (like wheat straw, rice straw, rice husk, sugarcane bagasse etc.) used as cheap feedstock for biofuels, have alternate competitive outlets such as animal fodder and domestic fuel, which increases their cost. The major advantage with *P. hysterophorus* is that it is a complete waste biomass with no known alternate outlet and in that way, it beats the cost competition with other biomasses mentioned above. Nonetheless, another yardstick for comparison is the extent of sugar release from *P. hysterophorus* as compared to other

biomass. The extensive comparison of the results of this study with published literature is given in Table 6.3.10. The method of pretreatment, enzyme hydrolysis and the sugar released thereafter was compared. It could be seen that the pentose sugar release from *P. hysterophorus* after pretreatment was higher than most of other biomass and was at par with other cheap biomass like switchgrass and water hyacinth. The amount of sugar released after enzymatic hydrolysis, was smaller because the cellulase activity of the enzyme isolated from *B. amyloliquefaciens* SS35 was very low. Other studies listed in Table 6.3.10 have used commercial mixtures of enzymes, which have far higher activity than the enzyme used in this study. Moreover, the conditions for enzymatic hydrolysis were not optimized. The optimized conditions of hydrolysis and delignification of pretreated biomass also boost the sugar release. Effect of ultrasound on delignification has been studied by various researchers previously (Table 6.3.11). The outcome of present study i.e. 90% lignin removal is comparable with the results from other reports, for example 96.2% (Yuan et al. 2010) and 99.64% lignin removal (Velmurugan and Muthukumar 2012) from *Populus tomentosa* biomass and sugarcane bagasse, respectively (Table 6.3.11).

Table 6.3.10 Comparative evaluation of sugar release from pretreatment of conventional lignocellulosic biomass and *Parthenium* spp.

Lignocellulosic biomass	PTT conditions	TRS on PTT (mg/g)	Enzymes	TRS during EH (mg/g)	Reference
Alfa-alfa	2.5% (w/v) H_2SO_4, 150°C, 20 min	145.0	Celluclast 1.5 L+*β*-glucosidase (Novozyme 188) 50 FPU/mL	201.0	Dien *et al*. 2006
Reed canary grass	2.5% (w/v) H_2SO_4, 150°C, 20 min	267.0	Celluclast 1.5 L+*β*-glucosidase (Novozyme 188) 50 FPU/mL	197.0	Dien *et al*. 2006
Switchgrass	2.5% (w/v) H_2SO_4, 150°C, 20 min	311.0	Celluclast 1.5 L+*β*-glucosidase (Novozyme 188) 50 FPU/mL	207.0	Dien *et al*. 2006
Switchgrass	Microwave, 0.1% alkali, 190°C, 30 min	136.0	Celluclast 1.5 L (12 FPU/g BM)+*β*-glucosidase (Novozyme 188) (21 U/g BM)	209.0	Hu and Wen 2008
Switchgrass (*Panicum virgatum*)	AFEX (0.9 g/g ammonia, 80°C, 20 min)	ND	Accelerase® (3.2 FPU/g BM)	385.0	Bals *et al*. 2010
Lantana camara	3% v/v H_2SO_4, 120°C for 45 min, delignification by Na_2SO_3+$NaClO_2$	187.0	Cellulase (*Trichoderma reesei*) (60 FPU/g BM)+*β*-glucosidase (Novozyme 188) (180 U/g BM)*	695.0*	Kuhad *et al*. 2010
Lantana camara	Chlorite treatment, 4% (w/v), 30 min	ND	Cellulase (60 FPU/g BM)+*β*-glucosidase (Novozyme 188) (180 U/g BM)*	925.0	Gupta *et al*. 2011
Prosopis juliflora	Chlorite treatment, 4% (w/v), 30 min	ND	Cellulase (60 FPU/g BM)+*β*-glucosidase (Novozyme 188) (180 U/g BM)*	864.0	Gupta *et al*. 2011
Kans grass (*Saccharum sponteneum*)	2% (v/v) H_2SO_4 at 120°C, 1.5 h	ND	Cellulase (20 FPU/g)+xylanase (6.63 U/mL) from *Trichoderma reesei*	69.08	Kataria and Ghosh 2011
Water hyacinth	4% H_2SO_4 + autoclaving, 75 min	356.0	Cellulase (Zytex) 70 FPU/g BM	723.0	Satyanagal-akshmi *et al*. 2011
Shea tree sawdust	Alkaline wet air oxidation	116.6*	Cellulase (25 FPU/g) (Zytex) +*β*-glucosidase (12.5 U/g)	131.0	Ayeni *et al*. 2013
Shea tree sawdust	NaOH-H_2O_2 assisted wet air oxidation	0.0	Cellulase (25 FPU/g) (Zytex) +*β*-glucosidase (12.5 U/g)	274.0	Ayeni *et al*. 2013
Parthenium hysterophorus	5% H_2SO_4 at 210°C, 6 h soaking, 30 min	96.8*	ND	ND	Ghosh *et al*. 2013
Mixed hardwood (*Q. mongolica*+ *R. pseudoacacia* L.+*C. crenata*)	H_2SO_4/H_2O in ratio of 1:4 (w/w), 170°C, pH 1.34, 60 min	120.0*	Cellulase complex (17.5 FPU/g)+*β*-glucosidase (12.5 CBU/g)	328.0*	Lim *et al*. 2013
Parthenium sp.	Biological (*Trametes hirsuta*), 7 days	ND	Accellerase®1500 (endoglucanase 2200 IU/g+*β*-glucosidase 525 IU/g)	485.64	Rana *et al*. 2013
Parthenium sp.	1% (v/v) H_2SO_4, 121°C, 20 min	ND	Accellerase®1500 (endoglucanase 2200 CMC IU/g+*β*-glucosidase 525 pNPG IU/g+xylanase 115 IU/g)	476.0	Pandiyan *et al*. 2014
Parthenium sp.	1% NaOH, room temperature, 1 h	ND	Accellerase®1500 (endoglucanase 2200 CMC IU/g+*β*-glucosidase 525 pNPG IU/g+xylanase 115 IU/g)	513.0	Pandiyan *et al*. 2014
Parthenium sp.	Biological (*Marasmiellus palmivorus* PK-27), 7d	ND	Accellerase®1500	410.0	Pandiyan *et al*. 2014
Parthenium hysterophorus	1% (v/v) H_2SO_4 + autoclaving for 30 min	285.3	Cellulase from *Bacillus amyloliquefaciens* SS35 (10 U/g BM)+*β*-glucosidase (Novozyme 188) (5 U/g BM)	187.4	This study

*as calculated from data reported in paper; *PTT, pretreatment; BM, biomass; EH, enzymatic hydrolysis; ND, not determined*

Table 6.3.11 Comparative assessment of results on ultrasound enhanced delignification of lignocellulosic biomass.

Raw material	Ultrasonic treatment conditions	Delignifying agents	Results	Reference
Wheat straw	100 W, 20 kHz, 60°C, 35 min	0.5 M NaOH (CH_3OH:H_2O 60:40)	67.4-78.5% lignin solubilized	Sun *et al.* 2002
Wheat straw	100 W, 20 kHz, 35°C, 35 min	0.5 M KOH pre-treatment and 2% H_2O_2-0.2% TAED post-treatment	43.3-46.2% lignin and 27.1-28.1% hemicellulose solubilization	Sun and Tomkinson 2002
Poplar (*Populus tomentosa*)	570 W, 20 kHz, 25°C, 30 min	95% ethanol, methanol, dioxane, dimethyl sulfoxide	96.2% lignin solubilized	Yuan *et al.* 2010
Sawdust	240 W, 22 kHz, room temperature	Aqueous soda solution	67.4% lignin removal	Baxi and Pandit 2012
Bamboo (*Neosinocalamus affinis*)	100 W, 20°C, 50 min	95% ethanol, 50 min NaOH (7%)/urea (12%)	13.4-16.4% lignin isolation with β-O-4 ether linked inter units	Li *et al.* 2012
Sugarcane bagasse	400 W, 24 kHz, 75°C, 61.97 min	3.25% w/v NaOH	99.64% lignin removal, sugar yield increased by 24.27% after enzymatic hydrolysis	Velmurugan and Muthukumar 2012
Newspaper pulp	100 W, 80% duty cycle, room temperature, 70 min	1 N NaOH	80% lignin removal	Subhedar and Gogate 2014
Parthenium hysterophorus	150 W, 20 kHz, 30°C, 10 min	1.5% w/v (0.375 N) NaOH	90% lignin removal, sugar yield increased by 46% after enzymatic hydrolysis	This study

6.4 Conclusions

Parthenium hysterophorus is the world's seven most devastating and hazardous weeds and is abundantly available in several parts of the world. This study treats the subject of effective utilization of this waste biomass (which has cellulose content of 45.2±1.81% w/w) for biofuels production. A comprehensive and comparative assessment of numerous pretreatment strategies for *P. hysterophorus*, covering all major physical, chemical and physicochemical methods have been presented in this study. The yardstick of assessment has been amount of fermentable sugars released during the pretreatment and the post-treatment enzymatic hydrolysis of pretreated biomass. Carboxymethylcellulase produced by *Bacillus amyloliquefaciens* SS35 and commercial *β*-glucosidase, were used for enzymatic hydrolysis of pretreated biomass. Among the different methods employed for pretreatment, the most efficient treatment was autoclaving of biomass at 121^{o}C and 15 psi pressure for 30 min in acidic (1% v/v, H_2SO_4) environment. Total reducing sugar (TRS) yield during this pretreatment was 285.32 mg/g biomass. Further enzymatic hydrolysis resulted in reducing sugar yield of 187.4 mg/g of pretreated biomass (9.37 g/L). The total fermentable sugar (TFS) yield from the optimized pretreatment was 397.7 mg/g raw biomass (39.77 g/100 g raw biomass). These results conclusively demonstrated the utility of *P. hysterophorus* for sustainable biofuels production.

A mechanistic insight into the enhancement of delignification process of the pretreated biomass by ultrasound with NaOH as the delignifying agent was explored. The approach was to couple the experiments with simulations of cavitation bubble dynamics. It was revealed that both physical and chemical effects of ultrasound and

cavitation contribute to delignification. The physical effects of transient cavitation, *viz.*, micro-turbulence and shock waves contribute to enhancement of depolymerization of lignin through hydrolysis. The chemical effect of transient cavitation, i.e. radical generation contributes to reduction in aromatic moieties in the lignin matrix by hydroxylation/oxidation. Transient cavitation is more intense at lower temperature and the hydroxylation/ oxidation induced by radicals generated from transient cavitation made significant contribution to overall delignification. The intensity of transient cavitation and hence, the magnitude of its physical and chemical effects is maximum at ambient or room temperature of 303 K. Thus, effective delignification was obtained under ultrasound treatment at room temperature and with lower requirement (1.5% w/v) of the delignifying agent, as compared to the conventional technique of mechanical agitation. However, similar extent of delignification with ultrasonic treatment at elevated temperature of 353 K (where physical and chemical effects of transient cavitation practically vanish) as compared to delignification at 303 K was a consequence of higher intrinsic reactivity of the delignifying agent that compensates for the lower physical and chemical effects of transient cavitation. A two-fold enhancement in kinetics of delignification was found with ultrasound treatment under the best operating conditions of temperature, biomass concentration and alkali concentration.

The main aim of delignification was to remove lignin to the maximum extent and to analyze the results of the effect of sonication on delignification from mechanistic point of view. The links between the physical and chemical effect of ultrasound and cavitation and the delignification process were explained on the basis

of results from experiments and simulations. The cellulose content in delignified biomass was also maximized and thus the yield of sugar in enzymatic hydrolysis process was enhanced by ~46%. The effects of different pretreatment methods and ultrasound assisted delignification on biomass structure and complexity were demonstrated by field emission scanning electron microscopy (FESEM), Fourier transform infrared (FTIR) spectroscopy and X-ray diffraction (XRD) techniques. Comparative assessment of the results with other conventional agricultural and forest residues shows that *P. hysterophorus* has the same potential for being the feedstock for biofuels.

References

Alvira, P., Tomas-Pejo, E., Ballesteros, M. and Negro, M. J. (2010) Pretreatment technologies for an efficient bioethanol production process based on enzymatic hydrolysis: A review. Bioresource Technology, 101, 4851-4861.

Ayeni, A. O., Banerjee, S., Omoleye, J. A., Hymore, F. K., Giri, B. S., Deshmukh, S. C., Pandey, R. A. and Mudliar, S. N. (2013) Optimization of pretreatment conditions using full factorial design and enzymatic convertibility of shea tree sawdust. Biomass Bioenergy, 48, 130-138.

Azzam, A. M. (1989) Pretreatment of cane bagasse with alkaline hydrogen peroxide for enzymatic hydrolysis of cellulose and ethanol fermentation. Journal of Environmental Science and Health, Part B, 24, 421-433.

Bals, B., Rogers, C., Jin, M., Balan, V. and Dale, B. (2010) Evaluation of ammonia fibre expansion (AFEX) pretreatment for enzymatic hydrolysis of switchgrass harvested in different seasons and locations. Biotechnology for Biofuels, 3, 1.

Barakat, A., Chuetor, S., Monlau, F., Solhy, A. and Rouau, X. (2014) Eco-friendly dry chemo-mechanical pretreatments of lignocellulosic biomass: Impact on energy and yield of the enzymatic hydrolysis. Applied Energy, 113, 97-105.

Barakat, A., de Vries, H. and Rouau, X. (2013) Dry fractionation process as an important step in current and future lignocellulosic biorefineries: A review. Bioresource Technology, 134, 362-373.

Baxi, P. B. and Pandit, A. B. (2012) Using cavitation for delignification of wood. Bioresource Technology 110, 697-700.

Binod, P., Sindhu, R., Singhania, R. R., Vikram, S., Devi, L., Nagalakshmi, S., Kurien, N., Sukumaran, R. K. and Pandey, A. (2010) Bioethanol production from rice straw: An overview. Bioresource Technology, 101, 4767-4774.

Bussemaker, M. J. and Zhang, D. (2013) Effect of ultrasound on lignocellulosic biomass as a pretreatment for biorefinery and biofuels applications. Industrial and Engineering Chemistry Research, 52, 3563-3580.

Bussemaker, M. J. and Zhang, D. (2014) A phenomenological investigation into the opposing effects of fluid flow on sonochemical activity at different frequency and power settings. 1. Overhead stirring. Ultrasonics Sonochemistry, 21, 436-445.

Bussemaker, M. J. and Zhang, D. (2014) A phenomenological investigation into the opposing effects of fluid flow on sonochemical activity at different frequency and power settings. 2. Fluid circulation at high frequencies. Ultrasonics Sonochemistry, 21, 485-492.

Bussemaker, M. J., Feng, Xu. And Zhang, D. (2013) Manipulation of ultrasonic effects on lignocellulose by varying the frequency, particle size, loading and stirring. Bioresource Technology, 148, 15-23.

Cabanelas, I. T. D., Arbib, Z., Chinalia, F. A., Souza, C. O., Perales, J. A., Almeida, P. F., Druzian J. I. and Nascimento, I. A. (2013) From waste to energy: Microalgae production in wastewater and glycerol. Applied Energy, 109, 283-290.

Caspeta, L., Caro-Bermúdez, M. A., Ponce-Noyola, T. and Martinez, A. (2014) Enzymatic hydrolysis at high-solids loadings for the conversion of agave

bagasse to fuel ethanol. Applied Energy, 113, 277-286.

Chandra, R., Takeuchi, H. and Hasegawa, T. (2012) Hydrothermal pretreatment of rice straw biomass: A potential and promising method for enhanced methane production. Applied Energy, 94, 129-140.

Chisti, Y. and Yan, J. (2011) Energy from algae: Current status and future trends: Algal biofuels - A status report. Applied Energy, 88, 3277-3279.

Choudhury, H. A., Choudhary, A., Sivakumar, M. and Moholkar, V. S. (2013) Mechanistic investigation of the sonochemical synthesis of zinc ferrite. Ultrasonics Sonochemistry, 20, 294-302.

Condon, E. U. and Odishaw, H. (1958) Handbook of Physics; McGraw Hill, New York.

Das, S. P., Ghosh, A., Gupta, A., Goyal, A. and Das, D. (2013) Lignocellulosic fermentation of wild grass employing recombinant hydrolytic enzymes and fermentative microbes with effective bioethanol recovery. BioMed Research International, Article ID 386063, 14 pages.

Dias, M. O. S., Junqueira, T. L., Jesus, C. D. F., Rossell, C. E. V., Filho, R. M. and Bonomi, A. (2012) Improving bioethanol production - Comparison between extractive and low temperature fermentation. Applied Energy, 98, 548-555.

Dien, B. S., Jung, H. G., Vogel, K. P., Casler, M. D., Lamb, J. F. S., Iten, L., Mitchell, R. B. and Sarath, G. (2006) Chemical composition and response to dilute-acid pretreatment and enzymatic saccharification of alfalfa, reed canarygrass and switchgrass. Biomass and Bioenergy, 30, 880-891.

Doktycz, S. J. and Suslick, K. S. (1990) Interparticle collisions driven by ultrasound.

Science , 247, 1067-1069.

Donohoe, B. S., Decker, S. R., Tucker, M. P., Himmel, M. E. and Vinzant, T. B. (2008) Visualizing lignin coalescence and migration through maize cell walls following thermochemical pretreatment. Biotechnology and Bioengineering, 101, 913-925.

Eriksson, T., Borjesson, J. and Tjerneld, F. (2002) Mechanism of surfactant effect in enzymatic hydrolysis of lignocellulose. Enzyme and Microbial Technology, 31, 353-364.

Fan, L. T., Gharpuray, M. M. and Lee, Y. H. (1987) In: Cellulose Hydrolysis Biotechnology Monographs. Springer, Berlin, p. 57.

Fraioli, V., Mancaruso, E., Migliaccio, M. and Vaglieco, M. B. (2014) Ethanol effect as premixed fuel in dual-fuel CI engines: Experimental and numerical investigations. Applied Energy,119, 394-404.

Garcia, A., Alriols, M. G., Llano-Ponte, R. and Labidi, J. (2011) Ultrasound-assisted fractionation of the lignocellulosic material. Bioresource Technology, 102, 6326-6330.

Ghosh, S., Haldar, S., Ganguly, A. and Chatterjee, P. K. (2013) Investigations on the kinetics and thermodynamics of dilute acid hydrolysis of *Parthenium hysterophorus* L. substrate. Chemical Engineering Journal, 229, 111-117.

Ghosh, S., Haldar, S., Shubhaneel N., Ganguly, A. and Chatterjee, P. K. (2012) Kinetic study of the acid hydrolysis of *Parthenium hysterophorus* L. for xylose yield in the production of lignocellulosic ethanol. IOSR Journal of Pharmacy and Biological Sciences, 3, 35-41.

Goering, H. K. and Van Soest, P. J. (1970) Forage fiber analyses (apparatus, reagents and some applications). USDA Agricultural Handbook No. 379. Washington, DC: Agricultural Research Service, US Department of Agriculture.

Gong, C. and Hart, D. P. (1998) Ultrasound induced cavitation and sonochemical yields. Journal of the Acoustical Society of America, 104, 2675-2682.

Goswami, P. P., Choudhury, H. A., Chakma, S. and Moholkar, V. S. (2013) Sonochemical synthesis and characterization of manganese ferrite nanoparticles. Industrial and. Engineering Chemistry Research, 52 (50), 17848-17855.

Gupta, R., Khasa, Y. P. and Kuhad, R. C. (2011) Evaluation of pretreatment methods in improving the enzymatic saccharification of cellulosic materials. Carbohydrate Polymers, 84, 1103-1109.

Hart, E. J. and Henglein, A. (1985) Free radical and free atom reactions in the sonolysis of aqueous iodide and formate solutions Journal of Physical Chemistry, 89, 4342-4347.

Hart, E. J. and Henglein, A. (1987) Sonochemistry of aqueous solutions: H_2-O_2 combustion in cavitation bubbles. Journal of Physical Chemistry, 91, 3654-3656.

Hideno, A., Inoue, H., Tsukahara, K., Fujimoto, S., Minowa, T., Inoue, S., Endo, T. and Sawayama, S. (2009) Wet disc milling pretreatment without sulfuric acid for enzymatic hydrolysis of rice straw. Bioresource Technology 100, 2706-2711.

Hirschfelder, J. O., Curtiss, C. F. and Bird, R. B. (1954) Molecular Theory of Gases and Liquids; Wiley, New York.

Ho, C. Y., Chang, J. J., Lee, Chin, T. Y., Shih, M. C., Li, W. H. and Huang, C. C. (2012) Development of cellulosic ethanol production process via co-culturing of artificial cellulosomal *Bacillus* and kefir yeast, Applied Energy, 100, 27-32.

Hu, Z. and Wen, Z. (2008) Enhancing enzymatic digestibility of switchgrass by microwave-assisted alkali pretreatment. Biochemical Engineering Journal, 38, 369-378.

Hua, I., Hochemer, R. H. and Hoffmann, M. R. (1995) Sonochemical degradation of *p*-Nitrophenol in a parallel plate near field acoustic processor. Environmental Science and Technology, 29, 2790-2796.

Ibrahim, M. M., El-Zawawy, W. K., Abdel-Fattah, Y. R., Soliman, N. A. and Agblevor, F. A. (2011) Comparison of alkaline pulping with steam explosion for glucose production from rice straw. Carbohydrate Polymer, 83, 720-726.

Kalva, A., Sivasankar, T. and Moholkar, V. S. (2009) Physical mechanism of ultrasound-assisted synthesis of biodiesel. Industrial and. Engineering Chemistry Research, 48, 534-544.

Kamm, B., Gruber, P. R. and Kamm, M. (2006) Biorefineries-Industrial processes and products: Status quo and future. Wiley-VCH Verlag GmbH and Co. KGa A, Weinheim.

Kataria, R. and Ghosh, S. (2011) Saccharification of Kans grass using enzyme

mixture from Trichoderma reesei for bioethanol production. Bioresource Technology, 102, 9970-9975.

Keller, J. B. and Miksis, M. J. (1980) Bubble oscillations of large amplitude. Journal of the Acoustical Society of America, 68, 628-633.

Kim, S. B., Kim, H. J. and Kim, C. J. (2006) Enhancement of the enzymatic digestibility of waste newspaper using tween. Applied Biochemistry and Biotechnology, 129/132, 486-95.

Kim, T. H. and Lee, Y. Y. (2005) Pretreatment and fractionation of corn stover by ammonia recycle percolation process. Bioresource Technology, 96, 2007-2013.

Koo, B. W., Min, B. C., Gwak, K. S., Lee, S. M., Choi, J. W., Yeo, H. and Choi, I. G. (2012) Structural changes in lignin during organosolv pretreatment of *Liriodendron tulipifera* and the effect on enzymatic hydrolysis. Biomass and Bioenergy, 42, 24-32.

Krishnan, S. J., Dwivedi, P. and Moholkar, V. S. (2006) Numerical investigation into the chemistry induced by hydrodynamic cavitation. Industrial and. Engineering Chemistry Research**,** 45, 1493-1504.

Kuhad, R. C., Gupta, R., Khasa, Y. P. and Singh, A. (2010) Bioethanol production from *Lantana camara* (red sage): Pretreatment, saccharification and fermentation. Bioresource Technology, 101, 8348-8354.

Kumar, M., Goyal, Y., Sarkar, A. and Gayen, K. (2012) Comparative economic assessment of ABE fermentation based on cellulosic and non-cellulosic feedstocks. Applied Energy, 93, 193-204.

Kumar, P., Barrett, D. M., Delwiche, M. J. and Stroeve, P. (2009a) Methods for pretreatment of lignocellulosic biomass for efficient hydrolysis and biofuel production. Industrial and. Engineering Chemistry Research, 48, 3713-3729.

Kumar, R., Mago, G., Balan, V. and Wyman, C. E. (2009b) Physical and chemical characterizations of corn stover and poplar solids resulting from leading pretreatment technologies. Bioresource Technology 100, 3948-3962.

Leighton, T. G. (1994) The acoustic bubble. Academic Press: San Diego.

Li, Q., Ji, G. S., Tang, Y. B., Gu, X. D., Fei, J. J. and Jiang, H. Q. (2012) Ultrasound-assisted compatible in situ hydrolysis of sugarcane bagasse in cellulase-aqueous-N-methylmorpholine-N-oxide system for improved saccharification. Bioresource Technology, 107, 251-257.

Lim, W. S., Kim, J. Y., Kim, H. Y., Choi, J. W., Choi, I. G. and Lee, J. W. (2013) Structural properties of pretreated biomass from different acid pretreatments and their effects on simultaneous saccharification and ethanol fermentation. Bioresource Technology, 139, 214-219.

Lima, C. S. S., Conceição, M. M., Silva, F. L. H., Lima, E. E., Conrado, L. S. and Leão, D. A. S. (2013) Characterization of acid hydrolysis of sisal. Applied Energy, 102, 254-259.

Nelson, N. (1944) A photometric adaptation of the Somogyi method for the determination of glucose, Journal of Biological Chemistry, 153, 375-380.

Pandiyan, K., Tiwari, R., Rana, S., Arora, A., Singh, S., Saxena, A. K. and Nain, L. (2014) Comparative efficiency of different pretreatment methods on enzymatic digestibility of *Parthenium* sp. World Journal of Microbiology

and Biotechnology, 30, 55-64.

Patel S. (2011) Harmful and beneficial aspects of *Parthenium hysterophorus*: an update. 3 Biotech, 1, 1-9.

Press, W. H., Teukolsky, S. A., Flannery, B. P. and Vetterling, W. T. (1992) Numerical Recipes; (2nd Ed.), Cambridge University Press, New York.

Rana, S., Tiwari, R., Arora, A., Singh, S., Kaushik, R., Saxena, A. K., Dutta, S. C. and Nain, L. (2013) Prospecting *Parthenium* sp. pretreated with Trametes hirsuta, as a potential bioethanol feedstock. Biocatalysis and Agricultural Biotechnology, 2, 152-158.

Ranjan, A. and Moholkar, V. S. (2012) Biobutanol: science, engineering, and economics. International Journal of Energy Research, 36, 277-323.

Ranjan, A. and Moholkar, V. S. (2013) Comparative study of various pretreatment techniques for rice straw saccharification for the production of alcoholic biofuels. Fuel, 112, 567-571.

Ranjan, A., Khanna, S. and Moholkar, V. S. (2013) Feasibility of rice straw as alternate substrate for biobutanol production. Applied Energy, 103, 32-38. (also refer "A Corrigendum to 'Feasibility of rice straw as alternative substrate for biobutanol production by Ranjan et al.' [Appl Energy, 103 (2013) 32-38]." Applied Energy, 116, 436-438.

Ranjan, A., Mayank, R. and Moholkar, V. S. (2013) Process optimization for butanol production from developed rice straw hydrolysate using *Clostridium acetobutylicum* MTCC 481 strain. Biomass Conversion and Biorefinery, 3, 143-155.

Reddy, B. R., Sivasankar, T., Sivakumar, M. and Moholkar, V. S. (2010) Physical facets of ultrasonic cavitational synthesis of zinc ferrite particles. Ultrasonics Sonochemistry, 17, 416-426.

Reid, R. C., Prausnitz, J. M. and Poling, B. E. (1987) Properties of Gases and Liquids; McGraw Hill, New York.

Reshamwala, S., Shawky, B. T. and Dale, B. E. (1995) Ethanol production from enzymatic hydrolysates of AFEX-treated coastal Bermuda grass and switchgrass. Applied Biochemistry and Biotechnology, 51/52, 43-55.

Rizzo, A. M., Prussi, M., Bettucci, L., Libelli, I. M. and Chiaramonti, D. (2013) Characterization of microalga *Chlorella* as a fuel and its thermogravimetric behavior. Applied Energy, 102, 24-31.

Saha, B. C. and Cotta, M. A. (2006) Ethanol production from alkaline peroxide pretreated enzymatically saccharified wheat straw. Biotechnology Progress, 22, 449-453.

Santori, G., Nicola, G. D., Moglie, M. and Polonara, F. (2012) A review analyzing the industrial biodiesel production practice starting from vegetable oil refining. Applied Energy, 92, 109-132.

Satyanagalakshmi, K., Sindhu, R., Binod, P., Janu, K. U., Sukumaran, R. K. and Pandey, A. (2011) Bioethanol production from acid pretreated water hyacinth by separate hydrolysis and fermentation. Journal of Scientific and Industrial Research, 70, 156-161.

Segal, L., Creely, J. J., Martin, A. E. Jr. and Conrad, C. M. (1962) An empirical method for estimating the degree of crystallinity of native cellulose using

the X-ray diffractometer. Textile Research Journal, 29, 786-794.

Shah, Y. T., Pandit, A. B. and Moholkar, V. S. (1999) Cavitation reaction engineering. Plenum Press, New York.

Sindhu, R., Kuttiraja, M., Binod, P., Sukumaran, R. K. and Pandey, A. (2014) Physicochemical characterization of alkali pretreated sugarcane tops and optimization of enzymatic saccharification using response surface methodology. Renewable Energy, 62, 362-368.

Singh, S., Bharadwaja, S. T. P., Yadav, P. K., Moholkar, V. S. and Goyal, A. (2014d) Mechanistic investigation in ultrasound-assisted (alkaline) delignification of *Parthenium hysterophorus* biomass. Industrial and Engineering Chemistry Research, 53, 14241−14252

Singh, S., Dikshit P. K., Moholkar V. S. and Goyal, A. (2014b) Purification and characterization of acidic cellulase from *Bacillus amyloliquefaciens* SS35 for hydrolyzing *Parthenium hysterophorus* biomass. Environmental Progress and Sustainable Energy. DOI: 10.1002/ep.12046.

Singh, S., Khanna, S., Moholkar, V. S. and Goyal, A. (2014c) Screening and optimization of pretreatments for *Parthenium hysterophorus* as feedstock for alcoholic biofuels. Applied Energy, 129, 195-206.

Singh, S., Moholkar, V. S. and Goyal A. (2013) Isolation, identification, and characterization of a cellulolytic *Bacillus amyloliquefaciens* strain SS35 from rhinoceros dung. ISRN Microbiology, Volume 2013, Article ID 728134.

Singh, S., Moholkar, V. S. and Goyal, A. (2014a) Optimization of

carboxymethylcellulase production from *Bacillus amyloliquefaciens* SS35. 3 Biotech, 4, 411-424.

Sivasankar, T. and Moholkar, V. S. (2009) Physical insights into the sonochemical degradation of recalcitrant organic pollutants with cavitation bubble dynamics. Ultrasonics Sonochemistry, 16, 769-781.

Sivasankar, T., Paunikar, A. W. And Moholkar, V. S. (2007) Mechanistic approach to enhancement of the yield of a sonochemical reaction. AIChE Journal, 53, 1132-1143.

SOLVAY Technical and Engineering Service (1967) Bulletin 6. Caustic Soda.

Somogyi, M. (1945) A new reagent for the determination of sugars. Journal of Biological Chemistry, 160, 61-68.

Storey, B. D. and Szeri, A. J. (2000) Water vapor, sonoluminescence and sonochemistry. Proceedings of Royal Society of London, Series A, 456, 1685-1709.

Subhedar, P. B. and Gogate, P. R. (2014) Alkaline and ultrasound assisted alkaline pretreatment for intensification of delignification process from sustainable raw-material. Ultrasonics Sonochemistry, 21, 216-225.

Sun, R. C. and Tomkinson, J. (2002) Comparitive study of lignins isolated by alkali and ultrasound assisted alkali extractions from wheat straw. Ultrasonics Sonochemistry, 9, 85-93.

Sun, R. C., Sun, X. F. and Ma, X. H. (2002) Effect of ultrasound on the structural and physicochemical of organosolv soluble hemicelluloses from wheat straw. Ultrasonics Sonochemistry, 9, 95-101.

Sun, X. F., Xu, F., Sun, R. C., Fowler, P. and Baird, M. S. (2005) Characteristics of degraded cellulose obtained from steam exploded wheat straw. Carbohydrate Research, 340, 97-106.

Sun, Y. and Cheng, J. (2002) Hydrolysis of lignocellulosic materials for ethanol production: a review. Bioresource Technology, 83, 1-11.

Suresh, K., Ranjan, A., Singh, S. and Moholkar, V. S. (2014) Mechanistic investigations in sono-hybrid techniques for rice straw pretreatment. Ultrasonics Sonochemistry, 21, 200-207.

Suslick, K. S. (1990) Sonochemistry. Science**,** 247, 1439-1445.

Talebnia, F., Karakashev, D. and Angelidaki, I. (2010) Production of bioethanol from wheat straw: An overview on pretreatment, hydrolysis and fermentation. Bioresource Technology, 101, 4744-4753.

TAPPI, 1992. Technical Association of Pulp and Paper Industry, Atlanta, Georgia, USA.

Tian, Y., Zhao, L., Meng, H., Sun, L. and Yan, J. (2009) Estimation of un-used land potential for biofuels development in (the) People's Republic of China. Applied Energy, 86, S77-S85.

Toegel, R., Gompf, B., Pecha, R. and Lohse, D. (2000) Does water vapor prevent upscaling sonoluminescence? Physical Review Letters, 85, 3165-3168.

Updegraff, D. M., (1969) Semimicro determination of cellulose in biological materials. Analytical Biochemistry, 32, 420-424.

Velmurugan, R. and Muthukumar, K. (2012) Ultrasound-assisted alkaline pretreatment of sugarcane bagasse for fermentable sugar production:

Optimization through response surface methodology. Bioresource Technology, 112, 293-299.

Vlasenko, E. Y., Ding, H., Labavitch, J. M. and Shoemaker, S. P. (1997) Enzymatic hydrolysis of pretreated rice straw. Bioresource Technology, 59, 109-119.

Washburn, E. W. (1928) International critical tables of numerical data, physics, chemistry and technology; volume 3, McGraw Hill, New York.

Wright, J. D. (1998) Ethanol from biomass by enzymatic hydrolysis. Chemical Engineering Progress, 84, 62-74.

Yan, J. and Lin, T. (2009) Biofuels in Asia. Applied Energy, 86, S1-S10.

Yoshioka, A., Seino, T., Tabata, M. and Takai, M. (2000) Homolytic scission of interunitary bonds in lignin induced by ultrasonic irradiation of MWL dissolved in dimethylsulfoxide. Holzforschung, 54, 357-364.

Young, F. R. (1989) Cavitation. McGraw Hill, London.

Yuan, T. Q., Xu, F., He, J. and Sun, R. C. (2010) Structural and physico-chemical characterization of hemicelluloses from ultrasound-assisted extractions of partially delignified fast-growing poplar wood through organic solvent and alkaline solutions. Biotechnology Advances, 28, 583-593.

Zhao, X., Zhang, L. and Liu, D. (2010) Pretreatment of Siam weed stem by several chemical methods for increasing the enzymatic digestibility. Biotechnology Journal, 5, 493-504.

Zheng, Y., Lee, C., Yu, C., Cheng, Y. S., Zhang, R., Jenkins, B. M. and Vander Gheynst, J. S. (2013) Dilute acid pretreatment and fermentation of sugar beet pulp to ethanol. Applied Energy, 105, 1-7.

Zheng, Y., Pan, Z. and Zhang, R. (2009) Overview of biomass pretreatment for cellulosic ethanol production. International Journal of Agriculture and Biological Engineering, 2, 51-68.

Chapter 7

Ultrasound induced enhancement of ethanol production from *Parthenium hysterophorus*: separate hydrolysis and fermentation

7.1 Introduction

Fast depletion of fossil fuel reserves has posed daunting threat to global energy security. Moreover, emission of greenhouse gases from industrial and vehicular exhaust has also raised serious concerns of global warming and climate change risks. As a common solution to both issues of energy security and climate change, the production of alternate liquid biofuels, which could substitute the fossil fuels, has been an immensely active research area for last one decade. Alcoholic biofuels such as bioethanol and biobutanol produced through fermentation route have shown great potential as alternate liquid transportation fuels. The economy of alcoholic biofuels production depends on the cost of substrate or feedstock for fermentation. Lignocellulosic biomass in the form of agricultural and forest residues and waste biomasses such as grasses and weeds have been explored as the potential feedstock for fermentation.

Conversion of lignocellulosic biomass to ethanol comprise three major steps, *viz*. processing and pretreatment of raw biomass, enzymatic hydrolysis of pretreated biomass and fermentation of enzymatic hydrolysate for ethanol production. In

addition to the cost of feedstock, the kinetics and yield of the enzymatic hydrolysis and fermentation processes also plays a major role in the overall efficiency and the economy of the process. Use of genetically modified or recombinant microbial strains that have higher yield, kinetics and selectivity is a conventional method for intensification of the processes. Another means of intensification of these processes, which has been investigated is the use of ultrasound irradiation of the enzymatic reaction mixture (Lee *et al*. 2008, Guiseppi-Elie *et al*. 2009, Dai *et al*. 2011, Malani *et al*. 2013, Nguyen and Le 2013, Souza *et al*. 2013, Sulaiman *et al*. 2013, Bashari *et al*. 2014, Malani *et al*. 2014, Subhedar and Gogate 2014) or fermentation broth (Wood *et al*. 1997, Schlafer *et al*. 2000, Launchen *et al*. 2003, Sulaiman *et al*. 2011, Khanna *et al*. 2012, Khanna *et al*. 2013, Ofori-Boateng and Lee 2014). Ultrasound and its secondary effect, cavitation, render several physical and chemical effects on the chemical and biochemical reaction systems, which are beneficial towards intensification of the process. Cavitation essentially involves nucleation, growth and transient implosive collapse of tiny gas/ vapor bubbles that cause immense energy concentration on an extremely short temporal and spatial scale (Suslick 1990). The principal physical effect of ultrasound and cavitation is in terms of generation of high intensity microturbulence in the system, while principal chemical effect is in terms of production of highly reactive radicals through thermal dissociation of vapor molecules entrapped in the bubble at the moment of transient collapse.

The objective of this study was to explore the mechanism of ultrasound induced enhancement of bioethanol production from waste biomass of *Parthenium hysterophorus* using the protocol of separate hydrolysis and fermentation. Enzymatic

hydrolysis of cellulosic biomass is an important step in the production of bioethanol. Enzyme being an expensive component of this process, the efficient hydrolysis of cellulose by cellulase is an important aspect for bioethanol production. The extent of enzymatic hydrolysis is a function of optimum values of the parameters involved, hydrolysis rate and yield of the process. In this study, the components of enzymatic hydrolysis were optimized using a statistical design of experiments, central composite design (CCD). The enzymatic hydrolysis of pretreated and delignified *P. hysterophorus* biomass was intensified by using ultrasound and the effects on kinetics of the process were evaluated. Influence of ultrasound on enzymatic hydrolysis processes has been explored immensely, however, there are very few reports aimed at fermentation. Previous authors (Wood *et al*. 1997, Schlafer *et al*. 2000, Launchen *et al*. 2003, Sulaiman *et al*. 2011, Neel *et al*. 2012, Ofori-Boateng and Lee 2014) have addressed the subject of ultrasound enhancement of bioethanol fermentation using various substrates and protocols. Although the previous literature has reported beneficial effects of ultrasound on bioethanol production, the overall focus of these studies has been on the results and not on the rationale. Many hypotheses have been proposed to explain the ultrasound-induced enhancements, yet the mechanism underlying these enhancements has remained largely unexplored. The links between physics of ultrasound and cavitation and the chemistry of fermentation have not been identified. In this study, the fundamental issue has been addressed. The approach was to couple the experimental results of conventional (with mechanical agitation) as well as ultrasound-assisted fermentation to a mathematical model as reported in other cases (Gupta *et al*. 2012, Philippidis 1992, Philippidis 1993, Shao *et*

al. 2009). This model comprises three simultaneous ordinary differential equations, one each for the time profiles of cell mass concentration, glucose concentration and ethanol concentration in the fermentation broth (Philippidis 1992). Such an approach has been earlier adopted for the analysis of ultrasound enhanced glycerol bioconversion (Khanna *et al*. 2012, Khanna *et al*. 2013), which revealed the important mechanistic facets of beneficial effects of ultrasound. After fitting the simulation results to the experimental data of fermentation (using Runge-Kutta ODE solver coupled with genetic algorithm code), the variations or trends in the kinetic and physiological parameters of the mathematical model, gave an interesting mechanistic account of the mechanism of influence of ultrasound on fermentation process, as described in the subsequent sections.

7.2 Materials and Methods

7.2.1 Materials

All the medium components and sodium hydroxide pellets were procured from HiMedia Pvt. Ltd., India. Sulfuric acid and chemicals used for reagent preparation for sugar estimation were purchased from Fisher Scientific, India. Glucose (99.5% purity), used as standard in HPLC and reducing sugar estimation was purchased from Sigma Aldrich, USA. Ethanol with 99.5% purity, used as standard in Gas chromatography was procured from Tedia Chemicals, USA.

7.2.2 Biomass collection and processing

P. hysterophorus plant biomass was collected from the campus of IIT Guwahati. Biomass was chopped, washed with water and dried at 60 ± 3^{o}C for 24 h prior to pretreatment. Ground biomass (particle size ~ 1 mm) was pretreated with 1% (v/v) H_2SO_4 + 30 min autoclaving (Chapter 6, Section 6.3.3) (Singh *et al*. 2014a) and the solid residue was further delignified by ultrasound assisted alkaline treatment (Chapter 6, Section 6.3.3.1) (Singh *et al*. 2014b).

7.2.3 Source of enzymes

Carboxymethylcellulase (CMCase) was produced by the isolate *Bacillus amyloliquefaciens* SS35 (Chapter 3, Section 3.2.3) (Singh *et al*. 2013). The specific activity of the enzyme was 1.0 U/mg (1.7 mg/mL) (Chapter 5, Section 5.3.1) (Singh *al*. 2014c), *β*-glucosidase (250 U/g) produced by *Aspergillus niger* (Novozyme 188) was procured from Sigma Aldrich (USA).

7.2.4 Microorganism for fermentation and culture conditions

Yeast strain *Saccharomyces cerevisiae* MTCC170 was procured from Institute of Microbial Technology (IMTECH), Microbial Type Culture Collection (MTCC), Chandigarh, India. The cultures were maintained in YEPD medium containing yeast extract (10.0 g/L), peptone (20.0 g/L) and dextrose (20 g/L).

7.2.5 Optimization of enzymatic hydrolysis by central composite design (CCD)

7.2.5.1 Experimental design, statistical analysis and model fitting

P. hysterophorus biomass pretreated with 1% H_2SO_4 + autoclaving and delignified by ultrasound assisted alkaline treatment was subjected to enzymatic hydrolysis. Delignified biomass consisted of cellulose 96.1 ± 0.6% (w/w of delignified biomass) and lignin 3.91 ± 0.2% (w/w of delignified biomass) (Chapter 6, Section 6.3.3.1). Two enzymes, *viz*. CMCase produced by *Bacillus amyloliquefaciens* SS35 and *β*-glucosidase from *Aspergillus niger* (Novozyme 188) were used for the hydrolysis. The experiments were performed in sodium citrate buffer (0.05 M, pH 5.0) supplemented with different concentrations of biomass, CMCase and *β*-glucosidase. The reactions were carried out in 150 mL Erlenmeyer flask with total reaction volume of 25 mL. The flasks were incubated at 30^{o}C and 150 rpm in an incubator shaker (Orbitek, Scigenics Biotech).

The central composite experimental design essentially fits a second-order polynomial model. A three-factor, five-level design was used in which five coded levels (-α, -1, 0, +1, +α) were assigned to each factor. α is the extended level with value of $(2)^{3/4}$ =1.682. A 2^3 full-factorial CCD experimental design with three

components, *viz*. biomass, CMCase and *β*-glucosidase concentrations at five coded levels was generated by Minitab statistical software (Release 15, Trial Version). This experimental design comprised 20 individual experiments ($=2^k + 2k + n_o$), where '*k*' is the number of independent variables and n_o is the number of replicate runs at center point of the variables. Each experiment was conducted in triplicate to assess reproducibility.

The experimental data (Table 7.3.1) were analyzed by the regression procedure to fit the following second-order polynomial equation (eq. 7.1):

$$Y = \beta_o + \sum_{i=1}^{k} \beta_i X_i + \sum_{i=1}^{k} \beta_{ii} X_i^2 + \sum_{i \neq j} \sum_{i} \beta_{ij} X_i X_j \qquad \text{(eq. 7.1)}$$

Notation: *Y* - response (total reducing sugar yield), *k* - number of factors or components, β_o - regression constant, β_i - linear coefficient, β_{ii} - quadratic coefficient and β_{ij} - interaction coefficient. The following equation (eq. 7.2) was used for coding (in the range of -1 to +1) the actual experimental values (given in the parentheses in the table) of the factors:

$$x_i = X_i - X_o/\Delta X_i, \qquad i = 1, 2, 3,..., k \qquad \text{(eq. 7.2)}$$

Where, x_i is the dimensionless value of an independent variable, X_i is the real value of an independent variable, X_o is the value of X_i at the center point and ΔX_i is the step change. The analysis of variance (ANOVA) was done as described in Section 4.2.6.3 of Chapter 4. Graphical representation of the fitted polynomial eq. 7.1 was given in the form of contour plots. Values and ANOVA of the linear, quadratic and interaction regression coefficients are given in Table 7.3.2A and B, respectively.

7.2.5.2 Experimental validation of optimization

Validation of optimization of enzymatic hydrolysis was carried out using the model predicted optimum values of parameters after analysis of results obtained from CCD experimental design. The experiments were performed with 3.88% w/v delignified biomass loading in sodium citrate buffer (0.05 M, pH 5.0) supplemented with CMCase (concentration 600 U/g delignified biomass) and *β*-glucosidase (concentration 50 U/g delignified biomass). The reactions were carried out in 150 mL Erlenmeyer flask with total reaction volume of 25 mL. The flasks were incubated at 30^{o}C and 150 rpm in an incubator shaker (Orbitek, Scigenics Biotech).

7.2.6 Intensification of enzymatic hydrolysis by ultrasound

The components of enzymatic hydrolysis were at their optimum values, obtained from CCD, in the process of intensification by ultrasound. An intermittent ultrasound irradiation was applied to the hydrolysis mixture using an ultrasound bath (Tran-sonic T-460, Elma, Germany, 2L) with the dimensions 25 cm × 15 cm × 10 cm, operating frequency of 35 kHz and power rating of 35 W. The actual power input to the liquid medium in the bath (i.e. water) was determined calorimetrically as 18.58 W (Sivasankar *et al*. 2007, Chakma and Moholkar 2011). This power is transmitted through the transducer attached to bottom of the bath. The diameter of this transducer was 4 cm. Therefore, the power dissipation to sonication medium is 1.48 W/cm^2 and the corresponding acoustic power amplitude was 150 kPa. The ultrasound was applied in a duty cycle of 10% (i.e. 1 min of sonication and 9 min of mechanical shaking in every 10 min of fermentation). The bath was filled with water and the

flask containing fermentation mixture was placed at the center of the bath. The flask was immersed to about 50% of its height in the water and the position of the Erlenmeyer flask was carefully maintained same in all experiments in view of spatial variation of the acoustic intensity (Moholkar *et al*. 2000, Moholkar *et al*. 2002). The schematic of reaction setup used in this study has been shown in Fig. 7.2.1. The temperature of the water in the bath was maintained at $30^{o} \pm 2^{o}C$ by replacement of small portions of initial water at regular intervals. Control experiments (mechanical shaking) were also carried out to validate the influence of ultrasound in test experiments (mechanical shaking and intermittent sonication). 200 μL aliquots of the reaction mixture were withdrawn intermittently from both control and test experiments to determine instantaneous total reducing sugar concentration. The hydrolysis was carried out till 96 and 14 h for control and test experiments, respectively, when the sugar yield became constant (< 5% difference) in the consecutive samples. Both test and control experiments were carried out in triplicate to assess the reproducibility of the results.

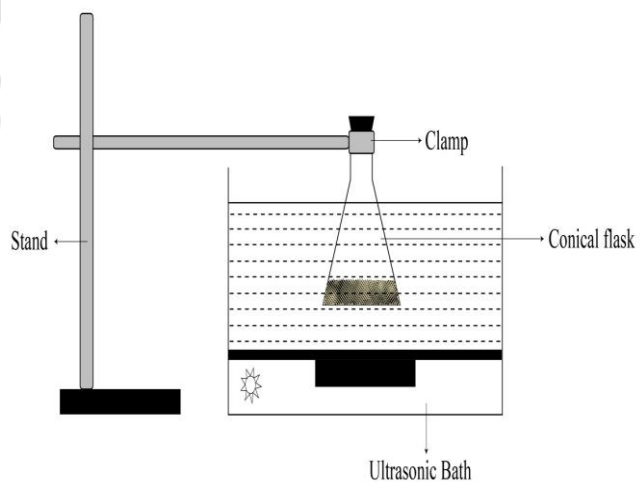

Fig. 7.2.1 Schematic setup for ultrasound assisted enzymatic hydrolysis (adopted from Bharadwaja 2014).

7.2.7 Fermentation of enzymatic hydrolysate and its intensification by ultrasound

Fermentation of the enzymatic hydrolysate (containing reducing monomeric sugars) was carried out using *Saccharomyces cerevisiae* MTCC170 in a 150 mL Erlenmeyer flask with working volume of 25 mL. In order to promote yeast growth, enzymatic hydrolysate was supplemented with yeast extract (10 g/L), KH_2PO_4 (2 g/L), $(NH_4)_2SO_4$ (1 g/L) and $MgSO_4 \cdot 7H_2O$ (1 g/L) (Karuppaiya *et al*. 2010) and medium pH was adjusted to 5.0. The mixture was inoculated with 10% (v/v) of *S. cerevisiae* MTCC170 and incubated at 30^{o}C and 150 rpm in an incubator shaker (Scigenics Biotech, Model: Orbitek). Ultrasound assisted fermentation was carried out under similar conditions of sonication as mentioned above in case of enzymatic hydrolysis (Section 7.2.6). In the test experiments, for every 10 min of treatment, sonication of the fermentation broth was carried out for 1 min with mechanical shaking of the flask for rest 9 min. The total fermentation period for control and test experiments was 30 and 15 h, respectively. The period of fermentation was decided on the change in percentage of sugar level in the consecutive samples withdrawn from fermentation broth. Fermentation was stopped when difference in sugar concentration in the two successive samples drawn from the broth was $\leq$ 5%. 200 µL aliquots of the fermentation broth were withdrawn intermittently to determine total reducing sugar, ethanol and cell mass concentration in fermentation broth. Both test and control experiments were conducted in triplicate to assess the reproducibility of the results. The average values of cell mass, sugar and ethanol concentration in triplicate experimental runs were considered for analysis.

7.2.8 Estimation of total reducing sugar and determination of cell mass

The reducing sugar content of the sample of fermentation broth was estimated by the method of Nelson (1944) and Somogyi (1945), using D-glucose as standard. Dry cell mass for yeast cells was determined by using an indirect method by plotting a calibration curve using intracellular protein content (g/L) and dry cell mass (g/L) of the yeast cells (Abd-Aziz *et al*. 2008). For the determination of dry cell mass, separate fermentation using pure glucose was carried out in a 500 mL Erlenmeyer flask with 200 mL culture broth under mechanical shaking. 1 mL samples of the fermentation broths were withdrawn at regular intervals in a pre-weighed micro-centrifuge tube and later centrifuged at 10000 ***g*** for 15 min. The pellet of yeast cells was dried at 50 ± 3^{o}C till constant weight was achieved. For determination of intracellular protein content, 500 µL cell suspension was withdrawn from the same flask and centrifuged at 10000 ***g*** for 15 min. The resulting cell pellet was washed with 10 mM phosphate buffer saline (PBS) pH 7.4 and yeast cells were ruptured by alkaline lysis method to obtain intracellular protein (Matsuo *et al*., 2006). Protein estimation was done by the method of Lowry *et al*. (1951) using bovine serum albumin (BSA) as standard. A calibration curve was plotted using dry cell mass (g/L) and intracellular protein content (g/L) of the yeast cells. Dry cell mass of the samples was calculated by determined intracellular protein content and comparing it with calibration plot.

7.2.9 Determination of change in morphology of yeast cells under ultrasound

Morphological changes of *S. cerevisiae* MTCC170 cells under the influence of ultrasound were investigated using Flow cytometry (BD Calibur™ Flow Cytometer, BD Biosciences, USA). Samples from both control and test experiments were analyzed using 488 nm laser and 530 nm emission filter. Morphological changes in the cells were evaluated by FSC (Forward Scatter) and SSC (Side Scatter). Forward-scattered light (FSC) is proportional to cell-surface area or size and side-scattered light (SSC) is proportional to cell granularity or internal complexity.

7.2.10 Determination of viability of yeast cells

Viability of *S. cerevisiae* MTCC170 cells before and after sonication was measured by methylene blue staining method (Painting and Kirsop, 1990). Yeast broth and methylene blue solution (0.1% w/v) were mixed in a ratio of 1:1 and incubated for 5 min. Cells were counted on hemocytometer at 40x magnification. The cell viability was calculated using the following formula:

$$\text{Viability (\%)} = \frac{\text{Number of live (unstained) cells}}{\text{Number of live (unstained) cells} + \text{Number of dead (stained) cells}} \times 100$$

7.2.11 Analytical Methods

The presence of hexose (glucose) sugar in the enzymatic hydrolysate was confirmed by HPLC analysis (Perkin-Elmer, Series 200, with a refractive index detector) using HiPlex-H column (300 mm × 5 µm × 4.6 mm, Varian). HPLC grade water (deionized water, Milli Q) was used as the mobile phase at a flow rate of 0.4

mL/min. The estimation of ethanol was done by Gas Chromatograph (Varian, CP 3800) using a CP Wax 52 CB capillary column (250 mm × 0.25 mm × 0.39 mm, Varian). The oven temperature was programmed from 45^{o}C to 100^{o}C with an increment of 3^{o}C/min and after 100^{o}C, an increment of 5^{o}C/min upto 200^{o}C. The injector and detector temperatures were kept at 230^{o}C and 250^{o}C, respectively. Nitrogen gas was used as a carrier at a flow rate of 2 mL/min. Glucose (99.5% purity) was used as standard in sugar analysis by HPLC and ethanol (99.5% purity) as standard in GC.

7.2.12 Mathematical model

Philippidis *et al*. (1992) reported a mathematical model for ethanol fermentation, which has been used in this study. The original model was developed for simultaneous saccharification and fermentation, but it can be adopted for present case where hydrolysis and fermentation have been carried out separately. Given below are the main equations of the model and the underlying assumptions.

(1) pH of the fermentation mixture stays practically same all along fermentation, and therefore, has no significant effects on enzyme activity and cell growth.

(2) Major products of metabolism of microorganism are ethanol and carbon dioxide.

(3) The growth medium provides an excess of all nutrients except for the carbon source (glucose), which has been derived by enzymatic hydrolysis of pretreated *P. hysterophorus*. The fermentation steps include: (a) diffusion of glucose towards cell wall, (b) uptake of glucose by cells, (c) glucose metabolism and ethanol synthesis and (d) ethanol secretion into the aqueous phase.

The process of fermentation of glucose to ethanol has been described by following three equations that give time variations of cell mass (*X*), glucose (*G*) and ethanol (*E*).

***Cell mass*:** Glucose is assumed to be the primary carbon source of the fermentative organism, which is metabolized into cell mass, *X*, with concomitant synthesis of ethanol and CO_2. Other metabolic products are produced in negligible amount. The Monod kinetic expression, which includes non-competitive substrate inhibition and non-competitive product inhibition, describes the microbial growth as a function of glucose and ethanol concentration:

$$\frac{dX}{dt} = \mu_m \times \left[\frac{G}{K_3 + G + G^2/K_I}\right] \times \left[\frac{K_{3E}}{K_{3E} + E}\right] \times X - k_d \times X \qquad \text{(eq. 7.3)}$$

where, μ_m - maximal specific growth rate of the microorganism, K_3 - Monod constant for glucose, K_I - substrate inhibition constant, K_{3E} - inhibition constant of cell growth by ethanol. The second term on the RHS is potential cell lysis, which is assumed to be proportional to cell mass concentration, *X*, and characterized by constant k_d, which is specific rate of cell death.

***Glucose*:** Consumption of glucose in the fermentation broth occurs via two mechanisms, cell mass synthesis (as described by equation 1) and as a source of cell maintenance requirement. Thus, the total glucose consumption rate by two mechanisms is:

$$\frac{dG}{dt} = -\left[\frac{1}{Y_{X/G}} \times \frac{d(X)}{dt} + m(X)\right] \qquad \text{(eq. 7.4)}$$

where, $Y_{X/G}$ - average yield coefficient of cell mass on the substrate (glucose), and *m*

- specific rate of substrate consumption for maintenance requirements. The above balance for glucose does not include additional term corresponding to ethanol fermentation, as ethanol is a product directly associated with energy generated by the fermentative microorganism.

Ethanol: Formation rate of ethanol has two contributions, *viz*. growth-associated ethanol formation and non-growth associated ethanol formation, and it also depends on concentration of glucose in the medium:

$$\frac{dE}{dt} = \left[a \times \left(\frac{dX}{dt} \right) + b(X) \right] \times \left[\frac{G}{K_4 + G} \right] \qquad \text{(eq. 7.5)}$$

where, a - constant for growth associated ethanol formation, b - constant for non-growth associated specific ethanol production, and K_4 - Monod constant for ethanol synthesis.

The above set of ordinary differential equations (ODEs) for three independent variables, *viz*. X, G and E, and the parameters therein characterize the fermentation process. These equations have total of 10 parameters, *viz*. K_3, K_I, K_{3E}, k_d, μ_m, a, b, $Y_{X/G}$, m and K_4. In order to get the physical insight into the ultrasound induced enhancement of fermentation, the numerical solution of above equations was compared with the experimental time profiles of X, G and E. The unknowns in this model were the kinetic and physiological parameters, whose optimum values need to be determined, so as to match the time profiles of the substrate, cell mass and ethanol concentrations calculated using the model with the experimental data. As per the findings of Philippidis *et al*. (1992), null value was assigned to the constant K_4. The main model of three ordinary differential equations was solved using Runge - Kutta

4th order method, and optimization of the parameters was done by calculating root mean square (RMS) error between experimental and model results using Genetic Algorithm (GA). GA minimizes the error and gives optimized values of parameters. The overall algorithm of model calculation is described in the flow chart shown in Fig. 7.2.2.

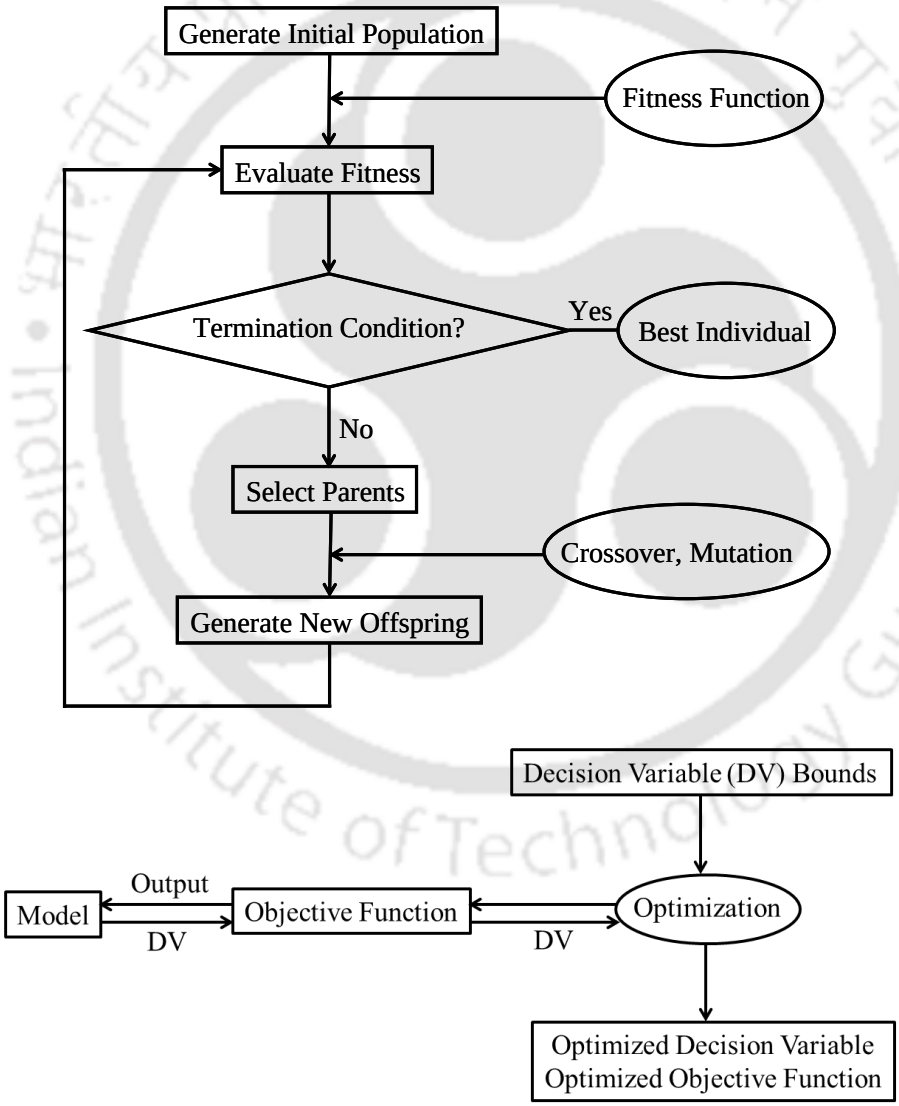

Fig. 7.2.2 Flowsheet depicting algorithm for fitting fermentation model to the experimental data and determination of model parameters with GA optimization.

7.3 Results and Discussion

7.3.1 Optimization of enzymatic hydrolysis of *P. hysterophorus* biomass

7.3.1.1 Optimization by central composite experimental design

The full factorial CCD matrix of the variables is given in Table 7.3.1, which shows the response (reducing sugar yield) obtained in each experiment and the standard deviation along with the model predicted responses. The results of second-order response model fitted to the coded data are given in Table 7.3.2A.

Table 7.3.1 Full factorial central composite design matrix of three components in coded and actual (in parentheses, g/L) values and the response of reducing sugar yield (mg/g).

Run order	Biomass concentration (X_1)	CMCase concentration (X_2)	β-glucosidase concentration (X_3)	Reducing sugar yield (mg/g)	
				*Experimental	Predicted
1	+α (80.0)	0 (400.0)	0 (35.0)	256.7 ± 11.3	248.41
2	0 (42.5)	0 (400.0)	0 (35.0)	340.3 ± 12.6	360.42
3	0 (42.5)	+α (600.0)	0 (35.0)	408.6 ± 11.2	407.74
4	-1 (20.2)	-1 (281.1)	+1 (43.9)	312.4 ± 8.90	309.98
5	0 (42.5)	0 (400.0)	0 (35.0)	340.3 ± 17.4	360.42
6	+1 (64.8)	-1 (281.1)	+1 (43.9)	310.1 ± 15.3	310.54
7	-1 (20.2)	-1 (281.1)	-1 (26.1)	289.3 ± 12.4	284.36
8	-1 (20.2)	+1 (518.9)	+1 (43.9)	430.0 ± 8.70	424.21
9	0 (42.5)	0 (400.0)	0 (35.0)	364.5 ± 13.2	360.42
10	+1 (64.8)	+1 (518.9)	-1 (26.1)	300.2 ± 10.2	302.77
11	0 (42.5)	0 (400.0)	-α (20.0)	336.2 ± 9.20	334.34
12	+1 (64.8)	+1 (518.9)	+1 (43.9)	410.3 ± 17.3	415.39
13	0 (42.5)	-α (200.0)	0 (35.0)	342.7 ± 12.4	343.35
14	-α (5.0)	0 (400.0)	0 (35.0)	200.6 ± 9.30	208.68
15	0 (42.5)	0 (400.0)	0 (35.0)	364.5 ± 8.10	360.42
16	+1 (64.8)	-1 (281.1)	-1 (26.1)	334.5 ± 13.2	340.43
17	-1 (20.2)	+1 (518.9)	-1 (26.1)	256.4 ± 12.8	256.09
18	0 (42.5)	0 (400.0)	0 (35.0)	376.4 ± 18.2	360.42
19	0 (42.5)	0 (400.0)	0 (35.0)	376.4 ± 17.2	360.42
20	0 (42.5)	0 (400.0)	+α (50.0)	448.9 ± 15.3	450.58

**Experimental values are mean ± SE (n = 3)*

The second-order regression equation fitted to this data is as follows:

$$Y_{\text{sugar yield}} = 360.420 + 11.813\ X_1 + 19.144\ X_2 + 34.559\ X_3 - 46.625\ X_1^2 + 5.348\ X_2^2 + 11.328\ X_3^2 - 2.347\ X_1X_2 - 13.877\ X_1X_3 + 35.627\ X_2X_3 \quad \text{(eq. 4.5)}$$

The overall regression coefficient (R^2) of the model was 0.9776 with adjusted coefficient of 0.9575. The predicted R^2 of 0.9440 is also in reasonable agreement with adjusted regression coefficient. This indicated that the model fits well to the experimental data. Table 7.3.2B represents the ANOVA of the fitted model. The insignificant *p* value of 0.948 for lack of fit implied that the model is significant.

Table 7.3.2 Statistical (CCD) analysis for optimization of enzymatic hydrolysis.

(A) Values of coefficients for second order regression model.

Model term	Coefficient estimate	*t*-value	*p*-value
Intercept	360.420	69.271	0.000*
Biomass concentration (X_1)	11.813	3.422	0.007*
CMCase concentration (X_2)	19.144	5.546	0.000*
β-glucosidase concentration (X_3)	34.559	10.011	0.000*
Biomass × Biomass (X_1^2)	-46.625	-13.874	0.000*
CMCase × CMCase (X_2^2)	5.348	1.591	0.143
β-glucosidase × β-glucosidase (X_3^2)	11.328	3.371	0.007*
Biomass × CMCase ($X_1 \times X_2$)	-2.347	-0.520	0.614
Biomass × β-glucosidase ($X_1 \times X_3$)	-13.877	-3.077	0.012*
CMCase × β-glucosidase ($X_2 \times X_3$)	35.627	7.899	0.000*

**Significant p values, $p \leq 0.05$; $R^2 = 0.9776$; Predicted $R^2 = 0.9440$; Adjusted $R^2 = 0.9575$*

(B) ANOVA for quadratic model.

Source	DF	SS	MS	*F*-value	*p*-value
Regression	9	71064.2	7896.0	48.52	0.000
Linear	3	36103.4	7740.5	47.56	0.000
Square	3	36103.4	12034.5	73.95	0.000
Interaction	3	11739.3	3913.1	24.04	0.000
Residual (Error)	10	1627.5	162.7		
Lack of fit	5	273.1	54.6	0.20	0.948
Pure Error	5	1354.3	270.9		
Total	19	72691.7			

DF - degrees of freedom; SS - sum of squares; MS - mean square

The *p* value zero for all linear, square and interaction coefficients indicated their significance. The *F*-value highest for square coefficient and lowest for interaction coefficients suggested that the combined effect of biomass, CMCase and *β*-glucosidase concentrations on reducing sugar yield is inadequate. The values of the components revealed by the statistical analysis and quadratic model for maximum sugar yield were as follows: biomass concentration = 38.8 g/L, CMCase concentration = 600 U/g of biomass and *β*-glucosidase concentration = 50 U/g of biomass. The maximum response (reducing sugar yield) predicted by the model under optimized concentrations of these three components have been depicted in the desirability function plot (Fig. 7.3.1).

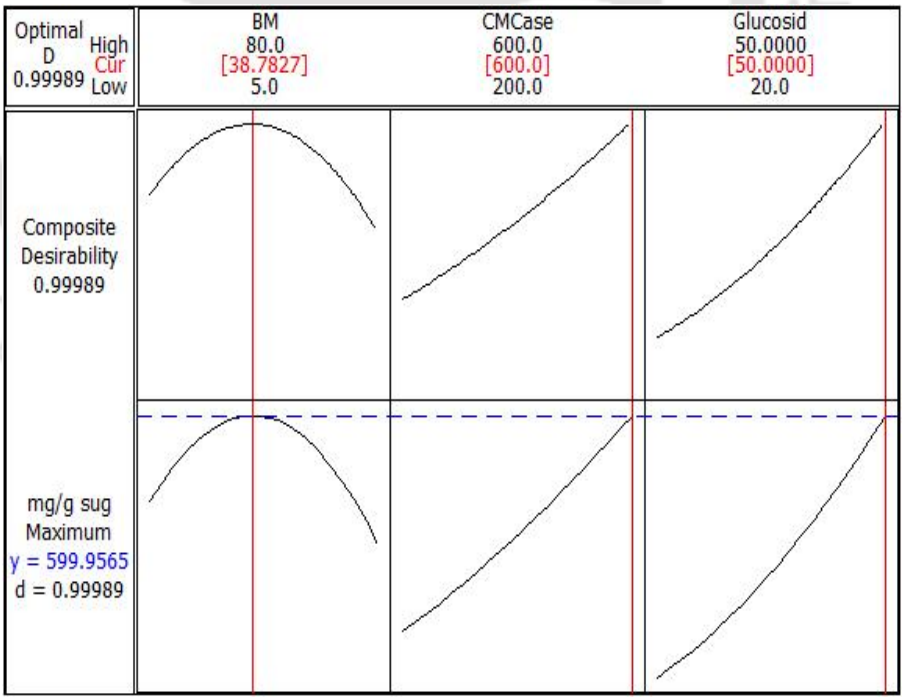

Fig. 7.3.1 Desirability function plot showing the optimum values of components of enzymatic hydrolysis.

The maximum reducing sugar yield for these parameters predicted by the model is 599.96 mg/g. The validation of this prediction was done by carrying out experiments in triplicate. The profile of total reducing sugar concentration and saccharification yield under optimized conditions has been shown in Figure 7.3.2. The experimental value of maximum reducing sugar yield obtained under optimized concentrations of the components was 593.4±16.3 mg/g, which was in good agreement with the predicted one. The reducing sugar yield under un-optimized conditions (as mentioned in Section 6.3.3.5 of Chapter 6) was 308.4 mg/g of biomass. Thus, the enhancement in sugar yield after optimization of enzymatic hydrolysis was approximately 2-fold. Also, in terms of raw biomass, sugar yield was increased by ~92% from 164.1 mg/g (Section 6.3.3.5, Chapter 6) to 315.5 mg/g of raw biomass.

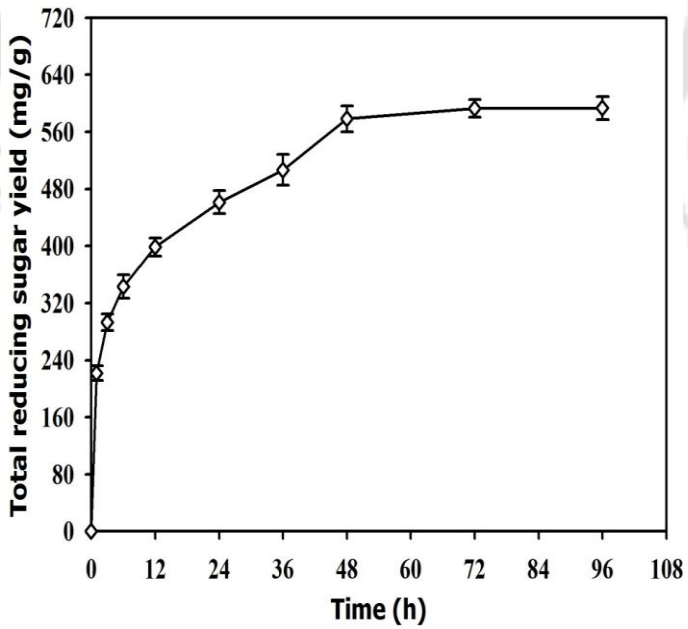

Fig. 7.3.2 Profile of sugar yield in enzymatic hydrolysis of *P. hysterophorus* biomass after optimization.

7.3.1.2 Interaction effects of the components

The interactive effects among the components have been assessed using contour plots shown in Fig. 7.3.3 (A-C). The trends in interactive effects observed were as follows: (1) the reducing sugar yield kept on increasing with increasing concentrations of CMCase. However, for biomass concentration, reducing sugar yield initially increased with increasing concentration and slightly reduced when biomass concentration crossed 70 g/L. The highest sugar yield was observed in a range of biomass concentration of 35-55 g/L (Fig. 7.3.3A). (2) with increasing concentration of β-glucosidase the reducing sugar yield increased constantly and was maximum for a β-glucosidase concentration of 50 U/g, trend with biomass concentration were similar as discussed previously (Fig. 7.3.3B), (3) sugar yield increased with the increase of both CMCase and β-glucosidase concentration and was maximum for maximum values of the concentration of both the enzymes (Fig. 7.3.3C).

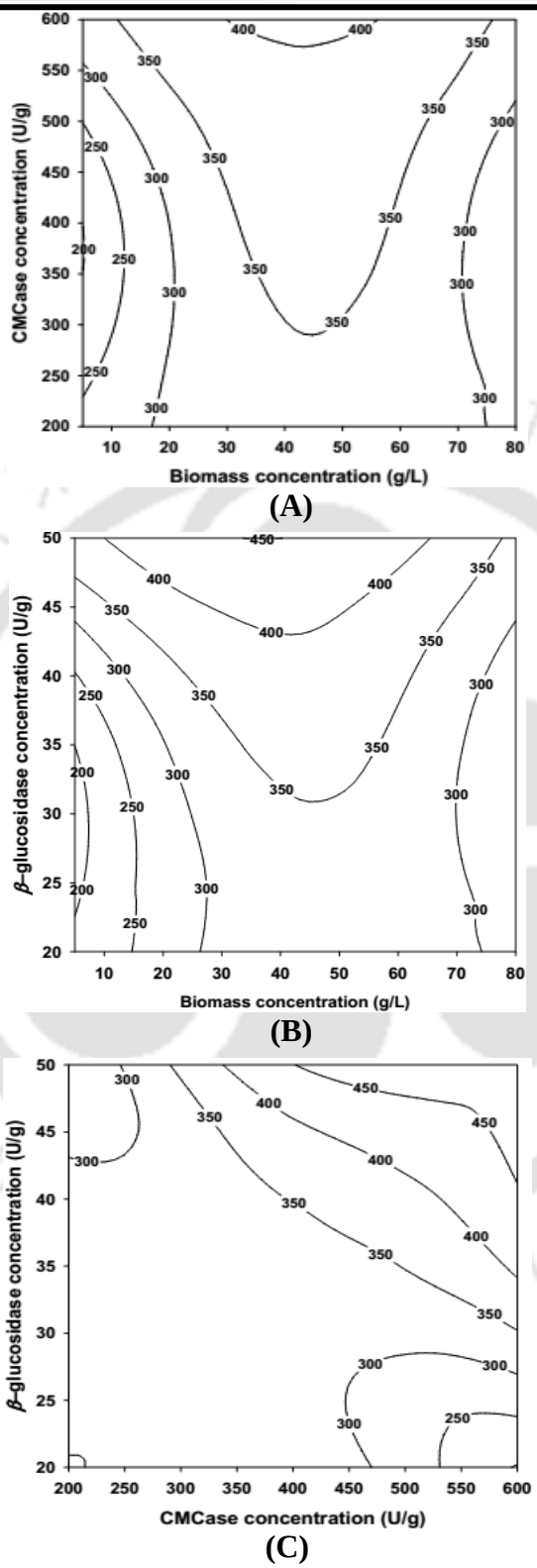

Fig. 7.3.3 Contour plots for reducing sugar yield showing the interactive effects of components of enzymatic hydrolysis: (A) concentrations of CMCase and Biomass, (B) concentrations of *β*-glucosidase and biomass, (C) concentrations of *β*-glucosidase and CMCase.

7.3.2 Intensification of enzymatic hydrolysis by ultrasound

7.3.2.1 Effect of sonication on saccharification

Ultrasound assisted enzymatic hydrolysis resulted in a sugar yield of 711.3 ± 18.6 mg/g within 14 h (Fig. 7.3.4). Thus, the time of hydrolysis was reduced by ~6-fold in comparison to control experiment (without ultrasound) where it was 96 h with a sugar yield of 593.4 ± 16.3 mg/g (Fig. 7.3.2). The sugar yield was increased by ~17%, after sonication. These observations are in accordance with the findings of other reports in literature (Table 7.3.4), however, in this study the enhancement in hydrolysis yields was very low. This could be a consequence of lesser efficiency of CMCase enzyme used in this study in comparison to commercial enzymes.

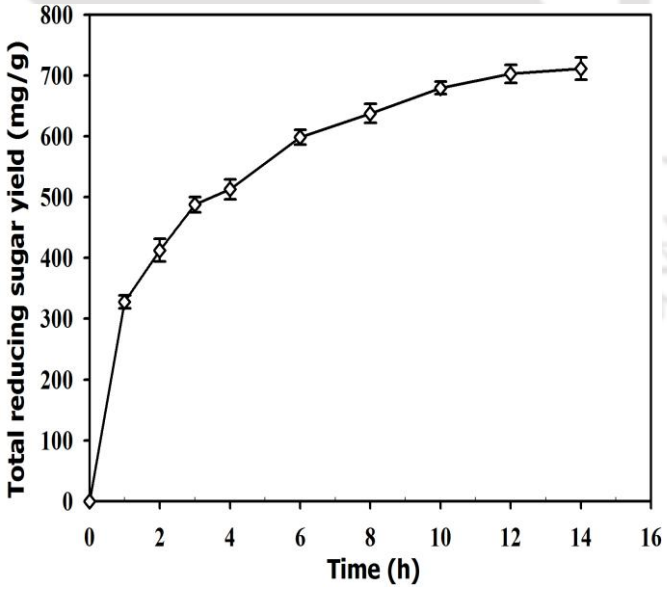

Fig. 7.3.4 Profile of enzymatic hydrolysis of *P. hysterophorus* biomass under the influence of ultrasound.

7.3.2.2 Effect of sonication on kinetics of enzymatic hydrolysis

Ultrasound-assisted enzymatic hydrolysis of *P. hysterophorus* biomass was carried out at different concentrations. The effect of sonication on kinetic parameters,

K_m and V_{max} was investigated by Lineweaver-Burk plots which were drawn using the data obtained from both control (Fig. 7.3.5A) and test experiments (Fig. 7.3.5B).

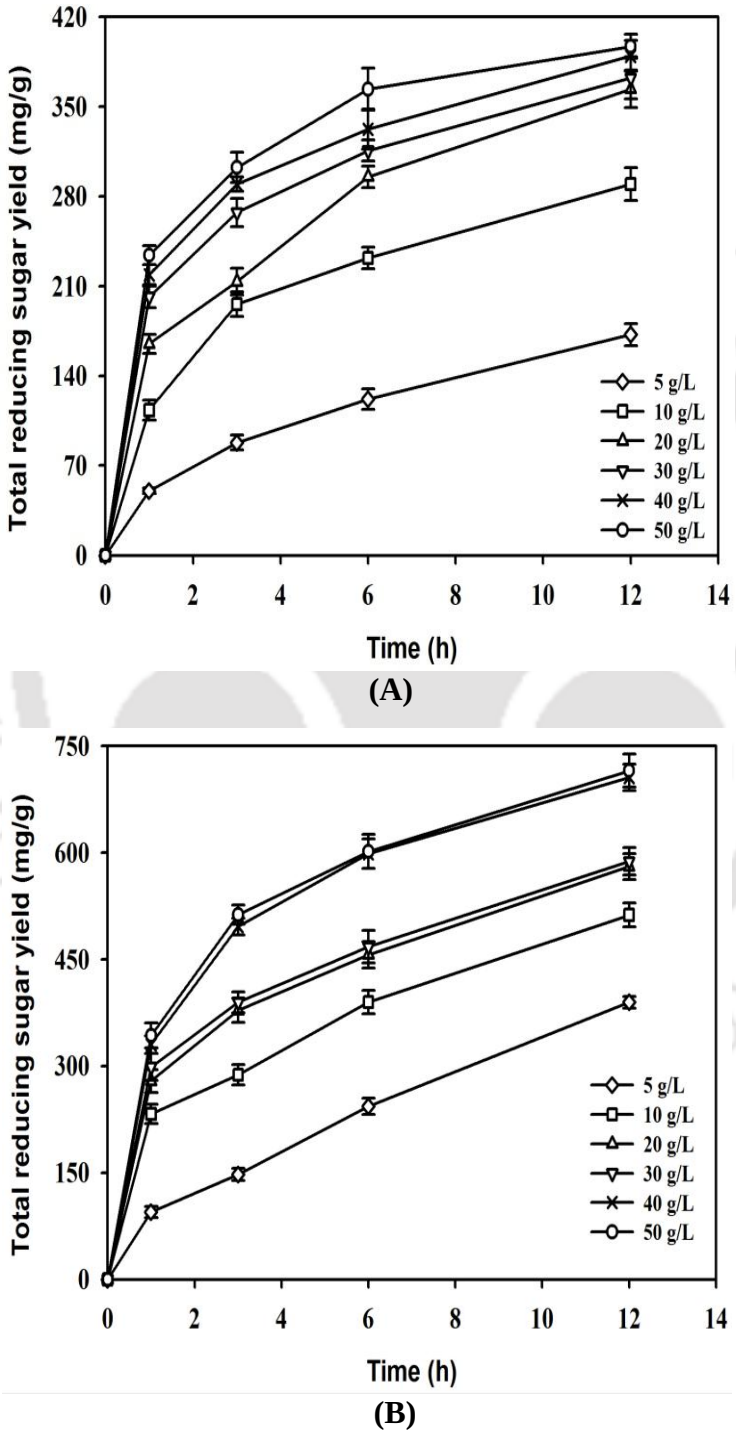

Fig. 7.3.5 Effect of substrate concentration on sugar yield in enzymatic hydrolysis (A) without ultrasound (control) and (B) with ultrasound (test).

The Lineweaver-Burk plots for control and test experiments have been shown in Fig. 7.3.6A and B, respectively. The values of K_m and V_{max} for ultrasound assisted enzymatic hydrolysis of *P. hysterophorus* biomass were found out to be 24.44 g/L and 0.055 mM/min, respectively. However, in case of hydrolysis without ultrasound (control experiments) the values of K_m and V_{max} were 42.77 g/L and 0.046 mM/min, respectively (Table 7.3.3).

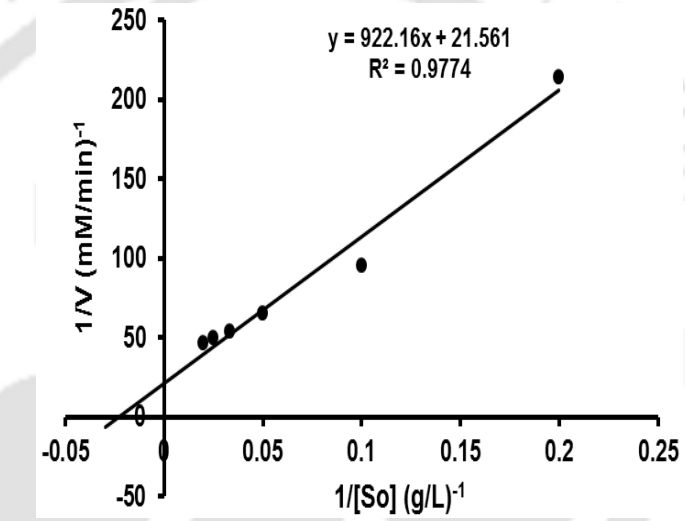

(A)

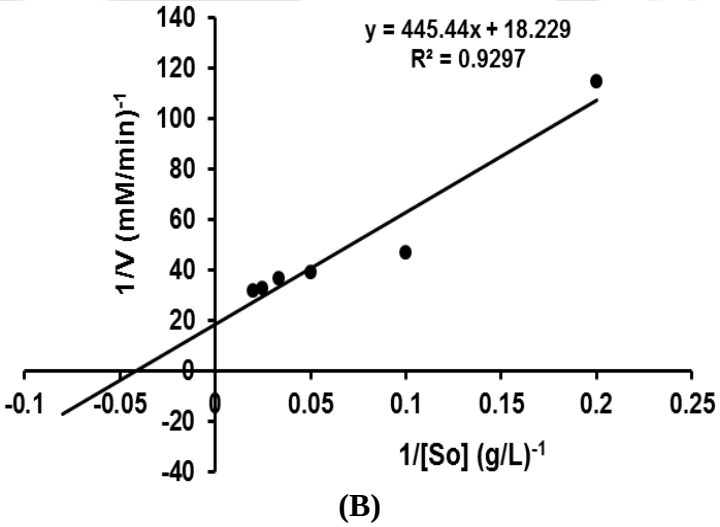

(B)

Fig. 7.3.6 Lineweaver-Burk plot for enzymatic hydrolysis (A) without ultrasound (control) and (B) with ultrasound (test).

Table 7.3.3 Effect of sonication on kinetic parameters of enzymatic hydrolysis.

Mode of enzymatic hydrolysis	Sugar yield (mg/g)	Reaction time (h)	K_m (g/L)	V_{max} (mM/min)
Without ultrasound	593.4 ± 16.3	96	42.77	0.046
With ultrasound	711.3 ± 18.6	14	24.44	0.055

The result obtained in this study indicated that the enhancement effects of ultrasound on the hydrolysis process are in terms of increase in rate of reaction as well as a reduced value of K_m. Increase in rate of reaction could be a consequence of enhancement in the convection in the medium and mass transfer characteristics. However, the reduced K_m value suggests that ultrasound facilitated substrate binding to the active site of the enzymes, possibly by enhancing pulsating motions within the enzyme molecule. Some comparable observations described earlier for different enzymatic reactions have been summarized in Table 7.3.4.

Table 7.3.4 Comparative assessment of results obtained from ultrasound assisted enzymatic hydrolysis with published literature.

Enzyme	Sonication Parameters	Observations	Reference
Commercial cellulase + *β*-glucosidase	20 kHz, 0.72-1.35 W/mL, 50°C, 20-60 min	Rate increases from 6.94×10^{-7} to 9.86×10^{-7} mol/(L s)	Imai *et al*. 2004
Glucose oxidase	23 kHz, Ultratip sonication	change in secondary structure of enzyme increased enzyme activity	Guiseppi-Elie *et al.* 2009
Commercial *α*-amylase	40 kHz, power output 132 W	Activation energy decreased by 80%, 3-fold higher enzyme activity	Souza *et al*. 2013
Cellulase	Intensity 17.33 W/cm^2, 30 min	Enzyme activity increased by 25%	Subhedar and Gogate 2014
1,3-ρropanediol dehydrogenase	35 W, 35 kHz, 75% duty cycle	K_m and V_{max} decreased and K_i increased	Khanna *et al*. 2013
Cellulolytic enzyme complex	132 W, 40 kHz	Sugar yield increased to two-fold	Lunelli *et al*. 2014
Commercial cellulase	60 W, 70% duty cycle, 6.5 h	~2.4-fold enhancement in released sugar concentration	Subhedar *et al*. 2015
Cellulase + *β*-glucosidase	35 W, 35 kHz, 10% duty cycle	K_m decreased and V_{max} increased, sugar yield increased by ~17%	This study

7.3.3 Comparative assessment of enzymatic hydrolysis

Each successive step of enzymatic hydrolysis led to an enhancement in sugar yield which has been presented in Table 7.3.5 in terms of raw biomass. Maximum enhancement recorded in optimization step which was 92%, showed the significance of this step in cellulosic ethanol production.

Table 7.3.5 Comparative assessment of enzymatic hydrolysis at various steps in terms of sugar yield on raw biomass.

Enzymatic hydrolysis step	Sugar yield (mg/g raw biomass)	Successive enhancement in yield (%)	Reference
Hydrolysis of pretreated (acid + autoclaving) biomass	131.7	-	Table 6.3.2A, Chapter 6
Hydrolysis of delignified (ultrasound assisted alkaline treatment of acid pretreated biomass) biomass	164.1	25	Section 6.3.3.5, Chapter 6
Optimization of enzymatic hydrolysis by central composite design	315.7	92	This study
Intensification of enzymatic hydrolysis by sonication	378.3	20	This study

7.3.4 Ethanol fermentation and its simulation

7.3.4.1 Intensification of fermentation with sonication

Fermentation of enzymatic hydrolysate obtained in previous step was carried out with and without sonication. The results obtained from both control (fermentation with mechanical shaking) and test (mechanical shaking and intermittent ultrasound) experiments have been presented in Tables 7.3.6 and 7.3.7, respectively. Fig. 7.3.7 and 7.3.8 represent the profiles of ethanol, cell mass and sugar concentrations in control and test experiments, respectively. The values of various parameters calculated from experimental data have been summarized in Table 7.3.8.

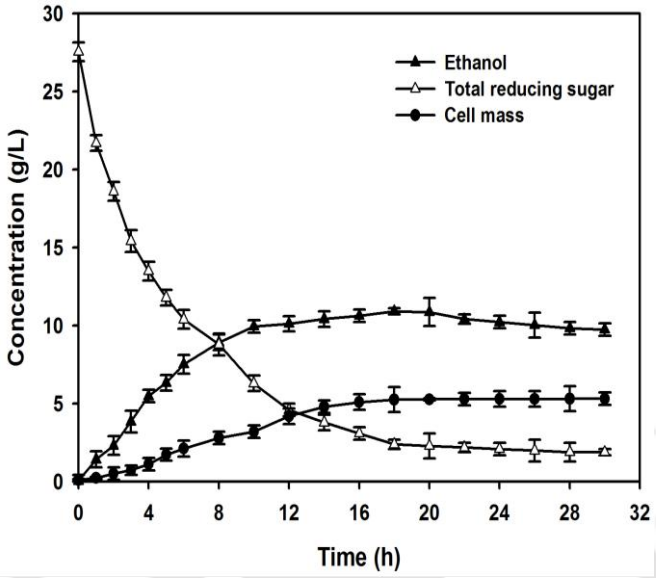

Fig. 7.3.7 Profiles of ethanol, total reducing sugar and cell mass in control (with mechanical agitation) experiments.

Table 7.3.6 Experimental data for the profiles of ethanol, sugar and cell mass in control experiments.

Time (h)	Ethanol concentration (g/L)	Sugar concentration (g/L)	cell mass concentration (g/L)
0	0.04 ± 0.4	27.56 ± 0.6	0.11 ± 0.05
1	1.43 ± 0.5	21.7 ± 0.5	0.24 ± 0.08
2	2.31 ± 0.6	18.6 ± 0.6	0.51 ± 0.4
3	3.85 ± 0.7	15.43 ± 0.7	0.73 ± 0.3
4	5.48 ± 0.4	13.5 ± 0.6	1.12 ± 0.4
5	6.34 ± 0.5	11.8 ± 0.5	1.73 ± 0.4
6	7.53 ± 0.6	10.4 ± 0.6	2.12 ± 0.5
8	8.93 ± 0.5	8.8 ± 0.7	2.8 ± 0.4
10	9.95 ± 0.4	6.3 ± 0.5	3.2 ± 0.4
12	10.12 ± 0.5	4.6 ± 0.4	4.2 ± 0.5
14	10.43 ± 0.5	3.8 ± 0.5	4.8 ± 0.4
16	10.64 ± 0.4	3.1 ± 0.4	5.1 ± 0.5
18	10.93 ± 0.2	2.4 ± 0.3	5.26 ± 0.8
20	10.87 ± 0.9	2.3 ± 0.8	5.28 ± 0.7
22	10.42 ± 0.3	2.2 ± 0.3	5.3 ± 0.4
24	10.23 ± 0.4	2.1 ± 0.4	5.3 ± 0.5
26	10.04 ± 0.8	2 ± 0.7	5.3 ± 0.5
28	9.84 ± 0.4	1.9 ± 0.6	5.31 ± 0.8
30	9.75 ± 0.4	1.9 ± 0.2	5.31 ± 0.4

Concentration values are mean ± standard error (n = 3)

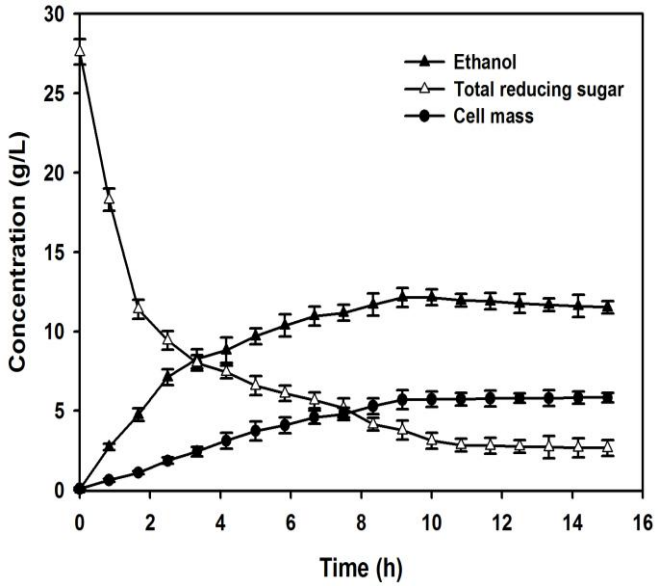

Fig. 7.3.8 Profiles of ethanol, total reducing sugar and cell mass in test (with mechanical agitation and intermittent ultrasound) experiments.

Table 7.3.7 Experimental data for the profiles of ethanol, sugar and cell mass in test experiments.

Time (h)	Ethanol concentration (g/L)	Sugar concentration (g/L)	cell mass concentration (g/L)
0	0.06 ± 0.02	27.6 ± 0.8	0.1 ± 0.08
0.8	2.71 ± 0.2	18.3 ± 0.7	0.63 ± 0.1
1.7	4.75 ± 0.4	11.4 ± 0.6	1.11 ± 0.11
2.5	7.12 ± 0.5	9.4 ± 0.6	1.86 ± 0.2
3.3	8.26 ± 0.6	8.0 ± 0.5	2.43 ± 0.3
4.2	8.81 ± 0.8	7.5 ± 0.4	3.12 ± 0.5
5.0	9.69 ± 0.5	6.6 ± 0.6	3.74 ± 0.6
5.8	10.37 ± 0.7	6.1 ± 0.5	4.1 ± 0.5
6.7	10.97 ± 0.6	5.7 ± 0.5	4.6 ± 0.4
7.5	11.17 ± 0.5	5.2 ± 0.6	4.8 ± 0.4
8.3	11.68 ± 0.7	4.2 ± 0.4	5.3 ± 0.5
9.2	12.14 ± 0.6	3.78 ± 0.6	5.7 ± 0.6
10.0	12.14 ± 0.5	3.1 ± 0.5	5.73 ± 0.5
10.8	11.96 ± 0.4	2.8 ± 0.4	5.74 ± 0.4
11.7	11.90 ± 0.5	2.8 ± 0.5	5.78 ± 0.5
12.5	11.76 ± 0.6	2.8 ± 0.4	5.79 ± 0.3
13.3	11.69 ± 0.4	2.7 ± 0.7	5.8 ± 0.5
14.2	11.59 ± 0.7	2.7 ± 0.6	5.83 ± 0.4
15.0	11.52 ± 0.4	2.7 ± 0.5	5.83 ± 0.3

Concentration values are mean ± standard error (n = 3)

Table 7.3.8 Summary of experimental results under control and test conditions.

Parameter	Control experiment*	Test experiment#
Maximum ethanol concentration (g/L)	10.93 ± 0.2	12.14 ± 0.5
Ethanol yield on glucose (g/g)	0.40	0.44
Ethanol yield on pretreated/delignified biomass (g/g)	0.28	0.31
Ethanol yield on raw biomass (g/g)	0.15	0.17
Ethanol productivity (g/L/h)	0.61	1.21
Maximum cell mass concentration (g/L)	5.26 ± 0.8	5.7 ± 0.5
Cell mass yield on glucose (g/g)	0.19	0.21
Cell mass yield on pretreated/delignified biomass (g/g)	0.14	0.15
Cell mass productivity (g/L/h)	0.29	0.57

**Maximum ethanol and cell mass concentration at 18 h of fermentation in control experiments and 10 h# in test experiments.*

An ethanol titer of 10.93 ± 0.2 g/L (0.4 g ethanol/g reducing sugar, 0.15 g ethanol/g raw biomass) and yeast cell concentration of 5.26 ± 0.8 g/L was achieved after 18 h of fermentation in control experiment. However, application of ultrasound on fermentation reduced the time to 10 h with an increased ethanol concentration of 12.14 ± 0.6 g/L (0.44 g/g reducing sugar, 0.166 g/g raw biomass) with cell mass 5.7 ± 0.5 g/L. Maximum ethanol and cell mass concentrations attained in the fermentation broth increased by ~10% with sonication. Moreover, the time of fermentation at which these values occurred reduced from 18 h in the control experiments to 10 h in test experiments. This essentially indicated a 2-fold rise in productivity with ultrasound irradiation. The results obtained in this study have been compared with the other reports in terms of ethanol productivity and ethanol yield (with respect to sugar and raw biomass) in Table 7.3.9.

Table 7.3.9 Comparison of the results obtained in this study with published literature.

Biomass/substrate	Organism	Mode of fermentation	Ethanol titer (g/L)	Ethanol productivity (g/L/h)	Ethanol yield (g/g of sugar)	Ethanol yield (g/g of raw biomass)	Reference
Waste paper	*Klebsiella oxytoca* P2	SSF with sonication	36.6	0.38*	0.36*	N. D.	Wood *et al*., 1997
Lantana camara	*Saccharomyces cerevisiae*	SHF without sonication	17.7	1.11	0.48	0.148	Kuhad *et al*. 2010
Saccharum spontaneum	*Saccharomyces cerevisiae* MTCC170	SHF without sonication	3.09	0.11	0.46	N. D.	Kataria and Ghosh 2011
Eichhornia crassipes	*Saccharomyces cerevisiae*	SHF without sonication	2.92	N. D.	0.04*	N. D.	Satyanagalakshmi *et al*. 2011
Lactose	*Kluyveromyces marxianus*	SHF with sonication	5.2	0.22	0.11	N. A.	Sulaiman *et al*. 2011
Prosopis juliflora	*Saccharomyces cerevisiae* HAU	SHF without sonication	34.78	3.16	0.45	N. D.	Gupta *et al*. 2012
Oil Palm fronds	*Saccharomyces cerevisiae*	SSF with sonication	18.2	3.64	0.29*	N. D.	Ofori-Boateng and Lee 2014
Parthenium hysterophorus	*Saccharomyces cerevisiae* MTCC170	SHF with sonication	12.14	1.21	0.44	0.166	This study
Parthenium hysterophorus	*Saccharomyces cerevisiae* MTCC170	SHF without sonication	10.93	0.61	0.40	0.149	This study

**calculated from the data given in paper. N. D., not determined. N. A., not applicable. SSF, Simultaneous saccharification and fermentation. SHF, separate hydrolysis and fermentation.*

7.3.4.2 Results from mathematical model of fermentations (with and without ultrasound)

The experimental and simulated time profiles of glucose, cell mass and ethanol concentration are shown in Fig. 7.3.9 and 7.3.10 for control (mechanical shaking) and test (mechanical shaking with intermittent sonication) experiments, respectively. As evident from the experimental profiles of glucose, cell mass and ethanol concentration in control (Fig. 7.3.7) and test (Fig. 7.3.8) experiments, the concentrations were almost constant after 16 h and 10 h of fermentation, respectively. The sugar concentration at that instant (3.1 g/L) was taken into consideration for deciding these points for modeling and GA optimization. The values of the kinetic and physiological parameters of the fermentation model fitted to the experimental data using GA optimization have been given in the Table 7.3.10.

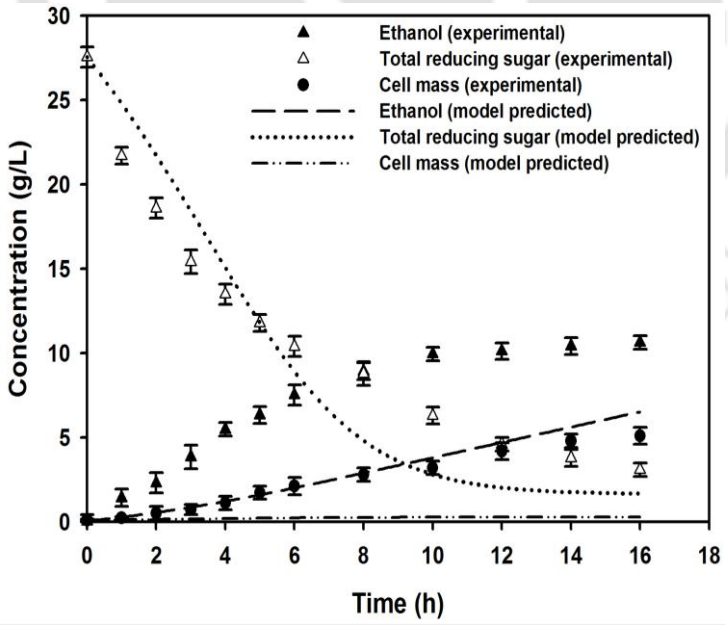

Fig. 7.3.9 Comparative representation of experimental and model predicted profiles of ethanol, total reducing sugar and cell mass in control experiment.

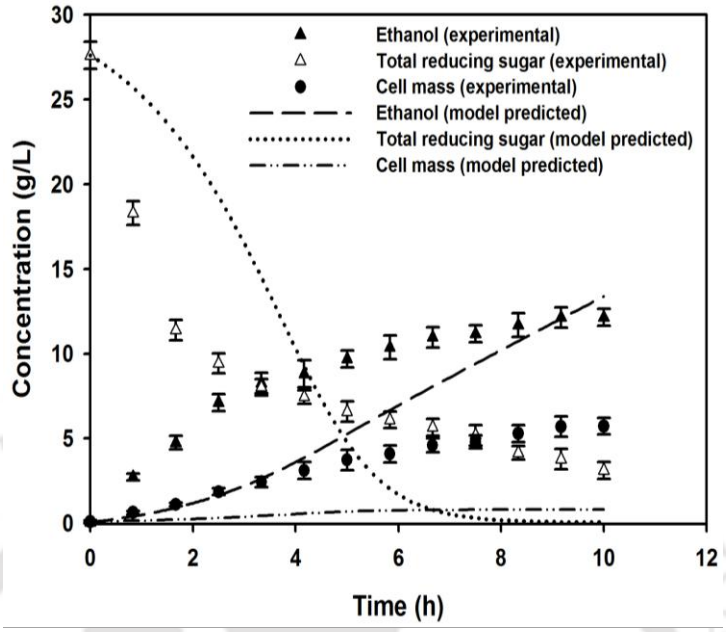

Fig. 7.3.10 Comparative representation of experimental and model predicted profiles of ethanol, total reducing sugar and cell mass in test experiment.

Table 7.3.10 Kinetic and physiological parameters in fermentation model fitted to experimental data with GA optimization.

Parameter	Control Experiment	Test Experiment
Monod constant for cell growth, K_3 (g/L)	26.19	20.08
Inhibition constant of cell growth by glucose, K_I (g/L)	83.44	96.45
Inhibition constant of cell growth by ethanol, K_{3E} (g/L)	49.99	47.61
Specific cell death rate, k_d (1/h)	0.083	0.005
Maximal specific growth rate, μ_m (1/h)	0.46	0.985
Constant for growth associated ethanol formation, a (g/g)	2.89	2.99
Non-growth associated specific ethanol production rate, b (g/g/h)	1.99	1.99
Average yield coefficient of cell mass on glucose, $Y_{X/G}$ (g/g)	0.002	0.026
Specific rate of substrate consumption for cell maintenance requirements, m (1/h)	0.271	0.116
Best fitness value for the model parameters	60	83

Comparison of the model parameters under test and control conditions indicated following trends:

1. Reduction in K_3 (Monod constant for glucose for cell growth) in test experiments indicating higher utilization of substrate for cell growth.
2. Increase in inhibition constant (K_I) for cell growth indicating greater tolerance of cells towards non-competitive inhibition by the substrate. On the other hand, the inhibition for cell growth by product (ethanol) remained practically unaltered with application of ultrasound, as seen from similar values of K_{3E} in control and test experiments.
3. The maximum specific growth rate increased, while the specific death rate reduced with ultrasound.

The trends in the kinetic and physiological parameters obtained by fitting the fermentation model to the experimental data gave an insight into the influence of ultrasound on various facets of fermentation process. Sonication of fermentation broth in test experiments caused reduction in Monod constant for cell growth, K_3. The reduction in K_3 (which is the substrate concentration required to achieve half of maximum specific growth rate of cell mass) is indicative of faster transport of glucose across the cell membrane due to which lesser bulk concentration of glucose is required to achieve maximum specific growth rate. In other words sonication assisted better utilization of glucose for cell growth, which was also supported by the rise in values of $Y_{X/G}$ and μ_{max}. Faster transport as well as utilization of glucose also resulted in rise in inhibition constant K_I, which essentially indicated that higher concentration of glucose is required for inhibition of cell growth. The reduction in K_3

and rise in K_I are thus synergistic effects of sonication on fermentation. Similar values of K_{3E} (i.e. inhibition constant due to product ethanol) remained practically same for both test and control experiments. This indicated that this is a sole physiological property of the cell which does not depend on its environment.

Ethanol is a product directly associated with energy generation by microorganism, which essentially means that it is a growth associated product. However, a value of 1.99 g/g/h for constant non-zero value of constant *b* in equation 3 indicates that ethanol formation occurred during stationary phase as well, which is non-growth associated production. The model for fermentation predicts same values of constants *a* and *b* for both control and test experiments. Thus, the mode of ethanol production does not get affected by sonication. However, for both control and test experiments, value of constant *a* was greater than that of *b*, which suggested that ethanol was predominantly a growth associated product.

The values of both k_d (specific cell death rate) and *m* (specific rate of substrate consumption for cell maintenance requirement) reduced with sonication. Cellular maintenance represents energy expenditure for repair of damaged cellular components and the transfer of nutrients and products in and out of the cells. It also includes the energy required for cell mobility and also for adjustment of the osmolarity of the cell's interior volume. The micro-convection generated by ultrasound waves assists the cell motility and de-agglomeration and the trans-membrane transport, which in turn regulates the osmolarity. Thus, under ultrasound irradiation the dependence of cells on substrate for maintenance reduces and larger fraction of glucose is utilized for ethanol production. The death phase of the cells

occurs mainly due to depletion of nutrients or accumulation of the toxic products. The strong microturbulence generated by the ultrasound assists efficient transfer of nutrients across the cells. Moreover, it also assists dilution of the toxic substances in the medium due to mixing. Both of these effects enhance the growth phase of the cells and reduce the death rate in the test experiments.

The results of simulations yielded practically similar values of constant for cell growth inhibition by ethanol (K_{3E}) in test and control experiments. This means that the mechanism by which ethanol inhibits cell growth is unaffected by physical or chemical effects of ultrasound and cavitation. Moulin *et al*. (1984) have reviewed various mechanisms of alcoholic inhibition of fermentation. There are two basic mechanisms through which ethanol inhibits the cell growth, *viz*. inhibition of the glycolytic enzymes (hexokinase being the most sensitive enzyme to non-competitive inhibition) and the effect on plasma membrane (i.e. modification of membrane fluidity, the transfer mechanisms and the activities of enzymes associated with membrane). The plasma membrane has a major role in regulating sugar and nutrient transport into the cell as well as the excretion of the metabolic products such as ethanol. Thomas and Rose (1979) and Leao and van Uden (1982) have attributed the inhibition of cell growth to decrease in the fluidity of the plasma membranes due to inhibitory effect of ethanol on action of one or more proteins involved in the transport of compounds in the cells and also modification of lipid content in the environment of the sugar transport system, which has major effect on the membrane permeability. These mechanisms are mostly of intrinsic type, which remain unaffected by the physical effect of microturbulence and microconvection induced by

ultrasound. Hence, the product inhibition constant, K_{3E}, does not change with sonication. The value of K_{3E} calculated in our model simulations (47.7 and 49.9 g/L for test and control experiments) matched closely with that reported in literature (50 g/L) (van Uden 1983).

7.3.5. Analysis of effect of ultrasound on viability and morphology of yeast cells

There was no significant change observed in SSC and FSC after sonication (Fig. 7.3.11A to D), which indicated that internal complexity and morphology of yeast cells remains same and thus corroborated no adverse effects on yeast cells.

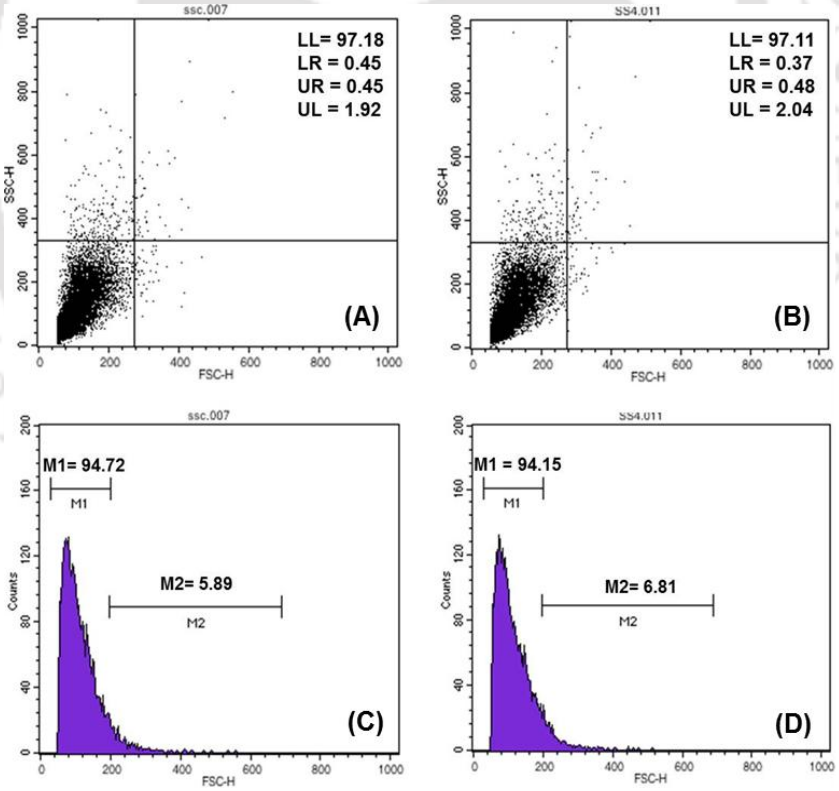

Fig. 7.3.11 Flow cytometric analysis for detecting morphological changes in *S. cerevisiae* MTCC170 cells under the influence of ultrasound (A) and (B) Acquisition dot plots (FSC versus SSC) of *S. cerevisiae* in control and test samples, respectively, (C) and (D) Histogram plots (Counts versus FSC) of *S. cerevisiae* in control and test samples, respectively.

The dead and viable yeast cells were distinguished as blue-stained and unstained cells, respectively by methylene blue staining method (Fig. 7.3.12A and B). Cell counting revealed that no cell death occurred due to ultrasonic irradiation and yeast cell viability was ~80% in both control and test samples. These results were in accordance with the outcomes from various studies, where the investigations on influence of sonication on yeast cells revealed that a mild and intermittent ultrasonic irradiation is not harmful to the cells (Wood *et al*. 1997, Radel *et al*. 2000, Sulaiman *et al*. 2011, Neel *et al*. 2012). However, the optimum sonication parameters such as ultrasound intensity and time of treatment (duty cycle) vary with the microorganisms.

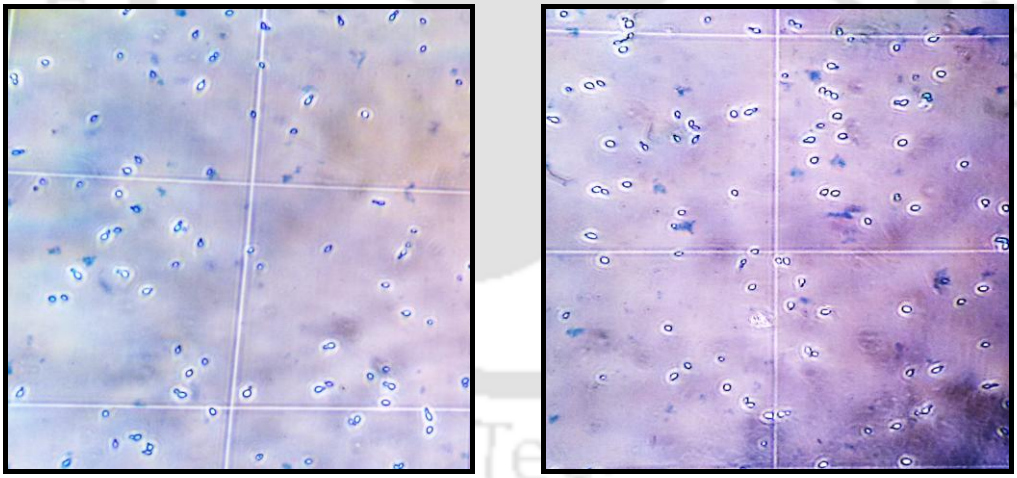

(A) **(B)**

Fig. 7.3.12 Micrographs of methylene blue stained yeast cells after completion of fermentation under (A) control experiments and (B) test experiments.

7.4 Conclusions

In this study, an attempted was made to get a physical insight into ultrasound induced enhancement in fermentation of hydrolyzate obtained from pretreatment and enzymatic hydrolysis of waste biomass *P. hysterophorus*. Results of fermentation (essentially the time profiles of substrate, cell concentration and ethanol concentration) with and without sonication were coupled to a model comprising of kinetic and physiological parameters that are characteristics of the mechanism of fermentation. The trends in these parameters gave an interesting account of the physical mechanism of ultrasound induced enhancement of ethanol fermentation. The results of this study revealed that the strong microturbulence and mild shock waves induced by ultrasound and cavitation augment trans-membrane transport of substrate and products as well as dilution of the toxic substances, both of which contributed to enhancement in cell growth with faster consumption of substrate and reduced cell death rate. The kinetics of ethanol formation rate showed a 2-fold enhancement with sonication in both cell mass and ethanol productivity. Nonetheless, the parameters related to intrinsic mechanisms of the cells, such as the inhibition constant for ethanol or the constants for growth and non-growth associated ethanol production remained unaffected by sonication. The results of this study provide important inputs in further mechanistic research in ultrasound-assisted bioethanol fermentation. The methodology adopted in this work can form a framework for investigations in other fermentation processes employing suitable mathematical models.

References

Abd-Aziz, S., Hung, G. S., Hassan, M. A., Karim, M. I. A. and Samat, N. (2008) Indirect method for quantification of cell biomass during solid state fermentation of palm kernel cake based on protein content. Asian Journal of Scientific Research 1, 385-393.

Bashari, M., Abdelhai, M. H., Abbas, S., Eibaid, A., Xu, X. and Jin, Z. (2014) Effect of ultrasound and high hydrostatic pressure (US/HHP) on the degradation of dextran catalyzed by dextranase. Ultrasonics Sonochemistry, 21, 76–83.

Bharadwaja, S. T. P. (2014) Mechanistic investigation in ultrasound assisted delignification and enzymatic hydrolysis of *Parthenium hysterophorus* for bioethanol production, M. Tech. thesis, Indian Institute of Technology Guwahati, Guwahati, Assam, India.

Chakma, S. and Moholkar, V. S. (2011) Mechanistic features of ultrasonic desorption of aromatic pollutants. Chemical Engineering Journal, 175, 356–367.

Dai, C., Ma, H., Gu X. and Tang, J. (2011) Ultrasound-accelerated enzymatic hydrolysis of defatted larva flour of *Tenebrio molitor* (L.). Journal of Food, Agriculture and Environment, 9, 101-106.

Gogate, P. R., Tatake, P. A., Kanthale, P. M. and Pandit, A. B. (2002) Mapping of sonochemical reactors: Review, analysis, and experimental verification. AIChE Journal, 48, 1542-1560.

Guiseppi-Elie, A., Choi, S. H. and Geckeler, K. E. (2009) Ultrasonic processing of enzymes: Effect on enzymatic activity of glucose oxidase. Journal of Molecular Catalysis B: Enzymatic, 58, 118–123.

Gupta, R., Kumar, S., Gomes, J. and Kuhad, R.C. (2012) Kinetic study of batch and fed-batch enzymatic saccharification of pretreated substrate and subsequent fermentation to ethanol. Biotechnology for Biofuels, 5, 16.

Imai, M., Ikari, K. and Suzuki, I. (2004) High-performance hydrolysis of cellulose using mixed cellulase species and ultrasonication pretreatment. Biochemical Engineering Journal, 17, 79-83.

Karuppaiya, M., Sasikumar, E., Viruthagiri, T. and Vijayagopal, V. (2010) Optimization of process variables using response surface methodology (RSM) for ethanol production from cashew apple juice by *Saccharomyces cerevisiae*. Asian Journal of Food and Agro-Industry, 3, 462-473.

Khanna, S., Jaiswal, S., Goyal, A. and Moholkar, V. S. (2012) Ultrasound enhanced bioconversion of glycerol by *Clostridium pasteurianum*: A mechanistic investigation. Chemical Engineering Journal, 200-202, 416-425.

Khanna, S., Jaiswal, S., Goyal, A. and Moholkar, V. S. (2013) Mechanistic investigation of ultrasonic enhancement of glycerol bioconversion by immobilized *Clostridium pasteurianum* on silica support. Biotechnology and Bioengineering, 110, 1637-1645.

Kuhad, R. C., Gupta, R., Khasa, Y. P. and Singh, A. (2010) Bioethanol production from *Lantana camara* (red sage): pretreatment, saccharification and fermentation. Bioresource Technology, 101, 8348-8354.

Lanchun, S., Bochu, W., Liancai, Z., Jie, L., Yanhong, Y. and Chuanren, D. (2003) The influence of low-intensity ultrasonic on some physiological characteristics of *Saccharomyces cerevisiae*. Colloids and Surfaces B:

Biointerfaces, 30, 61-66.

Leao, C. and van Uden, N. (1982) Effects of ethanol and other alkanols on the glucose transport system of *Saccharomyces cerevisiae*. Biotechnology and Bioengineering, 24, 2601-2604.

Lee, S. H., Nguyen H. M., Koo, Y. M. and Ha S. H. (2008) Ultrasound-enhanced lipase activity in the synthesis of sugar ester using ionic liquids. Process Biochemistry, 43, 1009–1012.

Lowry, O. H., Rosebrough, N. J., Farr, A. L. and Randall, R. J. (1951) Protein measurement with the Folin phenol reagent. Journal of Biological Chemistry, 193, 265-275.

Lunelli, F. C., Sfalcin, P., Souza, M., Zimmermann, E., Pra, V. D., Foletto, E. L., Jahn, S. L., Kuhn, R. C. and Mazutti, M. A. (2014) Ultrasound-assisted enzymatic hydrolysis of sugarcane bagasse for the production of fermentable sugars. Biosystems Engineering, 124, 24-28.

Malani, R. S., Khanna, S. and Moholkar, V. S. (2013) Sonoenzymatic decolourization of an azo dye employing immobilized horse radish peroxidase (HRP): A mechanistic study. Journal of Hazardous Materials, 256–257, 90–97.

Malani, R. S., Khanna, S., Chakma, S. and Moholkar, V. S. (2014) Mechanistic insight into sono-enzymatic degradation of organic pollutants with kinetic and thermodynamic analysis. Ultrasonics Sonochemistry 21, 1400–1406.

Matsuo, Y., Asakava, K., Toda, T. and Katayama, S. (2006) A rapid method for protein extraction from fission yeast. Bioscience, Biotechnology and Biochemistry, 70, 1992-1994.

Moholkar, V. S. Huitema, M., Rekveld, S. and Warmoeskerken, M. M. C. G. (2002) Characterization of an ultrasonic system using wavelet transforms. Chemical Engineering Science, 57, 617–629.

Moholkar, V. S., Sable, S. P. and Pandit, A. B. (2000) Mapping the cavitation intensity in an ultrasonic bath using the acoustic emission. AIChE Journal, 46, 684-694.

Moulin, G., Helen, B. and Galzy, P. (1984) Inhibition of alcoholic fermentation. Biotechnology and Genetic Engineering Reviews, 2, 365-382.

Neel, P. I., Gedanken, A., Schwarz, R. and Sendersky, E. (2012) Mild sonication accelerates ethanol production by yeast fermentation. Energy and Fuel, 26, 2352-2356.

Nelson, N. (1944) A photometric adaptation of the Somogyi method for the determination of glucose. Journal of Biological Chemistry, 153, 375-380.

Ofori-Boateng, C. and Lee, K. T. (2014) Ultrasonic-assisted simultaneous saccharification and fermentation of pretreated oil palm fronds for sustainable bioethanol production. Fuel, 119, 285-291.

Painting, K. and Kirsop, B. (1990) A quick method for estimating the percentage of viable cells in a yeast population, using methylene blue staining. World Journal of Microbiology and Biotechnology, 6, 346-347.

Pandiyan, K., Tiwari, R., Rana, S., Arora, A., Singh, S., Saxena, A. K. and Nain, L.

(2014) Comparative efficiency of different pretreatment methods on enzymatic digestibility of *Parthenium* sp. World Journal of Microbiology and Biotechnology, 30, 55-64.

Philippidis, G. P., Smith, T. K. and Wyman, C. E. (1993) Study of the enzymatic hydrolysis of cellulose for production of fuel ethanol by the simultaneous saccharification and fermentation process. Biotechnology and Bioengineering, 41, 846-853.

Philippidis, G. P., Spindler, D. D. and Wyman, C. E. (1992) Mathematical modeling of cellulose conversion to ethanol by simultaneous saccharification and fermentation process. Applied Biochemistry and Biotechnology, 34/35, 543-556.

Rana, S., Tiwari, R., Arora, A., Singh, S., Kaushik, R., Saxena, A. K., Dutta, S. C. and Nain, L. (2013) Prospecting *Parthenium* sp. pretreated with *Trametes hirsuta*, as a potential bioethanol feedstock. Biocatalysis and Agricultural Biotechnology, 2, 152-158.

Schlafer, O., Sievers, M., Klotzbucher, H. and Onyeche, T. I. (2000) Improvement of biological activity by low energy ultrasound assisted bioreactors. Ultrasonics, 38, 711-716.

Shao, X., Lynd, L. and Wyman, C.E. (2009) Kinetic modeling of cellulosic biomass to ethanol via simultaneous saccharification and fermentation: Part II. Experimental validation using waste paper sludge and anticipation of CFD analysis. Biotechnology and Bioengineering, 102, 66-72.

Singh, S., Bharadwaja, S. T. P., Yadav, P. K., Moholkar, V. S. and Goyal, A. (2014b)

Mechanistic investigation in ultrasound-assisted (alkaline) delignification of *Parthenium hysterophorus* biomass. Industrial and Engineering Chemistry Research, 53, 14241-14252.

Singh, S., Dikshit, P. K., Moholkar, V. S. and Goyal, A. (2014c) Purification and characterization of acidic cellulase from *Bacillus amyloliquefaciens* SS35 for hydrolyzing *Parthenium hysterophorus* biomass. Environmental Progress and Sustainable Energy, doi:10.1002/ep.12046.

Singh, S., Khanna, S., Moholkar, V. S. and Goyal, A. (2014a) Comparative assessment of pretreatment strategies for enzymatic saccharification of *Parthenium hysterophorus*. Applied Energy, 129, 195-206.

Singh, S., Moholkar, V. S. and Goyal, A. (2013) Isolation, identification and characterization of a cellulolytic *Bacillus amyloliquefaciens* strain SS35 from rhinoceros dung. ISRN Microbiology, Article ID 728134, 7 pages.

Sivasankar, T., Paunikar, A. W. and Moholkar, V. S. (2007) Mechanistic approach to enhancement of the yield of a sonochemical reaction. AIChE Journal, 53, 1132-1143.

Somogyi, M. (1945) A new reagent for the determination of sugars. Journal of Biological Chemistry, 160, 61-68.

Souza, M., Mezadri, E. T., Zimmerman, E., Leaes, E. X., Bassaco, M. M., Prá, V. D., Foletto, E., Cancellier, A., Terra, L. M., Jahn S. L. and Mazutti, M. A. (2013) Evaluation of activity of a commercial amylase under ultrasound-assisted irradiation. Ultrasonics Sonochemistry, 20, 89-94.

Subhedar, P. B. and Gogate, P. R. (2014) Enhancing the activity of cellulase enzyme using ultrasonic irradiations. Journal of Molecular Catalysis B: Enzymatic, 101 108–114.

Subhedar, P. B., Babu, N. R. and Gogate, P. R. (2015) Intensification of enzymatic hydrolysis of waste newspaper using ultrasound for fermentable sugar production. Ultrasonics Sonochemistry, 22, 326–332.

Sulaiman, A. Z., Ajit, A. and Chisti, Y. (2013) Ultrasound mediated enzymatic hydrolysis of cellulose and carboxymethyl cellulose. Biotechnology Progress, 29, 1448-1457.

Sulaiman, A. Z., Ajit, A. Yunus, R. M. and Chisti, Y. (2011) Ultrasound-assisted fermentation enhances bioethanol productivity. Biochemical Engineering Journal, 54, 141-150.

Suslick, K. S. (1990) Sonochemistry. Science, 247, 1439-1445.

Thomas, D. S. and Rose, A. H. (1979) Inhibitory effect of ethanol on growth and solute accumulation by *Saccharomyces cerevisiae* as affected by plasma membrane lipid composition. Archives of Microbiology, 122, 49-55.

van Uden, N. (1983) Effects of ethanol on temperature relation of viability and growth in yeast. CRC Critical Reviews in Biotechnology, 1, 263-272.

Wood, B. E., Aldrich, H. C. and Ingram, L. O. (1997) Ultrasound stimulates ethanol production during the simultaneous saccharification and fermentation of mixed waste office paper. Biotechnology Progress, 13, 232-237.

Chapter 8

Ultrasound induced enhancement of ethanol production from *Parthenium hysterophorus*: simultaneous saccharification and fermentation

8.1 Introduction

Bioethanol production from lignocellulosic biomass has been a highly active research area for past several years, as ethanol has shown high promise as an alternate liquid transportation fuel as well as oxygenate blend for gasoline. The conventional process for bioethanol production has two steps, viz. pretreatment and acid/enzymatic hydrolysis of lignocellulosic biomass followed by fermentation of the acid and/or enzymatic hydrolyzate. The cost of production of bioethanol is dependent on substrate as well as the efficiency of the process. Lignocellulosic biomass waste is abundant in the form of agro-residues, forest-residues and waste biomass (weed/grass) forms a potential low-cost feedstock for generation of bioethanol. Some typical examples of waste biomass whose carbohydrate content have been used for bioethanol production are *Saccharum spontaneum* (Kataria and Ghosh 2011), *Lantana camara* (Kuhad *et al*. 2010) and *Prosopis juliflora* (Gupta *et al*. 2012). In order to intensify the bioethanol productivity while at the same time reducing the cost of production, the process of simultaneous saccharification and fermentation (SSF)

has also been extensively investigated. This process has distinct advantages of milder operating conditions and requirement of a single fermentor vessel that combines the two steps of hydrolysis and fermentation mentioned above. In this process, hexose sugars released from enzymatic hydrolysis of cellulose in the biomass are simultaneously consumed by fermenting microorganisms. The enzymatic hydrolysis of cellulose itself is a two step process, in which first cellulase hydrolyzes the cellulose into cellobiose (dimer hexose sugar units), which are later split into monomeric hexose sugar units by cellobiase (or β-glucosidase). SSF process reduces the inhibitory effect of substrate (sugar) concentration on enzymes and also the probability of contamination by undesired invasive microorganisms (Galbe and Zacchi 2002). These features increase yield as well as kinetics of the saccharification as well as fermentation as compared to the conventional two-step process.

More recently, the technique of ultrasound irradiation or sonication of the fermentation broth for intensification of bioethanol fermentation has been used. Ultrasound is a well known technique for intensification of numerous physical and chemical processes. Ultrasound manifests its effect on the reaction system through phenomenon of cavitation, which includes nucleation, growth, oscillations and implosive transient collapse of tiny gas or vapor bubbles, which is driven by pressure variation generated in the medium during passage of ultrasound wave (Shah *et al*. 1999). Both ultrasound and cavitation render several physical and chemical effects on the reactions system, which are beneficial in enhancing the kinetics of the system. The most peculiar feature of energy introduction into the medium via ultrasound and cavitation is that implosive collapse of cavitation bubbles creates intense energy

concentration on an extremely small spatial and temporal scale. The main physical effect of ultrasound and cavitation is generation of intense micro-turbulence in the medium that gives very effective micro-mixing, which eliminates mass transfer limitations (Shah *et al*. 1999). The chemical effect of transient cavitation is generation of highly reactive radicals and other smaller species through dissociation of vapor entrapped in the bubble at the moment of transient collapse. Literature on application of ultrasound during bioethanol synthesis through SSF process is rather limited. Wood *et al*. (1997) reported bioethanol production using ultrasound (36 kHz, 150 W) assisted SSF process. They used waste paper as substrate and the microbial strain *Klebsiella oxytoca*. Bioethanol yield was found to increase by 20% by sonication. Ofori-Boateng and Lee (2014) investigated bioethanol production using SSF process from oil palm fronds as substrate and *S. cerevisiae* as the microbe. With ultrasound of 40 kHz frequency and 200 W intensity, 4-fold increment in bioethanol yield was observed within 5 h.

In order to effectively utilize the potential of ultrasound on intensification of the SSF process for bioethanol production, it is essential to understand the basic underlying physical mechanism. This would essentially mean identifying the links between physics of ultrasound and cavitation and the biochemistry of fermentation. In this chapter, this important issue has been addressed with the approach of coupling experimental results to a mathematical model. In this study, the fermentation model given by Philippidis *et al*. (1992) was used. It comprised 5 ordinary differential equations, *viz*. one each for cellulose, cellobiose, glucose, microbial cell concentration and ethanol. This model takes into account the essential physiology of

the SSF process. A major practical limitation of implementation of this model is difficulty in monitoring of the concentration of cellulose (which occurs in solid phase) and also the unstable intermediate of hexose-dimer cellobiose (which is rapidly decomposed into monomeric glucose) during fermentation (Shen and Agblevor 2010). Despite this limitation, fitting of the experimental data of microbial cell concentration and ethanol to their respective differential model equations reveals important mechanistic account of the influence of ultrasound on the SSF process. In this study the waste biomass *Parthenium hysterophorus* was used as substrate and *Saccharomyces cerevisiae* as the fermenting microorganism.

8.2 Materials, Methods and Mathematical Model

8.2.1 *Parthenium hysterophorus* biomass collection and processing

P. hysterophorus biomass was collected from the campus of (IIT Guwahati). Biomass was chopped (~ 5 cm), washed with water, dried at 60 ± 3^{o}C for 24 h and ground to a particle size of ~ 1 mm. Powdered biomass was pretreated with 1% (v/v) H_2SO_4 + 30 min autoclaving (Chapter 6, Section 6.3.3) (Singh *et al*. 2014a) and the solid residue was further delignified by ultrasound assisted alkaline treatment (Chapter 6, Section 6.3.3.1) (Singh *et al*. 2014b).

8.2.2 Chemicals and reagents

All components of fermentation medium were procured from HiMedia Pvt. Ltd., India. Glucose (99.5% purity, as standard for HPLC and for reducing sugar estimation) was procured from Sigma Aldrich, USA. Ethanol (99.5% purity) was procured from Tedia Chemicals, USA. All other chemicals were procured from Fischer Scientific, India.

8.2.3 Source of enzymes

Carboxymethylcellulase (CMCase) was produced from *Bacillus amyloliquefaciens* SS35 isolated from rhinoceros dung (Chapter 3, Section 3.2.3) (Singh *et al*. 2013). The specific activity of the enzyme was 1.0 U/mg (1.7 mg/mL) (Chapter 5, Section 5.3.1) (Singh *et al*. 2014c), *β*-glucosidase (250 U/g) produced from *Aspergillus niger* (Novozyme 188) was procured from Sigma Aldrich, USA.

8.2.4 Microorganism and fermentation conditions

Saccharomyces cerevisiae MTCC170, used for ethanol fermentation, was procured from Microbial Type Culture Collection (MTCC), Institute of Microbial Technology (IMTECH), Chandigarh, India and was maintained in YEPD medium containing yeast extract (10 g/L), peptone (20 g/L) and dextrose (20 g/L).

8.2.5 Simultaneous saccharification and fermentation: Control experiment

Simultaneous saccharification and fermentation (SSF) of pretreated and delignified *P. hysterophorus* was carried out by using the enzymes, CMCase and *β*-glucosidase and microbe *S. cerevisiae* MTCC170. 3.88% (w/v) pretreated and delignified *P. hysterophorus* biomass was added to fermentation medium, which consisted of yeast extract (10 g/L), KH_2PO_4 (2 g/L), $(NH_4)_2SO_4$ (1 g/L) and $MgSO_4 \cdot 7H_2O$ (1 g/L) (pH 5.0) (Karuppaiya *et al*. 2010). This mixture was supplemented with CMCase and *β*-glucosidase with concentrations of 600 U/g and 50 FPU/g of delignified biomass, respectively. SSF was carried out in a 150 mL Erlenmeyer flask with working volume of 25 mL. The medium was inoculated with 10% (v/v) of previously grown culture of *S. cerevisiae* MTCC170 and incubated at 30^{o}C and 150 rpm in an incubator shaker (Scigenics Biotech, Orbitek).

8.2.6 Simultaneous saccharification and fermentation: Test experiment

Ultrasound-assisted fermentation (test experiment) was carried out in an ultrasound bath (Tran-sonic T-460, Elma, Germany, 2L) operating at a frequency of 35 kHz and power rating of 35 W. The actual power input and dissipation in the

water of the bath was 18.58 W and 1.48 W/cm^2, respectively which corresponds to acoustic power amplitude of 150 kPa (Chapter 7, Section 7.2.7). The reaction set up and sonication cycles (10%) were similar as described in Section 7.2.7 of Chapter 7. The temperature of the bath was maintained at 30^o ± 2^{o}C by replacing small portions of initial water at regular intervals.

200 µL aliquots of the fermentation broth were withdrawn intermittently in both control and test experiments to determine total reducing sugar, ethanol and cell mass concentration in fermentation broth. The total fermentation period for control and test experiments was set at 78 and 35 h, respectively, based on the concentration of residual sugar in the samples of fermentation broth. The fermentation was stopped when the sugar concentration became constant (< 2% difference) in the consecutive samples withdrawn from fermentation broth. Both test and control experiments were performed thrice to assess the reproducibility of the results.

8.2.7 Determination of total reducing sugar, cell mass and cell viability

The aliquots (200 µL) withdrawn from fermentation broth were analysed for residual reducing sugar using D-glucose as standard by the method of Nelson (1944) and Somogyi (1945). Dry cell mass for yeast cells was determined by using a calibration curve of intracellular protein content (g/L) versus dry cell mass (g/L) Abd-Aziz *et al*. 2008) which was drawn by following the method described in Section 7.2.9 of Chapter 7. Viability of *S. cerevisiae* MTCC170 cells in the samples before and after sonication was determined using methylene blue staining method (Painting and Kirsop 1990) as described in Section 7.2.11 of Chapter 7.

8.2.8 Analytical methods

The presence of glucose in the aliquots of fermentation broth was confirmed with HPLC analysis (Perkin-Elmer, Series 200, with a refractive index detector) using HiPlex-H column (300 mm × 5 μm × 4.6 mm, Varian). HPLC grade water (deionized water, Milli Q) was used as the mobile phase at a flow rate of 0.4 mL/min with glucose (99.5% purity) as standard in sugar analysis. The estimation of ethanol was done by Gas Chromatography (Varian, CP 3800) using a CP Wax 52 CB capillary column (250 mm × 0.25 mm × 0.39 mm, Varian) with ethanol (99.5% purity) as the standard. The oven temperature was programmed from 45^{o}C to 100^{o}C with an increment of 3^{o}C/min and after 100^{o}C, an increment of 5^{o}C/min up to 200^{o}C. The injector and detector temperatures were kept at 230^{o}C and 250^{o}C, respectively. Nitrogen gas was used as a carrier at a flow rate of 2 mL/min.

8.2.9 Mathematical model

The ethanol fermentation model for SSF, developed by Philippidis *et al*. (1992) was used in this study. This model is essentially based on the HCH-1 model of enzymatic hydrolysis of cellulose reported by Holtzapple *et al*. (1984). This model makes several assumptions as follows: (1) No distinction between two components of cellulase, *viz*. endoglucanase and exoglucanase; (2) exogenous addition of cellulose hydrolysing enzymes, *viz*. cellulase and *β*-glucosidase to the SSF system; (3) cellulose is hydrolyzed to cellobiose by cellulase with negligible formation of glucose; (4) pH of the fermentation broth remains practically constant during SSF process; (5) major metabolic products of SSF process are ethanol and CO_2, (6) the

carbon source for metabolism (glucose) is derived from cellulose, while the growth medium provides sufficient excess of all other nutrients and (7) the activities of cellulase and β-glucosidase enzymes are assumed to remain constant throughout the process. The model of Philippidis *et al*. (1992) proposes that cellulose to ethanol conversion process in SSF mode comprises of the following steps: (1) cellulase diffusion towards cellulose, (2) adsorption of cellulase on surface of cellulose, (3) hydrolysis of cellulose to cellobiose, (4) diffusion of cellobiose into aqueous phase, (5) hydrolysis of cellobiose to glucose (catalyzed by β-glucosidase), (6) glucose diffusion towards cells, (7) glucose uptake by cells, (8) glucose to ethanol conversion and (9) ethanol secretion into aqueous phase. The model comprises of five ordinary differential equations for cellulose (eq. 8.1), cellobiose (eq. 8.2), glucose (eq. 8.3), cell mass (eq. 8.4) and ethanol (eq. 8.5) as follows:

Cellulose:

$$\frac{d(C)}{dt} = \left(\frac{k_1 \alpha_t (E_1)_t}{\left[K_e + (E_1)_t\right]\left[1 + \frac{(B)}{K_{1B}} + \frac{(G)}{K_{1G}}\right]} \right) \times \left(\frac{K_{1E}}{K_{1E} + (E)} \right) \qquad \text{(eq. 8.1)}$$

Cellobiose:

$$\frac{d(B)}{dt} = 1.06 \left(\frac{k_1 \alpha_t (E_1)_t}{\left[K_e + (E_1)_t\right]\left[1 + \frac{(B)}{K_{1B}} + \frac{(G)}{K_{1G}}\right]} \frac{K_{1E}}{K_{1E} + (E)} \right) - \left(\frac{k_2 (E_2)(B)}{K_m \left[1 + \frac{(G)}{K_{2G}}\right] + (B)\left[1 + \frac{(B)}{K_{2B}}\right]} \frac{K_{2E}}{K_{2E} + (E)} \right) \qquad \text{(eq. 8.2)}$$

Glucose:

$$\frac{d(G)}{dt} = 1.05\left(\frac{k_2(E_2)(B)}{K_m\left[1+\frac{(G)}{K_{2G}}\right]+(B)\left[1+\frac{(B)}{K_{2B}}\right]} \frac{K_{2E}}{K_{2E}+(E)} \right) - \left(\frac{1}{Y_{X/G}} \frac{d(X)}{dt} + m(X) \right) \quad \text{(eq. 8.3)}$$

Cell mass:

$$\frac{d(X)}{dt} = \left(\frac{\mu_m(G)}{K_3+(G)+\frac{(G)^2}{K_I}} \frac{K_{3E}}{K_{3E}+(E)}(X) \right) - \left(k_d(X)\right) \quad \text{(eq. 8.4)}$$

Ethanol:

$$\frac{d(E)}{dt} = \left(a\frac{d(X)}{dt} + b(X) \right) \times \left(\frac{(G)}{K_4+(G)} \right) \quad \text{(eq. 8.5)}$$

Notation: *C*, *B*, *G*, *X*, *E* - concentrations of cellulose, cellobiose, glucose, cell mass and ethanol, respectively, *a*, *b* - constants for ethanol formation, growth associated and non-growth associated, respectively, α_t - available surface area for cellulose, $(E_1)_t$ - total concentration of cellulase in the solution, (E_2) - concentration of β-glucosidase in the solution, k_d - specific rate of cell death, k_1, k_2 - specific rates of cellulose and cellobiose hydrolysis, respectively, K_I - constant of cell growth inhibition by glucose, K_m - Michaelis constant of β-glucosidase for cellobiose, K_3, K_4 - Monod constants of glucose for cell growth and ethanol synthesis, respectively, K_{1B}, K_{2B} - Inhibition constants of cellulase and β-glucosidase by cellobiose, respectively, *t* - time, K_{1G}, K_{2G} - inhibition constants of cellulase and β-glucosidase by glucose, respectively, K_{1E}, K_{2E}, K_{3E} - Inhibition constants of cellulase, β-

glucosidase and cell growth by ethanol, respectively, m -specific rate of substrate consumption for maintenance requirements, μ_m - maximal specific growth rate, $Y_{X/G}$ - average yield coefficient of cell mass on substrate (glucose).

The following changes have been made in original model equations of Philippidis *et al*. (1992) in view of experimental conditions of present experiments. In view of acid + autoclaved biomass that results in high reduction of cellulose crystallinity and increase in porosity, the value of substrate reactivity coefficient (ϕ) is set to 1. The values of two parameters, *viz*. adsorption constants for cellulase and β-glucosidase onto lignin are set to zero in view of use of delignified biomass as the substrate in SSF process. The concentration of lignin in the biomass is also assumed to be zero. The zero value has been assigned to parameter K_4 (Monod constant of glucose for ethanol synthesis) as per the results of Philippidis *et al*. (1992) which demonstrated that ethanol formation was not directly dependent on the glucose concentration.

As stated earlier, due to limitations of experimental facilities used in this study, the concentration of cellulose (existing in solid phase) and the intermediate dimeric cellobiose during the fermentation process, could not be monitored. However, the instantaneous concentration of glucose in the fermentation broth was monitored. Therefore, while fitting the experimental data, only the equations for cell mass and ethanol were used. These equations have a total of 7 parameters, *viz*. K_3, K_I, K_{3E}, k_d, μ_m, a and b. The glucose concentration profile obtained during SSF experiments was fitted to a polynomial expression and which was used to determine

instantaneous glucose concentration in the broth at a particular time, by numerical integration of the differential equations for cell mass and ethanol.

Fitting of these equations to the experimental profiles of cell mass and ethanol would yield the numerical values of these model parameters, which represent kinetic and physiological facets of the SSF system. Variations in the values of these model parameters for the test and control experiments give a mechanistic account of the influence of ultrasound on the SSF system. For determination of the optimum values of the model parameters - so as to match the experimental and model predicted trends, the main model of two simultaneous ordinary differential equations was solved using Runge-Kutta 4^{th} order method and the solution was coupled to Genetic Algorithm (GA) optimization module of MATLAB. Optimization of the model parameters was done by calculating root mean square (RMS) error between experimental and model results. GA module minimizes this error, yielding optimized values of the model parameters. The overall algorithm of simulations of fermentation with the model is depicted in the flow chart given in Section 7.2.13 of Chapter 7 (Fig. 7.2.2).

8.3 Results and Discussion

8.3.1 Simultaneous saccharification and fermentation (SSF): with and without sonication

The profiles of ethanol, total reducing sugar and cell mass in control experiment are shown in Figure 8.3.1 and Table 8.3.1, for the test experiment the profiles are shown in Figure 8.3.2 and Table 8.3.2. The summary of the results of the SSF process is given in Table 8.3.3; the values in parentheses are the results of SHF experiments (Chapter 7, Section 7.3.4). The SSF with mechanical shaking resulted in a maximum ethanol concentration of 10.57 g/L after 54 h of fermentation, with an ethanol yield of 0.27 g/g of pretreated biomass (0.15 g ethanol/g raw biomass). At the same time, the cell mass concentration of 4.37 g/L was achieved with a yield of 0.11 g cell mass/g of pretreated biomass. Ethanol and cell mass productivities in control experiment were 0.2 g/L/h and 0.08 g/L/h, respectively. The most notable effect of sonication on SSF was in terms of reduction in time of fermentation. With sonication 3-fold reduction in fermentation time was observed with only 18.3 h in test experiment against 54 h in control experiment. However, while comparing with the SHF which showed fermentation period of just 10 h (not inclusive of the time of cellulose hydrolysis prior to fermentation) after sonication, the SSF after sonication gave slower reaction kinetics. In ultrasound assisted SSF, ethanol titer was increased to 15.62 g/L (from 10.57 g/L) with a yield of 0.4 g ethanol/g pretreated biomass or 0.21 g ethanol/ g raw biomass. Due to the reduction in overall fermentation time period and the enhancement in ethanol and cell mass concentrations, the ethanol and cell mass productivities increased by 4-fold in the test experiment, *viz*. 0.85 g/L/h and 0.36 g/L/h, respectively, as compared with the control experiment.

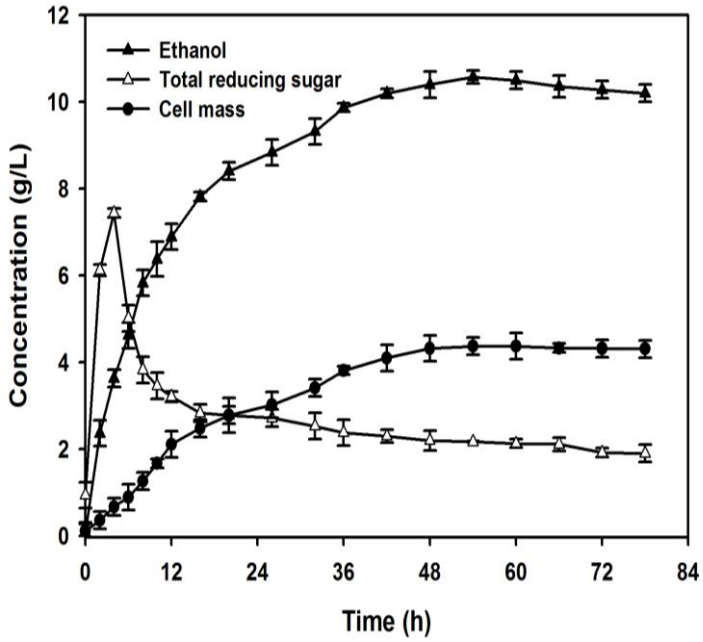

Fig. 8.3.1 Profiles of ethanol, glucose and cell mass in control experiment (with mechanical shaking of SSF system).

Table 8.3.1 Experimental data for the profiles of ethanol, glucose and cell mass in control experiments.

Time (h)	Ethanol concentration (g/L)	Sugar concentration (g/L)	cell mass concentration (g/L)
0	0.07 ± 0.20	0.94 ± 0.30	0.11 ± 0.20
2	2.36 ± 0.30	6.13 ± 0.13	0.36 ± 0.20
4	3.63 ± 0.20	7.44 ± 0.10	0.67 ± 0.20
6	4.62 ± 0.30	5.01 ± 0.30	0.89 ± 0.30
8	5.83 ± 0.30	3.82 ± 0.30	1.26 ± 0.20
10	6.38 ± 0.40	3.46 ± 0.30	1.67 ± 0.10
12	6.89 ±0.30	3.21 ± 0.12	2.11 ± 0.30
16	7.82 ± 0.10	2.83 ± 0.20	2.48 ± 0.20
20	8.41 ± 0.20	2.78 ± 0.20	2.78 ± 0.40
26	8.84 ± 0.30	2.72 ± 0.20	3.02 ± 0.30
32	9.32 ± 0.30	2.53 ± 0.30	3.41 ± 0.20
36	9.87 ± 0.10	2.38 ± 0.30	3.81 ± 0.10
42	10.2 ± 0.10	2.30 ± 0.15	4.10 ± 0.30
48	10.4 ± 0.30	2.20 ± 0.23	4.32 ± 0.30
54	10.57 ± 0.15	2.17 ± 0.01	4.37 ± 0.20
60	10.5 ± 0.20	2.13 ± 0.10	4.37 ± 0.30
66	10.36 ± 0.25	2.11 ± 0.15	4.33 ± 0.10
72	10.28 ± 0.20	1.92 ± 0.10	4.32 ± 0.20
78	10.20 ± 0.20	1.90 ± 0.20	4.31 ± 0.20

Concentration values are mean ± standard error (n = 3)

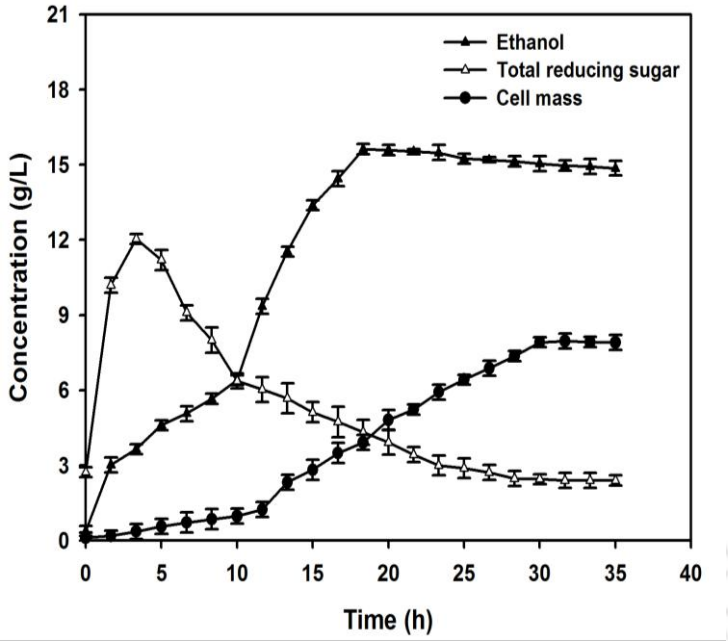

Fig. 8.3.2 Profiles of ethanol, glucose and cell mass in test experiment (with sonication of SSF system at 10% duty cycle).

Table 8.3.2 Experimental data for the profiles of ethanol, glucose and cell mass in test experiments.

Time (h)	Ethanol concentration (g/L)	Sugar concentration (g/L)	cell mass concentration (g/L)
0	0.03 ± 0.20	2.73 ± 0.20	0.11 ± 0.20
1.7	2.46 ± 0.30	10.19 ± 0.30	0.85 ± 0.20
3.3	3.65 ± 0.20	12.04 ± 0.20	1.79 ± 030
5.0	4.59 ± 0.20	11.19 ± 0.40	2.42 ± 0.30
6.7	5.07 ± 0.30	9.09 ± 0.30	3.54 ± 0.40
8.3	5.65 ± 0.20	8.00 ± 0.50	3.86 ± 0.40
10.0	6.39 ± 0.20	6.36 ± 0.30	4.12 ± 0.30
11.7	9.35 ± 0.30	6.02 ± 0.50	4.82 ± 0.30
13.3	11.53 ± 0.20	5.68 ± 0.60	5.13 ± 0.30
15.0	13.38 ± 0.20	5.12 ± 0.40	5.83 ± 0.40
16.7	14.43 ± 0.30	4.73 ± 0.60	6.23 ± 0.40
18.3	15.62 ± 0.20	4.37 ± 0.50	6.53 ± 0.30
20.0	15.58 ± 0.20	3.92 ± 0.50	6.56 ± 0.40
21.7	15.52 ± 0.10	3.43 ± 0.30	6.58 ± 0.20
23.3	15.48 ± 0.30	3.00 ± 0.40	6.55 ± 0.30
25.0	15.23 ± 0.20	2.89 ± 0.40	6.56 ± 0.20
26.7	15.19 ± 0.10	2.72 ± 0.30	6.87 ± 0.30
28.3	15.13 ± 0.20	2.48 ± 0.30	7.36 ± 0.20
30.0	15.03 ± 0.30	2.45 ± 0.20	7.91 ± 0.20
31.7	14.96 ± 0.20	2.40 ± 0.30	7.96 ± 0.30
33.3	14.92 ± 0.30	2.40 ± 0.30	7.92 ± 0.20
35.0	14.86 ± 0.30	2.40 ± 0.20	7.90 ± 0.30

Concentration values are mean ± standard error (n = 3)

Table 8.3.3 Summary of results of control and test experiments (Results of SHF experiments are given in parentheses for comparison).

Parameter	Control Experiment (with mechanical shaking)*	Test Experiment (with intermittent sonication)[#]
Maximum ethanol concentration (g/L)	10.57 ± 0.15 (10.93 ± 0.20)**	15.62 ± 0.20 (12.14 ± 0.50)[##]
Ethanol yield on pretreated/delignified biomass (g/g)	0.27 (0.28)**	0.40 (0.31)[##]
Ethanol yield on raw biomass (g/g)	0.15 (0.15)**	0.21 (0.17)[##]
Ethanol productivity (g/L/h)	0.20 (0.61)**	0.85 (1.21)[##]
Maximum cell mass concentration (g/L)	4.37 ± 0.20 (5.26 ± 0.80)**	6.53 ± 0.30 (5.73 ± 0.50)[##]
Cell mass yield on pretreated/delignified biomass (g/g)	0.11 (0.14)**	0.17 (0.15)[##]
Cell mass productivity (g/L/h)	0.08 (0.29)**	0.36 (0.57)[##]

**Parameter values recorded at 54 h of fermentation in control experiments and at 18.3 h[#] in test experiments.*
***Maximum ethanol and cell mass concentration at 18 h of fermentation in control experiments and 10 h[##] in test experiments.*
Concentration values are mean ± standard error (n = 3)

The values of the physiological parameters in the differential equations for cell mass and ethanol, obtained with GA optimization are listed in Table 8.3.4. Experimental and model predicted profiles of ethanol and cell mass in control and test experiments are depicted in Fig. 8.3.3 and Fig. 8.3.4, respectively. Comparative analysis of the values of the physiological parameters obtained from fitting of the fermentation model to the experimental data give a mechanistic account of the influence of ultrasound on the SSF process. The trends in the values of model parameters for the control and test experiments (Table 8.3.4) and the explanations for these trends are as follows:

1. The value of K_3 (Monod constant for glucose for cell growth) was reduced in ultrasound-assisted SSF (test experiment), which indicated higher utilization of substrate for cell growth. This is attributed to faster transport of glucose across cell membrane due to strong micro-convection generated by ultrasound. Due to enhanced mass transfer, lesser bulk concentration of glucose is required to achieve maximum specific growth rate. This is also evident from rise in the value of μ_m in test experiments.

Table 8.3.4 Kinetic and physiological parameters in fermentation model fitted to experimental data with GA optimization.

Parameter	Control Experiment	Test Experiment
Monod constant for cell growth, $\boldsymbol{K_3}$ (g/L)	25.01	20.02
Inhibition constant of cell growth by glucose, $\boldsymbol{K_I}$ (g/L)	50.06	60.02
Inhibition constant of cell growth by ethanol, $\boldsymbol{K_{3E}}$ (g/L)	30.03	30.01
Specific cell death rate, $\boldsymbol{k_d}$ (1/h)	0.12	0.09
Maximal specific growth rate, $\boldsymbol{\mu_m}$ (1/h)	0.48	0.61
Constant for growth associated ethanol formation, $\boldsymbol{a}$ (g/g)	2.98	2.99
Non-growth associated specific ethanol production rate, $\boldsymbol{b}$ (g/g/h)	1.99	1.99
Best fitness value for the model parameters	60	86

2. Under the influence of ultrasound, the maximal specific cell growth rate (μ_m) was increased and the specific cell death rate (k_d) was reduced. The main causes of cell death are depletion of nutrients or accumulation of toxic products in the medium. The microturbulence and intense mixing generated by ultrasound assists the transfer of nutrients across the cells and dilution of toxic substances in the vicinity of the cell, respectively. Both of these effects eventually result in enhanced growth

of the cells, with reduced death rate.

3. The rise in K_I (inhibition constant of cell growth by glucose) indicated rise in tolerance of cells towards non-competitive inhibition by the substrate, or in other words, the inhibitory concentration of glucose shifted to a higher value. The reduction in both K_3 and K_I may be the result of the faster transport and utilization of glucose due to intense mixing introduced by ultrasound and this essentially is the synergistic effect of sonication on the fermentation.
4. Similar values of K_{3E} (inhibition constant of cell growth by ethanol) in control and test experiments showed that the inhibition for cell growth by product (ethanol) remained practically unaltered. It indicated that this property solely depends on physiology of the cells and not on its environment. Hence, it remained unaffected by the physical or chemical effects induced by ultrasound and cavitation. This effect can be further explained on the basis of intrinsic properties of the cells related to ethanol inhibition. There are two major causes leading to cell growth inhibition by ethanol: (a) inhibition of enzymes involved in glycolytic pathway and (b) effects on plasma membrane (fluidity, transport mechanisms or the enzymes associated with the membrane) (Moulin *et al*. 1984). These properties are mostly of intrinsic type, which remain unaffected by the physical or chemical effects of ultrasound.
5. Production of ethanol is directly related to the energy generation by microorganisms making this process growth-associated. However, a non-zero value (1.99 g/g/h) of *b* (non-growth associated specific ethanol production rate) indicated that ethanol formation takes place during stationary phase as well. The

value of *a* (constant for growth associated ethanol formation) was greater than *b* in both control and test experiments, which suggested that ethanol production is predominantly a growth associated process.

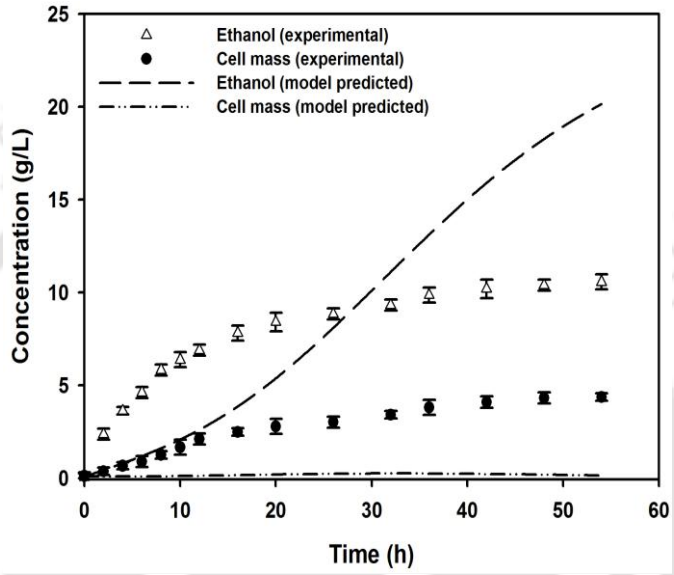

Fig. 8.3.3 Comparative representation of experimental and model predicted profiles of ethanol and cell mass in control experiment.

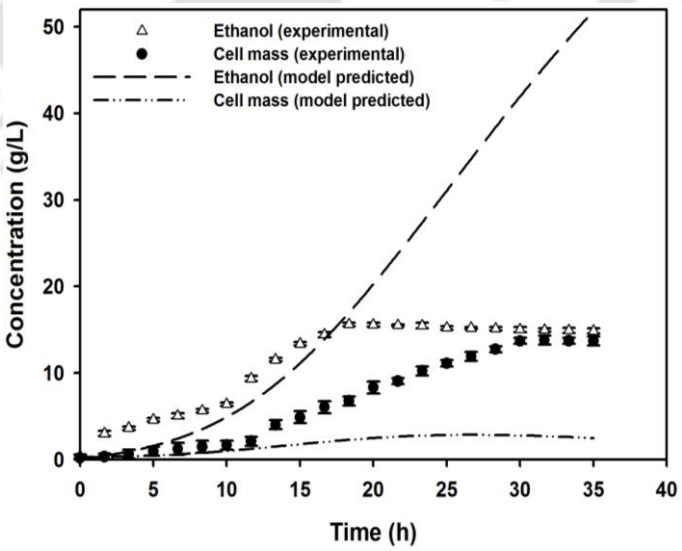

Fig. 8.3.4 Comparative representation of experimental and model predicted profiles of ethanol and cell mass in test experiment.

8.3.2 Comparative analysis of fermentation in SHF and SSF modes

The comparison of the results obtained in SSF (Table 8.3.3, Section 8.3.1) with that of SHF gives interesting accounts of links between physical effects of sonication and mode of fermentation. The higher value of ethanol concentration (15.62±0.20 g/L) in ultrasound-assisted SSF could be a consequence of acceleration of fermentation and enzymatic hydrolysis under sonication. The ethanol productivity in SHF was higher (1.21 g/L/h) than in SSF (0.85 g/L/h). These values could be misnomer indicating SHF process to be more efficient than SSF. However, it should be noted that the productivity in SHF process was determined on the basis of fermentation period only (and does not include hydrolysis time). Also, in test experiments the cell mass concentration was higher than control for both SHF and SSF, however, variations were reverse when compared between SHF and SSF. For control conditions, in SSF cell mass concentration was lower (4.37±0.20 g/L) than in SHF (5.26±0.80 g/L), however, for test experiment, SSF showed higher cell mass (6.53±0.30 g/L) than SHF (5.73±0.50 g/L). A plausible explanation for this could be same as stated earlier that ultrasound enhances not only fermentation but also the enzymatic hydrolysis. In SSF control experiment, the slower hydrolysis due to relatively lower convection induced by mechanical shaking, may lead to a lower instantaneous sugar concentration at any point of time than in SHF, resulting in lower cell mass. In SSF test experiment, the enhancement in cellulose hydrolysis due to strong micro-convection induced by sonication can significantly increase the instantaneous sugar levels in the broth, even higher than that in SHF mode, which could lead to higher cell mass production.

8.3.3 Effect of sonication on cell viability

Methylene blue staining (Fig. 8.3.5A and B) and viable cell count revealed that no cell death occurred due to sonication. Cell viability in control and test experiment samples was ~ 83% and ~ 84%, respectively. However, the effects of ultrasound on viability of yeast cells, investigated in previous studies (Wood *et al*. 1997, Radel *et al*. 2000, Sulaiman *et al*. 2011) explained that the destructive effects of sonication are due to pressure amplitude, frequency, power dissipation and exposure time (duty cycle). In a study by Radel *et al*. (2000), continuous exposure (60 min) of *S. cerevisiae* cells to the ultrasound of 2.2 MHz at an electrical power input of 14 W, killed 25% of the cells. Sulaiman *et al*. (2011) observed that the viability of yeast cells decreased with the increase in duty cycle and remained ≥70% throughout the fermentation at maximum duty cycle (40%) when *Kluyveromyces marxianus* cells were exposed to a sonication intensity of 11.8 W/cm^2 or a power input of 15 W.

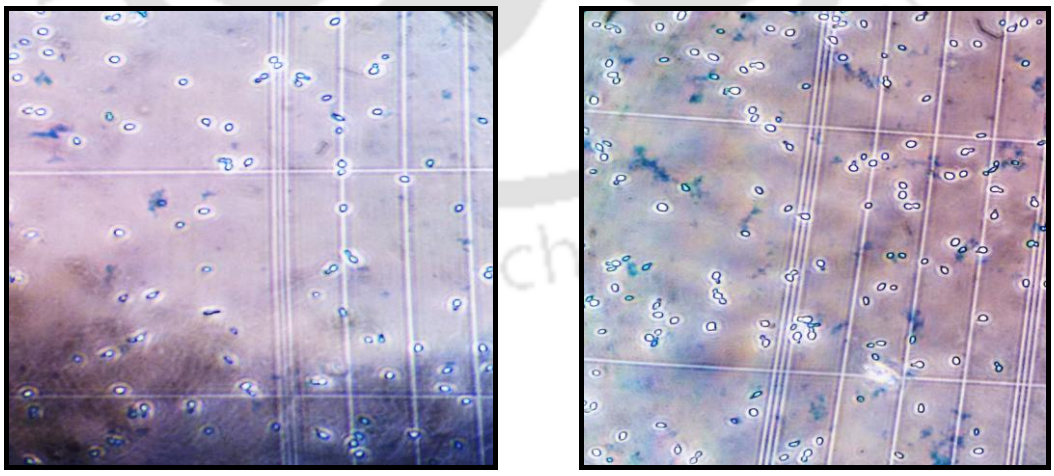

(A) **(B)**

Fig. 8.3.5 Micrographs of methylene blue stained yeast cells after completion of fermentation in (A) control and (B) test experiment showing unstained viable *S. cerevisiae* MTCC170 cells and blue stained dead cells.

8.3.4 Comparative assessment of the results of SSF in this study with literature

The results obtained in this study were compared with other reports in terms of ethanol titer, productivity and yield (with respect to raw biomass) (Table 8.3.5). It could be inferred from the data that ethanol yield with respect to raw biomass in the present study is at par with the previous reports. The results of the current study are remarkable despite the use of cellulase enzyme from a natural isolate for biomass hydrolysis. This result can be attributed to the physical effect of ultrasound and cavitation, which enhance the mass transfer in the system and thus, kinetics and yield of the SSF process.

Table 8.3.5 Comparison of the results of present study with published literature.

Biomass	Organism	SSF under sonication	Ethanol titer (g/L)	Ethanol productivity (g/L/h)	Ethanol yield (g/g of raw biomass)	Reference
Waste paper	*Klebsiella oxytoca* P2	Yes	36.6	0.38*	N. D.	Wood *et al.* 1997
Paper sludge	*Kluyveromyces marxianus* Y01070	No	8.8	0.12	0.33	Kadar *et al.* 2004
Paper sludge	*S. cerevisiae*	No	9.0	0.13	0.33	Kadar *et al.* 2004
Rice straw	*S. cerevisiae* D4A	No	12.7	0.11*	0.12	Ko *et al.* 2009
Saccharina japonica	*Pichia angophorae* KCTC 17574, *P. stipitis* KCTC 7228, *S. cerevisiae* KCCM 1129, *Pachysolen tannophilus* KCTC 7937	No	7.7	0.12*	N. D.	Jang *et al.* 2012
Rice straw	*S. cerevisiae* AYH306	No	58.7	0.49	0.13	Sun and Tao 2013
Oil Palm fronds	*S. cerevisiae*	Yes	18.2	3.64	N. D.	Ofori-Boateng and Lee 2014
Parthenium hysterophorus	*Saccharomyces cerevisiae* MTCC170	No	10.57	0.20	0.27	This study
Parthenium hysterophorus	*Saccharomyces cerevisiae* MTCC170	Yes	15.62	0.85	0.40	This study

*N. D., not determined; *as calculated from data reported in paper*

8.4 Conclusions

In this study, an attempt was made to get a physical insight into ultrasound induced enhancement in bioethanol synthesis from waste biomass *P. hysterophorus* using simultaneous saccharification and fermentation mode. The results of fermentation with and without sonication were coupled to a model comprising kinetic and physiological parameters that are characteristics of the mechanism of fermentation. The trends of these parameters gave an interesting account of the physical mechanism of ultrasound induced enhancement of ethanol fermentation. The results of this study revealed that strong microturbulence and mild shock waves induced by ultrasound and cavitation augment trans-membrane transport of substrate and products as well as dilution of the toxic substances, both of which contribute to enhancement in cell growth with faster consumption of substrate and reduced cell death rate. The ethanol productivity as well as cell mass productivity by SSF showed a 4-fold enhancement after sonication. Nonetheless, the parameters related to intrinsic mechanisms of the cells, such as the inhibition constant for ethanol or the constants for growth and non-growth associated ethanol production remained unaffected by sonication. The methylene blue staining method for determination of yeast cell viability revealed that sonication was not adversely affecting the cells. The work presented in this study could give important inputs in further mechanistic research in ultrasound-assisted bioethanol fermentation. The methodology adopted in this work can form a framework for investigations in other fermentation processes employing suitable mathematical models.

References

Abd-Aziz, S., Hung. G. S., Hassan, M. A., Karim, M. I. A. and Samat, N. (2008) Indirect method for quantification of cell biomass during solid state fermentation of palm kernel cake based on protein content. Asian Journal of Scientific Research, 1, 385-393.

Galbe, M. and Zacchi, G. (2002) A review of the production of ethanol from softwood. Applied Microbiology and Biotechnology, 59, 618-628.

Gupta, R., Kumar, S., Gomes, J. and Kuhad, R. C. (2012) Kinetic study of batch and fed-batch enzymatic saccharification of pretreated substrate and subsequent fermentation to ethanol. Biotechnology for Biofuels, 5, 16.

Holtzapple, M. T., Caram, H. S. and Humphrey, A. E. (1984) The HCH-1 model of enzymatic cellulose hydrolysis. Biotechnology and Bioengineering, 26, 775-780.

Jang, J. S., Cho, Y. K., Jeong, G. T. and Kim, S. K. (2012) Optimization of saccharification and ethanol production by simultaneous saccharification and fermentation (SSF) from seaweed, *Saccharina japonica*. Bioprocess and Biosystem Engineering, 35, 11-18.

Kadar, Zs., Szengyel, Zs. and Réczey, K. (2004) Simultaneous saccharification and fermentation (SSF) of industrial wastes for the production of ethanol. Industrial Crops and Products, 20, 103-110.

Karuppaiya, M., Sasikumar, E., Viruthagiri, T. and Vijayagopal, V. (2010) Optimization of process variables using response surface methodology (RSM) for ethanol production from cashew apple juice by *Saccharomyces cerevisiae*.

Asian Journal of Food and Agro-Industry, 3, 462-473.

Kataria, R. and Ghosh, S. (2011) Saccharification of Kans grass using enzyme mixture from *Trichoderma reesei* for bioethanol production. Bioresource Technology, 102, 9970-9975.

Ko, J. K., Bak, J. S., Jung, M. W., Lee, H. J., Choi, I. G., Kim, T. H. and Kim K. H. (2009) Ethanol production from rice straw using optimized aqueous-ammonia soaking pretreatment and simultaneous saccharification and fermentation processes. Bioresource Technology, 100, 4374-4380.

Kuhad, R. C., Gupta, R., Khasa, Y. P. and Singh A. (2010) Bioethanol production from *Lantana camara* (red sage): pretreatment, saccharification and fermentation. Bioresource Technology, 101, 8348-8354.

Moulin, G., Helen, B. and Galzy, P. (1984) Inhibition of alcoholic fermentation. Biotechnology and Genetic Engineering Reviews, 2, 365-382.

Nelson, N. (1944) A photometric adaptation of the Somogyi method for the determination of glucose. Journal of Biological Chemistry, 153, 375-380.

Ofori-Boateng, C. and Lee, K. T. (2014) Ultrasonic-assisted simultaneous saccharification and fermentation of pretreated oil palm fronds for sustainable bioethanol production. Fuel, 119, 285-291.

Painting, K. and Kirsop B. (1990) A quick method for estimating the percentage of viable cells in a yeast population, using methylene blue staining. World Journal of Microbiology and Biotechnology, 6, 346-347.

Philippidis, G. P., Spindler, D. D. and Wyman, C. E. (1992) Mathematical modeling of cellulose conversion to ethanol by simultaneous saccharification and

fermentation process. Applied Biochemistry and Biotechnology, 34/35, 543-556.

Radel, S., McLoughlin, A. J., Gherardini, L., Doblhoff-Dier, O. and Benes, E. (2000) Viability of yeast cells in well controlled propagating and standing ultrasonic plane waves. Ultrasonics, 38, 633-637.

Shah, Y. T., Pandit, A. B., Moholkar, V. S. (1999) Cavitation reaction engineering; Plenum Press: New York.

Shen, J. and Agblevor, F. A. (2010) Modeling semi-simultaneous saccharification and fermentation of ethanol production from cellulose. Biomass and Bioenergy, 34, 1098-1107.

Singh, S., Bharadwaja, S. T. P., Yadav, P. K., Moholkar, V. S. and Goyal, A. (2014b) Mechanistic investigation in ultrasoundassisted (alkaline) delignification of *Parthenium hysterophorus* biomass. Industrial and Engineering Chemistry Research, 53, 14241−14252.

Singh, S., Dikshit, P. K., Moholkar, V. S. and Goyal, A. (2014c) Purification and characterization of acidic cellulase from *Bacillus amyloliquefaciens* SS35 for hydrolyzing *Parthenium hysterophorus* biomass. Environmental Progress and Sustainable Energy. doi:10.1002/ep.12046.

Singh, S., Khanna, S., Moholkar, V. S. and Goyal, A. (2014a) Comparative assessment of pretreatment strategies for enzymatic saccharification of *Parthenium hysterophorus*. Applied Energy, 129, 195-206.

Singh, S., Moholkar, V. S. and Goyal, A. (2013) Isolation, identification and characterization of a cellulolytic *Bacillus amyloliquefaciens* strain SS35 from

rhinoceros dung. ISRN Microbiology, Article ID 728134, 7 pages.

Somogyi, M. (1945) A new reagent for the determination of sugar. Journal of Biological Chemistry, 160, 61-68.

Sun, W. L. and Tao, W. Y. (2013) Simultaneous saccharification and fermentation of rice straw pretreated by a sequence of dilute acid and dilute alkali at high dry matter content. Energy Source, Part A, 35, 741-752.

Wood, B. E., Aldrich, H. C. and Ingram, L. O. (1997) Ultrasound stimulates ethanol production during the simultaneous saccharification and fermentation of mixed waste office paper. Biotechnology Progress, 13, 232−237.

Chapter 9

Overview of the thesis and scope for future work

9.1 Overview

Ethanol production by lignocellulosic biomass follows three successive steps *viz*. pretreatment, enzymatic hydrolysis of pretreated biomass and fermentation. The economics of bioethanol production depends mainly on availability and cost of the substrate. Moreover, the efficiency of enzymatic hydrolysis of biomass, pretreatment and fermentation also plays an important role in bioethanol production. In present work, an attempt is made to develop, optimize and intensify a complete process for bioethanol production comprising of the three steps mentioned above.

As a first approach to process development, a natural cellulase producing strain *Bacillus amyloliquefaciens* SS35 was isolated from rhinoceros dung and endoglucanase (carboxymethylcellulase) production from the isolate was optimized by statistical design. The enzyme was purified, characterized and subsequently used for hydrolysis of pretreated and delignified *Parthenium hysterophorus* (Carrot grass), a noxious weed. Also, biomass pretreatment methods were optimized in subsequent step, i.e. acid hydrolysis and alkaline delignification. Delignification process was

coupled with ultrasound and the mechanism of the process has been suggested with the help of simulations of cavitation bubble dynamics. Enzymatic hydrolysis of pretreated and delignified *P. hysterophorus* biomass was also optimized by statistical method. The kinetics and yield of the hydrolysis process was enhanced by applying ultrasound. Effect of sonication and its underlying mechanism on the enzymatic hydrolysis system was investigated with help of kinetic analysis.

The final step in process development was fermentation, which was carried out using enzyme hydrolyzate as sugar source and *Saccharomyces cerevisiae* MTCC170 as the microbe. In order to boost the kinetics and yield of fermentation, ultrasonic irradiation was applied. The effect of ultrasonic treatment on sugar consumption, ethanol yield, cell growth, viability and other parameters of fermentation process was investigated. Further, separate hydrolysis and fermentation (SHF) processes were combined as simultaneous saccharification and fermentation (SSF) and the process was carried out under same conditions of ultrasound as in case of SHF. The experimental results from both the processes were fitted in a mathematical model and the effects of ultrasonic irradiation on various parameters related to kinetics of fermentation were studied. The major findings of this study addressing different facets of bioethanol production process have been summarized herewith.

Chapter 1 gives a general introduction and motivation for the thesis work. The global status of bioethanol production has been described briefly along with present scenario and future prospects of bioethanol production in India. Bioethanol production by lignocellulosic biomass has been reviewed from view point of major

challenges and potential solutions. Significance and aim of the thesis has been described briefly.

Chapter 2 describes the review of literature focused on governing factors and strategies for bioethanol production from lignocellulosic biomass. The literature reviewed in this chapter covers topics of cellulase production from microorganisms, and optimization, purification, characterization and applications of cellulase. In addition, literature published in area of pretreatment strategies for lignocellulosic biomass, enzymatic saccharification of pretreated biomass, fermentation of enzyme hydrolysate for ethanol production have been critically reviewed and discussed in this chapter. Subsequently, the literature in the area of application of ultrasound for intensification of various chemical and biochemical processes and its mechanistic insight using various mathematical models has also been reviewed and analyzed. Finally, the grey areas in bioethanol research have been identified and justification for the present thesis work has been given.

Chapter 3 deals with the first step of process development, i.e. isolation, screening, identification and characterization of cellulolytic *B. amyloliquefaciens* SS35 from rhinoceros dung. Cellulose hydrolysing bacteria were isolated from rhinoceros dung and tested for clear zone formation around the colonies on Bushnell Haas (BH) medium (pH 7.0) agar plates supplemented with carboxymethylcellulose (CMC). Isolates were screened on the basis of carboxymethylcellulase (CMCase) production in liquid medium. Out of 36 isolates, isolate no. 35 exhibited maximum CMCase activity of 0.079 U/mL and was selected for identification by using biochemical tests and phylogenetic analyses. The isolate was a Gram-positive, spore forming bacterium with rod-shaped cells. SEM (scanning electron microscopy)

analysis showed that the dimension of a single cell of isolate SS35 was 0.5-0.6 µm × 1.5-1.6 µm. The isolate showed positive results for catalase and nitrate tests and negative results for urease and H_2S production. Amylase production by isolate SS35 was indicated by hydrolysis of starch on the agar plate. Sugar fermentation profile of the isolate SS35 indicated that the bacterium was able to ferment the sugars cellobiose, dextrose, fructose, maltose, mannitol, rhamnose, sucrose, xylose, salicin, arabinose, inositol, trehalose, mannose and could not ferment the sugars adonitol, raffinose, dulcitol, galactose, melibiose, sorbitol, inulin and lactose. The results of antibiotic sensitivity and resistance of isolate SS35 showed that the isolate was resistant to penicillin, cephaloridin, ampicillin, ticarcillin, cefixime and cefoperazone, a prominent attribute of genus *Bacillus*. The isolate was identified as *Bacillus amyloliquefaciens* SS35 based on nucleotide homology and phylogenetic analysis using 16S rRNA and gyrase A gene sequences.

Chapter 4 describes the optimization of carboxymethylcellulase production from *B. amyloliquefaciens* SS35 by statistical designs. Optimization of the medium components and fermentation parameters for enhancing CMCase activity by *B. amyloliquefaciens* SS35 was carried out. The statistical experimental designs were applied in two steps *viz*. medium optimization and optimization of fermentation parameters. For medium optimization, Plackett-Burman design followed by Central Composite Design (CCD) was used, while for optimization of fermentation parameters one variable at a time method followed by central composite design was used. In case of medium optimization, Plackett -Burman factorial design revealed that carbon and nitrogen sources in the medium were the significant factors for enzyme production. The results from a 2^3-central composite design were fit in a

second-order polynomial model, which showed a good agreement between predicted and adjusted coefficient of determination values with R^2 = 0.8642 and 0.9575, respectively. At the concentration of 18.05 g/L CMC, 8 g/L yeast extract and 2 g/L peptone, the CMCase activity was found to be 0.553 ± 0.021 U/mL, after experimental validation of the model predicted value (0.553 U/mL). In optimization of fermentation parameters, the results from a 2^4-central composite design were fit in a second-order polynomial model, which showed an agreement between predicted and adjusted coefficient of determination values with R^2 = 94.22% and 84.73%, respectively. The optimum fermentation parameters for optimized medium were: initial medium pH 5.65, incubation temperature 40^{o}C, shaking speed 120 rpm and inoculum size 6.96% v/v. After experimental validation of the model with predicted CMCase activity of 0.710 U/mL under optimized conditions, CMCase activity was found to be 0.693 ± 0.043 U/mL. Thus, enhancement in CMCase activity was 3-fold after medium optimization, and 4-fold after both medium and fermentation parameters optimization. The CMCase production by *B. amyloliquefaciens* SS35 is predominantly influenced by the medium components in comparison to fermentation parameters.

Chapter 5 dealt with the purification and characterization of endoglucanase from *B. amyloliquefaciens* SS35. Purification of CMCase was carried out by ammonium sulphate fractionation method and anion exchange chromatography using DEAE-Sepharose, which resulted in yield of 12.4 and 2.1%, respectively and both the purification steps showed the purification fold of 4.6 and 18.5, respectively. The molecular weight of the CMCase was approximately, 37 kDa as determined by SDS-polyacrylamide gel electrophoresis and zymogram analysis. The optimal temperature

for CMCase activity was 55°C and the pH was 5.0. The enzyme was highly stable in the temperature range of 20-40°C and pH range of 5.0-9.0 for more than 20 h with significant residual CMCase activity of 80%. Endoglucanase activity at pH 5.0 and stability at 30^{o}C reflected the significance of the enzyme in the simultaneous saccharification and fermentation process of ethanol production using lignocellulosic biomass, since most of the ethanol fermenting organisms are truly mesophilic and acidophilic. The CMCase activity was significantly inhibited by Fe^{3+}, Zn^{2+}, Hg^{2+} ions and enhanced by Co^{2+}, Ca^{2+}, K^{+}, Na^{+} and Mn^{2+} ions. The study of effect of various ions on CMCase activity may be helpful in selecting or excluding the same ions in an SSF (simultaneous saccharification and fermentation) process as medium component for the microorganism. The purified CMCase hydrolysed CMC, barley-*β*-D-glucan, lichenan, hydroxyethylcellulose, starch and xylan. These observations showed that the enzyme was able to hydrolyse *β*-1,3 and *β*-1,4 glucosidic bonds preferably, making it a good candidate for hydrolysis of cellulosic biomass. However, no detectable activities were observed with avicel and *p*NPG indicating that the enzyme lacks exoglucanase and cellobiase (*β*-glucosidase) activities, respectively. The kinetic parameters using CMC, viz. K_m and V_{max} for CMCase were 0.33 mg/mL and 4.19 µmoles/mg/min, respectively. The efficiency of the enzyme was checked by hydrolysing *P. hysterophorus* and a maximum total reducing sugar (TRS) yield was 271.5 mg/g of biomass. The above results indicated that the CMCase isolated and purified in this study has high potential for application in hydrolysis of lignocellulosic biomass, which is an important step in synthesis of bioalcohols through fermentation.

Chapter 6 describes the screening and optimization of pretreatments and ultrasound-assisted (alkaline) delignification of *P. hysterophorus* biomass. The comparative assessment of pretreatment strategies and optimization of ultrasound-assisted alkaline delignification for the lignocellulosic biomass, *P. hysterophorus*, which has cellulose content of 45.2 ± 1.81% (w/w), was done. In case of screening and optimization of pretreatment process for *P. hysterophorus* biomass, the yardstick of assessment was amount of fermentable sugars released during enzymatic hydrolysis of pretreated biomass. Different biomass samples, pretreated with various methods were characterized by SEM and FTIR analyses to observe the effect of pretreatment on structure and constitution of biomass. Various physical, chemical and physicochemical methods have been employed for the pretreatment with aim of exposure of cellulose moieties in biomass for enzymatic action during hydrolysis. Carboxymethylcellulase (1.0 U/mg, 1.7 mg/mL) produced by the isolate *B. amyloliquefaciens* SS35 and *β*-glucosidase (Novozyme 188), were used for enzymatic hydrolysis of pretreated biomass. Among the different methods employed for pretreatment, the most efficient treatment was revealed to be autoclaving of biomass at 121^{o}C and 15 psi pressure for 30 min in acidic environment (1%, v/v or 0.36 N sulphuric acid). TRS yield during this pretreatment, mainly due to hydrolysis of hemicellulosic fraction of biomass, has been 285.3 mg/g biomass. Enzymatic hydrolysis of pretreated biomass resulted in reducing sugar yield of 187.4 mg/g of pretreated biomass (9.37 g/L). The total fermentable sugar yield from the optimized pretreatment was 397.7 mg/g raw biomass (39.77 g/100 g raw biomass). In addition, ultrasound assisted delignification of *P. hysterophorus* biomass has also been attempted in this study from the mechanistic point of view. The approach of study

was to couple simulations of cavitation bubble dynamics to the experiments on delignification in order to identify the links between chemistry of delignification and physics of cavitation. Optimum conditions for delignification with ultrasound have been identified as: temperature = 303 K, NaOH concentration = 1.5% (w/v) and biomass concentration = 2% (w/v). Characterization of delignified biomass was carried out using FTIR spectroscopy, XRD and FESEM techniques. Kinetic analysis of delignification at optimum conditions has revealed 2-fold enhancement with ultrasound as compared to mechanically agitated treatment. Enzymatic hydrolysis of delignified biomass resulted in reducing sugar yield of 308.4 mg/g of delignified biomass (15.42 ± 0.33 g/L) after 84 h of hydrolysis.

Chapter 7 deals with the investigations on separate enzymatic hydrolysis of *P. hysterophorus* biomass and subsequent fermentation of hydrolysate. The efficiency (in terms of yield and kinetics) of conventional hydrolysis and fermentation processes was improved by employing intermittent ultrasonic irradiation at a duty cycle of 10%. The optimization of hydrolysis process was carried out by a 2^3-central composite design and the results were fitted in a second-order polynomial model, which showed an agreement between predicted and adjusted coefficient of determination values with R^2 = 94.4% and 95.75%, respectively. The optimum parameters for enzymatic hydrolysis were: biomass loading = 38.8 g/L, CMCase concentration = 600 U/g of biomass, and glucosidase concentration = 50 U/g of biomass. After experimental validation of the model predicted response (sugar yield), which was 599.95 mg/g reducing sugar yield, sugar yield obtained was 593.4 ± 16.3 mg/g. Thus, enhancement in yield was 2-fold after optimization of the process. Ultrasound-assisted enzymatic hydrolysis was carried under optimum

conditions obtained from CCD experimental design. It was observed that maximum sugar (yield was 711.3 ± 18.6 mg/g) was released within 14 h of hydrolysis as compared to 96 h (sugar yield was 593.4 ± 16.3 mg/g) for control experiment without ultrasound. To account for the enhancement of enzymatic hydrolysis, experiments were carried out to analyze the reaction kinetics using Lineweaver-Burk plots. The values of V_{max} and K_m for ultrasound assisted process were found out to be 0.055 mM/min and 24.44 g/L as compared to 0.046 mM/min and 42.77 g/L for hydrolysis without ultrasound. This result indicated that the enhancement effect of ultrasound on the hydrolysis process is in terms of both increase in rate of reaction and a reduced value of K_m relative to control implies an increased affinity of the enzymes for the substrate. Increase in rate of reaction could be a consequence of enhancement in the convection in the medium and mass transfer characteristics. However, the reduced K_m value suggests that ultrasound facilitated substrate binding to the active site of the enzymes, possibly by enhancing pulsating motions within the enzyme molecule. The hydrolysate was fermented to ethanol using yeast strain *Saccharomyces cerevisiae* MTCC170 and also the influence of ultrasound on fermentation was investigated. The experiments with the application of ultrasound, were carried out in an ultrasonic bath (Transonic T-460, Elma, Germany, 2 L, with dimensions 25 cm × 15 cm × 10 cm) operating at a frequency of 35 kHz and power input of 35 W. The duty cycle of sonication was 10% (1 min ON and 9 min OFF). In case of control experiment an ethanol titer of 10.93 g/L (0.4 g/g reducing sugar) was achieved after 18 h of fermentation. The time of fermentation was reduced to 10 h in ultrasound-assisted process and resulted to an ethanol concentration of 12.14 g/L (0.44 g/g reducing sugar). The influence of ultrasound on the fermentation process

needs to be mapped on the basis of variation in the four parameters, k_d, μ_m, $Y_{X/G}$ and m. The experimental data were fitted to a saccharification/ fermentation model. This model is based on the HCH-1 model for heterogeneous cellulose hydrolysis followed by ethanol fermentation modeled with Monod - type kinetics. This model comprised of five ordinary differential equations, one each cellulose, cellobiose, microbial cell mass, substrate (sugar) and ethanol. These equations were solved using Runge-Kutta solver coupled to a genetic algorithm code. The kinetic parameters in the model were assigned a lower and upper bound. For the SHF operation there were 8 model parameters. The genetic algorithm code was used to find the best set of values of the parameters within the bounds defined a priori, based on typical values of the parameters reported in literature. Comparison of the parameters for SHF operation - with and without ultrasound helped in determining the extent of influence of ultrasound on the process. The major trends in parameters were as follows: (1) the specific growth rate of microbial cells increases with ultrasound, (2) the specific death rate of cells decreases with ultrasound, (3) the yield of microbial cell mass per unit sugar consumed increases with ultrasound, while the consumption rate of substrate for cell maintenance reduces with ultrasound. Other parameters such as Monod constant for substrate and inhibition constant for substrate did not alter with ultrasound. These results are attributed to enhanced mass transfer characteristics of the process in presence of ultrasound, i. e. diffusion of substrate/ product across cell wall. Moreover, ultrasound can help desorption of the product gases such as CO_2 from the solution, and at the same time, high convection generated by ultrasound can improve transfer and dissolution of oxygen in the broth so as to maintain the

dissolved oxygen concentration close to saturation levels. These results are manifested in faster rate of hydrolysis and fermentation.

Chapter 8 deals with the simultaneous saccharification and fermentation (SSF) of pretreated and delignified *P. hysterophorus* biomass. All physical parameters of fermentation and ultrasound were same as described above in SHF process, except the components of the process, *viz*. pretreated and delignified *P. hysterophorus* biomass was used as substrate and the enzymes were added directly in fermentation broth. The results of control experiment (without ultrasound) revealed that the maximum ethanol production was achieved at 54^{th} h of fermentation with an ethanol titer of 10.57 g/L. However, test (ultrasound-assisted fermentation) experiment resulted in ethanol titer of 15.62 g/L after 18.3 h. The experimental data (i.e. time profiles of cell mass, sugar and ethanol concentrations) obtained from SSF experiments (both with and without ultrasound), were fitted to the saccharification/ fermentation model, as described above. For the SSF operation, there were 9 model parameters. The genetic algorithm code was used to find the best set of values of the parameters within the bounds defined a priori, based on typical values of the parameters reported in literature. Comparison of the parameters for SSF process - with and without ultrasound helped in determining the extent of influence of ultrasound on the process. The influence of ultrasound on parameter values followed the same trend as in case of SHF process. The trends obtained in SSF process were interpreted on similar grounds as in case of SHF experiments, mentioned above.

Figure 9.1 gives a schematic representation of the major results and findings of the present thesis.

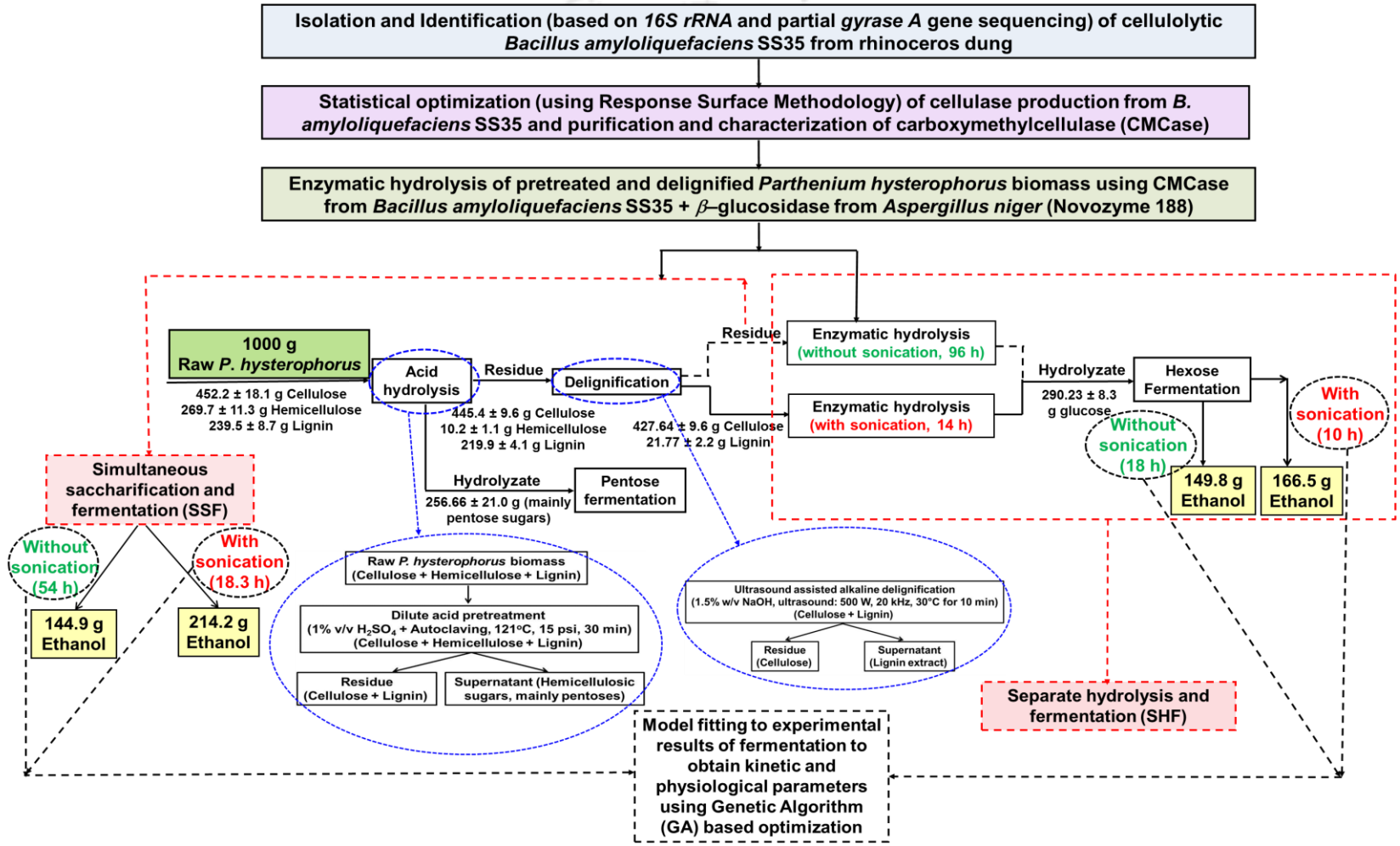

Fig. 9.1 Schematic representation of the major results and findings of the thesis (* for greater details on pentose fermentation, please refer to STP Bharadwaja, *Mechanistic investigation in ultrasound assisted delignification and enzymatic hydrolysis of Parthenium hysterophorus for bioethanol production*, M.Tech. thesis, IIT Guwahati, Guwahati (2014).

9.2 Scope for future work

The present thesis has established *P. hysterophorus* based bioethanol production process at laboratory level. As noted in Chapter 1, the cost of the substrate constitutes the major component of the total cost of production of bioethanol. The process reported in this thesis is based on the waste biomass of *P. hysterophorus* and owing to its negligible cost the process can have feasible economics, which may lead to its chances of commercially accepted. However, more research work is required before such an endeavor. Some suggestions for future work in this regard have been given which are as follows:

1. The laboratory scale process reported in this thesis can first be attempted using a bench scale sono-bioreactor.
2. Since CMCase is an inducible enzyme and a cheap carbon source is crucial for the competitiveness for enzymes production at low cost, the potential of the *B. amyloliquefaciens* SS35 to produce CMCase using inexpensive carbon sources different from technical grade carboxymethylcellulose can be investigated. Also carboxymethylcellulose can be replaced by cellulose rich biomass, for example, pretreated and delignified *Parthenium hysterophorus* biomass.
3. Intensification of CMCase production from *Bacillus amyloliquefaciens* SS35 can also be carried out by sonication.
4. In the present thesis the fermentation has been carried out in batch mode. This could be improved to either fed-batch or continuous modes, since these modes of operations are more suitable for large scale processes.
5. The ultrasound enhanced processes need further optimization in terms of ultrasound power input as well as frequency, which were kept constant in present

thesis. This factor is crucial, as it directly affects the operating cost of the process, and thus, needs to be optimized with systematic approach.

6. Combined fermentation of hexose and pentose hydrolysates can also be attempted using suitable microbial cultures. The relatively slower kinetics of consumption of pentose sugars (as reported in literature) can be boosted with ultrasound.

Research outputs of the thesis

Publications in International Journals

Published/Accepted

1. **Singh S.**, Agarwal M.[§], Sarma S.[§], Goyal A. and Moholkar V.S. (**2015**) Mechanistic insight into ultrasound induced enhancement of simultaneous saccharification and fermentation of *Parthenium hysterophorus* for ethanol production. ***Ultrasonics Sonochemistry***, 26, 249–256. ([§]equally contributed)
2. **Singh S.**, Sarma S.[§], Agarwal M.[§], Goyal A. and Moholkar V.S. (**2015**). Ultrasound enhanced ethanol production from *Parthenium hysterophorus*: A mechanistic investigation. ***Bioresource Technology***, 188, 287–294. ([§]equally contributed)
3. **Singh S.**, Dikshit P.K., Moholkar V.S. and Goyal A. (**2014**) Purification and characterization of acidic cellulase from *Bacillus amyloliquefaciens* SS35 for hydrolyzing *Parthenium hysterophorus* biomass. ***Environmental Progress and Sustainable Energy***, DOI: 10.1002/ep.12046.
4. **Singh S.**[§], Bharadwaja S.T.P.[§] ,Moholkar V.S. and Goyal A. (**2014**) Mechanistic investigation in ultrasound–assisted (alkaline) delignification of *Parthenium hysterophorus* biomass. ***Industrial and Engineering Chemistry Research***, 53, 14241-14252. ([§]equally contributed)
5. **Singh S.**, Khanna S., Moholkar V.S. and Goyal A. (**2014**) Comparative assessment of pretreatment strategies for enzymatic saccharification of *Parthenium hysterophorus*. ***Applied Energy***, 129, 195–206.
6. **Singh S.**, Moholkar V.S. and Goyal A. (**2014**) Optimization of carboxymethylcellulase production from *Bacillus amyloliquefaciens* SS35. ***3 Biotech***, 4, 411-424.
7. **Singh S.**, Moholkar V.S. and Goyal A. (**2013**) Isolation, identification, and characterization of a cellulolytic *Bacillus amyloliquefaciens* strain SS35 from rhinoceros dung. ***ISRN Microbiology***, Volume 2013, Article ID 728134, 7 pages.

Manuscript under preparation

8. **Singh S.**, Goyal A. and Moholkar V.S. Enzymatic hydrolysis of *Parthenium hysterophorus* using cellulase isolated from *Bacillus amyloliquefaciens* SS35: Statistical optimization and ultrasound–assisted intensification.

Conference presentations from thesis work

International

1. **Singh S.**, Goyal A. and Moholkar V.S. (**2015**) Bioethanol production from *Parthenium hysterophorus* (carrot grass): Ultrasound enhanced enzymatic hydrolysis and fermentation. 4th Annual International Conference on Sustainable Energy and Environmental Sciences (SEES 2015), February 9-10, 2015, Singapore. (**Oral Presentation**)
2. **Singh S.**, Sarma S., Goyal A. and Moholkar V.S. (**2014**) Ultrasound-enhanced Bioethanol production from *Parthenium hysterophorus* (carrot grass) by simultaneous saccharification and fermentation. Indo-US Conference on Advanced Lignocellulosic Biofuels (Indo-US CALB-2014), November 10-11, 2014, CSIR-Indian Institute of Chemical Technology, Hyderabad, India. (Poster Presentation) (**Received Best Poster Award, Third Prize**)
3. **Singh S.**, Moholkar V.S. and Goyal A. (**2014**) Ultrasound-assisted intensification of bioethanol production from *Parthenium hysterophorus*. International Conference on Emerging Trends in Biotechnology and 11th Convention of the Biotech Research Society, India (BRSI-2014). November 6-9, 2014, Jawaharlal Nehru University, New Delhi, India. (Poster Presentation)
4. **Singh S.**, Moholkar V.S. and Goyal A. (**2014**) Bioethanol production by pretreatment, hydrolysis and fermentation of *Parthenium hysterophorus*. International Conference on Energy Technology, Power Engineering and Environmental Sustainability. June 21–22, 2014, Jawaharlal Nehru University, New Delhi, India. Abstract published in *International Journal of Applied Research*, 9(9), 1149. (**Oral Presentation**)
5. **Singh S.**, Dikshit P.K., Moholkar V.S. and Goyal A. (**2014**) Statistical optimization of enzymatic hydrolysis of *Parthenium hysterophorus* by response surface methodology. International Conference on Harnessing Natural Resources for Sustainable Development: Global Trend, January 29–31, 2014, Cotton College, Guwahati, Assam, India. (**Oral Presentation**)
6. **Singh S.**, Moholkar V.S. and Goyal A. (**2013**) Optimization of pretreatment strategies for enzymatic saccharification of *Parthenium hysterophorus* for bioethanol production. International Symposium on Frontier Discoveries and Innovations in Microbiology and its Interdisciplinary Relevance (54th Annual Conference of Association of Microbiologists of India) (AMI–2013), November 17–20, 2013, Maharshi Dayanand University, Rohtak, Haryana, India. (Poster Presentation)
7. **Singh S.**, Dikshit P.K., Moholkar V.S. and Goyal A. (**2012**) Stability and specificity studies of cellulase produced from a facultative thermophilic and acidophilic *Bacillus amyloliquefaciens* SS35. International Conference on Industrial Biotechnology and 9th Convention of the Biotech Research Society, India (BRSI–2012), November 21–23, 2012, Punjabi University, Patiala, Punjab, India. (Poster Presentation) **(Received Best Poster Award)**

8. **Singh S.**, Dikshit P.K., Moholkar V.S. and Goyal A. (**2011**) Screening, isolation and optimization of culture conditions of cellulose hydrolytic bacteria from rhinoceros dung. International Conference on Microbial Biotechnology for Sustainable Development (52nd Annual Conference of Association of Microbiologists of India) (AMI–2011), November 3–6, 2011, Panjab University, Chandigarh, Punjab, India. (Poster Presentation)

National

1. **Singh S.**, Bharadwaja S.T.P., Moholkar V.S. and Goyal A. (**2014**) Ultrasound assisted delignification of acid pretreated *Parthenium hysterophorus* for enzymatic hydrolysis. National Seminar on Emerging Bio-inputs in Biotechnology for a Green Environment, Department of Bioengineering and Technology, May 9–10, 2014, Gauhati University Institute of Science and Technology, Gauhati University, Assam, India. (**Oral Presentation**)
2. **Singh S.**, Moholkar V.S. and Goyal A. (**2013**) Statistical optimization of medium composition for cellulase production from an isolate *Bacillus amyloliquefaciens* SS35. UGC–SAP National Seminar cum DBT–BIF Workshop on Recent advances in Microbial Biotechnology and Molecular Evolution. March 1-4, 2013, Tezpur University, Tezpur, Assam, India. (**Oral Presentation**)
3. **Singh S.**, Moholkar V.S. and Goyal A. (**2010**) Screening, isolation and optimization of culture conditions of cellulolytic bacterium (SS10) isolated from microbial biodiversity rich Assam**.** National Conference on Emerging Trends in Biopharmaceuticals: Relevance to Human Health. November 11-13, 2010, Thapar University, Patiala, Punjab, India. (Poster Presentation)